SYNTHESIS AND CHARACTERIZATION OF C_2 SYMMETRIC LIQUID CRYSTALLINE MATERIALS

by

KYLE ANDREW HOPE-ROSS

B.Sc., The University of British Columbia, 2005

A THESIS SUBMITTED IN PARTIAL FULFILLMENT OF THE REQUIREMENTS FOR THE DEGREE OF

MASTER OF SCIENCE

in

THE FACULTY OF GRADUATE STUDIES

(Forestry)

THE UNIVERSITY OF BRITISH COLUMBIA

(Vancouver)

August 2008

Abstract

A number of compounds were synthesized with the ultimate goal being the synthesis of C_2 symmetric molecules which displayed thermotropic liquid crystalline behaviour. The compounds prepared were 4-alkoxy benzophenones, 3,4-bis-alkoxy benzophenones, 4-alkoxy dibenzylidene acetones, 3,4-bis-alkoxy dibenzylidene acetones and 4'-alkoxy-1,9-diphenyl-nona-1,3,6,8-tetraen-5-ones. The length of the linear alkoxy side chain was varied from C_6H_{13} to $C_{12}H_{25}$.

All compounds were characterized by FTIR, ^{1}H, and ^{13}C NMR spectroscopy. Mesophase behaviour of the synthesized compounds was investigated using differential scanning calorimetry and polarizing optical microscopy.

It was determined that both the alkoxy side chain length, as well as the number of alkoxy side chains have an effect on the ability of this class of C_2 symmetric compounds to self-assemble into liquid crystalline phases. In addition, the overall core size and extent of conjugation also affected mesophase formation. The mono-alkoxy benzophenones and dibenzylidene acetones were non-mesogenic, while all four of the mono-alkoxy 1,9-diphenyl-nona-1,3,6,8-tetraen-5-ones (alkoxy side chain of lengths C_6H_{13}, C_8H_{17}, $C_{10}H_{21}$ and $C_{12}H_{25}$) self-assembled into nematic liquid crystalline phases. Increasing the number of alkoxy side chains from one to two per aromatic moiety helped induce liquid crystalline formation: the corresponding bis-C_6H_{13} benzophenone and bis-C_6H_{13}, bis-C_8H_{17}, and bis-$C_{10}H_{21}$ dibenzylidene acetones were mesogenic, displaying smectic A (benzophenone) and nematic (dibenzylidene acetone) mesophases respectively.

Table of Contents

List of Tables

List of Figures

List of Schemes

List of Abbreviations and Symbols

bs: broad singlet

cm^{-1}: wavenumbers

Col_h: hexagonal columnar

Cr: crystal; crystalline

δ: delta; chemical shift

ΔH: enthalpy change

d: doublet

dba: dibenzylidene acetone

DCM: dichloromethane

dd: doublet of doublets

DDQ: 2,3-dichloro-5,6-dicyano-*p*-benzoquinone

DIBAL: di-*iso*-butyl aluminum hydride

DMF: N,N-dimethyl formamide

DMSO: dimethyl sulfoxide

DSC: Differential Scanning Calorimetry

dt: doublet of triplets

Et_2O: diethyl ether

EtOH: ethanol

EDG: electron donating group

EWG: electron withdrawing group

FTIR: Fourier Transform Infrared Spectroscopy

g: grams

h: hours

$HNEt_2$: diethyl amine

Hz: hertz

I: Isotropic

J: coupling constant

kJ: kilojoule

LAH: lithium aluminum hydride, $LiAlH_4$

LC: liquid crystalline

LCD: liquid crystal display

LED: light-emitting diode

NaOMe: sodium methoxide

NMR: Nuclear Magnetic Resonance Spectroscopy

M: molar

Me: methyl

mL: millilitres

mmol: millimoles

mol: mole; moles

mp: melting point

MeOH: methanol

MHz: megahertz

N: nematic

OLED: organic light-emitting diode

PCC: pyridinium chlorochromate

POM: polarizing optical microscopy; polarizing optical microscope

ppm: parts per million

PTLC: preparative thin layer chromatography

pyr.: pyridine

q: quartet

quin.: quintet

rt: room temperature

s: singlet

Sm: Smectic

σ: Hammett parameter for electronegativity

t: triplet

THF: tetrahydrofuran

T_c: clearing temperature

T_m: melting temperature

XRD: X-Ray Diffraction

Acknowledgments

I would like to acknowledge my professors, friends and fellow students at the University of British Columbia, who have made this a memorable journey.

I thank Dr. John F. Kadla, whose support and encouragement have helped me through this process.

I thank Drs. Mark MacLachlan and Shawn Mansfield for their input and advice.

To my fellow lab-mates I offer many thanks for their friendship and advice, in particular: Drs. Fadi Asfour, Batia Bar-Nir, Jennifer Braun and Ms. Magdalena Mazur.

I would like to thank Ms. Emilie Voisin and Dr. Vance Williams for their help and advice in the characterization of the liquid crystalline mesophases.

I acknowledge the following academics who have provided me with liquid crystalline images for the introductory chapter: Dr. Oleg Lavrentovich and Dr. Mary Neubert (Liquid Crystal Institute at Kent State University) as well as Dr. Torsten Hegmann (University of Manitoba).

I would also like to thank my parents, who have provided me with unconditional love and encouragement throughout my education.

Finally, a very special thank you is owed to Jessica Erickson, without whose love and support this undertaking would not have been possible.

Chapter 1

Introduction

1.1 Liquid Crystals

1.1.1 Background and Theory

Liquid crystal research began in 1888 when Austrian botanist Friedrich Reinitzer observed that cholesteryl benzoate melted from a solid to a cloudy liquid at 145.5 °C and then melted again at 178.5 °C to a clear liquid.[1,2] Reinitzer sought the help of German physicist Otto Lehman, who built the first heating stage for a microscope. Together they observed the different textures under the microscope and it was Lehman who later coined the term 'liquid crystal'.[3] These early observations and techniques laid the groundwork for liquid crystal research today. For instance, a major requirement for a substance to be classified as liquid crystalline is the property of multiple melting points, and every modern liquid crystal research laboratory is equipped with a hot stage microscope.

Traditionally, it is taught that there are three phases of matter: solid, liquid and gas. A liquid crystal is any material that displays a fourth phase of matter intermediate between the isotropic liquid phase and the anisotropic crystalline phase. This fourth phase of matter (the liquid crystalline phase) is referred to as the mesophase (from the Greek *mesos,* meaning between). Any molecule which exhibits liquid crystalline behaviour is referred to as a mesogen. Many common substances display mesogenic behaviour, including soaps and cholesterol derivatives.[4]

Liquid crystals can be classified into two groups: lyotropic liquid crystals and thermotropic liquid crystals. Lyotropic liquid crystals are molecules which must be dissolved in a solvent to exhibit mesogenic behaviour and display phase transitions as a function of solute concentration as well as temperature. Thermotropic liquid crystals display phase transitions solely as a function of temperature. Soaps are an example of lyotropic liquid crystals, whereas cholesteryl benzoate is an example of a thermotropic liquid crystal. This thesis will focus on thermotropic liquid crystals.

1.1.2 Classes of Thermotropic Liquid Crystals

Thermotropic liquid crystals exhibit different mesophases depending upon their molecular structure and ordering in the liquid crystalline phase. There are four commonly accepted mesophases: the nematic, chiral nematic, smectic and columnar phases.[5]

Nematic (from the Greek *nema,* meaning thread) liquid crystals display long-range directional order, but no positional order. All of the molecules are aligned in the same direction, along a director axis. **Figure 1.1** presents a schematic of the long-range directional ordering present in nematic liquid crystals (**a**), and a representative texture observed under a polarizing optical microscope (POM) (**b**).

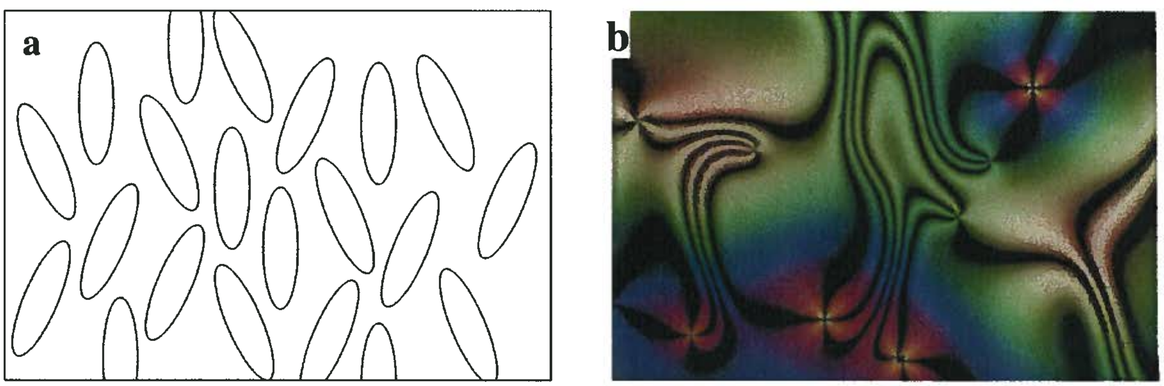

Figure 1.1: **a**) Schematic of a nematic liquid crystal,[4] **b**) Representative texture of a nematic liquid crystal (courtesy of O. Lavrentovich; http://www.lci.kent.edu/defect.html).

The chiral nematic phase, or cholesteric phase (as it was first observed in cholesterol derivatives), is a subset of the nematic phase and is formed with optically active molecules. Each layer of molecules in the chiral nematic phase is twisted in the same direction from the layer of molecules above it. This twisting produces chirality similar to the chirality present in screws. The chirality in chiral nematic liquid crystals can originate from either a chiral mesogen or a chiral dopant added to a non-chiral mesogen in small amounts. The layers of twisted nematics lead to the concept of *pitch*, an important property of chiral nematic liquid crystals.[4] The pitch of a chiral nematic liquid crystal is defined as the distance between two parallel layers which are twisted by 360°. The chirality in liquid crystalline molecules leads to unique optical properties, such as the selective reflection of circularly polarized light and high optical activity. **Figure 1.2** presents a schematic of the layers of twisted nematic phases present in chiral nematic liquid crystals (**a**), and a representative fingerprint texture observed under POM (**b**). The pitch *n* is related to the fingerprint texture: as the pitch increases, so does the thickness of ridges in the fingerprint texture.

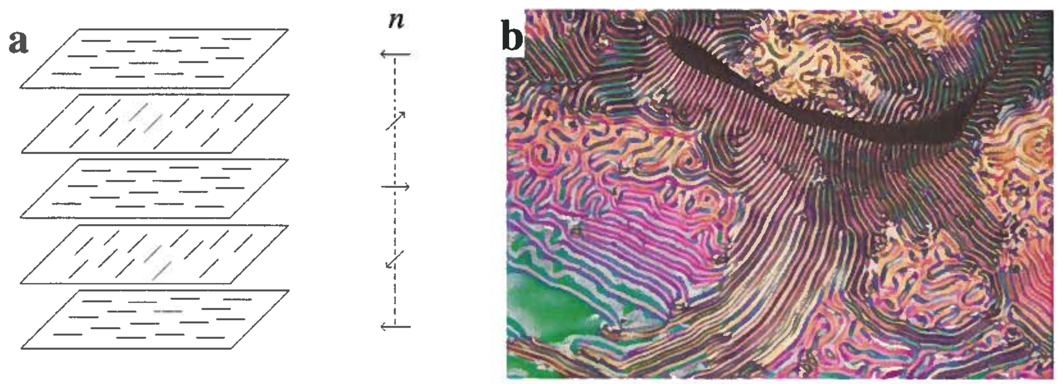

Figure 1.2: **a**) Schematic of a chiral nematic liquid crystal: layers of twisted nematics,[4] **b**) Representative fingerprint texture of a chiral nematic liquid crystal (courtesy of T. Hegmann; http://home.cc.umanitoba.ca/%7Ehegmann/Site/Photos.html#0).

Smectic (from the Greek *smectos*, meaning soap) liquid crystals display both long range directional and positional order, and are thus more organized and energetically stable than nematic phases. The smectic mesophases can be further divided into subclasses A, B, C, etc., simply labeled by when they were discovered (A being discovered first).[5]The smectic A mesophase consists of parallel rows and columns of molecules, and the smectic B mesophase displays a more hexagonal packing of molecules. The smectic C mesophase is structurally similar to the smectic A mesophase, but consists of molecules which are tilted with respect to the layer. Smectic C thus differs from smectic A by the magnitude of the distance between parallel layers of molecules. **Figure 1.3** presents schematic examples of the most common smectic phases: smectic A (**a**), smectic B (**b**), and smectic C (**c**) mesophases, and a representative texture is shown in **Figure 1.4**.[4]

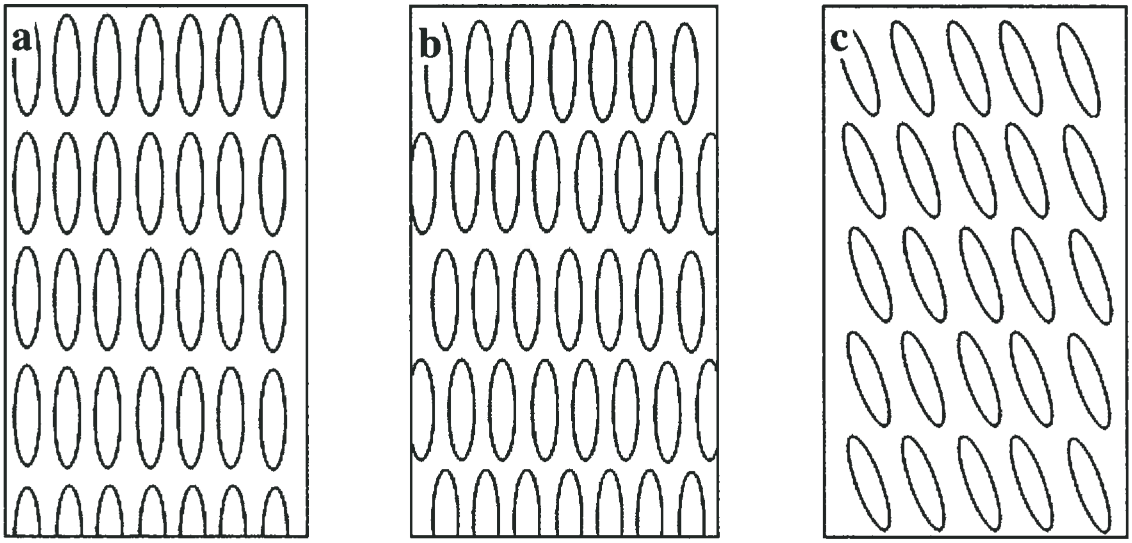

Figure 1.3: Schematic of smectic mesophases **a**) Sm A, **b**) Sm B and **c**) Sm C.[4]

Figure 1.4: Representative texture of a smectic A liquid crystal (courtesy of M. Neubert; http://www.lci.kent.edu/fans.html).

In the columnar phase, disc-shaped molecules traditionally self-assemble based on π-stacking interactions. Columnar mesophases are further classified as either hexagonal, where the disc-like molecules are arranged in a hexagonal array, or rectangular, where the disc-like molecules are arranged in a rectangular array. **Figure 1.5** displays a schematic example of a hexagonal columnar mesophase (**a**) and a representative texture of a hexagonal columnar liquid crystal (**b**).

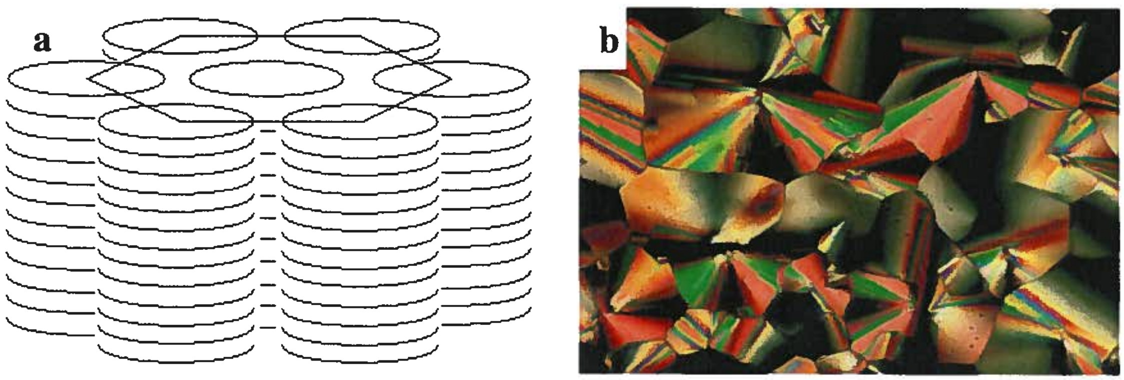

Figure 1.5: **a**) Schematic of the hexagonal columnar mesophase,[4] **b**) Representative texture of a hexagonal columnar liquid crystal (courtesy of T. Hegmann; http://home.cc.umanitoba.ca/%7Ehegmann/Site/Photos.html#4).

1.1.3 Structural Characteristics of Liquid Crystals

There are three general molecular shapes which lead to mesogenic behaviour: rod-like, disc-like and board-like. Rod-like mesogens such as *p*-sexiphenyl[4] (**Figure 1.6**) are called calamitic liquid crystals, which tend to form either smectic or nematic mesophases.[4]

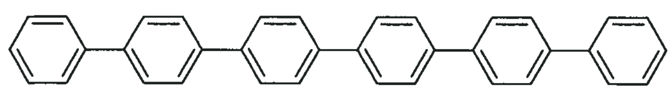

Figure 1.6: Structure of *p*-sexiphenyl.[4]

Disc-like mesogens are called discotic liquid crystals. These tend to form columnar and nematic mesophases and include molecules such as poly-functionalized aromatics, for example 1,2,3,4,5,6-hexakis-heptyl benzoate[4] (**Figure 1.7**).

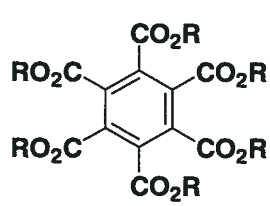

Figure 1.7: 1,2,3,4,5,6-hexakis-heptyl benzoate ($R = C_7H_{15}$).[4]

Mesogens which are neither calamitic nor discotic are called sanidic liquid crystals.[4] Typically sanidic liquid crystals are composed of flat, board-like structures, which can be induced by intermolecular hydrogen bonding, as seen in 2,3,4-tris-hexyloxy cinnamic acid[4] (**Figure 1.8**). Sanidic liquid crystals tend to form nematic mesophases.

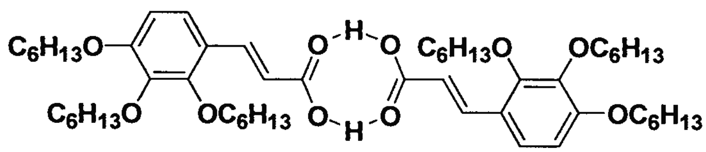

Figure 1.8: Intermolecularly hydrogen bonded 2,3,4-tris-hexyloxy cinnamic acid complex.[4]

Thermotropic liquid crystals can be characterized by the various phase transitions that occur during heating. A liquid crystalline material displays multiple discrete temperature transitions between the isotropic liquid phase and the anisotropic crystalline phase. The temperature at which the transition from anisotropic solid to anisotropic liquid crystalline phase is known as the melting temperature T_m, and the temperature at which the anisotropic liquid changes to an isotropic liquid is known as the clearing temperature T_c.[5] There may also be temperature transitions within the anisotropic liquid crystalline phase between different mesophases, such as a smectic to nematic transition.[5] The phase transitions can be observed using thermal analysis, e.g. differential scanning calorimetry (DSC),[6] and the mesophases identified by polarizing optical microscopy (POM).[4]

Differential scanning calorimetry is a thermal analytical technique used to measure phase changes and temperature transitions. The DSC measures the difference in the amount of energy required to heat a sample versus a reference as a function of temperature.[6] **Figure 1.9** displays a DSC thermogram of a liquid crystalline material showing the phase transition from crystal to liquid crystal (**a**) and from liquid crystal to isotropic liquid (**b**). **Figure 1.10** displays POM images corresponding to the **a**) crystalline phase, **b**) nematic liquid crystalline phase and **c**) isotropic liquid phase.

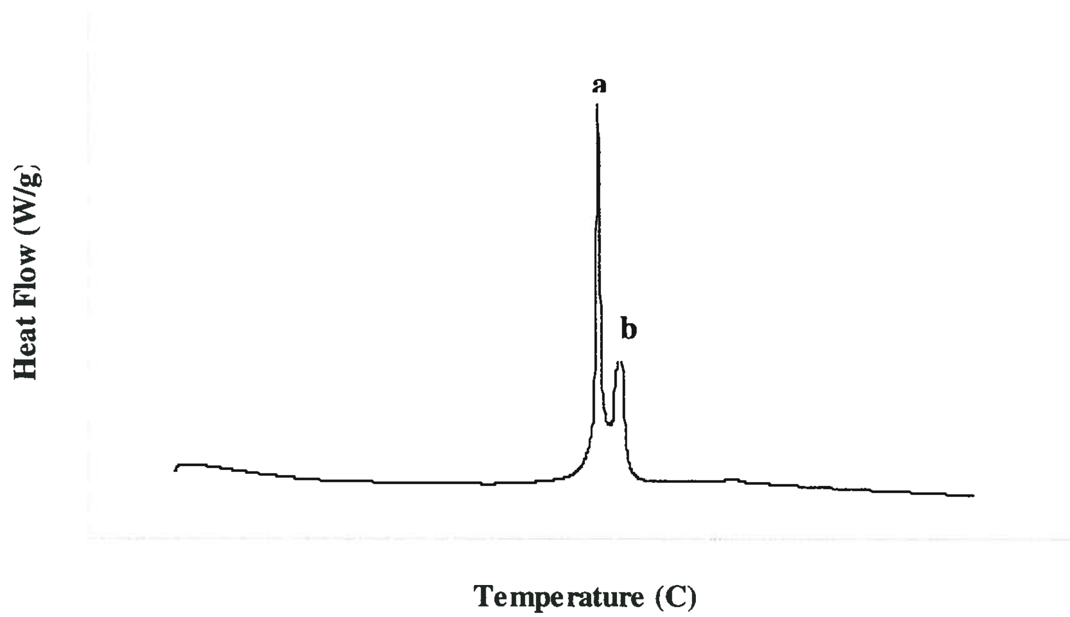

Figure 1.9: DSC thermogram of a liquid crystalline material displaying the **a**) crystal to liquid crystal and **b**) liquid crystal to isotropic liquid phase transitions.

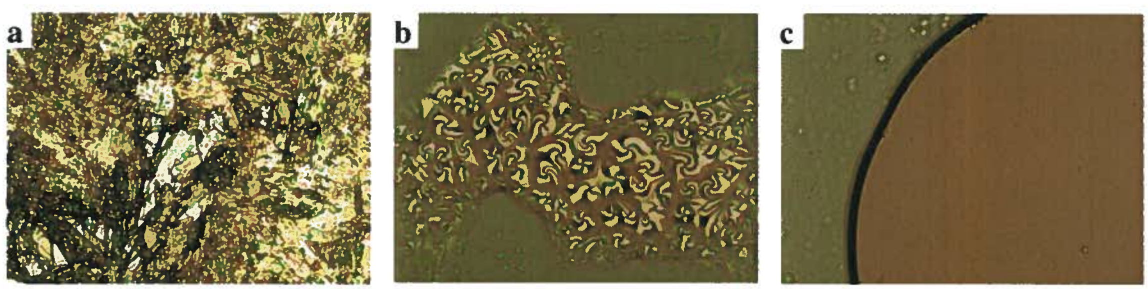

Figure 1.10: POM images representing the **a**) crystalline phase, **b**) nematic liquid crystalline phase and **c**) isotropic liquid phase.

The output of a DSC is a plot of heat flow (in mW or W/g) vs. temperature (in °C or K). As the sample material undergoes a phase change or temperature transition, more or less heat is required to maintain the same temperature as the reference. In the case of exothermic transitions such as crystallization, less heat flow is required, which results in a negative peak. In the case of endothermic transitions such as melting, more heat flow is required, which results in a positive peak. DSC thermograms of thermotropic liquid crystals generally exhibit an endothermic peak corresponding to the transition from the anisotropic crystalline phase to the liquid crystalline phase (the melting point), as well as an endothermic peak corresponding to the transition from the liquid crystalline phase to the isotropic liquid phase (the clearing point).

Crystal to liquid crystal or crystal to isotropic transitions generally have transition enthalpies on the order of 30-50 kJ/mol, while liquid crystal to isotropic transitions have enthalpies on the order of 1-8 kJ/mol. There may also be transitions from one liquid crystalline phase to another liquid crystalline phase, which have transition enthalpies in the same range as liquid crystal to isotropic transitions (i.e. 1-8 kJ/mol).[5]

By contrast, polarizing optical microscopy (POM) is a qualitative analytical technique that allows the physical observation of phase transitions, and thereby facilitates the direct characterization of the different types of liquid crystalline phases, based on characteristic textures and the concept of birefringence.[5]

Birefringence, or double refraction, is an important property of liquid crystalline materials.[5] Birefringent materials have different indices of refraction for light polarized parallel to the director axis and for light polarized perpendicular to the director axis. Essentially, light of different polarization travels at different velocities through the medium. Isotropic liquids, however, do not display birefringence. Liquid crystalline mesophases can thus be characterized by the observation that they flow like a liquid, but are birefringent, or optically anisotropic.[5] **Figure 1.11** displays a POM image of a nematic liquid crystalline material under crossed polars showing birefringence. The dark areas represent regions where the transmission axis of the first polarizer is parallel to the director axis, and no light is transmitted. The light areas, on the other hand, represent regions where the transmission axis isn't aligned with the director axis, and light is transmitted.

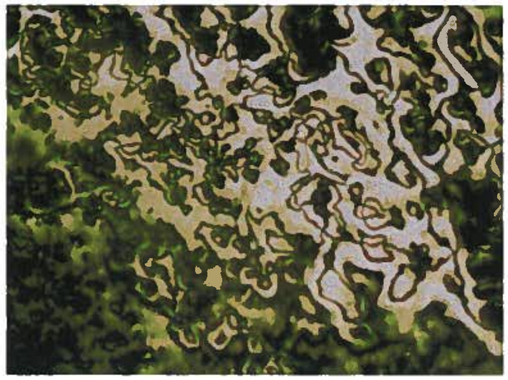

Figure 1.11: POM image of a nematic liquid crystal displaying birefringence.

The typical setup for a polarizing optical microscope consists of a microscope equipped with polarizing filters connected to a hot stage with a temperature controller. Often, a digital camera is connected to preview and capture images.

Employing POM to characterize liquid crystalline phases is still a subjective technique, however, and needs to be done in combination with differential scanning calorimetry and X-ray diffraction (XRD).

1.1.4 Applications of Thermotropic Liquid Crystals

Thermotropic liquid crystals have a wide variety of applications, including temperature sensors,[1,5] light-emitting diodes,[7] photovoltaic solar cells,[8] and most notably displays (LCDs).[9] The applications of liquid crystals take advantage of the novel combination of ordering, electrical, optical and physical properties.

Temperature sensors exploit the fact that chiral nematic liquid crystals can exhibit large colour changes with small changes in temperature. As such, liquid crystals can be used for temperature mapping of both electrical systems and body parts.[1,5]

In the mapping of electrical systems, circuit boards or various electrical components are coated with a liquid crystalline material, which maps the temperature distribution over the entire device.[1] Using this technique, the components which are running at elevated temperatures, or displaying more resistance, are easily observed.

Temperature sensors are also used in the medical industry to map skin temperature. By using liquid crystals, a large area of skin can be mapped to provide the clinician with more information about the skin rather than using a series of point temperatures. This information can be useful in determining circulation and tissue anomalies. A specific example of this is in the detection of tumors, where skin temperature is higher in the vicinity of a tumor.[5]

A second application of thermotropic liquid crystals is in organic light-emitting diodes (OLEDs).[7] LEDs are semiconductor diodes which emit a narrow spectrum of light when electrons fall into a lower energy level. Traditional LEDs are composed of semiconductor materials such as aluminum gallium arsenide and zinc selenide, whereas OLEDs are composed of small molecule crystals, liquid crystals, or polymers. To function as LEDs, the organic molecules must contain conjugated π bonds.[7] OLEDs have an advantage over traditional LEDs because they can be handled in the solution phase. This decreases processing costs as well as increasing the ease of thin film deposition. Thermotropic liquid crystals are attractive materials for OLEDs due to their electronic properties, their inherent ability to self assemble, as well as their hole-transporting properties.[10]

A third application of thermotropic liquid crystals is in photovoltaic solar cells.[8] A photovoltaic solar cell is a device that converts solar energy into electrical energy by means of the photovoltaic effect. Also composed of semiconductors, the advantages of using thermotropic liquid crystals over traditional semiconductors are similar to those for OLEDs.

Probably the most common and well known application of liquid crystals is that of the liquid crystal display (LCD).[9] LCDs are found in digital watches, digital calculators, flat-screen televisions and computer monitors. Materials for use in LCDs have a few basic requirements, namely a twisted nematic or chiral nematic mesophase, the property of birefringence and a mesophase range of appropriate temperatures. In order to be useful in a LCD application, the molecule must be liquid crystalline at temperatures between -10 °C and 60 °C. The material must also be kinetically and thermodynamically stable, and colourless.

1.2 Factors Influencing the Formation of Liquid Crystalline Mesophases

The typical small molecule thermotropic liquid crystal contains a rigid, usually aromatic core with flexible, usually aliphatic side chains. It has been shown that there are a number of factors which influence the formation of liquid crystalline mesophases. Among the factors are molecular shape,[11,12] core size,[13,14] electronics,[13,15] and alkyl side chain length.[16,17] As mesophase formation is largely dependent on π-π stacking interactions,[13] any factor which influences the ability of the molecules to π stack will influence the ability of molecules to self assemble.

1.2.1 Molecular Shape

Molecular shape is very important in the self-assembly of molecules into the liquid crystalline phase. In order for a molecule to exhibit mesogenic behaviour, it must be highly geometrically anisotropic,[11] i.e. rod-shaped or disk-shaped. In addition, molecules which do not display distinct hydrophilic and hydrophobic regions are unlikely to self-assemble into liquid crystalline mesophases. It is generally accepted that thermotropic liquid crystalline molecules are composed of flat, rigid cores (usually aromatic) and multiple long, flexible side chains (usually aliphatic).[12]

1.2.2 Core Size

Core size has been shown to play a role in the ability of molecules to self-assemble. Recently, Williams *et al.*[13] prepared a series of discotic liquid crystals based on a phenanthrene core. They condensed 2,3,6,7-tetra(hexyloxy)phenanthrene-9,10-dione with a series of 1,2-diamines (**Scheme 1.1**) and examined the phase behaviour. Only the compound with the largest core (compound **c**) exhibited a liquid crystalline mesophase, whereas the other two (compounds **a** and **b**) did not. The researchers suggest that dispersion forces are an important contributor to π-stacked structures, and as dispersion forces are favoured by increased surface area, it is intuitive that larger molecules should demonstrate a greater propensity to self-assemble.

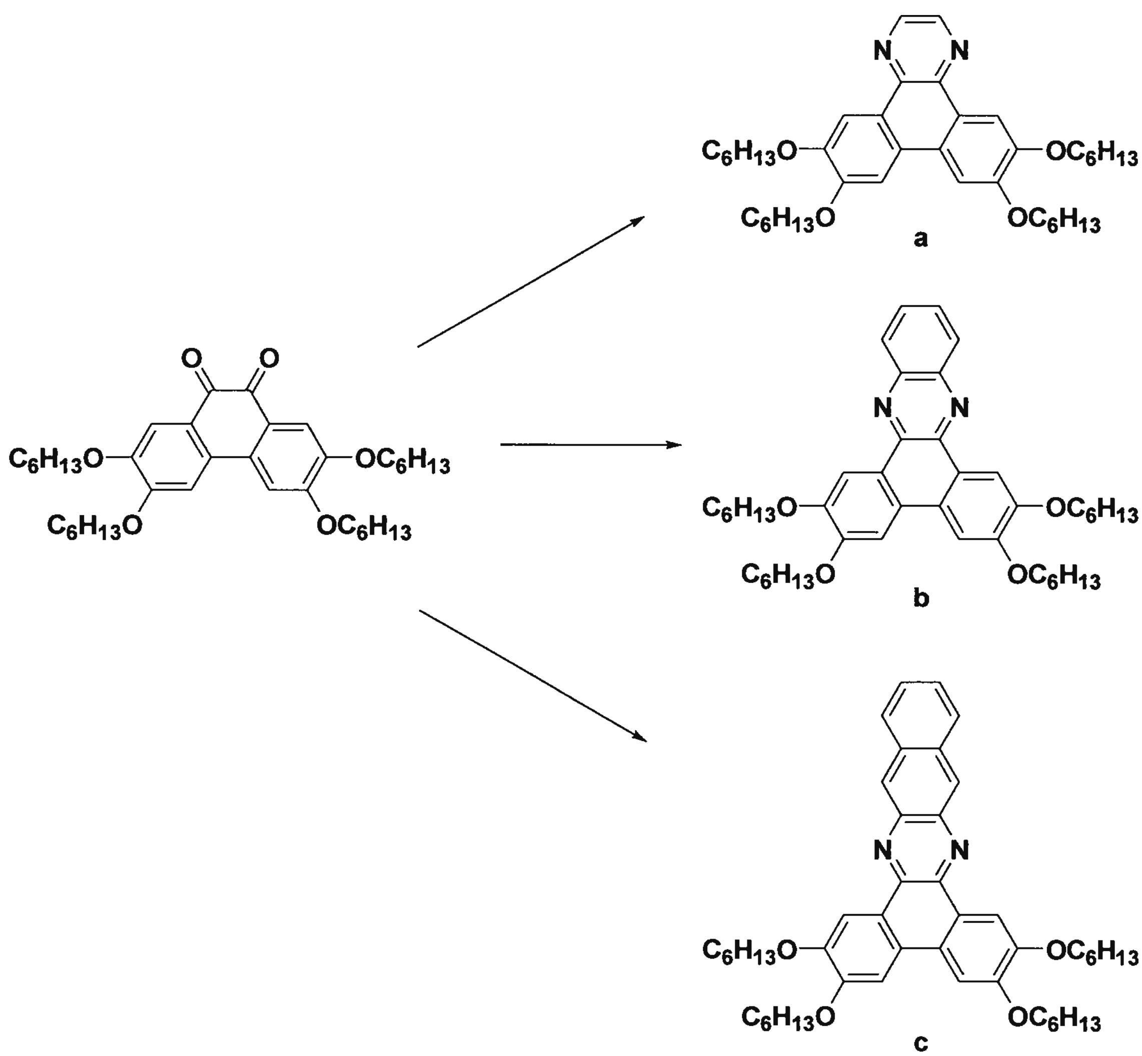

Scheme 1.1: Condensation of phenanthrene-9,10-dione with various diamines.[13]

In another study, Warman *et al.*[14] examined the effect of core size on the clearing temperatures of various discotic liquid crystalline materials. Defining core size as the number of atoms in the aromatic core, the researchers looked at compounds derived from triphenylene (18 carbons) to hexabenzocoronene (42 carbons). They found that the average clearing temperature (from a number of examples) increased with increasing core size. This result concurs with the conclusion of Williams *et al*[13] that a larger core size directly impacts the π-stacking, which in turn stabilizes the mesophase.

1.2.3 Electronics

Electronics also have a strong influence on self-assembly. In the aforementioned study, Williams *et al.*[13] also investigated the effect of electron-withdrawing and electron-donating groups on the phenanthrene derivative (**Figure 1.12**). They found that only the compounds with an electron-withdrawing substituent (X = F, Cl, CO_2CH_3, CN, NO_2) exhibited liquid crystalline mesophases, and those with electron-donating substituents (X = H, CH_3, OCH_3) did not. In the compounds displaying liquid crystallinity, they also found a strong correlation between the clearing temperature of the mesogens and the Hammett parameters σ_m and σ_p for electronegativity (the Hammett parameters σ_m and σ_p are determined by taking the difference in pK_a of benzoic acid and the pK_a of the appropriately *meta* or *para* substituted benzoic acid). The researchers suggest that "π-stacking is favoured by the addition of electron-withdrawing groups, which help to minimize the repulsive interactions between adjacent aromatic π-systems".

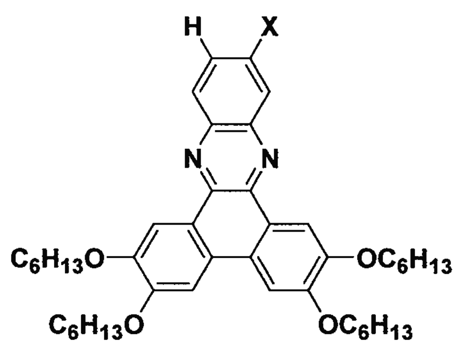

Figure 1.12: The effect of electronics on the mesophase behaviour of phenanthrene derivatives (X = H, CH_3, OCH_3, F, Cl, CO_2CH_3, CN, NO_2).[13]

Further evidence for the importance of electronics on the ability for molecules to self-assemble has been provided by Lai *et al.*[15] In a study similar to that of Williams *et al.*[13]

they prepared a series of benzoxazole derivatives (**Figure 1.13**) and investigated the effects of polar groups on the mesomorphic behaviour. They found that for X = H and OH, no mesophase was observed, for electron-donating groups, EDG (X = CH_3, OCH_3, NMe_2), a nematic mesophase was observed and for electron-withdrawing groups, EWG (X = F, Cl, Br, CF_3, NO_2, CN, CO_2CH_3), a smectic A mesophase was observed. However, unlike the Williams study,[13] no strong correlations between clearing temperatures or mesophase temperature ranges and Hammett parameters for electronegativity were found.

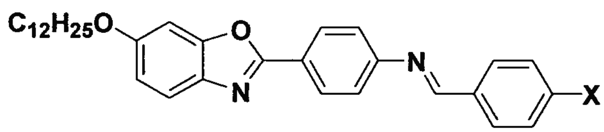

Figure 1.13: The effect of electronics on the mesophase behaviour of benzoxazole derivatives (X = H, OH, CH_3, OCH_3, NMe_2, F, Cl, Br, CF_3, NO_2, CN, CO_2CH_3).[15]

1.2.4 Alkyl Side Chain Length

Finally, alkyl and alkoxy side chain length has also been demonstrated to have a dramatic effect on mesophase formation. In a study by Lai *et al.*,[16] the effect of alkoxy chain length on mesophase behaviour was investigated. The researchers prepared a series of benzoxazole derivatives with a dodecyloxy group on one side and an alkoxy group of varying length on the opposing side (**Figure 1.14**). They found that the compounds with the shorter alkoxy chains (n = 1, 3, 4) exhibited nematic liquid crystalline phases, and the compounds with the longer alkoxy chains (n = 6, 7, 8, 10, 12, 14) exhibited smectic C phases. The mesogens displaying smectic C phases also showed increased clearing temperatures with increasing chain length. This result is intuitive when one considers the degree of ordering in nematic versus smectic mesophases. The nematic mesophase contains only directional order, whereas the smectic mesophase contains both positional and directional order. The increased alkoxy chain length increases the molecular ordering in the mesophase, resulting in more stable mesophases (and higher clearing temperatures).

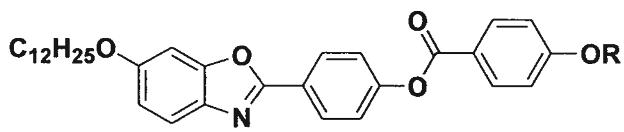

Figure 1.14: The effect of alkyl chain length on the mesophase behaviour of benzoxazole derivatives ($R = (CH_2)_nH$ n = 1, 3, 4, 6, 7, 8, 10, 12, 14).[16]

In a similar study, Engel *et al.*[17] prepared a series of octa-alkyl substituted phthalocyanines (**Figure 1.15**) and varied the alkyl chain lengths from $R = C_5H_{11}$ to $R = C_{10}H_{21}$. The authors report that chain lengths greater than $R = C_4H_9$ are required to induce liquid crystallinity. The researchers also found that both T_m and T_c decreased with increasing alkyl chain length, with the latter decreasing linearly with increasing alkyl chain length.

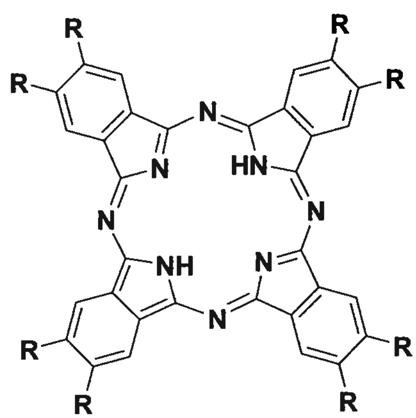

Figure 1.15: The effect of alkyl chain length on the mesophase behaviour of phthalocyanine derivatives ($R = C_5H_{11}$, C_6H_{13}, C_8H_{17}, $C_{10}H_{21}$).[17]

Mesophase formation is strongly dependent on a number of factors that influence self-assembly. Molecular shape, core size, electronics and alkyl side chain length all impact the ordering abilities of mesogenic molecules and are therefore critical in the design of new liquid crystalline materials.

1.3 Benzophenone Derivatives

Based on the established requirements of a rigid core and flexible side chains, it seems that benzophenone bearing one or more alkoxy side chains is a suitable target for liquid crystalline materials. Benzophenones exhibit both the electron-rich core and rigidity necessary for liquid crystallinity. To date, however, no simple liquid crystalline benzophenone derivatives (ie. benzophenones bearing alkyl or alkoxy side chains) have been prepared.

In fact, a study was conducted which predicted that benzophenone was not a suitable core for mesogenic compounds.[18] To illustrate this point, the researchers prepared two benzophenone derivatives (4-pentyl-4'-methoxy-benzophenone (**a**) and 4-heptyloxy-4'-octyl-benzophenone (**b**), **Figure 1.16**), both of which did not exhibit liquid crystalline behaviour. However, two noticeable characteristics of these compounds exist: the lack of symmetry and the fact that one side bears an alkyl chain while the other side bears an alkoxy chain. These minor issues could affect the molecular ordering sufficiently to inhibit mesophase formation.

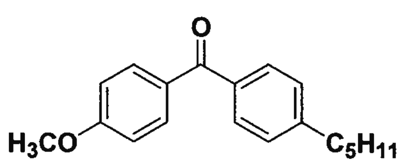

a

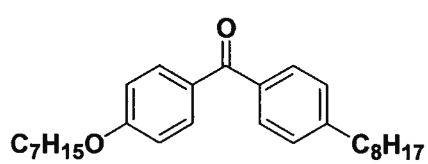

b

Figure 1.16: Non-mesogenic benzophenone derivatives.[18]

Nonetheless, benzophenone derived liquid crystalline materials are not unknown. A series of substituted benzophenone esters of cholesterol have been prepared (**Figure 1.17**), and their mesophase behaviour investigated.[19] All of the compounds prepared exhibit a cholesteric mesophase, and the derivatives with alkyl chains longer than C_6 also exhibited two different unidentified smectic mesophases.

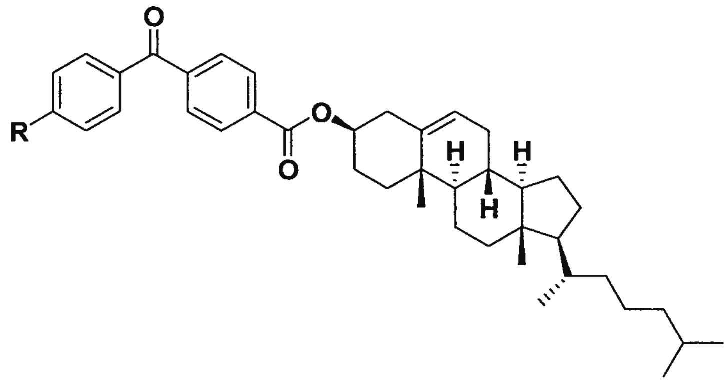

Figure 1.17: Cholesteryl 4-(4-alkylbenzoyl)benzoates (R = $(CH_2)_nH$, n = 0-15).[19]

In addition, a number of polymeric liquid crystals have been prepared which contain the benzophenone moiety.[20] Based on the above evidence; benzophenone appears to be a viable rigid core for the investigation of new liquid crystalline materials provided important factors such as symmetry and alkoxy side chain length are taken into consideration.

1.4 Dibenzylidene Acetone Derivatives

Another potential mesogenic core is 1,5-diphenyl-penta-1,4-dien-3-one (**Figure 1.18**), commonly referred to as dibenzylidene acetone or dba. Dba is structurally analogous to benzophenone in that it simply contains an olefin spacer between the ketone carbonyl and the aromatic rings. Dba is easily prepared from benzaldehyde and acetone,[21] and is a frequently used ligand in organometallic chemistry, typically on palladium.[22]

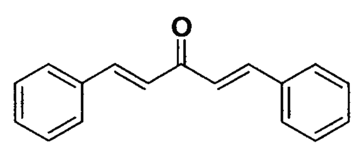

Figure 1.18: Structure of dibenzylidene acetone (dba).

Compounds containing a dba core are attractive synthetic targets for liquid crystalline materials as they contain an electron-rich, rigid conjugated core, and they can be easily prepared with a variety of functional groups in a minimum number of synthetic steps.

1.5 Cinnamaldehyde Derivatives

Cinnamic acid and cinnamaldehyde derivatives are well-known mesogenic substances, with the linear 4-alkoxy cinnamic acids among the first reported.[23] Derivatives with linear alkoxy chains ranging in length from n = 1 to n = 16 have been reported, and all exhibit liquid crystalline behaviour. The derivatives with shorter chains ($n < 9$) exhibit nematic mesophases, while the derivatives with longer chains ($n > 9$) exhibit both smectic and nematic mesophases. The series showed a trend of both decreasing melting and clearing temperatures with increasing alkoxy chain length. As the alkoxy chain length increased ($n > 9$), the temperature range of the smectic mesophase increased, indicating a greater stability of the mesophase. Interestingly, only the E isomers gave rise to liquid crystalline mesophases, whereas the Z isomers melt directly from the crystalline solid to the isotropic liquid. This indicates a strong dependency on molecular shape for mesophase ordering. Moreover, the methyl and ethyl esters do not exhibit liquid crystalline behaviour, indicating an intermolecular hydrogen-bonding effect is likely creating dimers with increased core sizes. In addition, 2,3,4-tris-hexyloxy cinnamic acid is an often-cited example for the sanidic class of mesogenic molecules,[24] with the same intermolecular hydrogen-bonding model proposed (**Figure 1.8**, *vide supra*). Based on these results and the presence of a rigid aromatic core, cinnamaldehyde derivatives with a 1,9-diphenyl-nona-1,3,6,8-tetraen-4-one core represent feasible structures towards liquid crystalline materials.

1.6 Hypothesis

The hypothesis for this research is that benzophenone (**a**), dibenzylidene acetone (**b**) and 1,9-diphenyl-nona-1,3,6,8-tetraen-4-one (**c**) (**Figure 1.19**, *vide supra*) will provide suitable rigid, electron-rich cores for liquid crystalline materials. By varying the alkoxy side chain length and number of side chains, a comprehensive system will be developed that will allow the systematic study of various factors influencing mesophase formation.

In addition, it is hypothesized that three variables studied: alkoxy side chain length, the number of alkoxy side chains, and the core size and conjugation will all strongly impact liquid crystalline mesophase formation.

Based on previous evidence, the length of the alkoxy side chain should have a strong influence on mesophase formation. Longer alkoxy chains should lead to mesophases with broader temperature ranges as well as decreased melting temperatures T_m.

In addition, the number of alkoxy side chains should greatly affect molecular self-assembly. Increased differentiation between the aromatic core and aliphatic side chains should lead to greater organization in the liquid phase which, in turn, should lead to wider liquid crystalline mesophases. Furthermore, the addition of multiple side chains should decrease the alkoxy chain length required to induce liquid crystalline mesophase formation.

Finally, the core size and conjugation should have a dramatic effect on the ability of the molecules to self-assemble into liquid crystalline mesophases. When changing from benzophenone (**a**) to dibenzylidene acetone (**b**) to 1,9-diphenyl-nona-1,3,6,8-tetra-en-5-one (**c**) (**Figure 1.19**), not only is the core size increasing, but so is the number of carbon atoms in the core as well as the extent of conjugation in the core. This increase in core size and conjugation will increase the ability of the molecules to π stack, which should result in a broader mesophase temperature range.

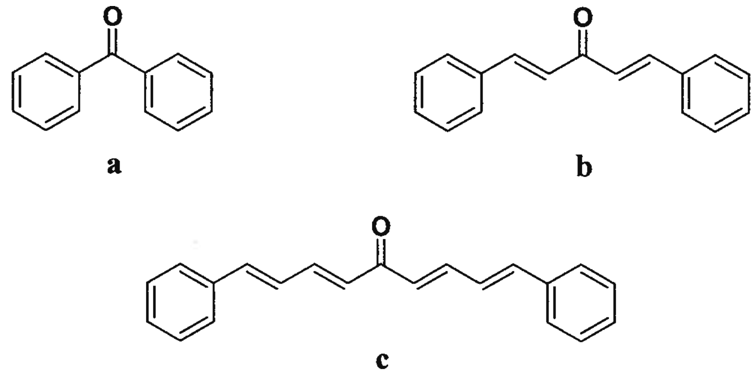

Figure 1.19 Structures of benzophenone (**a**), dibenzylidene-acetone (**b**), and 1,9-diphenyl-nona-1,3,6,8-tetraen-5-one (**c**).

1.7 Thesis Outline

Mesophase formation is strongly dependent on a number of factors that influence self-assembly. Molecular shape, core size, electronics and alkyl side chain length all impact the ordering abilities of mesogenic molecules and are therefore critical in the design of new liquid crystalline materials.

The objective of this research is to investigate how a number of factors influence liquid crystalline mesophase formation. The variables that will be investigated are: 1) the length of the alkoxy side chain on the mesogen, 2) the number of alkoxy side chains on the mesogen, and 3) the size and conjugation of the mesogen's core.

Based on the rigid molecular shape and electron-rich core, benzophenone derivatives are ideal molecules for mesogenic compounds. Appending one or more alkoxy side chains of varying length should create the distinct hydrophobic and hydrophilic regions necessary for liquid crystallinity. In addition, by extending the core and the conjugation by inserting olefin spacers between the ketone and aromatic rings, a large number of potential compounds for liquid crystalline materials can be studied.

A series of C_2-symmetric molecules will be prepared with 1, 2 or 3 linear alkoxy side chains ranging in length from C_6H_{13} to $C_{12}H_{25}$. Three different cores will be examined:

benzophenone (**a**), dibenzylidene-acetone (**b**), and 1,9-diphenyl-nona-1,3,6,8-tetraen-5-one (**c**) (**Figure 1.19**, *vide supra*). These molecules are attractive targets for liquid crystalline materials based on the bioavailability of the precursors, specifically from plant and wood sources.[25] Based on their calamitic rod-like molecular shapes, these compounds have the potential to be useful as materials for liquid crystal displays.

The compounds will be characterized by FTIR, ^{1}H NMR and ^{13}C NMR spectroscopy, and the phase behaviour studied by differential scanning calorimetry. The nature of the mesophases will be investigated using polarizing optical microscopy.

1.7.1 Mono-alkoxy Benzophenone Compounds

The plan for the synthesis of the mono-alkoxy benzophenone derivatives is simply a Williamson ether synthesis[26] starting from commercially available 4,4'-dihydroxy-benzophenone and the appropriate n-alkyl bromide (**Scheme 1.2**).

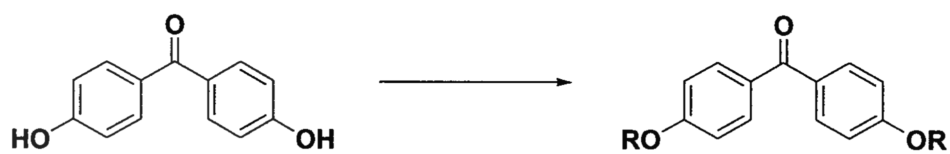

Scheme 1.2: Proposed synthesis of mono-alkoxy benzophenones (R = C_6H_{13}, C_8H_{17}, $C_{10}H_{21}$, $C_{12}H_{25}$).

Of the mono-alkoxy target compounds, the C_8, C_{10} and C_{12} derivatives have been prepared for various materials applications,[27-29] but their mesophase behaviour has not been reported.

1.7.2 Bis-alkoxy Benzophenone Compounds

The proposed synthesis of the bis-alkoxy benzophenone derivatives **2e-h** is a Friedel-Crafts acylation[30] reaction to couple 1,2-alkoxy-benzenes with 3,4-bis-alkoxy-benzoyl chlorides. The 1,2-alkyloxy-benzenes are prepared by a Williamson ether synthesis starting from catechol and the appropriate n-alkyl bromides. The 3,4-bis-alkoxy-benzoyl chlorides are prepared from the corresponding benzoic acids and thionyl chloride. The benzoic acids are produced from protection of 3,4-dihydroxy-benzoic acid as its methyl ester, Williamson ether synthesis to append the alkoxy chains and saponification of the protecting ester (**Scheme 1.3**).

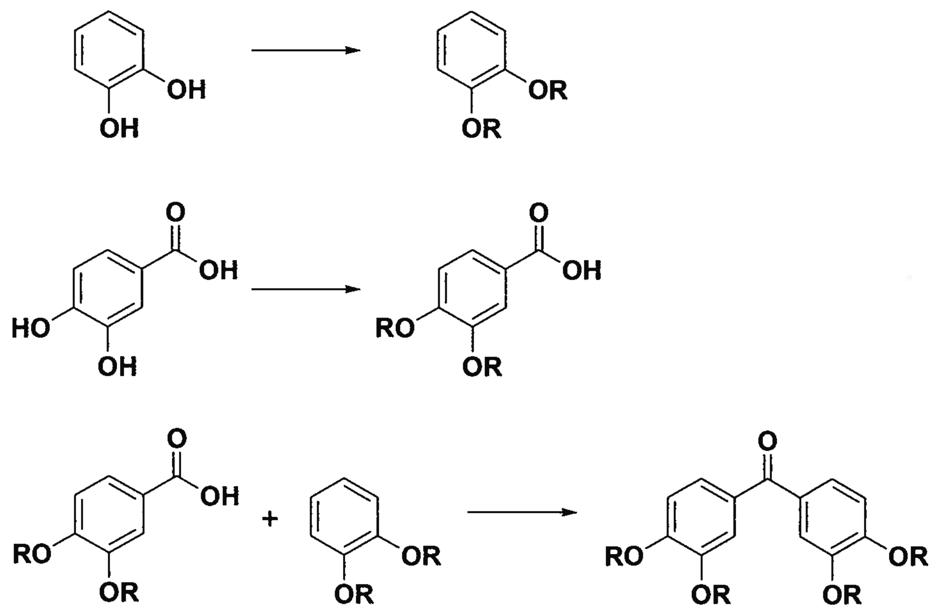

Scheme 1.3: Proposed synthesis of bis-alkoxy benzophenones (R = C_6H_{13}, C_8H_{17}, $C_{10}H_{21}$, $C_{12}H_{25}$).

Of the bis-alkoxy target compounds, the preparation of the C_{12} derivative has been previously reported as a precursor towards self-assembled field effect transistors,[31] however, no data has been reported on its mesophase behaviour.

1.7.3 Tris-alkoxy Benzophenone Compounds

The strategy for the synthesis of the tris-alkoxy benzophenone derivatives is analogous to that for the bis-alkoxy benzophenone derivatives. For these compounds gallic acid (3,4,5-

trihydroxy benzoic acid, **Figure 1.20a**) and pyrogallol (1,2,3-trihydroxy benzene, **Figure 1.20b**) will be used instead of 3,4-dihydroxy benzoic acid and catechol, respectively.

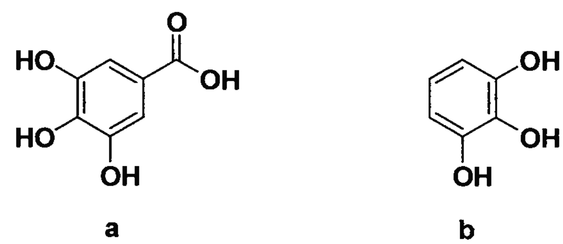

Figure 1.20: Gallic acid (**a**) and pyrogallol (**b**).

1.7.4 Dibenzylidene Acetone Compounds

The synthetic plan for the construction of the dibenzylidene acetone derivatives is a bidirectional aldol condensation between two equivalents of the appropriate alkoxy-substituted benzaldehydes and one equivalent of acetone.[32] The alkoxy-substituted benzaldehydes are prepared by Williamson ether synthesis starting from 4-hydroxy-benzaldehyde, 3,4-dihydroxy-benzaldehyde or 3,4,5-trihydroxy-benzaldehyde and the appropriate alkyl bromide (**Scheme 1.4**).

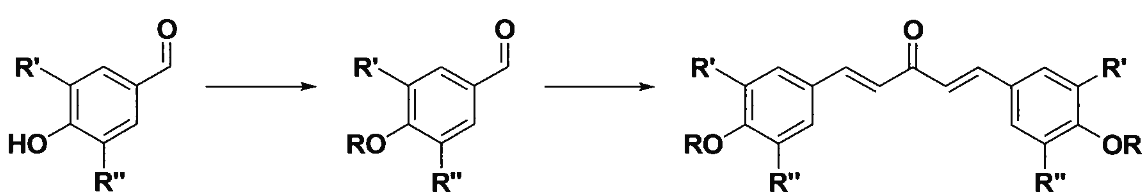

Scheme 1.4: Proposed synthesis of the dibenzylidene acetones (R = C_6H_{13}, C_8H_{17}, $C_{10}H_{21}$, $C_{12}H_{25}$; R' = H, OR; R" = H, OR).

1.7.5 Mono-alkoxy 1,9-Diphenyl-nona-1,3,6,8-tetraen-5-one Compounds

The plan for the synthesis of the mono-alkoxy 1,9-diphenyl-nona-1,3,6,8-tetraen-5-one compounds is to start with commercially available *p*-coumaric acid (3-(4-hydroxy-phenyl)-2-propenoic acid). The acid is first protected as an ester, and the alkoxy chain installed using Williamson conditions. Then partial reduction of the ester to the aldehyde followed by a bidirectional aldol condensation with acetone affords the target molecules in 4 synthetic steps (**Scheme 1.5**).

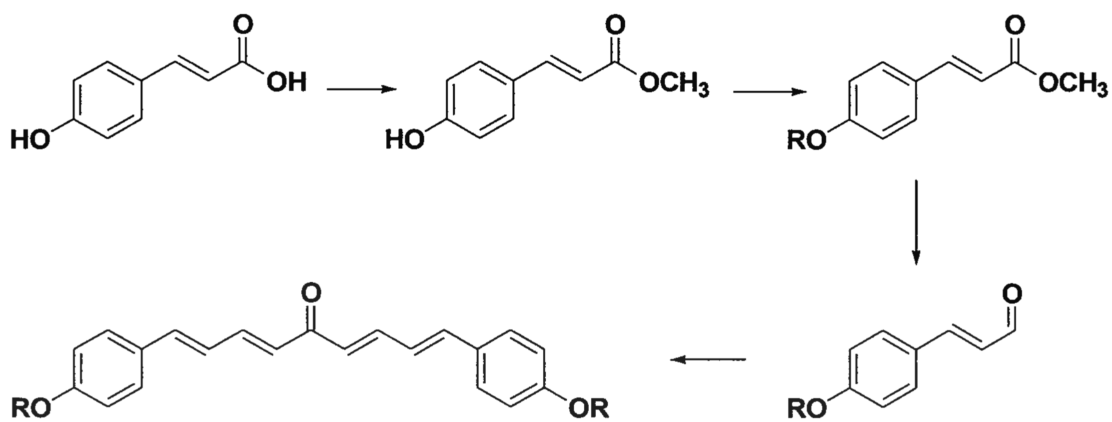

Scheme 1.5: Proposed synthesis of the mono-alkoxy 1,9-diphenyl-nona-1,3,6,8-tetraen-5-ones (R = C_6H_{13}, C_8H_{17}, $C_{10}H_{21}$, $C_{12}H_{25}$).

1.7.6 Bis-alkoxy and Tris-alkoxy 1,9-Diphenyl-nona-1,3,6,8-tetraen-5-one Compounds

The proposed synthesis of the bis-alkoxy and tris-alkoxy 1,9-diphenyl-nona-1,3,6,8-tetraen-5-one compounds is analogous to that of the mono-alkoxy analogues, but instead of starting with *p*-coumaric acid, the substituted cinnamic acid esters would be achieved via a Knoevenagel condensation[33] between 3,4-bis-alkoxy or 3,4,5-tris-alkoxy benzaldehydes and mono-ethyl malonic acid (**Scheme 1.6**). The same sequence of partial reduction to the aldehyde followed by a bidirectional aldol condensation as above (**Scheme 1.5**) leads to the analogous bis-alkoxy and tris-alkoxy 1,9-diphenyl-nona-1,3,6,8-tetraen-5-ones.

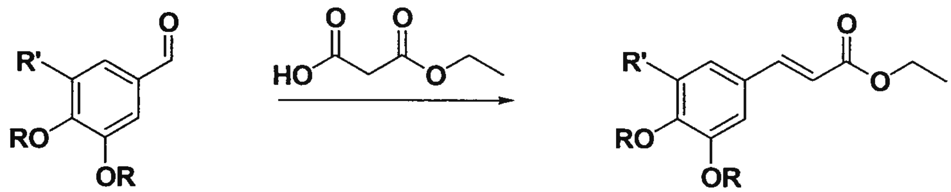

Scheme 1.6: Knoevenagel condensation towards substituted cinnamic acid ethyl esters (R = C_6H_{13}, C_8H_{17}, $C_{10}H_{21}$, $C_{12}H_{25}$; R' = H, OR).

Chapter 2

Materials and Methods

2.1 General

All chemicals were purchased from Sigma-Aldrich (Oakville, ON), and used without further purification, unless otherwise noted. Solvents were purchased from Fisher Scientific (Nepean, ON), and used as received. Tetrahydrofuran (THF) and 1,4-dioxane were distilled from sodium benzophenone (benzophenone ketyl radical). Dichloromethane (CH_2Cl_2) was distilled from P_2O_5 for Friedel-Crafts acylation reactions. All reactions were monitored by TLC, which was performed on Merck Alumafoil 60 Å TLC plates with UV254 indicator (Fisher Scientific). Flash Chromatography was performed on 60 Å 70-230 mesh Silica Gel purchased from Fisher Scientific. Preparative Thin Layer Chromatography (PTLC) was performed on 20 cm Analtech Uniplate 2000 μm preparative TLC plates with UV254 indicator (Fisher Scientific).

^1H and ^{13}C nuclear magnetic resonance (NMR) spectra were recorded using a 300 MHz Bruker Avance Ultrashield NMR Spectrometer (300.13 and 75.03 MHz, respectively) at concentrations of approximately 10 mg/mL and referenced to $CDCl_3$ (7.28 ppm) or deutero-acetone (2.05 ppm). The number of scans used was 16 for ^1H NMR and 3072 for ^{13}C NMR. Signal assignments were made with the assistance of ACDLabs NMR prediction software. ^{13}C signals containing multiple nuclei were estimated by integration.[34] Fourier Transform Infrared (FTIR) spectra were recorded on a Perkin Elmer Spectrum One FTIR spectrometer by thin film deposition on ZnSe plates. Melting points were determined using a Mel-Temp melting point apparatus, and are uncorrected.

Differential scanning calorimetry (DSC) was carried out on a TA Instruments DSC Q1000. All experiments were run with 1-3 mg of sample in aluminum hermetic pans at heating rates of 10 °C/min. and cooling rates of 5 °C/min. unless otherwise noted. The samples were initially analysed at temperatures between -90 °C and 250 °C, with subsequent runs performed only in the temperature range displaying phase transitions.

Polarizing optical microscopy (POM) was performed on an Olympus BX41 Microscope equipped with an Instec HCS402 Hot Stage and STC200 Temperature Controller. All samples that exhibited multiple endothermic transitions on heating or multiple exothermic transitions on cooling by DSC analysis were characterized by POM. In a typical experiment 5-10 mg of sample was heated to the clearing point which was estimated by DSC and cooled slowly to observe the liquid crystalline textures. POM images were captured with a Lumenera Infinity1 Digital Camera, and were recorded and analyzed using InfinityCapture software.

2.2 Synthesis

2.2.1 Synthesis of Benzophenone Compounds

2.2.1.1 Mono-alkoxy Benzophenone Compounds

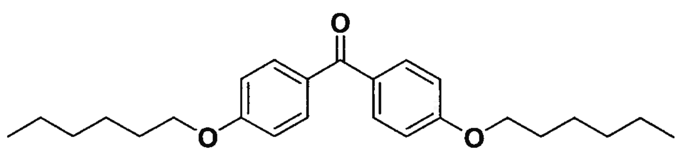

2a

bis-(4-hexyloxy-phenyl)-methanone (**2a**) To a solution of 4,4′-dihydroxybenzophenone (**1**, 0.50 g, 2.33 mmol) and potassium carbonate (1.29 g, 9.34 mmol) in acetone (25 mL) was added 1-bromohexane (1.54 g, 9.34 mmol) dropwise. The resulting mixture was allowed to reflux for 48 hours, then poured into water and extracted with CH_2Cl_2 (2 × 100 mL). The combined organic layers were washed with water (300 mL), dried over $MgSO_4$, filtered and the solvent removed *in vacuo*. Recrystallization from acetone afforded **2a** (0.86 g, 97 %) as white crystals, mp. 102-105 °C; FTIR (thin film, cm^{-1}): 2955, 2938, 2863, 1636, 1604, 1256, 853, 764; ^{1}H NMR (300 MHz, $CDCl_3$) δ 7.79 (d, J = 8.66 Hz, 4H); 6.96 (d, J = 8.66 Hz, 4H); 4.05 (t, J = 6.58 Hz, 4H); 1.84 (quin, J = 6.58 Hz, 4H); 1.56-1.31 (m, 12H); 0.94 (t, J = 6.58 Hz, 6H); ^{13}C NMR (300 MHz, $CDCl_3$) δ 194.5; 162.4; 132.2; 130.6; 113.9; 68.2; 31.6; 29.1; 25.7; 22.6; 14.0.

bis-(4-octyloxy-phenyl)-methanone (**2b**) was prepared in a method analogous to **2a** (0.78 g, 77 %); mp. 96-99 °C; FTIR (thin film, cm^{-1}): 2920, 2851, 1634, 1604, 1254, 854, 763; ^{1}H NMR (300 MHz, $CDCl_3$) δ 7.79 (d, J = 8.88 Hz, 4H); 6.96 (d, J = 8.88 Hz, 4H); 4.05 (t, J = 6.58 Hz, 4H); 1.84 (quin, J = 6.58 Hz, 4H); 1.56-1.23 (m, 20H); 0.91 (t, J = 6.58 Hz, 6H); ^{13}C NMR (300 MHz, $CDCl_3$) δ 194.5; 162.4; 132.2; 130.6; 113.9; 68.3; 31.8; 29.3; 29.2; 29.1; 26.0; 22.7; 14.1.

bis-(4-decyloxy-phenyl)-methanone (**2c**) was prepared in a method analogous to **2a** (0.69 g, 75 %); mp. 99-101 °C [lit.[28] 100 °C]; FTIR (thin film, cm^{-1}): 2956, 2924, 2859, 1635, 1604, 1255, 852, 764; ^{1}H NMR (300 MHz, $CDCl_3$) δ 7.79 (d, J = 8.66 Hz, 4H); 6.96 (d, J = 8.66 Hz, 4H); 4.05 (t, J = 6.58 Hz, 4H); 1.84 (quin, J = 6.58 Hz, 4H); 1.54-1.22 (m, 28H); 0.91 (t, J = 6.58 Hz, 6H); ^{13}C NMR (300 MHz, $CDCl_3$) δ 194.5; 162.4; 132.2; 130.6; 113.9; 68.3; 31.9; 29.6; 29.5; 29.4; 29.3; 29.1; 26.0; 22.7; 14.1.

bis-(4-dodecyloxy-phenyl)-methanone (**2d**) was prepared in a method analogous to **2a** (0.82 g, 64 %); mp. 102-105 °C; FTIR (thin film, cm^{-1}): 2921, 2851, 1635, 1603, 1257, 763; ^{1}H NMR (300 MHz, $CDCl_3$) δ 7.79 (d, J = 8.66 Hz, 4H); 6.96 (d, J = 8.66 Hz, 4H); 4.05 (t, J = 6.58 Hz, 4H); 1.84 (quin, J = 6.58 Hz, 4H); 1.55-1.22 (m, 36H); 0.90 (t, J = 6.58 Hz, 6H); ^{13}C NMR (300 MHz, $CDCl_3$) δ 194.5; 162.4; 132.2; 130.6; 113.9; 68.3; 31.9; 29.7; 29.64; 29.59; 29.56; 29.4; 29.3; 29.1; 26.0; 22.7; 14.1.

2.2.1.2 Bis-alkoxy Benzophenone Compounds

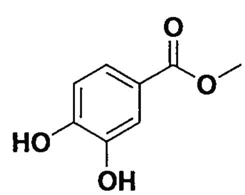

4

methyl-3,4-dihydroxy-benzoate (**4**). To a solution of 3,4-dihydroxy-benzoic acid (**3**, 5.00 g, 32.44 mmol) in methanol (150 mL) was added concentrated sulfuric acid (2.70 mL, 48.66 mmol). The mixture was heated to reflux for 18 hours, and cooled to room temperature. Solvent was removed *in vacuo*, and ethyl acetate (100 mL) was added. The solution was washed with H_2O (150 mL) and the organic layer separated. The aqueous layer was extracted with EtOAc (100 mL) and the combined organics were washed with H_2O (2 × 200 mL), dried over $MgSO_4$, filtered and the solvent removed *in vacuo*. The resulting solid was washed with $CHCl_3$, filtered and air dried to afford **4** as an off-white solid, (4.41 g, 82 %); mp. 133-137 °C [lit.[35] 134-135 °C]; FTIR (thin film, cm^{-1}): 3465, 3270, 1677, 1613, 1444, 1293, 1240, 1185, 1092, 984, 764; ^{1}H NMR (300 MHz, acetone-d^6) δ 8.45 (bs, 2H); 7.51 (d, J = 1.97 Hz, 1H); 7.45 (dd, J_1 = 8.33 Hz, J_2 = 1.97 Hz, 1H); 6.91 (d, J = 8.33 Hz, 1H); 3.82 (s, 3H); ^{13}C NMR (300 MHz, acetone-d^6) δ 166.1; 149.9; 144.7; 122.4; 122.0; 116.3; 114.9; 51.0.

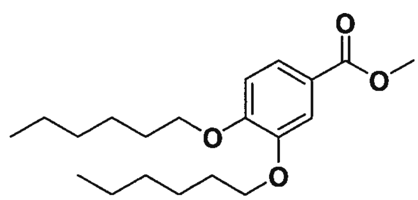

5e

methyl-3,4-bis-hexyloxy-benzoate (5e). To a solution of methyl-3,4-dihydroxy-benzoate (**4,** 1.50 g, 8.92 mmol) in acetone (100 mL) was added 1-bromohexane (5.89 g, 35.68 mmol). The resulting mixture was heated to reflux for 72 hours. The reaction mixture was cooled to room temperature, poured into H_2O (100 mL), extracted with $CHCl_3$ (2 × 150 mL), washed with H_2O (2 × 200 mL), dried over $MgSO_4$, filtered and the solvent removed *in vacuo*. Vacuum distillation (28-35 °C, 0.30 mmHg) to remove excess 1-bromohexane afforded **5e** (2.89 g, 96 %) as a clear, light yellow oil. FTIR (thin film, cm^{-1}): 2932, 1720, 1514, 1291, 1270, 1215, 1133; ^{1}H NMR (300 MHz, $CDCl_3$) δ 7.65 (dd, J_1 = 8.44 Hz, J_2 = 1.97 Hz, 1H); 7.56 (d, J = 1.97 Hz, 1H); 6.88 (d, J = 8.44 Hz, 1H); 4.064 (t, J = 6.58 Hz, 2H); 4.057 (t, J = 6.58 Hz, 2H); 3.90 (s, 3H); 1.86 (quin, J = 6.58 Hz, 2H); 1.85 (quin, J = 6.58 Hz, 2H); 1.56-1.28 (m, 12H); 0.93 (t, J = 6.58 Hz, 6H); ^{13}C NMR (300 MHz, $CDCl_3$) δ 167.0; 153.2; 148.5; 123.5; 122.4; 114.2; 111.9; 69.3; 69.0; 51.9; 31.57; 31.55; 29.1; 29.0; 25.7; 25.6; 22.59; 22.58; 14.01; 13.99.

methyl-3,4-bis-octyloxy-benzoate (5f) was prepared in a method analogous to **5e** to afford a clear, yellow oil that crystallized on standing, (3.50 g, 100 %); mp. 33-35 °C [lit.[36] 108-110 °C]; FTIR (thin film, cm^{-1}): 2927, 1721, 1291, 1270, 1215; ^1H NMR (300 MHz, $CDCl_3$) δ 7.65 (dd, J_1 = 8.44 Hz, J_2 = 1.97 Hz, 1H); 7.56 (d, J = 1.97 Hz, 1H); 6.88 (d, J = 8.44 Hz, 1H); 4.06 (t, J = 6.58 Hz, 2H); 4.05 (t, J = 6.58 Hz, 2H); 3.90 (s, 3H); 1.86 (quin, J = 6.58 Hz, 2H); 1.85 (quin, J = 6.58 Hz, 2H); 1.56-1.24 (m, 20H); 0.91 (t, J = 6.58 Hz, 6H); ^{13}C NMR (300 MHz, $CDCl_3$) δ 167.0; 153.2; 148.5; 123.5; 122.4; 114.3; 111.9; 69.3; 69.0; 51.9; 31.82; 31.80; 29.36; 29.34; 29.26; 29.24; 29.18; 29.08; 26.01; 25.97; 22.7 (2C); 14.1 (2C).

methyl-3,4-bis-decyloxy-benzoate (**5g**) was prepared in a method analogous to **5e** with the following exceptions: recrystallized from MeOH to afford **5g** as a white powder (3.88 g, 97 %); mp. 44-47 °C [lit.[37] 73-74 °C]; FTIR (thin film, cm^{-1}): 2926, 2855, 1721, 1290, 1270, 1214; ^1H NMR (300 MHz, $CDCl_3$) δ 7.65 (dd, J_1 = 8.44 Hz, J_2 = 1.64 Hz, 1H); 7.55 (d, J = 1.64 Hz, 1H); 6.88 (d, J = 8.44 Hz, 1H); 4.06 (t, J = 6.58 Hz, 2H); 4.05 (t, J = 6.58 Hz, 2H); 3.90 (s, 3H); 1.92-1.79 (m, 4H); 1.55-1.21 (m, 28H); 0.90 (t, J = 6.58 Hz, 6H); ^{13}C NMR (300 MHz, $CDCl_3$) δ 167.0; 153.2; 148.5; 123.5; 122.4; 114.3; 111.9; 69.3; 69.0; 51.9; 31.9 (2C); 29.62; 29.60; 29.58; 29.56; 29.40; 29.38; 29.3 (2C); 29.2; 29.1; 26.01; 25.97; 22.7 (2C); 14.1 (2C).

methyl-3,4-bis-dodecyloxy-benzoate (**5h**) was prepared in a method analogous to **5g** (2.90 g, 97 %); mp. 51-54 °C [lit.[38] 54-55 °C]; FTIR (thin film, cm^{-1}): 2925, 2854, 1721, 1291, 1270, 1214; ^1H NMR (300 MHz, $CDCl_3$) δ 7.65 (dd, J_1 = 8.44 Hz, J_2 = 1.86 Hz, 1H); 7.56 (d, J = 1.86 Hz, 1H); 6.88 (d, J = 8.44 Hz, 1H); 4.06 (t, J = 6.58 Hz, 2H); 4.05 (t, J = 6.58 Hz, 2H); 3.90 (s, 3H); 1.92-1.78 (m, 4H); 1.56-1.21 (m, 36H); 0.90 (t, J = 6.58 Hz, 6H); ^{13}C NMR (300 MHz, $CDCl_3$) δ 167.0; 153.2; 148.5; 123.5; 122.4; 114.3; 111.9; 69.3; 69.0; 51.9; 31.9 (2C); 29.70 (2C); 29.66 (2C); 29.63 (2C); 29.61 (2C); 29.42; 29.37 (3C); 29.2; 29.1; 26.01; 25.98; 22.7 (2C); 14.1 (2C).

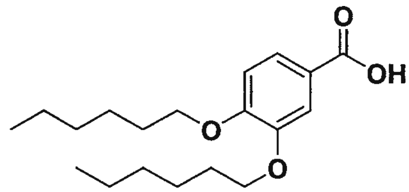

6e

3,4-bis-hexyloxy-benzoic acid (6e). To a solution of methyl-3,4-bis-hexyloxy-benzoate (**5e,** 2.50 g, 7.43 mmol) in methanol (75 mL) was added aqueous (15 mL) KOH (0.83 g, 14.86 mmol) dropwise. The resulting solution was heated to reflux for 24 hours, poured into 2.0 M HCl (100 mL), and extracted with CH_2Cl_2 (3 × 75 mL). The combined organic layers were washed with H_2O (2 × 200 mL), dried over $MgSO_4$, filtered and the solvent removed *in vacuo*. The crude product was washed with MeOH/ H_2O (1:1), filtered and air dried to afford **6e** as a white powder (2.26 g, 94 %); mp. 124-127 °C [lit.[39] 128 °C]; FTIR (thin film, cm^{-1}): 2955, 2929, 2857, 1669, 1586, 1441, 1272, 1228, 1141; ^{1}H NMR (300 MHz, $CDCl_3$) δ 7.75 (dd, J_1 = 8.44 Hz, J_2 = 1.86 Hz, 1H); 7.61 (d, J = 1.86 Hz, 1H); 6.91 (d, J = 8.44 Hz, 1H); 4.09 (t, J = 6.58 Hz, 2H); 4.07 (t, J = 6.58 Hz, 2H); 1.93-1.80 (m, 4H); 1.57-1.27 (m, 12H); 0.93 (t, J = 6.58 Hz, 6H); ^{13}C NMR (300 MHz, $CDCl_3$) δ 171.7; 154.0; 148.6; 124.5; 121.3; 114.5; 111.9; 69.3; 69.0; 31.57; 31.54; 29.1; 29.0; 25.67; 25.63; 22.60; 22.58; 14.0 (2C).

3,4-bis-octyloxy-benzoic acid (6f) was prepared in a method analogous to **6e**. (3.26 g, 99 %); mp. 119-121 °C [lit.[40] 125 °C]; FTIR (thin film, cm^{-1}): 2924, 2851, 1668, 1273, 1227, 1140; ^{1}H NMR (300 MHz, $CDCl_3$) δ 7.74 (dd, J_1 = 8.44 Hz, J_2 = 1.97 Hz, 1H); 7.61 (d, J = 1.97 Hz, 1H); 6.91 (d, J = 8.44 Hz, 1H); 4.09 (t, J = 6.58 Hz, 2H); 4.07 (t, J = 6.58 Hz, 2H); 1.93-1.80 (m, 4H); 1.56-1.24 (m, 20H); 0.91 (t, J = 6.58 Hz, 6H); ^{13}C NMR (300 MHz, $CDCl_3$) δ 171.4; 154.0; 148.6; 124.5; 121.3; 114.6; 111.9; 69.3; 69.0; 31.82; 31.80; 29.36; 29.33; 29.27; 29.25; 29.1; 29.0; 26.00; 25.96; 22.7 (2C); 14.1 (2C).

3,4-bis-decyloxy-benzoic acid (6g) was prepared in a method analogous to **6e** (2.55 g, 88 %); mp. 118-120 °C [lit.[41] 123 °C]; FTIR (thin film, cm^{-1}): 2847, 1666, 1275, 1224, 1139; ^{1}H NMR (300 MHz, $CDCl_3$) δ 7.74 (dd, J_1 = 8.44 Hz, J_2 = 1.64 Hz, 1H); 7.61 (d, J

= 1.64 Hz, 1H); 6.91 (d, J = 8.44 Hz, 1H); 4.09 (t, J = 6.58 Hz, 2H); 4.07 (t, J = 6.58 Hz, 2H); 1.93-1.80 (m, 4H); 1.57-1.23 (m, 28H); 0.91 (t, J = 6.58 Hz, 6H); ^{13}C NMR (300 MHz, $CDCl_3$) δ 171.4; 154.0; 148.6; 124.5; 121.3; 114.6; 111.9; 69.3; 69.0; 31.9 (2C); 29.62; 29.60; 29.58; 29.56; 29.40; 29.37; 29.35 (2C); 29.1; 29.0; 26.00; 25.96; 22.7 (2C); 14.1 (2C).

3,4-bis-dodecyloxy-benzoic acid (6h) was prepared in a method analogous to **6e** (2.43 g, 91 %); mp. 117-119 °C [lit.[42] 120 °C]; FTIR (thin film, cm^{-1}): 2916, 2848, 1668, 1277, 1225; ^{1}H NMR (300 MHz, $CDCl_3$) δ 7.74 (dd, J_1 = 8.44 Hz, J_2 = 1.97 Hz, 1H); 7.62 (d, J = 1.97 Hz, 1H); 6.91 (d, J = 8.44 Hz, 1H); 4.09 (t, J = 6.58 Hz, 2H); 4.07 (t, J = 6.58 Hz, 2H); 1.92-1.79 (m, 4H); 1.57-1.24 (m, 36H); 0.91 (t, J = 6.58 Hz, 6H); ^{13}C NMR (300 MHz, $CDCl_3$) δ 170.7; 154.1; 148.8; 124.5; 121.4; 114.6; 112.2; 69.5; 69.2; 31.9 (2C); 29.63 (2C); 29.60 (2C); 29.57 (2C); 29.55 (2C); 29.35; 29.32; 29.29 (2C); 29.2; 29.1; 25.98; 25.95; 22.6 (2C); 14.1 (2C).

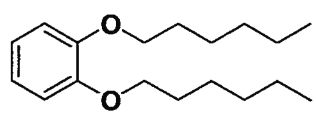

8e

1,2-bis-hexyloxy-benzene (8e). To a solution of catechol (**7**, 2.00 g, 18.16 mmol) and potassium carbonate (10.04 g, 72.65 mmol) in acetone (100 mL) was added 1-bromohexane (12.00 g, 72.65 mmol) dropwise. The resulting mixture was refluxed for 48 hours, then poured into water and extracted with CH_2Cl_2 (2 × 100 mL). The combined organic layers were washed with water (300 mL), dried over $MgSO_4$, filtered and the solvent removed *in vacuo*. Excess 1-bromohexane was removed by vacuum distillation (30 °C, 0.20 mmHg) and flash chromatography (CH_2Cl_2) afforded **8e** (4.92 g 97 %) as a clear, colourless oil. FTIR (thin film, cm^{-1}): 2931, 2860, 1502, 1469, 1254, 1223, 739; ^{1}H NMR (300 MHz, $CDCl_3$) δ 6.91 (s, 4H); 4.01 (t, J = 6.58 Hz, 4H); 1.84 (quin, J = 6.58 Hz, 4H); 1.56-1.29 (m, 12H); 0.93 (t, J = 6.58 Hz, 6H); ^{13}C NMR (300 MHz, $CDCl_3$) δ 149.3; 121.0; 114.2; 69.3; 31.6; 29.3; 25.7; 22.6; 14.0.

1,2-bis-octyloxy-benzene (8f) was prepared in a method analogous to **8e** (8.73 g, 96 %); FTIR (thin film, cm^{-1}): 2927, 2856, 1503, 1469, 1254, 1223; ^{1}H NMR (300 MHz, $CDCl_3$) δ 6.91 (s, 4H); 4.01 (t, *J* = 6.58 Hz, 4H); 1.84 (quin, *J* = 6.58 Hz, 4H); 1.55-1.24 (m, 20H); 0.91 (t, *J* = 6.58 Hz, 6H); ^{13}C NMR (300 MHz, $CDCl_3$) δ 149.3; 121.0; 114.2; 69.3; 31.8; 29.41; 29.37; 29.3; 26.1; 22.7; 14.1.

1,2-bis-decyloxy-benzene (8g) was prepared in a method analogous to **8e** with the following exception: instead of flash chromatography, the material was recrystallized from hexanes to afford **8g** as a white powder, 2.66 g, 94 %; mp. 38-40 °C [lit.[43] 41 °C]; FTIR (thin film, cm^{-1}): 2925, 2854, 1504, 1468, 1554, 1254, 1223, 738; ^{1}H NMR (300 MHz, $CDCl_3$) δ 6.91 (s, 4H); 4.01 (t, *J* = 6.58 Hz, 4H); 1.83 (quin, *J* = 6.58 Hz, 4H); 1.54-1.22 (m, 28H); 0.90 (t, *J* = 6.58 Hz, 6H); ^{13}C NMR (300 MHz, $CDCl_3$) δ 149.3; 121.0; 114.2; 69.3; 31.9; 29.64; 29.59; 29.5; 29.4 (4C); 26.1; 22.7; 14.1.

1,2-bis-dodecyloxy-benzene (8h) was prepared in a method analogous to **8g** (4.05 g, 100 %); mp. 44-46 °C [lit.[44] 46 °C]; FTIR (thin film, cm^{-1}): 2921, 2851, 1507, 1467, 1258, 1223, 1123; ^{1}H NMR (300 MHz, $CDCl_3$) δ 6.91 (s, 4H); 4.01 (t, *J* = 6.58 Hz, 4H); 1.83 (quin, *J* = 6.58 Hz, 4H); 1.54-1.23 (m, 36H); 0.90 (t, *J* = 6.58 Hz, 6H); ^{13}C NMR (300 MHz, $CDCl_3$) δ 149.3; 121.0; 114.2; 69.3; 31.9; 29.71; 29.66; 29.65 (2C); 29.45; 29.37 (2C); 26.1; 22.7; 14.1.

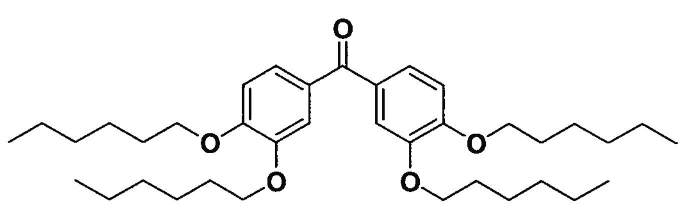

9e

bis-(3,4-bis-hexyloxy-phenyl)-methanone (9e). To a solution of 3,4-bis-hexyloxy-benzoic acid (**6e**, g, 1.06 mmol) and diethylamine (0.50 mL) in CH_2Cl_2 (15 mL) was added $SOCl_2$ (5 mL) dropwise. The solution was heated to reflux for 1.5 hours. Excess $SOCl_2$, pyridine, and CH_2Cl_2 were removed *in vacuo*, and the resultant acid chloride was added as a solution in CH_2Cl_2 (15 mL) to a mixture of $AlCl_3$ (0.14 g, 1.06 mmol) and 1,2-bis-hexyloxy-benzene (**8e**, 0.29 g, 1.06 mmol) in CH_2Cl_2 (15 mL) at 0°C under N_2. The reaction mixture was stirred for 1.0 hour, warmed to room temperature and stirred overnight. The greenish reaction mixture was quenched with H_2O (10 mL), poured into 2.0M HCl (200 mL) and extracted with CH_2Cl_2 (3 × 75 mL). The combined organic layers were washed with water (200 mL) and brine (200 mL), dried over $MgSO_4$, filtered and the solvent removed *in vacuo*. Recrystallization from acetone afforded **9e** (0.37 g, 60 %) as a white powder; mp. 44-48 °C; FTIR (thin film, cm^{-1}): 2931, 2860, 1649, 1595, 1513, 1428, 1266, 1135, 1017, 760; ^1H NMR (300 MHz, $CDCl_3$) δ 7.42 (d, J = 1.86 Hz, 2H); 7.37 (dd, J_1 = 8.33 Hz, J_2 = 1.86 Hz, 2H); 6.90 (d, J = 8.33 Hz, 2H); 4.09 (t, J = 6.58 Hz, 4H); 4.06 (t, J = 6.58 Hz, 4H); 1.93-1.79 (m, 8H); 1.58-1.30 (m, 24H); 0.93 (t, J = 6.58 Hz, 6H); 0.92 (t, J = 6.58 Hz, 6H); ^{13}C NMR (300 MHz, $CDCl_3$) δ 194.6; 152.8; 148.7; 130.7; 124.7; 114.7; 111.5; 69.3; 69.1; 31.58; 31.56; 29.2; 29.1; 25.69; 25.66; 22.6 (4C); 14.0 (4C).

bis-(3,4-bis-octyloxy-phenyl)-methanone (9f) was prepared in a method analogous to **9e** (0.58 g, 67 %); mp. 55-58 °C; FTIR (thin film, cm^{-1}): 2926, 2856, 1647, 1595, 1513, 1468, 1428, 1266, 1135, 1026, 760; ^1H NMR (300 MHz, $CDCl_3$) δ 7.42 (d, J = 1.86 Hz, 2H); 7.37 (dd, J_1 = 8.33 Hz, J_2 = 1.86 Hz, 2H); 6.90 (d, J = 8.33 Hz, 2H); 4.09 (t, J = 6.58 Hz, 4H); 4.06 (t, J = 6.58 Hz, 4H); 1.93-1.79 (m, 8H); 1.55-1.23 (m, 40H); 0.95-0.86 (m, 12H); ^{13}C NMR (300 MHz, $CDCl_3$) δ 194.6; 152.8; 148.7; 130.7; 124.7; 114.7; 111.5; 69.3; 69.1; 31. 8 (4C); 29.37; 29.35; 29.27 (4C); 29.2; 29.1; 26.02; 26.00; 22.7 (4C); 14.1 (4C).

bis-(3,4-bis-decyloxy-phenyl)-methanone (9g) was prepared in a method analogous to **9e** (0.60 g, 69 %); mp. 63-66 °C; FTIR (thin film, cm^{-1}): 2924, 2854, 1650, 1595, 1514, 1467, 1428, 1338, 1265, 1199, 1126; ^1H NMR (300 MHz, $CDCl_3$) δ 7.42 (d, J = 1.86 Hz, 2H); 7.37 (dd, J_1 = 8.33 Hz, J_2 = 1.86 Hz, 2H); 6.90 (d, J = 8.33 Hz, 2H); 4.09 (t, J = 6.58 Hz, 4H); 4.06 (t, J = 6.58 Hz, 4H); 1.93-1.79 (m, 8H); 1.56-1.22 (m, 56H); 0.90 (t, J = 6.58 Hz, 12H); ^{13}C NMR (300 MHz, $CDCl_3$) δ 194.6; 152.8; 148.7; 130.7; 124.7; 114.7;

111.5; 69.3; 69.1; 31.9 (4C); 29.62 (4C); 29.58 (4C); 29.42; 29.40; 29.35 (4C); 29.2; 29.1; 26.03; 26.00; 22.7 (4C); 14.1 (4C).

bis-(3,4-bis-dodecyloxy-phenyl)-methanone (9h) was prepared in a method analogous to **9e** (0.52 g, 56 %); mp. 70-73 °C; FTIR (thin film, cm^{-1}): 2923, 2853, 1647, 1595, 1513, 1467, 1429, 1266, 1124, 1031, 759; ^1H NMR (300 MHz, $CDCl_3$) δ 7.42 (d, J = 1.86 Hz, 2H); 7.36 (dd, J_1 = 8.33 Hz, J_2 = 1.86 Hz, 2H); 6.90 (d, J = 8.33 Hz, 2H); 4.09 (t, J = 6.58 Hz, 4H); 4.06 (t, J = 6.58 Hz, 4H); 1.93-1.79 (m, 8H); 1.55-1.20 (m, 75H); 0.90 (t, J = 6.58 Hz, 12H); ^{13}C NMR (300 MHz, $CDCl_3$) δ 194.6; 152.8; 148.7; 130.7; 124.7; 114.7; 111.5; 69.3; 69.1; 31.9 (4C); 29.70 (4C); 29.66 (4C); 29.6 (8C); 29.43; 29.40; 29.37 (4C); 29.2; 29.1; 26.04; 26.01; 22.7 (4C); 14.1 (4C).

2.2.1.3 Tris-alkoxy Benzophenone Compounds

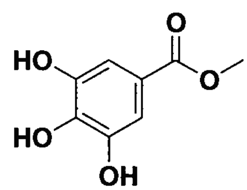

11

methyl-3,4,5-tris-hydroxy benzoate (11). To a solution of gallic acid (**10**, 10.0 g, 58.78 mmol) in MeOH (200 mL) was added concentrated sulfuric acid (3.92 mL, 70.54 mmol) dropwise, and the reaction mixture was heated to reflux for 24 hours. The solution was cooled to room temperature, poured into H_2O (200 mL), extracted with EtOAc (2 × 200 mL), washed with H_2O (2 × 200 mL), dried over $MgSO_4$, filtered and the solvent removed *in vacuo* to afford **11** (7.50 g, 69 %) as a white powder; mp. 198-202 °C [lit.[45] 202 °C]; ^1H NMR (300 MHz, acetone-d^6) δ 8.23 (bs, 2H); 8.04 (bs, 1H); 7.13 (s, 2H); 3.80 (s, 3H); ^{13}C NMR (300 MHz, $CDCl_3$) δ 166.4; 145.2; 137.9; 120.9; 108.9; 51.0.

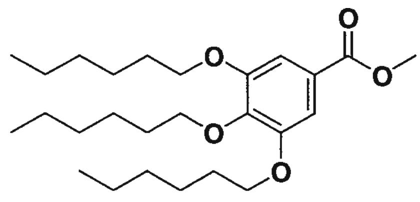

12i

methyl-3,4,5-tris-hexyloxy-benzoate (12i) To a solution of methyl-3,4,5-tris-hydroxy benzoate (**11**, 4.00 g, 21.7 mmol) and potassium carbonate (18.0 g, 130.3 mmol) in acetone (150 mL) was added 1-bromohexane (21.5 g, 130.3 mmol) dropwise. The resulting solution was heated to 80°C and stirred for 24 hours. The mixture was poured into water (200 mL) and extracted with CH_2Cl_2 (2 × 150 mL). The combined organic layers were washed with water (2 × 200 mL), dried over $MgSO_4$, filtered and the solvent removed *in vacuo*. The resulting liquid was vacuum distilled (22-30 °C, 0.18 mmHg) to remove excess 1-bromohexane. Flash chromatography (CH_2Cl_2) afforded **12i** as a clear yellow oil (8.50 g, 90 %); ^{1}H NMR (300 MHz, $CDCl_3$) δ 7.27 (s, 2H); 4.04 (t, J = 6.58 Hz, 2H); 4.03 (t, J = 6.58 Hz, 4H); 3.91 (s, 3H); 1.89-1.71 (m, 6H); 1.56-1.30 (m, 18H); 0.96-0.89 (m, 9H); ^{13}C NMR (300 MHz, $CDCl_3$) δ166.9; 152.8; 142.4; 124.7; 108.0; 73.5; 69.2; 52.1; 31.7; 31.5; 30.3; 29.3; 25.74; 25.69; 22.7; 22.6; 14.1; 14.0.

methyl-3,4,5-tris-octyloxy-benzoate (12j) was prepared in a method analogous to **12i** (4.00 g, 94 %); ^{1}H NMR (300 MHz, $CDCl_3$) δ ^{13}C NMR (300 MHz, $CDCl_3$) δ 7.27 (s, 2H); 4.04 (t, J = 6.58 Hz, 2H); 4.03 (t, J = 6.58 Hz, 4H); 3.91 (s, 3H); 1.88-1.71 (m, 6H); 1.55-1.25 (m, 30H); 0.94-0.87 (m, 9H); ^{13}C NMR (300 MHz, $CDCl_3$) δ166.9; 152.8; 142.4; 124.7; 108.0; 73.5; 69.2; 52.1; 31.9; 31.8; 30.3; 29.5; 29.34; 29.31; 29.28; 26.08; 26.04; 22.69; 22.67; 14.1.

methyl-3,4,5-tris-decyloxy-benzoate (12k) was prepared in a method analogous to **12i** with the following exception: instead of flash chromatography, the material was recrystallized from MeOH to afford **12k** as a white powder (9.32 g, 95 %); ^{1}H NMR (300 MHz, $CDCl_3$) δ 7.27 (s, 2H); 4.04 (t, J = 6.58 Hz, 2H); 4.03 (t, J = 6.58 Hz, 4H); 3.91 (s, 3H); 1.88-1.71 (m, 6H); 1.55-1.43 (m, 6H); 1.42-1.23 (m, 36H); 0.90 (t, J = 6.58 Hz, 9H); [13]C NMR (300 MHz, $CDCl_3$) δ167.0; 152.8; 124.6; 108.03; 107.99; 73.5; 69.2 (2C); 52.1; 31.9 (3C); 30.3; 29.72; 29.66; 29.63 (3C); 29.58 (4C); 29.39 (4C); 29.34 (2C); 29.31 (2C); 26.08; 26.05; 22.7 (3C); 14.1 (3C).

methyl-3,4,5-tris-dodecyloxy-benzoate (12l) was prepared in a method analogous to **12k** (5.70 g, 100 %); mp 40-42°C; [1]H NMR (300 MHz, $CDCl_3$) δ 7.27 (s, 2H); 4.07-3.99 (m, 6H); 3.91 (s, 3H); 1.90-1.71 (m, 54H); 0.90 (t, J = 6.80 Hz, 9H); [13]C NMR (300 MHz, $CDCl_3$) δ 166.9; 152.8; 142.4; 124.6; 108.0; 73.5; 69.2; 52.1; 31.9 (3C); 30.3; 29.73 (3C); 29.70 (3C); 26.66 (2C); 29.64 (4C); 29.57; 29.40 (3C); 29.37 (2C); 29.3 (2C); 26.09; 26.06; 22.7 (3C); 14.1 (3C).

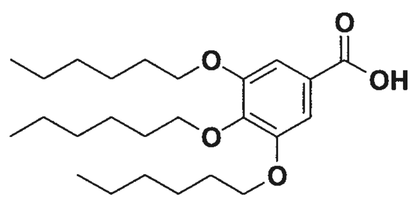

13i

3,4,5-tris-hexyloxy-benzoic acid (13i) To a solution of methyl-3,4,5-tris-hexyloxy-benzoate (**12i,** 4.00g, 9.16 mmol) in MeOH (100 mL) was added aqueous (10 mL) potassium hydroxide (1.03 g, 18.32 mmol). The resulting solution was allowed to reflux for 24 hours. The mixture was cooled to room temperature, poured into 2.0 M HCl (100 mL) and extracted with CH_2Cl_2 (3 × 75 mL). The combined organic layers were washed with H_2O (2 × 200 mL), dried over $MgSO_4$, filtered and the solvent removed *in vacuo*. Recrystallization from MeOH/H_2O (1:1) afforded **13i** as a white fluffy powder (3.60 g, 93 %); mp. 38-40 °C [lit.[28] 39 °C]; [1]H NMR (300 MHz, $CDCl_3$) δ 7.34 (s, 2H); 4.07 (t, J = 6.58 Hz, 2H); 4.05 (t, J = 6.58 Hz, 4H); 1.85 (quin., J = 6.58 Hz, 4H); 1.77 (quin., J = 6.58 Hz, 2H); 1.57-1.29 (m, 18H); 0.97-0.88 (m, 9H); [13]C NMR (300 MHz, $CDCl_3$) δ 171.3; 152.9; 143.2; 123.5; 108.6; 73.6; 69.2; 31.7; 31.5; 30.3; 29.2; 25.74; 25.69; 22.67; 22.62; 14.07; 14.02.

3,4,5-tris-octyloxy-benzoic acid (13j) was prepared in a method analogous to **13i** (1.95 g, 93 %); mp 52-54 °C [lit.[46] 53 °C]; ^{1}H NMR (300 MHz, $CDCl_3$) δ 7.34 (s, 2H); 4.07 (t, *J* = 6.58 Hz, 2H); 4.05 (t, *J* = 6.58 Hz, 4H); 1.84 (quin., *J* = 6.58 Hz, 4H); 1.77 (quin., *J* = 6.58 Hz, 2H); 1.56-1.25 (m, 30H); 0.91 (t, *J* = 6.58 Hz, 9H); ^{13}C NMR (300 MHz, $CDCl_3$) δ 171.4; 152.9; 143.2; 123.5; 108.6; 73.6; 69.2; 31.9; 31.8; 30.3; 29.5; 29.34 (3C); 29.28 (4C); 26.1; 26.0; 22.69; 22.67; 14.1 (3C).

3,4,5-tris-decyloxy-benzoic acid (13k) was prepared in a method analogous to **13i** (1.56 g, 85 %); mp 47-50 °C [lit.[28] 51 °C]; ^{1}H NMR (300 MHz, $CDCl_3$) δ 7.34 (s, 2H); 4.07 (t, *J* = 6.58 Hz, 2H); 4.05 (t, *J* = 6.58 Hz, 4H); 1.84 (quin., *J* = 6.58 Hz, 4H); 1.77 (quin., *J* = 6.58 Hz, 2H); 1.57-1.22 (m, 42H); 0.90 (t, *J* = 6.58 Hz, 9H); ^{13}C NMR (300 MHz, $CDCl_3$) δ 171.4; 152.9; 143.2; 123.5; 108.6; 73.6; 69.2; 31.94; 31.92; 30.3; 29.73; 29.67; 29.64; 29.58; 29.56; 29.40 (3C); 29.35; 29.29; 26.1; 26.0; 22.7 (3C); 14.1 (3C).

3,4,5-tris-dodecyloxy-benzoic acid (13l) was prepared in a method analogous to **13i** (2.53 g, 94 %); mp 48-51 °C [lit.[46] 56 °C]; ^{1}H NMR (300 MHz, $CDCl_3$) δ 7.35 (s, 2H); 4.07 (t, *J* = 6.58 Hz, 2H); 4.05 (t, *J* = 6.58 Hz, 4H); 1.90-1.70 (m, 6H); 1.56-1.19 (m, 54H); 0.90 (t, *J* = 6.58 Hz, 9H); ^{13}C NMR (300 MHz, $CDCl_3$) δ 171.6; 152.9; 143.2; 123.6; 108.6; 73.6; 69.2; 31.9 (3C); 30.3; 29.73 (3C); 29.70 (3C); 29.66 (2C); 29.64 (5C); 29.56; 29.40 (2C); 29.37 (2C); 29.3 (2C); 26.08; 26.05; 22.7 (3C); 14.1 (3C).

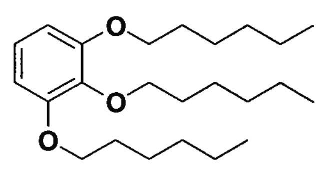

15i

1,2,3-tris-hexyloxy-benzene (15i). To a solution of 1,2,3-trihydroxy benzene (**14**, 2.00 g, 15.86 mmol) and potassium carbonate (13.15 g, 95.16 mmol) in acetone (150 mL) was added 1-bromohexane (11.78 g, mmol) dropwise. The reaction mixture was heated to reflux for 120 hours, poured into water and extracted with CH_2Cl_2 (2 × 100 mL). The combined organic layers were washed with water (2 × 200 mL), dried over $MgSO_4$, filtered and the solvent removed *in vacuo*. The crude product was vacuum distilled (24-30 °C, 0.22 mmHg) to remove excess 1-bromohexane, and flash chromatography (CH_2Cl_2) afforded **15i** (5.20 g, 87 %) as a clear, yellow oil; ^1H NMR (300 MHz, $CDCl_3$) δ 6.93 (t, J = 8.33 Hz, 1H); 6.56 (d, J = 8.33 Hz, 2H); 3.99 (t, J = 6.58 Hz, 4H); 3.97 (t, J = 6.58 Hz, 2H); 1.87-1.71 (m, 6H); 1.56-1.27 (m, 18H); 0.93 (t, J = 6.58 Hz, 9H); ^{13}C NMR (300 MHz, $CDCl_3$) δ 153.4; 138.5; 123.1; 106.8; 73.4; 69.1; 31.8; 31.6; 30.3; 29.4; 25.8 (3C); 22.7; 22.6; 14.1; 14.0.

1,2,3-tris-octyloxy-benzene (15j) was prepared in a method analogous to **15i** (5.70 g, 78 %); ^1H NMR (300 MHz, $CDCl_3$) δ 6.92 (t, J = 8.22 Hz, 1H); 6.56 (d, J = 8.22 Hz, 2H); 3.99 (t, J = 6.58 Hz, 4H); 3.97 (t, J = 6.58 Hz, 2H); 1.81 (quin., J = 6.58 Hz, 4H); 1.77 (quin., J = 6.58 Hz, 2H); 1.55-1.22 (m, 30H); 0.91 (t, J = 6.58 Hz, 9H); ^{13}C NMR (300 MHz, $CDCl_3$) δ 153.4; 138.5; 123.1; 106.8; 73.4; 69.1; 31.9; 31.8; 30.4; 29.6; 29.5; 29.4 (3C); 29.3; 26.14; 26.12; 22.70; 22.67; 14.1 (3C).

1,2,3-tris-decyloxy-benzene (15k) was prepared in a method analogous to **15i** with the following exception: recrystallized from hexanes to afford **15k** (6.40 g, 74 %) as a white powder; mp. 42-46 °C; ^1H NMR (300 MHz, $CDCl_3$) δ 6.92 (t, J = 8.33 Hz, 1H); 6.56 (d, J = 8.33 Hz, 2H); 3.99 (t, J = 6.58 Hz, 4H); 3.96 (t, J = 6.58 Hz, 2H); 1.87-1.71 (m, 6H); 1.57-1.19 (m, 42H); 0.90 (t, J = 6.58 Hz, 9H); ^{13}C NMR (300 MHz, $CDCl_3$) δ 153.4; 138.5; 123.1; 106.8; 73.4; 69.1; 31.95; 31.92; 30.4; 29.8; 29.69; 29.65 (3C); 29.60; 29.45; 29.43 (3C); 29.40; 29.35; 26.2; 26.1; 22.7 (3C); 14.1 (3C).

1,2,3-tris-dodecyloxy-benzene (15l) was prepared in a method analogous to **15k** (3.76 g 75 %); mp. 53-55 °C; ^1H NMR (300 MHz, $CDCl_3$) δ 6.92 (t, J = 8.22 Hz, 1H); 6.56 (d, J = 8.22 Hz, 2H); 3.99 (t, J = 6.58 Hz, 4H); 3.96 (t, J = 6.58 Hz, 2H); 1.87-1.71 (m, 6H); 1.55-1.21 (m, 54H); 0.91 (t, J = 6.58 Hz, 9H); ^{13}C NMR (300 MHz, $CDCl_3$) δ 153.4; 138.5; 123.1; 106.8; 73.4; 69.1; 31.9 (3C); 30.4; 29.8 (3C); 29.71 (3C); 29.66 (7C); 29.44 (4C); 29.40; 29.37 (2C); 26.2; 26.1; 22.7 (3C); 14.1 (3C).

2.2.2 Synthesis of Dibenzylidene Acetone Compounds

2.2.2.1 Mono-alkoxy Dibenzylidene Acetone Compounds

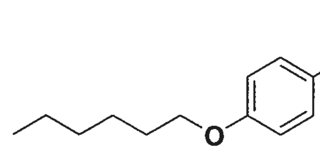

18a

4-hexyloxy-benzaldehyde (18a). To a solution of 4-hydroxybenzaldehyde (**17**, 5.0 g, 40.9 mmol) and potassium carbonate (11.3 g, 81.9 mmol) in DMF (150 mL) was added 1-bromohexane (15.8 g, 81.9 mmol) as a solution in DMF (30 mL). The resulting solution was stirred at room temperature for 20 hours. The reaction mixture was poured into water (200 mL), extracted with CH_2Cl_2 (2 × 150 mL), washed with water (2 × 200 mL), dried over $MgSO_4$, filtered and the solvent removed *in vacuo*. Residual DMF and excess 1-bromohexane were removed by vacuum distillation (24-31 °C, 0.20 mmHg) to afford **18a** (8.4 g, 100 %) as a clear, orange liquid; FTIR (thin film, cm^{-1}): 2932, 2859, 1692, 1602, 1577, 1510, 1312, 1257, 1161, 832; ^1H NMR (300 MHz, $CDCl_3$) δ 9.90 (s, 1H); 7.84 (d, J = 8.44 Hz, 2H); 7.01 (d, J = 8.44 Hz, 2H); 4.06 (t, J = 6.58 Hz, 2H); 1.83 (quin, J = 6.58 Hz, 2H); 1.56-1.29 (m, 6H); 0.93 (t, J = 6.58 Hz, 3H); ^{13}C NMR (300 MHz, $CDCl_3$) δ 190.8; 164.3; 132.0; 129.8; 114.8; 68.4; 31.5; 29.0; 25.6; 22.6; 14.0.

4-octyloxy-benzaldehyde (18b) was prepared in a method analogous to **18a** (14.3g, 93 %); FTIR (thin film, cm^{-1}): 2928, 2856, 1697, 1602, 1578, 1509, 1312, 1259, 1215, 1160, 832; ^1H NMR (300 MHz, $CDCl_3$) δ 9.90 (s, 1H); 7.84 (d, J = 8.55 Hz, 2H); 7.01 (d, J = 8.55 Hz, 2H); 4.06 (t, J = 6.58 Hz, 2H); 1.83 (quin, J = 6.58 Hz, 2H); 1.55-1.25 (m, 10H); 0.91 (t, J = 6.58 Hz, 3H); ^{13}C NMR (300 MHz, $CDCl_3$) δ 190.8; 164.3; 132.0; 129.8; 114.8; 68.4; 31.8; 29.3; 29.2; 29.1; 26.0; 22.6; 14.1.

4-decyloxy-benzaldehyde (18c) was prepared in a method analogous to **18a** (10.4 g, 97 %); FTIR (thin film, cm^{-1}): 2926, 2855, 1696, 1603, 1578, 1510, 1312, 1259, 1216, 1160, 833; ^{1}H NMR (300 MHz, $CDCl_3$) δ 9.89 (s, 1H); 7.84 (d, J = 8.22 Hz, 2H); 7.00 (d, J = 8.22 Hz, 2H); 4.05 (t, J = 6.58 Hz, 2H); 1.83 (quin, J = 6.58 Hz, 2H); 1.55-1.20 (m, 14H); 0.90 (t, J = 6.58 Hz, 3H); ^{13}C NMR (300 MHz, $CDCl_3$) δ 190.8; 164.3; 132.0; 129.8; 114.7; 68.4; 31.9; 29.5 (2C); 29.34; 29.31; 29.1; 26.0; 22.7; 14.1.

4-dodecyloxy-benzaldehyde (18d) was prepared in a method analogous to **18a** (2.1 g, 86 %); FTIR (thin film, cm^{-1}): 2926, 2854, 1698, 1602, 1578, 1509, 1311, 1259, 1215, 1160, 832; ^{1}H NMR (300 MHz, $CDCl_3$) δ 9.90 (s, 1H); 7.84 (d, J = 8.33 Hz, 2H); 7.01 (d, J = 8.33 Hz, 2H); 4.06 (t, J = 6.58 Hz, 2H); 1.83 (quin, J = 6.58 Hz, 2H); 1.55-1.23 (m, 14H); 0.90 (t, J = 6.58 Hz, 3H); ^{13}C NMR (300 MHz, $CDCl_3$) δ 190.8; 164.3; 132.0; 129.8; 114.8; 68.4; 31.9; 29.65; 29.64; 29.58; 29.55; 29.3 (2C); 29.1; 26.0; 22.7; 14.1.

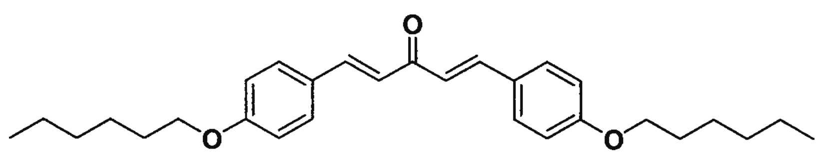

19a

1,5-bis-(4-hexyloxy-phenyl)-penta-1,4-dien-3-one (19a). A solution of sodium hydroxide (0.39 g, 9.75 mmol) in water (5 mL) and ethanol (5 mL) was cooled to 0°C for 30 minutes. To this solution was added reagent grade acetone (0.11g, 1.95 mmol) and 4-hexyloxy-benzaldehyde (**18a,** 0.80 g, 3.90 mmol). The resulting solution was stirred at room temperature for 72 hours, poured into water (200mL), extracted with CH_2Cl_2 (2 × 150 mL) and washed with water (250 mL). The organic layers were combined, dried over $MgSO_4$, filtered and the solvent removed *in vacuo.* The crude material was recrystallized from EtOH to afford **19a** as yellow crystals (0.49 g, 58 %); mp. 97-100 °C; FTIR (thin film, cm^{-1}): 2934, 2869, 1651, 1599, 1574, 1512, 1177, 1030, 983; ^{1}H NMR (300MHz, $CDCl_3$) δ 7.72 (d, J = 15.78 Hz, 2H); 7.58 (d, J = 8.66 Hz, 4H); 6.97 (d, J = 15.78 Hz, 2H); 6.94 (d, J = 8.66 Hz, 4H); 4.02 (t, J = 6.58 Hz, 4H); 1.82 (quin, J = 6.58 Hz, 4H); 1.54-1.29 (m, 12H); 0.93 (t, J = 6.58 Hz, 6H); ^{13}C NMR (300MHz, $CDCl_3$) δ 188.9; 161.2; 142.7; 130.1; 127.4; 123.4; 114.9; 68.2; 31.6; 29.1; 25.7; 22.6; 14.0.

1,5-bis-(4-octyloxy-phenyl)-penta-1,4-dien-3-one (19b) was prepared in a method analogous to **19a** (1.61 g, 70 %); mp. 92-98 °C; FTIR (thin film, cm^{-1}): 2928, 2853, 1646, 1591, 1571, 1511, 1257, 1175, 984; ^{1}H NMR (300MHz, $CDCl_3$) δ 7.72 (d, *J* = 16.0 Hz, 2H); 7.58 (d, *J* = 8.66 Hz, 4H); 6.97 (d, *J* = 16.0 Hz, 2H); 6.94 (d, *J* = 8.66 Hz, 4H); 4.02 (t, *J* = 6.58 Hz, 4H); 1.82 (quin, *J* = 6.58 Hz, 4H); 1.54-1.26 (m, 20H); 0.91 (t, *J* = 6.58 Hz, 6H); ^{13}C NMR (300MHz, $CDCl_3$) δ 188.9; 161.2; 142.7; 130.1; 127.4; 123.4; 114.9; 68.2; 31.8; 29.3; 29.2; 29.2; 26.0; 22.7; 14.1.

1,5-bis-(4-decyloxy-phenyl)-penta-1,4-dien-3-one (3c) was prepared in a method analogous to **19a** (0.77 g, 74 %); mp. 84-88 °C; FTIR (thin film, cm^{-1}): 2921, 2852, 1649, 1627, 1595, 1511, 1251, 1177, 1023, 980, 836; ^{1}H NMR (300 MHz, $CDCl_3$) δ 7.72 (d, *J* = 15.89 Hz, 2H); 7.58 (d, *J* = 8.55 Hz, 4H); 6.97 (d, *J* = 15.89 Hz, 2H); 6.94 (d, *J* = 8.55 Hz, 4H); 4.02 (t, *J* = 6.47 Hz, 4H); 1.82 (quin, *J* = 6.47 Hz, 4H); 1.55-1.22 (m, 28H); 0.91 (t, *J* = 6.47 Hz, 6H); ^{13}C NMR (300 MHz, $CDCl_3$) δ 188.9; 161.2; 142.7; 130.1; 127.4; 123.4; 114.9; 68.2; 31.9; 29.56; 29.55; 29.4; 29.3; 29.2; 26.0; 22.7; 14.1.

1,5-bis-(4-dodecyloxy-phenyl)-penta-1,4-dien-3-one (19d) was prepared in a method analogous to **19a** (1.93 g, 68 %); mp. 93-97 °C; FTIR (thin film, cm^{-1}): 2955, 2919, 2850, 1647, 1623, 1594, 1511, 1465, 1252, 1022, 979, 835, 822; ^{1}H NMR (300 MHz, $CDCl_3$) δ 7.71 (d, *J* = 15.89 Hz, 2H); 7.58 (d, *J* = 8.66 Hz, 4H); 6.97 (d, *J* = 15.89 Hz, 2H); 6.94 (d, *J* = 8.66 Hz, 4H); 4.02 (t, *J* = 6.58 Hz, 4H); 1.82 (quin, *J* = 6.58 Hz, 4H); 1.51-1.23 (m, 36H); 0.90 (t, *J* = 6.58 Hz, 6H); ^{13}C NMR (300 MHz, $CDCl_3$) δ 188.9; 161.2; 142.7; 130.1; 127.4; 123.4; 114.9; 68.2; 31.9; 29.7; 29.6; 29.6; 29.6; 29.4; 29.4; 29.2; 26.0; 22.7; 14.1.

2.2.2.2 Bis-alkoxy Dibenzylidene Acetone Compounds

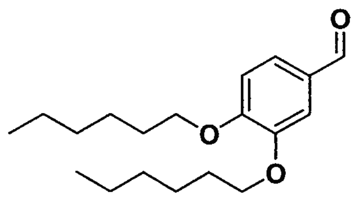

21e

3,4-bis-hexyloxy-benzaldehyde (21e). To a solution of 3,4-dihydroxy-benzaldehyde (**20**, 3.0 g, 21.7 mmol) and potassium carbonate (12.0 g, 86.9 mmol) in DMF (150 mL) was added 1-bromohexane as a solution in DMF (30 mL) dropwise. The resulting mixture was stirred at room temperature for 20 hours, poured into water (200 mL) and extracted with CH_2Cl_2 (2 × 150 mL). The combined organic layers were washed with water (3 × 150 mL), dried over $MgSO_4$, filtered and the solvent removed *in vacuo*. Vacuum distillation (25-32 °C, 0.21 mmHg) to remove excess DMF and alkyl bromide afforded **21e** (6.0 g, 90 %) as a white/brown powder; mp. 40-42 °C [lit.[47] 40-42 °C]; FTIR (thin film, cm^{-1}): 2931, 2860, 1690, 1595, 1584, 1510, 1436, 1269, 1239, 1134; ^{1}H NMR (300 MHz, $CDCl_3$) δ 9.85 (s, 1H); 7.47-7.37 (m, 2H); 6.97 (d, J = 8.00 Hz, 1H); 4.14-4.02 (m, 4H); 1.94-1.79 (m, 4H); 1.57-1.26 (m, 12H); 0.98-0.85 (m, 6H); ^{13}C NMR (300 MHz, $CDCl_3$) δ 191.0; 154.7; 149.5; 129.9; 126.6; 111.8; 111.0; 69.14; 69.12; 31.54; 31.51; 29.03; 28.95; 25.65; 25.61; 22.59; 22.57; 14.0 (2C).

3,4-bis-octyloxy-benzaldehyde (21f) was prepared in a method analogous to **21e** (2.32 g, 89 %); mp. 48-51 °C [lit.[48] 52-54 °C]; FTIR (thin film, cm^{-1}): 2926, 2855, 1689, 1596, 1585, 1510, 1270, 1134; ^{1}H NMR (300 MHz, $CDCl_3$) δ 9.85 (s, 1H); 7.46-7.40 (m, 2H); 6.97 (d, J = 8.00 Hz, 1H); 4.13-4.03 (m, 4H); 1.93-1.77 (m, 4H); 1.56-1.16 (m, 20H); 0.95-0.82 (m, 6H); ^{13}C NMR (300 MHz, $CDCl_3$) δ 191.0; 154.7; 149.5; 129.9; 126.6; 111.8; 111.0; 69.1 (2C); 31.8 (2C); 29.34; 29.32; 29.26; 29.24; 29.08; 28.99; 25.98; 25.95; 22.7 (2C); 14.1 (2C).

3,4-bis-decyloxy-benzaldehyde (21g) was prepared in a method analogous to **21e** (7.9 g, 100 %); mp. 58-62 °C [lit.[48] 62 °C]; FTIR (thin film, cm^{-1}): 2922, 2851, 1687, 1585, 1510, 1467, 1278, 1237, 1134; ^1H NMR (300 MHz, $CDCl_3$) δ 9.85 (s, 1H); 7.47-7.37 (m, 2H); 6.97 (d, J = 8.00 Hz, 1H); 4.13-4.03 (m, 4H); 1.94-1.80 (m, 4H); 1.57-1.18 (m, 28H); 0.94-0.86 (m, 6H); ^{13}C NMR (300 MHz, $CDCl_3$) δ 191.0; 154.7; 149.5; 129.9; 126.6; 111.8; 111.0; 69.16; 69.13; 31.9 (2C); 29.61; 29.58; 29.56 (2C); 29.38; 29.34 (3C); 29.08; 29.00; 25.98; 25.95; 22.7 (2C); 14.1 (2C).

3,4-bis-dodecyloxy-benzaldehyde (21h) was prepared in a method analogous to **21e** (16.9 g, 98 %); mp. 62-65 °C [lit.[49] 70 °C]; FTIR (thin film, cm^{-1}): 2919, 2850, 1687, 1597, 1586, 1511, 14667, 1278, 1238, 1134; ^1H NMR (300 MHz, $CDCl_3$) δ 9.85 (s, 1H); 7.48-7.39 (m, 2H); 6.97 (d, J = 8.11 Hz, 1H); 4.15-4.03 (m, 4H); 1.93-1.80 (m, 4H); 1.57-1.19 (m, 36H); 0.90 (t, J = 6.58 Hz, 6H); ^{13}C NMR (300 MHz, $CDCl_3$) δ 191.0; 154.7; 149.5; 129.9; 126.5; 111.8; 111.1; 69.18; 69.14; 31.9 (2C); 29.69 (2C); 29.65 (2C); 29.61 (2C); 29.59 (2C); 29.35 (4C); 29.08; 29.00; 25.99; 25.95; 22.7 (2C); 14.1 (2C).

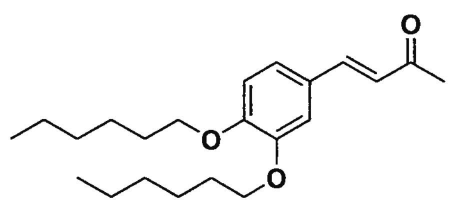

22e

4-(3,4-bis-hexyloxy-phenyl)-but-3-en-2-one (22e). To a solution of 3,4-bis-hexyloxy-benzaldehyde (**21e**, 2.50 g, 8.16 mmol) in acetone (50 mL) was added sodium methoxide (25 % wt solution in MeOH, 1.9 mL, 8.97 mmol) dropwise. The resulting solution was stirred for 1.0 hour, poured into H_2O (150 mL) and extracted with CH_2Cl_2 (2 × 200 mL). The combined organic layers were washed with H_2O (2 × 200 mL), dried over $MgSO_4$, filtered and the solvent removed *in vacuo*. The resulting dark yellow oil was recrystallized from MeOH to afford **22e** (1.90 g, 84 %) as a yellow powder; mp. 72-74 °C; FTIR (thin film, cm^{-1}): 2931, 2860, 1667, 1596, 1512, 1468, 1250, 1138; ^1H NMR

(300 MHz, $CDCl_3$) δ 7.46 (d, J = 16.22 Hz, 1H); 7.13-7.08 (m, 2H); 6.88 (d, J = 8.88 Hz, 1H); 6.60 (d, J = 16.22 Hz, 1H); 4.05 (t, J = 6.58 Hz, 2H); 4.04 (t, J = 6.58 Hz, 2H); 2.38 (s, 3H); 1.85 (quin., J = 6.58 Hz, 4H); 1.56-1.29 (m, 12H); 0.97-0.89 (m, 6H); ^{13}C NMR (300 MHz, $CDCl_3$) δ 198.4; 151.7; 149.3; 143.7; 127.2; 125.1; 123.0; 113.0; 112.2; 69.3; 69.1; 31.57; 31.56; 29.2; 29.1; 27.3; 25.68; 25.66; 22.61; 22.59; 14.0 (2C).

4-(3,4-bis-octyloxy-phenyl)-but-3-en-2-one (**22f**) was prepared in a method analogous to **22e** (0.39 g, 70 %); mp. 78-80 °C; FTIR (thin film, cm^{-1}): 2955, 2926, 2858, 1683, 1665, 1643, 1591, 1515, 1466, 1266, 1236, 1140; ^{1}H NMR (300 MHz, $CDCl_3$) δ 7.46 (d, J = 16.22 Hz, 1H); 7.13-7.07 (m, 2H); 6.88 (d, J = 8.77 Hz, 1H); 6.60 (d, J = 16.22 Hz, 1H); 4.05 (t, J = 6.58 Hz, 2H); 4.03 (t, J = 6.58 Hz, 2H); 2.38 (s, 3H); 1.85 (quin, J = 6.58 Hz, 4H); 1.55-1.24 (m, 20H); 0.91 (t, J = 6.58 Hz, 6H); ^{13}C NMR (300 MHz, $CDCl_3$) δ 198.3; 151.7; 149.3; 143.7; 127.2; 125.1; 123.0; 113.0; 112.3; 69.4; 69.1; 31.82; 31.81; 29.4; 29.34; 29.27; 29.26; 29.2; 29.1; 27.3; 26.01; 25.99; 22.7 (2C); 14.1 (2C).

4-(3,4-bis-decyloxy-phenyl)-but-3-en-2-one (**22g**) was prepared in a method analogous to **22e** (1.54 g, 70 %); mp. 71-74 °C; FTIR (thin film, cm^{-1}): 2925, 2854, 1669, 1596, 1512, 1467, 1249, 1138; ^{1}H NMR (300 MHz, $CDCl_3$) δ 7.46 (d, J = 16.33 Hz, 1H); 7.14-7.08 (m, 2H); 6.88 (d, J = 8.00 Hz, 1H); 6.60 (d, J = 16.33 Hz, 1H); 4.08-4.00 (m, 4H); 2.38 (s, 3H); 1.85 (quin, J = 6.58 Hz, 4H); 1.55-1.21 (m, 28H); 0.90 (t, J = 6.58 Hz, 6H); ^{13}C NMR (300 MHz, $CDCl_3$) δ 198.4; 151.7; 149.3; 143.7; 127.2; 125.1; 123.0; 113.0; 112.3; 69.4; 69.1; 31.9 (2C); 29.63; 29.61; 29.58 (2C); 29.41; 29.39; 29.35 (2C); 29.2; 29.1; 27.3; 26.02; 25.99; 22.7 (2C); 14.1 (2C).

4-(3,4-bis-dodecyloxy-phenyl)-but-3-en-2-one (**22h**) was prepared in a method analogous to **22e** (0.54 g, 100 %); mp. 66-70 °C; FTIR (thin film, cm^{-1}): 2923, 2853, 1668, 1595, 1513, 1468, 1250, 1139; ^{1}H NMR (300 MHz, $CDCl_3$) δ 7.46 (d, J = 16.11 Hz, 1H); 7.13-7.08 (m, 2H); 6.88 (d, J = 8.77 Hz, 1H); 6.60 (d, J = 16.11 Hz, 1H); 4.05 (t, J = 6.58 Hz, 2H); 4.03 (t, J = 6.58 Hz, 2H); 2.38 (s, 3H); 1.85 (quin, J = 6.58 Hz, 4H); 1.55-1.21 (m, 36H); 0.90 (t, J = 6.58 Hz, 6H); ^{13}C NMR (300 MHz, $CDCl_3$) δ 198.3;

151.7; 149.3; 143.7; 127.2; 125.1; 123.0; 113.0; 112.3; 69.4; 69.1; 31.9 (2C); 29.69 (2C); 29.66 (2C); 29.64 (2C); 29.61 (2C); 29.42; 29.39; 29.37 (2C); 29.2; 29.1; 27.3; 26.02; 25.99; 22.7 (2C); 14.1 (2C).

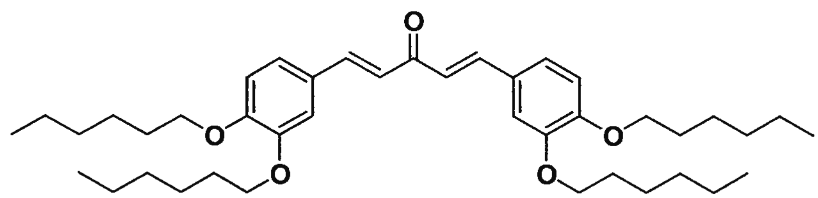

1,5-bis-(3,4-bis-hexyloxy-phenyl)-penta-1,4-dien-3-one (**23e**). To a solution of 4-(3,4-bis-hexyloxy-phenyl)-but-3-en-2-one (**22e**, 0.50 g, 1.44 mmol) and 3,4-bis-hexyloxy-benzaldehyde (**21e,** 0.44 g, 1.44 mmol) in methanol (20 mL) was added sodium methoxide (25 % wt solution in MeOH, 0.94 mL, 4.33 mmol) dropwise. The resulting mixture was heated to reflux for 48 hours, poured into 1.0 M HCl (200 mL) and extracted with CH_2Cl_2 (3 × 75 mL). The combined organic layers were washed with H_2O (2 × 200 mL), dried over $MgSO_4$, filtered and the solvent removed *in vacuo*. Recrystallization from acetone afforded **23e** (0.52 g, 57 %) as a yellow powder; mp. 62-65 °C; FTIR (thin film, cm^{-1}): 2955, 2931, 2860, 1648, 1618, 1595, 1511, 1468, 1432, 1258, 1234, 1172, 1137, 1095, 1017; ^{1}H NMR (300 MHz, $CDCl_3$) δ 7.69 (d, J = 15.78 Hz, 2H); 7.21-7.15 (m, 4H); 6.95 (d, J = 15.78 Hz, 2H); 6.90 (d, J = 8.33 Hz, 2H); 4.07 (t, J = 6.58 Hz, 4H); 4.06 (t, J = 6.58 Hz, 4H); 1.87 (quin, J = 6.58 Hz, 4H); 1.86 (quin, J = 6.58 Hz, 4H); 1.56-1.26 (m, 24H); 0.94 (t, J = 6.58 Hz, 6H); 0.93 (t, J = 6.58 Hz, 6H); ^{13}C NMR (300 MHz, $CDCl_3$) δ 188.8; 151.6; 149.2; 143.1; 127.8; 123.5; 123.1; 113.0; 112.6; 69.4; 69.1; 31.59; 31.56; 29.2; 29.1; 25.71; 25.67; 22.62; 22.59; 14.03; 14.01.

1,5-bis-(3,4-bis-octyloxy-phenyl)-penta-1,4-dien-3-one (**23f**) was prepared in a method analogous to **23e** (0.57 g, 61 %); mp. 62-65 °C; FTIR (thin film, cm^{-1}): 2925, 2854, 1648, 1618, 1583, 1514, 1468, 1338, 1260, 1173, 1138, 1096, 984; ^{1}H NMR (300 MHz, $CDCl_3$) δ 7.69 (d, J = 15.78 Hz, 2H); 7.21-7.15 (m, 4H); 6.95 (d, J = 15.78 Hz, 2H); 6.90 (d, J = 8.22 Hz, 2H); 4.06 (t, J = 6.58 Hz, 8H); 1.92-1.81 (m, 8H); 1.55-1.26 (m, 40H); 0.91 (t, J = 6.58 Hz, 12H); ^{13}C NMR (300 MHz, $CDCl_3$) δ 188.8; 151.6; 149.2; 143.1;

127.8; 123.5; 123.1; 113.0; 112.7; 69.4; 69.1; 31.83; 31.82; 29.39; 29.35; 29.29 (2C); 29.26; 29.1; 26.04; 26.01; 22.7 (2C); 14.1 (2C).

1,5-bis-(3,4-bis-decyloxy-phenyl)-penta-1,4-dien-3-one (23g) was prepared in a method analogous to **23e** (0.92 g, 50 %); mp. 68-73 °C; FTIR (thin film, cm^{-1}): 2921, 2851, 1649, 1589, 1514, 1467, 1262, 1235, 1173, 1138, 982; ^{1}H NMR (300 MHz, $CDCl_3$) δ 7.68 (d, *J* = 15.78 Hz, 2H); 7.21-7.15 (m, 4H); 6.94 (d, *J* = 15.78 Hz, 2H); 6.89 (d, *J* = 8.22 Hz, 2H); 4.06 (t, *J* = 6.58 Hz, 8H); 1.86 (quin, *J* = 6.58 Hz, 8H); 1.56-1.22 (m, 56H); 0.90 (t, *J* = 6.58 Hz, 12H); ^{13}C NMR (300 MHz, $CDCl_3$) δ 188.8; 151.6; 149.2; 143.1; 127.8; 123.5; 123.1; 113.1; 112.7; 69.4; 69.1; 31.9 (4C); 29.64; 29.61; 29.59; 29.58; 29.43; 29.40; 29.35 (4C); 29.3; 29.1; 26.04; 26.00; 22.7 (4C); 14.1 (4C).

1,5-bis-(3,4-bis-dodecyloxy-phenyl)-penta-1,4-dien-3-one (23h) was prepared in a method analogous to **23e** (0.24 g, 56 %); mp. 70-75 °C; FTIR (thin film, cm^{-1}): 2924, 2854, 1650, 1617, 1595, 1510, 1468, 1432, 1260, 1170, 1137, 1093; ^{1}H NMR (300 MHz, $CDCl_3$) δ 7.68 (d, *J* = 15.78 Hz, 2H); 7.21-7.15 (m, 4H); 6.94 (d, *J* = 15.78 Hz, 2H); 6.89 (d, *J* = 8.22 Hz, 2H); 4.06 (t, *J* = 6.58 Hz, 8H); 1.86 (quin, *J* = 6.58 Hz, 8H); 1.54-1.20 (m, 72H); 0.90 (t, *J* = 6.58 Hz, 12H); ^{13}C NMR (300 MHz, $CDCl_3$) δ 188.8; 151.6; 149.2; 143.1; 127.8; 123.5; 123.1; 113.1; 112.7; 69.4; 69.1; 31.9 (4C); 29.72; 29.70; 29.66 (4C); 29.65 (4C); 29.62 (4C); 29.45; 29.40; 29.37 (4C); 29.3; 29.2; 26.05; 26.01; 22.7 (4C); 14.1 (4C).

2.2.2.3 Tris-alkoxy Dibenzylidene Acetone Compounds

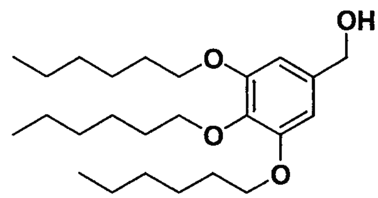

24i

3,4,5-tris-hexyloxy-benzyl alcohol (24i). To a slurry of $LiAlH_4$ (0.55 g, 14.43 mmol) in freshly distilled THF (30 mL) at 0°C under $Ar_{(g)}$ was added **24i** (3.00 g, 6.87 mmol) as a solution in THF (30 mL). The resulting mixture was stirred at 0°C for 30 min, heated to room temperature and stirred for 48 hours. The reaction was quenched with H_2O (40 mL), poured into 1.0 M HCl (100 mL) and extracted with Et_2O (2 × 150 mL). The combined organic layers were washed with a saturated NaCl solution (2 × 150 mL), dried over $MgSO_4$, filtered and the solvent removed *in vacuo* to afford a whitish yellow waxy solid, **24i** (7.49 g, 100 %); mp. 38-41 °C; ^{1}H NMR (300 MHz, $CDCl_3$) δ 6.58 (s, 2H); 4.61 (d, J = 5.70 Hz, 2H); 3.99 (t, J = 6.58 Hz, 4H); 3.96 (t, J = 6.58 Hz, 2H); 1.87-1.71 (m, 6H); 1.61 (t, J = 5.70 Hz, 1H); 1.55-1.43 (m, 6H); 1.42-1.26 (m, 18H); 0.91 (t, J = 6.58 Hz, 9H); ^{13}C NMR (300 MHz, $CDCl_3$) δ 6.58 (s, 2H); 4.61 (s, 2H); 3.99 (t, J = 6.58 Hz, 4H); 3.96 (t, J = 6.58 Hz, 2H); 1.87-1.71 (m, 6H); 1.55-1.27 (m, 18H); 0.92 (t, J = 6.58 Hz, 9H) ^{13}C NMR (300 MHz, $CDCl_3$) δ 153.3; 137.6; 136.0; 105.4; 73.4; 69.1; 65.7; 31.8; 31.6; 30.3; 29.4; 25.8; 22.7; 22.6; 14.1; 14.0.

3,4,5-tris-octyloxy-benzyl alcohol (24j) was prepared in a method analogous to **24i** (7.57 g, 100 %); ^{1}H NMR (300 MHz, $CDCl_3$) δ 6.58 (s, 2H); 4.61 (d, J = 5.70 Hz, 2H); 3.99 (t, J = 6.58 Hz, 4H); 3.96 (t, J = 6.58 Hz, 2H); 1.87-1.71 (m, 6H); 1.61 (t, J = 5.70 Hz, 1H); 1.55-1.43 (m, 6H); 1.42-1.26 (m, 30H); 0.91 (t, J = 6.58 Hz, 9H); ^{13}C NMR (300 MHz, $CDCl_3$) δ 153.3; 137.6; 136.0; 105.4; 73.4; 69.1; 65.7; 31.9; 31.8; 30.3; 29.6; 29.42 (2C); 29.37 (3C); 29.3 (2C); 26.13; 26.10; 22.69; 22.67; 14.1 (3C).

3,4,5-tris-decyloxy-benzyl alcohol (24k) was prepared in a method analogous to **24i** (1.74 g, 91 %); mp 35-37 °C; ^{1}H NMR (300 MHz, $CDCl_3$) δ 6.58 (s, 2H); 4.61 (d, J = 5.81 Hz, 2H); 3.99 (t, J = 6.58 Hz, 4H); 3.96 (t, J = 6.58 Hz, 2H); 1.87-1.70 (m, 6H); 1.59 (t, J = 5.81 Hz, 1H); 1.55-1.22 (m, 42H); 0.90 (t, J = 6.58 Hz, 9H); ^{13}C NMR (300 MHz, $CDCl_3$) δ 153.3; 137.7; 136.0; 105.4; 73.4; 69.1; 65.7; 31.95; 31.92 (2C); 30.3; 29.8; 29.69; 29.65 (2C); 29.62; 29.60 (2C); 29.42 (5C); 29.36 (2C); 26.14; 26.10 (2C); 22.7 (3C); 14.1 (3C).

3,4,5-tris-dodecyloxy-benzyl alcohol (24l) was prepared in a method analogous to **24i** (5.36 g, 89 %); mp. 44-48 °C; ^{1}H NMR (300 MHz, $CDCl_3$) δ 6.58 (s, 2H); 4.62 (d, J = 5.81 Hz, 2H); 3.99 (t, J = 6.58 Hz, 4H); 3.96 (t, J = 6.58 Hz, 2H); 1.87-1.71 (m, 6H); 1.60 (t, J = 5.81 Hz, 1H) 1.54-1.23 (m, 54H); 0.90 (t, J = 6.58 Hz, 9H); ^{13}C NMR (300 MHz, $CDCl_3$) δ153.3; 137.7; 136.0; 105.4; 73.4; 69.1 (2C); 65.7; 31.9 (3C); 30.3; 29.8 (3C); 29.71 (3C); 29.66 (7C); 29.42 (3C); 29.40 (2C); 29.37 (2C); 26.14; 26.11; 22.7 (3C); 14.1 (3C).

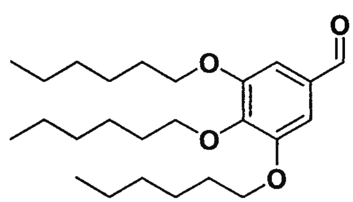

25i

3,4,5-tris-hexyloxy-benzaldehyde (25i). To a slurry of pyridinium chlorochromate (7.39 g, 34.3 mmol) in CH_2Cl_2 (150 mL) was added 3,4,5-tris-hexyloxy-benzyl alcohol (**24i**, 7.0 g, 17.1 mmol) as a solution in CH_2Cl_2 (20 mL) dropwise over 5 minutes. The mixture was allowed to stir at room temperature for 3.5 hours, filtered and washed with Et_2O (150 mL). The filtrate was washed with water (200 mL) and separated. The aqueous portion was extracted with CH_2Cl_2 (150 mL). The combined organic layers were washed with H_2O (2 × 200 mL), dried over $MgSO_4$, filtered and the solvent removed *in vacuo*. Flash chromatography (CH_2Cl_2) afforded **25i** as a clear, yellow oil (5.85 g, 84 %); ^{1}H NMR (300 MHz, $CDCl_3$) δ 9.85 (s, 1H); 7.10 (s, 2H); 4.08 (t, J = 6.58 Hz, 2H); 4.06 (t, J = 6.58

Hz, 4H); 1.85 (quin. $J = 6.58$ Hz, 4H); 1.77 (quin. $J = 6.58$ Hz, 2H); 1.56-1.26 (m, 18H); 0.96-0.89 (m, 9H); ^{13}C NMR (300 MHz, $CDCl_3$) δ 191.3; 153.5; 143.9; 131.4; 107.9; 73.6; 69.3; 31.7; 31.5; 30.3; 29.2; 25.73; 25.66; 22.7; 22.6; 14.1; 14.0.

3,4,5-tris-octyloxy-benzaldehyde (25j) was prepared in a method analogous to **25i** (4.48 g, 100 %); ^{1}H NMR (300 MHz, $CDCl_3$) δ 9.85 (s, 1H); 7.10 (s, 2H); 4.08 (t, $J = 6.58$ Hz, 2H); 4.05 (t, $J = 6.58$ Hz, 4H); 1.85 (quin, $J = 6.58$ Hz, 4H); 1.77 (quin, $J = 6.58$ Hz, 2H); 1.55-1.22 (m, 30H); 0.91 (t, $J = 6.58$ Hz, 9H); ^{13}C NMR (300 MHz, $CDCl_3$) δ 191.3; 153.5; 143.9; 131.4; 107.9; 73.6; 69.3; 31.9; 31.8; 30.3; 29.5; 29.35; 29.33 (3C); 29.26 (3C); 26.06; 26.01; 22.68; 22.67; 14.1 (3C).

3,4,5-tris-decyloxy-benzaldehyde (25k) was prepared in a method analogous to **25i** (1.43 g, 96 %); ^{1}H NMR (300 MHz, $CDCl_3$) δ 9.85 (s, 1H); 7.10 (s, 2H); 4.08 (t, $J = 6.58$ Hz, 2H); 4.05 (t, $J = 6.58$ Hz, 4H); 1.85 (quin, $J = 6.58$ Hz, 4H); 1.77 (quin, $J = 6.58$ Hz, 2H); 1.55-1.22 (m, 42H); 0.90 (t, $J = 6.58$ Hz, 9H); ^{13}C NMR (300 MHz, $CDCl_3$) δ 191.3; 153.5; 143.9; 131.4; 107.9; 73.6; 69.3; 31.93; 31.91; 30.3; 29.72; 29.66; 29.62 (2C); 29.58 (2C); 29.54; 29.38 (3C); 29.34 (2C); 29.26 (2C); 26.06; 26.03; 22.7 (3C); 14.1 (3C).

3,4,5-tris-dodecyloxy-benzaldehyde (25l) was prepared in a method analogous to **25i** (0.89 g, 89 %); mp 44-47 °C; ^{1}H NMR (300 MHz, $CDCl_3$) δ 9.85 (s, 1H); 7.10 (s, 2H); 4.08 (t, $J = 6.58$ Hz, 2H); 4.05 (t, $J = 6.58$ Hz, 4H); 1.85 (quin, $J = 6.58$ Hz, 4H); 1.77 (quin, $J = 6.58$ Hz, 2H); 1.55-1.21 (m, 54H); 0.90 (t, $J = 6.58$ Hz, 9H); ^{13}C NMR (300 MHz, $CDCl_3$) δ 191.3; 153.5; 143.9; 131.4; 107.9; 73.6; 69.3; 31.9 (3C); 30.3; 29.74; 29.72 (2C); 29.69 (3C); 29.66 (2C); 29.6 (4C); 29.5; 29.38 (2C); 29.37 (3C); 29.26 (2C); 26.07; 26.03; 22.7 (3C); 14.1 (3C).

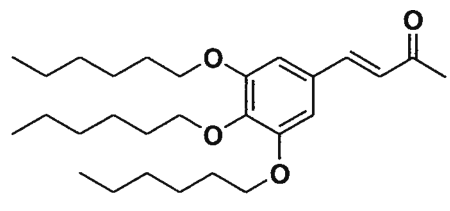

26i

4-(3,4,5-tris-hexyloxy-phenyl)-but-3-en-2-one (26i). To a solution of 3,4,5-tris-hexyloxy-benzaldehyde (**25i**, 2.50 g, 8.16 mmol) in acetone (50 mL) was added sodium methoxide (25 % wt solution in MeOH, 1.9 mL, 8.97 mmol) dropwise. The resulting solution was stirred for 1.0 hour, poured into 1.0 M HCl (100 mL) and extracted with CH_2Cl_2 (2 × 200 mL). The combined organic layers were washed with H_2O (2 × 200 mL), dried over $MgSO_4$, filtered and the solvent removed *in vacuo*. Flash chromatography ($CHCl_3$) afforded **26i** as a yellow powder (1.06 g, 38 %); mp. 72-74 °C; ^{1}H NMR (300 MHz, $CDCl_3$) δ 7.42 (d, J = 16.22 Hz, 1H); 6.76 (s, 2H); 6.61 (d, J = 16.22 Hz, 1H); 4.02 (t, J = 6.58 Hz, 2H); 4.01 (t, J = 6.58 Hz, 4H); 2.39 (s, 3H); 1.84 (quin, J = 6.58 Hz, 4H); 1.76 (quin, J = 6.58 Hz, 4H); 1.57-1.28 (m, 18H); 0.93 (t, J = 6.58 Hz, 6H); 0.92 (t, J = 6.58 Hz, 3H); ^{13}C NMR (300 MHz, $CDCl_3$) δ 198.3; 153.4; 143.9;129.4; 126.2; 106.9; 73.6; 69.2; 31.7; 31.6; 30.3; 29.3; 27.3; 25.74; 25.71; 22.7; 22.6; 14.1; 14.0.

4-(3,4,5-tris-octyloxy-phenyl)-but-3-en-2-one (26j) was prepared in a method analogous to **32i** (0.25 g, 47 %); ^{1}H NMR (300 MHz, $CDCl_3$) δ 7.42 (d, J = 16.22 Hz, 1H); 6.76 (s, 2H); 6.61 (d, J = 16.22 Hz, 1H); 4.01 (t, J = 6.58 Hz, 6H); 2.39 (s, 3H); 1.84 (quin., J = 6.58 Hz, 4H); 1.77 (quin., J = 6.58 Hz, 2H); 1.54-1.22 (m, 30H); 0.91 (t, J = 6.58 Hz, 9H); ^{13}C NMR (300 MHz, $CDCl_3$) δ 198.3; 153.4; 143.9; 140.7; 129.4; 126.2; 106.9; 73.6; 69.2; 31.9; 31.8; 30.3; 29.5; 29.4 (5C); 29.3 (2C); 27.3; 26.1 (3C); 22.69; 22.67; 14.1 (3C).

4-(3,4,5-tris-decyloxy-phenyl)-but-3-en-2-one (26k) was prepared in a method analogous to **26i** (1.44 g, 67 %); ^{1}H NMR (300 MHz, $CDCl_3$) δ 7.42 (d, J = 16.22 Hz, 1H); 6.76 (s, 2H); 6.61 (d, J = 16.22 Hz, 1H); 4.01 (t, J = 6.58 Hz, 6H); 2.39 (s, 3H); 1.83 (quin., J = 6.58 Hz, 4H); 1.76 (quin., J = 6.58 Hz, 2H); 1.55-1.21 (m, 42H); 0.90 (t, J =

6.58 Hz, 9H); ^{13}C NMR (300 MHz, $CDCl_3$) δ 198.3; 153.4; 143.9; 140.7; 129.4; 126.2; 106.9; 73.6; 69.2; 31.94; 31.91; 30.3; 29.73; 29.66; 29.64 (2C); 29.58 (3C); 29.40 (3C); 29.35 (4C); 27.3; 26.1 (3C); 22.7 (3C); 14.1 (3C).

4-(3,4,5-tris-dodecyloxy-phenyl)-but-3-en-2-one (26l) was prepared in a method analogous to **26i** (0.20 g 38 %); ^{1}H NMR (300 MHz, $CDCl_3$) δ 7.42 (d, *J* = 16.22 Hz, 1H); 6.76 (s, 2H); 6.61 (d, *J* = 16.22 Hz, 1H); 4.01 (t, *J* = 6.58 Hz, 6H); 2.39 (s, 3H); 1.83 (quin., *J* = 6.58 Hz, 4H); 1.76 (quin., *J* = 6.58 Hz, 2H); 1.56-1.20 (m, 54H); 0.90 (t, *J* = 6.58 Hz, 9H); ^{13}C NMR (300 MHz, $CDCl_3$) δ 198.3; 153.4; 143.9; 140.7; 129.4; 126.2; 106.9; 73.6; 69.2; 31.9 (3C); 30.3; 29.73 (3C); 29.70 (3C); 29.66 (2C); 29.64 (4C); 29.58; 29.40 (3C); 29.37 (4C); 27.3; 26.1 (3C); 22.7 (3C); 14.1 (3C).

2.2.3 Synthesis of 1,9-Diphenyl-nona-1,3,6,8-tetraen-5-one Compounds

2.2.3.1 Mono-alkoxy 1,9-Diphenyl-nona-1,3,6,8-tetraen-5-one Compounds

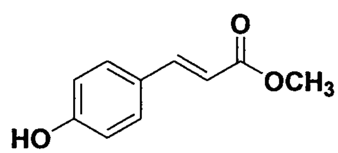

29

methyl-4-hydroxy-cinnamate (29). To a solution of 4-hydroxy-cinnamic acid (**28**, 5.00 g, 30.46 mmol) in methanol (50 mL) was added concentrated H_2SO_4 (2.54 mL, 45.67 mmol) dropwise. The resulting solution was allowed to reflux for 20 hours, was cooled to room temperature, poured into H_2O (100 mL) and extracted with EtOAc (2 × 150 mL). The combined organic layers were washed with H_2O (200 mL), $NaHCO_{3\,(sat)}$ (200 mL), again with H_2O (200 mL), dried over $MgSO_4$, filtered and the solvent removed *in vacuo*. Recrystallization from hexanes afforded **29** (5.26 g, 97 %) as a white powder; mp. 135-138 °C. [lit.[50] 136-137 °C]; FTIR (thin film, cm^{-1}): 3389, 1685, 1636, 1607, 1330, 1198, 1179, 987, 834; ^{1}H NMR (300 MHz, $CDCl_3$) δ 7.67 (d, *J* = 15.89 Hz, 1H); 7.44 (d, *J* = 8.55 Hz, 2H); 6.88 (d, *J* = 8.55 Hz, 2H); 6.32 (d, *J* = 15.89 Hz, 1H); 6.00 (s, 1H); 3.83 (s, 3H); ^{13}C NMR (300 MHz, $CDCl_3$) δ 168.3; 158.0; 144.9; 130.0; 127.0; 115.9; 115.0; 51.8.

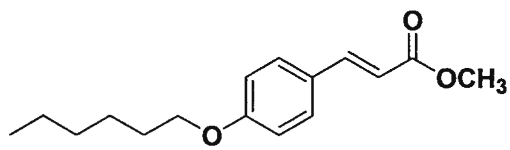

30a

methyl-4-hexyloxy-cinnamate (**30a**) To a solution of methyl-4-hydroxy-cinnamate (**29,** 1.00 g, 5.61 mmol) and K_2CO_3 (1.55 g, 11.22 mmol) in acetone (40 mL) was added 1-bromohexane (1.85 g, 11.22 mmol) as a solution in acetone (10 mL). The resulting mixture was heated to reflux 20 hours, poured into H_2O (100 mL) and extracted with CH_2Cl_2 (2 × 100 mL). The combined organic layers were washed with H_2O (2 × 200 mL), dried over $MgSO_4$, filtered and the solvent removed *in vacuo*. Recrystallization from hexanes afforded **30a** (2.67 g, 91 %) as a white powder; mp. 77-80 °C; FTIR (thin film, cm^{-1}): 2940, 2870, 1711, 1606, 1513, 1258, 1168, 993, 835; ^1H NMR (300 MHz, $CDCl_3$) δ 7.67 (d, J = 15.89 Hz, 1H); 7.48 (d, J = 8.66 Hz, 2H); 6.91 (d, J = 8.66 Hz, 2H); 6.32 (d, J = 15.89 Hz, 1H); 4.00 (t, J = 6.58 Hz, 2H); 3.81 (s, 3H); 1.81 (quin., J = 6.58 Hz, 2H); 1.54-1.29 (m, 6H); 0.90 (t, J = 6.58 Hz, 3H); ^{13}C NMR (300 MHz, $CDCl_3$) δ 167.8; 161.0; 144.6; 129.7; 126.9; 115.1; 114.8; 68.2; 51.5; 31.5; 29.1; 25.7; 22.6; 14.0.

methyl-4-octyloxy-cinnamate (**30b**) was prepared in a method analogous to **30a** (4.81 g, 98 %); mp. 65-69 °C; FTIR (thin film, cm^{-1}): 2923, 1709, 1603; 1512, 1288, 1252, 1167, 1000, 826; ^1H NMR (300 MHz, $CDCl_3$) δ 7.67 (d, J = 16.00 Hz, 1H); 7.48 (d, J = 8.66 Hz, 2H); 6.91 (d, J = 8.66 Hz, 2H); 6.32 (d, J = 16.00 Hz, 1H); 4.00 (t, J = 6.58 Hz, 2H); 3.81 (s, 3H); 1.81 (quin., J = 6.58 Hz, 2H); 1.54-1.23 (m, 14H); 0.91 (t, J = 6.58 Hz, 3H); ^{13}C NMR (300 MHz, $CDCl_3$) δ 167.8; 161.0; 144.6; 129.7; 126.9; 115.1; 114.8; 68.2; 51.5; 31.8; 29.3; 29.22; 29.16; 26.0; 22.6; 14.1.

methyl-4-decyloxy-cinnamate (**30c**) was prepared in a method analogous to **30a** (2.41 g, 90 %); mp. 61-63 °C; FTIR (thin film, cm^{-1}): 2920, 2851, 1724, 1513, 1286, 1179, 982, 823; ^{1}H NMR (300 MHz, $CDCl_3$) δ 7.67 (d, J = 15.89 Hz, 1H); 7.48 (d, J = 8.66 Hz, 2H); 6.91 (d, J = 8.66 Hz, 2H); 6.32 (d, J = 15.89 Hz, 1H); 4.00 (t, J = 6.58 Hz, 2H); 3.81 (s, 3H); 1.81 (quin., J = 6.58 Hz, 2H); 1.53-1.23 (m, 14H); 0.90 (t, J = 6.58 Hz, 3H); ^{13}C NMR (300 MHz, $CDCl_3$) δ 167.8; 161.0; 144.6; 129.7; 126.9; 115.1; 114.8; 68.2; 51.5; 31.9; 29.6 (2C); 29.4; 29.3; 29.2; 26.0; 22.7; 14.1.

methyl-4-dodecyloxy-cinnamate (30d) was prepared in a method analogous to **30a** (1.74 g, 90 %); mp. 65-70 °C; FTIR (thin film, cm^{-1}): 2919, 2850, 1725, 1513, 1286, 1179, 981, 837, 822; ^{1}H NMR (300 MHz, $CDCl_3$) δ 7.67 (d, J = 16.00 Hz, 1H); 7.48 (d, J = 8.66 Hz, 2H); 6.91 (d, J = 8.66 Hz, 2H); 6.32 (d, J = 16.00 Hz, 1H); 4.00 (t, J = 6.58 Hz, 2H); 3.81 (s, 3H); 1.81 (quin., J = 6.58 Hz, 2H); 1.53-1.22 (m, 18H); 0.90 (t, J = 6.58 Hz, 3H); ^{13}C NMR (300 MHz, $CDCl_3$) δ 167.8; 161.0; 144.6; 129.7; 126.9; 115.1; 114.8; 68.2; 51.6; 31.9; 29.65; 29.64; 29.58; 29.56; 29.37; 29.34; 29.2; 26.0; 22.7; 14.1.

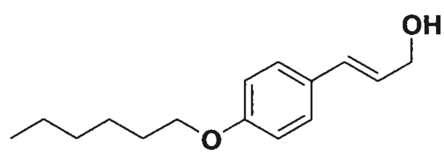

31a

4-hexyloxy-cinnamyl alcohol (31a) To a solution of methyl-4-hexyloxy-cinnamate (**30a**, 1.50 g, 5.72 mmol) in anhydrous toluene (30 mL) under N_2 at 0°C was added DIBAL-H (1.0 M solution in toluene, 14.29 mL, 14.29 mmol) dropwise. The resulting mixture was allowed to stir for 1.0 hour, warmed to room temperature and stirred for 3 hours. The reaction mixture was slowly quenched with H_2O (3 mL), poured into 2.0 M HCl (100 mL) and extracted with $CHCl_3$ (3 × 75 mL). The combined organic layers were washed with H_2O (2 × 200 mL), dried over $MgSO_4$, filtered and the solvent removed *in vacuo.* Recrystallization from hexanes afforded **31a** (1.25 g, 93 %) as a white powder; mp. 64-69 °C; FTIR (thin film, cm^{-1}): 2955, 2931, 2860, 1468, 1245, 971; 834; ^{1}H NMR (300 MHz, $CDCl_3$) δ 7.33 (d, J = 8.66 Hz, 2H); 6.89 (d, J = 8.66 Hz, 2H); 6.57 (d, J = 15.89 Hz, 1H); 6.25 (dt, J_1 = 15.89 Hz, J_2 = 5.81 Hz, 1H); 4.31 (t, J = 5.81 Hz, 2H); 3.97 (t, J =

6.58 Hz, 2H); 1.80 (quin., J = 6.58 Hz, 2H); 1.54-1.29 (m, 11H); 0.93 (t, J = 6.58 Hz, 3H); ^{13}C NMR (300 MHz, $CDCl_3$) δ 158.9; 131.1; 129.2; 127.6; 126.1; 114.6; 68.1; 64.0; 31.6; 29.2; 25.7; 22.6; 14.0.

4-octyloxy-cinnamyl alcohol (31b) was prepared in a method analogous to **31a** (0.86 g, 96 %); mp. 67-70 °C; FTIR (thin film, cm^{-1}): 2921, 2855, 1465, 1253, 969, 844; ^{1}H NMR (300 MHz, $CDCl_3$) δ 7.33 (d, J = 8.66 Hz, 2H); 6.87 (d, J = 8.66 Hz, 2H); 6.57 (d, J = 15.89 Hz, 1H); 6.25 (dt, J_1 = 15.89 Hz, J_2 = 5.92 Hz, 1H); 4.32 (t, J = 5.92 Hz, 2H); 3.97 (t, J = 6.58 Hz, 2H); 1.80 (quin., J = 6.58 Hz, 2H); 1.53-1.22 (m, 11H); 0.91 (t, J = 6.58 Hz, 3H); ^{13}C NMR (300 MHz, $CDCl_3$) δ 158.9; 131.1; 129.2; 127.6; 126.1; 114.6; 68.1; 64.0; 31.8; 29.4; 29.26; 29.24; 26.0; 22.7; 14.1.

4-decyloxy-cinnamyl alcohol (31c) was prepared in a method analogous to **31a** (1.72 g, 95 %); mp. 69-72 °C; FTIR (thin film, cm^{-1}): 2918, 2850, 1465, 1253, 969, 843; ^{1}H NMR (300 MHz, $CDCl_3$) δ 7.33 (d, J = 8.66 Hz, 2H); 6.87 (d, J = 8.66 Hz, 2H); 6.57 (d, J = 15.89 Hz, 1H); 6.25 (dt, J_1 = 15.89 Hz, J_2 = 6.03 Hz, 1H); 4.31 (d, J = 5.92 Hz, 2H); 3.97 (t, J = 6.58 Hz, 2H); 1.80 (quin., J = 6.58 Hz, 2H); 1.54-1.22 (m, 14H); 0.91 (t, J = 6.58 Hz, 3H); ^{13}C NMR (300 MHz, $CDCl_3$) δ 158.9; 131.1; 129.2; 127.6; 126.1; 114.6; 68.1; 64.0; 31.9; 29.58; 29.56; 29.4; 29.32; 29.26; 26.0; 22.7; 14.1.

4-dodecyloxy-cinnamyl alcohol (31d) was prepared in a method analogous to **31a** (0.88 g, 96 %); mp. 80-83 °C; FTIR (thin film, cm^{-1}): 2917, 2850, 1464, 1254, 960, 844; ^{1}H NMR (300 MHz, $CDCl_3$) δ 7.33 (d, J = 8.66 Hz, 2H); 6.87 (d, J = 8.66 Hz, 2H); 6.57 (d, J = 15.89 Hz, 1H); 6.25 (dt, J_1 = 15.89 Hz, J_2 = 5.92 Hz, 1H); 4.32 (t, J = 5.92 Hz, 2H); 3.97 (t, J = 6.58 Hz, 2H); 1.80 (quin., J = 6.58 Hz, 2H); 1.54-1.20 (m, 18H); 0.90 (t, J = 6.58 Hz, 3H); ^{13}C NMR (300 MHz, $CDCl_3$) δ 158.9; 131.1; 129.2; 127.6; 126.1; 114.6; 68.1; 64.0; 31.9; 29.66; 29.64; 29.60; 29.58; 29.40; 29.35; 29.26; 26.0; 22.7; 14.1.

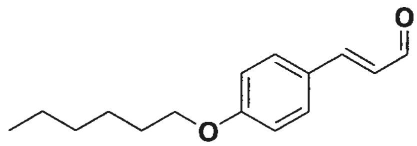

32a

4-hexyloxy-cinnamaldehyde (**32a**). To a solution of 2,3-dichloro-5,6-dicyano-1,4-*p*-benzoquinone (DDQ, 1.78 g, 7.84 mmol) in freshly distilled 1,4-dioxane (40 mL) under N_2 was added 4-hexyloxy-cinnamyl alcohol (**31a**, 1.75 g, 7.47 mmol) as a solution in 1,4-dioxane (40 mL). The resulting solution was allowed to stir for 1 hour. The reaction mixture was filtered and the solvent removed *in vacuo*. Flash chromatography (hexanes:EtOAc, 4:1) afforded **32a** (1.73 g, 100 %) as a clear yellow oil that crystallized on standing. FTIR (thin film, cm^{-1}): 2932, 2859, 1682, 1602, 1512, 1251, 1175, 1127; ^{1}H NMR (300 MHz, $CDCl_3$) δ 9.67 (d, J = 7.67 Hz, 1H); 7.53 (d, J = 8.66 Hz, 2H); 7.44 (d, J = 15.78 Hz, 1H); 6.95 (d, J = 8.66 Hz, 2H); 6.63 (dd, J_1 = 15.78 Hz, J_2 = 7.67 Hz, 1H); 4.03 (t, J = 6.58 Hz, 2H); 1.82 (quin., J = 6.58 Hz, 2H); 1.55-1.22 (m, 6H); 0.93 (t, J = 6.58 Hz, 3H); ^{13}C NMR (300 MHz, $CDCl_3$) δ 193.7; 161.9; 152.8; 130.3; 126.6; 126.4; 115.1; 68.3; 31.5; 29.1; 25.7; 22.6; 14.0.

4-octyloxy-cinnamaldehyde (**32b**) was prepared in a method analogous to **32a** (2.22 g, 100 %); FTIR (thin film, cm^{-1}): 2927, 2856, 1678, 1602, 1512, 1260, 1174, 1127; ^{1}H NMR (300 MHz, $CDCl_3$) δ 9.67 (d, J = 7.67 Hz, 1H); 7.53 (d, J = 8.66 Hz, 2H); 7.44 (d, J = 15.89 Hz, 1H); 6.95 (d, J = 8.66 Hz, 2H); 6.63 (dd, J_1 = 15.89 Hz, J_2 = 7.67 Hz, 1H); 4.02 (t, J = 6.58 Hz, 2H); 1.82 (quin., J = 6.58 Hz, 2H); 1.54-1.23 (m, 10H); 0.91 (t, J = 6.58 Hz, 3H); ^{13}C NMR (300 MHz, $CDCl_3$) δ193.7; 161.9; 152.8; 130.3; 126.6; 126.4; 115.1; 68.3; 31.8; 29.3; 29.2; 29.1; 26.0; 22.6; 14.1.

4-decyloxy-cinnamaldehyde (**32c**) was prepared in a method analogous to **32a** with the following exception: recrystallized from hexanes to afford **32c** (0.48 g, 97 %) as a light yellow powder; mp. 31-33 °C [lit.[51] 32-33 °C]; FTIR (thin film, cm^{-1}): 2925, 2854, 1679, 1602, 1512, 1468, 1260, 1175, 1127; ^{1}H NMR (300 MHz, $CDCl_3$) δ 9.67 (d, J = 7.67 Hz, 1H); 7.53 (d, J = 8.66 Hz, 2H); 7.44 (d, J = 15.89 Hz, 1H); 6.95 (d, J = 8.66 Hz, 2H);

6.63 (dd, J_1 = 15.89 Hz, J_2 = 7.67 Hz, 1H); 4.02 (t, J = 6.58 Hz, 2H); 1.82 (quin., J = 6.58 Hz, 2H); 1.54-1.22 (m, 14H); 0.90 (t, J = 6.58 Hz, 3H); ^{13}C NMR (300 MHz, $CDCl_3$) δ 193.7; 161.9; 152.8; 130.3; 126.6; 115.1; 68.3; 31.9; 29.5 (2C); 29.4; 29.3; 29.1; 26.0; 22.7; 14.1.

4-dodecyloxy-cinnamaldehyde (32d) was prepared in a method analogous to **32c**. (0.50 g, 100 %); mp. 40-44 °C; FTIR (thin film, cm^{-1}): 2921, 2852, 1675, 1603, 1513, 1470, 1251, 967; ^1H NMR (300 MHz, $CDCl_3$) δ 9.67 (d, J = 7.67 Hz, 1H); 7.53 (d, J = 8.66 Hz, 2H); 7.44 (d, J = 15.78 Hz, 1H); 6.95 (d, J = 8.66 Hz, 2H); 6.63 (dd, J_1 = 15.78 Hz, J_2 = 7.67 Hz, 1H); 4.02 (t, J = 6.58 Hz, 2H); 1.82 (quin., J = 6.58 Hz, 2H); 1.54-1.20 (m, 18H); 0.90 (t, J = 6.58 Hz, 3H); ^{13}C NMR (300 MHz, $CDCl_3$) δ 193.7; 161.9; 152.8; 130.3; 126.6; 115.1; 68.3; 31.9; 29.65; 29.63; 29.58; 29.56; 29.4 (2C); 29.1; 26.0; 22.7; 14.1.

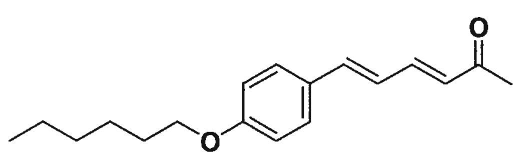

33a

6-(4-hexyloxy-phenyl)-hexa-3,5-dien-2-one (33a). To a solution of 4-hexyloxy-cinnamaldehyde (**32a**, 0.50 g, 2.15 mmol) and acetone (1.25 g, 21.52 mmol) in MeOH (20 mL) at 25 °C was added aqueous (5mL) NaOH (0.43 g, 10.76 mmol). The reaction mixture was allowed to stir for 1.0 hour, warmed to 40 °C and stirred for 24 hours. The yellow reaction mixture was poured into 2.0 M HCl (200 mL), and extracted with CH_2Cl_2 (3 × 75 mL). The combined organic layers were washed with H_2O (2 × 200 mL), dried over $MgSO_4$, filtered and the solvent removed *in vacuo*. Recrystallization from MeOH afforded **33a** (0.51 g, 87 %) as a yellow powder; mp. 73-76 °C; FTIR (thin film, cm^{-1}): 2955, 2938, 2862, 1661, 1259, 990, 840; ^1H NMR (300 MHz, $CDCl_3$) δ 7.43 (d, J = 8.66 Hz, 2H); 7.31 (dd, J_1 = 15.46 Hz, J_2 = 10.52 Hz, 1H); 6.93 (d, J = 15.46 Hz, 1H); 6.90 (d, J = 8.66 Hz, 2H); 6.78 (dd, J_1 = 15.46 Hz, J_2 = 10.52 Hz, 1H); 6.23 (d, J = 15.46

Hz, 1H); 4.00 (t, $J = 6.58$ Hz, 2H); 2.33 (s, 3H); 1.81 (quin., $J = 6.58$ Hz, 2H); 1.53-1.29 (m, 6H); 0.93 (t, $J = 6.58$ Hz, 3H); ^{13}C NMR (300 MHz, $CDCl_3$) δ 198.4; 160.2; 144.1; 141.2; 129.3; 128.8; 128.6; 124.4; 114.9; 68.2; 31.6; 29.2; 27.3; 25.7; 22.6; 14.0.

6-(4-octyloxy-phenyl)-hexa-3,5-dien-2-one (33b) was prepared in a method analogous to **33a** (0.49 g, 85 %); mp. 75-78 °C; FTIR (thin film, cm^{-1}): 2955, 2922, 2857, 1661, 1256, 990, 840; ^{1}H NMR (300 MHz, $CDCl_3$) δ 7.43 (d, $J = 8.66$ Hz, 2H); 7.30 (dd, $J_1 = 15.46$ Hz, $J_2 = 10.52$ Hz, 1H); 6.92 (d, $J = 15.46$ Hz, 1H); 6.90 (d, $J = 8.66$ Hz, 2H); 6.77 (dd, $J_1 = 15.46$ Hz, $J_2 = 10.52$ Hz, 1H); 6.23 (d, $J = 15.46$ Hz, 1H); 4.00 (t, $J = 6.58$ Hz, 2H); 2.33 (s, 3H); 1.81 (quin., $J = 6.58$ Hz, 2H); 1.55-1.23 (m, 10H); 0.91 (t, $J = 6.58$ Hz, 3H); ^{13}C NMR (300 MHz, $CDCl_3$) δ198.4; 160.2; 144.1; 141.2; 129.3; 128.8; 128.6; 124.4; 114.9; 68.2; 31.8; 29.3; 29.22; 29.19; 27.3; 26.0; 22.7; 14.1.

6-(4-decyloxy-phenyl)-hexa-3,5-dien-2-one (33c) was prepared in a method analogous to **33a** (0.49 g, 86 %); mp. 82-86 °C. IR (thin film, cm^{-1}): 2919, 2850, 1661, 1257, 990, 840; ^{1}H NMR (300 MHz, $CDCl_3$) δ 7.43 (d, $J = 8.55$ Hz, 2H); 7.30 (dd, $J_1 = 15.46$ Hz, $J_2 = 10.63$ Hz, 1H); 6.93 (d, $J = 15.46$ Hz, 1H); 6.90 (d, $J = 8.55$ Hz, 2H); 6.77 (dd, $J_1 = 15.46$ Hz, $J_2 = 10.63$ Hz, 1H); 6.23 (d, $J = 15.46$ Hz, 1H); 4.00 (t, $J = 6.58$ Hz, 2H); 2.33 (s, 3H); 1.81 (quin., $J = 6.58$ Hz, 2H); 1.54-1.20 (m, 14H); 0.90 (t, $J = 6.58$ Hz, 3H); ^{13}C NMR (300 MHz, $CDCl_3$) δ 198.4; 160.2; 144.1; 141.2; 129.3; 128.8; 128.6; 124.4; 114.9; 68.2; 31.9; 29.5 (2C); 29.4; 29.3; 29.2; 27.3; 26.0; 22.7; 14.1.

6-(4-dodecyloxy-phenyl)-hexa-3,5-dien-2-one (33d) Prepared in a method analogous to **33a** (0.49 g, 88 %); mp. 85-89 °C; FTIR (thin film, cm^{-1}): 2918, 2849, 1661, 1262, 990, 840; ^{1}H NMR (300 MHz, $CDCl_3$) δ 7.43 (d, $J = 8.66$ Hz, 2H); 7.30 (dd, $J_1 = 15.46$ Hz, $J_2 = 10.63$ Hz, 1H); 6.93 (d, $J = 15.46$ Hz, 1H); 6.90 (d, $J = 8.66$ Hz, 2H); 6.77 (dd, $J_1 = 15.46$ Hz, $J_2 = 10.63$ Hz, 1H); 6.23 (d, $J = 15.46$ Hz, 1H); 4.00 (t, $J = 6.58$ Hz, 2H); 2.33 (s, 3H); 1.81 (quin., $J = 6.58$ Hz, 2H); 1.54-1.21 (m, 18H); 0.90 (t, $J = 6.58$ Hz, 3H); ^{13}C NMR (300 MHz, $CDCl_3$) δ 198.4; 160.2; 144.1; 141.2; 129.3; 128.8; 128.6; 124.4; 114.9; 68.2; 31.9; 29.66; 29.64; 29.58; 29.56; 29.37; 29.34; 29.2; 27.3; 26.0; 22.7; 14.1.

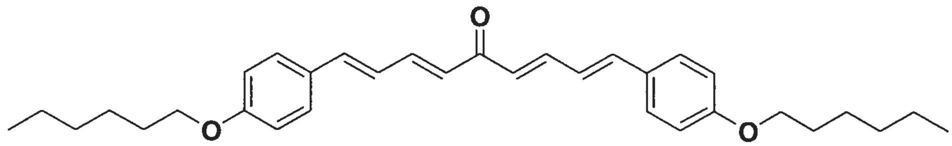

34a

1,9-Bis-(4-hexyloxy-phenyl)-nona-1,3,6,8-tetraen-5-one (**34a**). To a solution of 6-(4-hexyloxy-phenyl)-hexa-3,5-dien-2-one (**33a**, 0.20 g, 0.73 mmol) and 4-hexyloxy-cinnamaldehyde (**32a**, 0.17 g, 0.73 mmol) in THF (15 mL) was added NaOMe (25 wt % in MeOH, 0.48 mL, 2.20 mmol) dropwise. The resulting dark orange solution was allowed to stir for 30 minutes, was poured into 2.0 M HCl (100mL) and extracted with CH_2Cl_2 (2 × 100 mL). The combined organic layers were washed with H_2O (2 × 200 mL), dried over $MgSO_4$, filtered and the solvent removed *in vacuo*. Recrystallization from acetone afforded **34a** as a green/yellow solid (0.22 g, 62 %); mp. 147-151 °C; FTIR (thin film, cm^{-1}): 2926, 2851, 1655, 1592, 1509, 1464, 1359, 1257, 1174, 1071, 1005, 854, 821; ^{1}H NMR (300 MHz, $CDCl_3$) δ 7.48 (dd, J_1 = 15.13 Hz, J_2 = 10.41 Hz, 2H); 7.44 (d, J = 8.66 Hz, 4H); 6.95 (d, J = 15.46 Hz, 2H); 6.90 (d, J = 8.66 Hz, 4H); 6.84 (dd, J_1 = 15.46 Hz, J_2 = 10.41 Hz, 2H); 6.53 (d, J = 15.13 Hz, 2H); 4.00 (t, J = 6.58 Hz, 4H); 1.81 (quin., J = 6.58 Hz, 4H); 1.55-1.30 (m, 12H); 0.91 (t, J = 6.58 Hz, 6H); ^{13}C NMR (300 MHz, $CDCl_3$) δ 189.0; 160.2; 143.3; 141.2; 128.8; 128.7; 128.1; 124.8; 114.9; 68.2; 31.6; 29.2; 25.7; 22.6; 14.0.

1,9-Bis-(4-octyloxy-phenyl)-nona-1,3,6,8-tetraen-5-one (**34b**) was prepared in a method analogous to **34a** (0.21 g, 58 %); mp. 133-137 °C; FTIR (thin film, cm^{-1}): 2922, 2851, 1654, 1593, 1563, 1510, 1467, 1360, 1261, 1174, 1074, 999, 855, 825; ^{1}H NMR (300 MHz, $CDCl_3$) δ 7.48 (dd, J_1 = 15.46 Hz, J_2 = 10.52 Hz, 2H); 7.44 (d, J = 8.66 Hz, 4H); 6.95 (d, J = 15.46 Hz, 2H); 6.90 (d, J = 8.66 Hz, 4H); 6.84 (dd, J_1 = 15.46 Hz, J_2 = 10.52 Hz, 2H); 6.53 (d, J = 15.46 Hz, 2H); 4.00 (t, J = 6.58 Hz, 4H); 1.81 (quin., J = 6.58 Hz, 4H); 1.54-1.22 (m, 20H); 0.91 (t, J = 6.58 Hz, 6H); ^{13}C NMR (300 MHz, $CDCl_3$) δ 189.0; 160.2; 143.3; 141.2; 128.8; 128.7; 128.1; 124.8; 114.9; 68.2; 31.8; 29.3; 29.23; 29.21; 26.0; 22.7; 14.1.

1,9-Bis-(4-decyloxy-phenyl)-nona-1,3,6,8-tetraen-5-one (**34c**) was prepared in a method analogous to **34a** (0.25 g, 60 %); mp. 116-144 °C; FTIR (thin film, cm^{-1}): 2921, 2851, 1653, 1592, 1564, 1510, 1467, 1358, 1259, 1174, 1072, 998, 855, 824; ^1H NMR (300 MHz, $CDCl_3$) δ 7.48 (dd, J_1 = 15.13 Hz, J_2 = 10.41 Hz, 2H); 7.44 (d, J = 8.66 Hz, 4H); 6.95 (d, J = 15.46 Hz, 2H); 6.90 (d, J = 8.66 Hz, 4H); 6.84 (dd, J_1 = 15.46 Hz, J_2 = 10.41 Hz, 2H); 6.53 (d, J = 15.13 Hz, 2H); 4.00 (t, J = 6.58 Hz, 4H); 1.81 (quin., J = 6.58 Hz, 4H); 1.54-1.22 (m, 28H); 0.91 (t, J = 6.58 Hz, 6H); ^{13}C NMR (300 MHz, $CDCl_3$) δ 189.0; 160.2; 143.3; 141.2; 128.9; 128.7; 128.1; 124.8; 114.9; 68.2; 31.9; 29.56; 29.55; 29.4; 29.3; 29.2; 26.0; 22.7; 14.1.

1,9-Bis-(4-dodecyloxy-phenyl)-nona-1,3,6,8-tetraen-5-one (**34d**) was prepared in a method analogous to **34a** (0.28 g, 76 %); mp. 115-147 °C; FTIR (thin film, cm^{-1}): 2921, 2851, 1653, 1592, 1510, 1359, 1259, 1174, 1072, 999, 854; ^1H NMR (300 MHz, $CDCl_3$) δ 7.48 (dd, J_1 = 15.13 Hz, J_2 = 10.52 Hz, 2H); 7.44 (d, J = 8.66 Hz, 4H); 6.95 (d, J = 15.46 Hz, 2H); 6.90 (d, J = 8.66 Hz, 4H); 6.83 (dd, J_1 = 15.46 Hz, J_2 = 10.52 Hz, 2H); 6.53 (d, J = 15.13 Hz, 2H); 4.00 (t, J = 6.58 Hz, 4H); 1.81 (quin., J = 6.58 Hz, 4H); 1.54-1.21 (m, 36H); 0.91 (t, J = 6.58 Hz, 6H); ^{13}C NMR (300 MHz, $CDCl_3$) δ 188.9; 160.2; 143.3; 141.2; 128.9; 128.7; 128.1; 124.9; 114.9; 68.2; 31.9; 29.64; 29.61; 29.4; 29.3; 29.2; 26.0; 22.7; 14.1.

2.2.3.2 Bis-alkoxy 1,9-Diphenyl-1,3,6,8-tetraen-5-one Compounds

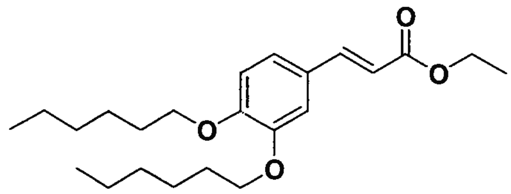

35e

3-(3,4-bis-hexyloxy-phenyl)-acrylic acid ethyl ester (35e). To a solution of 3,4-bis-hexyloxy benzaldehyde (**21e**, 2.00 g, 6.53 mmol) and mono-ethyl malonate (1.29 g, 9.79 mmol) in pyridine (45 mL) was added piperidine (0.64 mL, 6.53 mmol) dropwise. The resulting solution was heated to 80 °C for 16 hours. The reaction mixture was cooled to room temperature, poured into 2.0 M HCl (250 mL) and extracted with CH_2Cl_2 (2 × 200 mL). The combined organic layers were washed with H_2O (2 × 200 mL), dried over $MgSO_4$, filtered and the solvent remove *in vacuo*. Recrystallization from hexanes afforded **35e** (2.10 g, 85 %) as a light brown powder; mp. 36-39 °C; FTIR (thin film, cm^{-1}): 2932, 2860, 1711, 1634, 1598, 1512, 1469, 1305, 1259, 1164, 1138; ^1H NMR (300 MHz, $CDCl_3$) δ 7.63 (d, *J* = 16.00 Hz, 1H); 7.11-7.05 (m, 2H); 6.86 (d, *J* = 8.77 Hz, 1H); 6.30 (d, *J* = 16.00 Hz, 1H); 4.27 (q, *J* = 7.13 Hz, 2H); 4.03 (t, *J* = 6.58 Hz, 2H); 4.02 (t, *J* = 6.58 Hz, 2H); 1.84 (quin., *J* = 6.58 Hz, 4H); 1.57-1.26 (m, 15H); 0.93 (t, *J* = 6.58 Hz, 3H); 0.92 (t, *J* = 6.58 Hz, 3H); ^{13}C NMR (300 MHz, $CDCl_3$) δ 167.3; 151.3; 149.2; 144.7; 127.3; 122.6; 115.6; 113.0; 112.2; 69.3; 69.1; 60.3; 31.6 (2C); 29.2; 29.1; 25.7 (2C); 22.6 (2C); 14.4; 14.0 (2C).

3-(3,4-bis-octyloxy-phenyl)-acrylic acid ethyl ester (35f) was prepared in a method analogous to **35e** (2.68 g, 90 %); mp. 42-45 °C; FTIR (thin film, cm^{-1}): 2927, 2856, 1711, 1634, 1598, 1512, 1468, 1305, 1261, 1164, 1138; ^1H NMR (300 MHz, $CDCl_3$) δ 7.63 (d, *J* = 15.89 Hz, 1H); 7.12-7.05 (m, 2H); 6.86 (d, *J* = 8.77 Hz, 1H); 6.30 (d, *J* = 15.89 Hz, 1H); 4.27 (q, *J* = 7.13 Hz, 2H); 4.04 (t, *J* = 6.58 Hz, 2H); 4.03 (t, *J* = 6.58 Hz, 2H); 1.84 (quin., *J* = 6.58 Hz, 4H); 1.57-1.26 (m, 23H); 0.94-0.87 (m, 6H); ^{13}C NMR (300 MHz,

$CDCl_3$) δ 167.3; 151.3; 149.2; 144.7; 127.3; 122.6; 115.7; 113.0; 112.2; 69.3; 69.1; 60.3; 31.8 (2C); 29.4; 29.34; 29.27; 29.26; 29.2; 29.1; 26.01; 25.99; 22.7 (2C); 14.4; 14.0 (2C).

3-(3,4-bis-decyloxy-phenyl)-acrylic acid ethyl ester (35g) was prepared in a method analogous to **35e** (3.08 g, 96 %); mp. 52-55 °C; FTIR (thin film, cm^{-1}): 2925, 2855, 1710, 1634, 1597, 1512, 1467, 1305, 1260, 1163, 1138; ^1H NMR (300 MHz, $CDCl_3$) δ 7.63 (d, J = 15.89 Hz, 1H); 7.12-7.05 (m, 2H); 6.87 (d, J = 8.88 Hz, 1H); 6.30 (d, J = 15.89 Hz, 1H); 4.27 (q, J = 7.13 Hz, 2H); 4.04 (t, J = 6.58 Hz, 2H); 4.03 (t, J = 6.58 Hz, 2H); 1.84 (quin., J = 6.58 Hz, 4H); 1.56-1.21 (m, 31H); 0.90 (t, J = 6.58 Hz, 6H); ^{13}C NMR (300 MHz, $CDCl_3$) δ 167.3; 151.3; 149.2; 144.7; 127.3; 122.6; 115.6; 113.0; 112.3; 69.3; 69.1; 60.3; 31.9 (2C); 29.63; 29.61; 29.58 (2C); 29.41; 29.39; 29.35 (2C); 29.2; 29.1; 26.01; 25.99; 22.7 (2C); 14.4; 14.0 (2C).

3-(3,4-bis-dodecyloxy-phenyl)-acrylic acid ethyl ester (35h) was prepared in a method analogous to **35e** (3.29 g, 96 %); mp. 59-62 °C; FTIR (thin film, cm^{-1}): 2918, 2849, 1706, 1633, 1595, 1517, 1467, 1435, 1422, 1341, 1305, 1251, 1223, 1171, 1139, 1049, 978, 841; ^1H NMR (300 MHz, $CDCl_3$) δ 7.63 (d, J = 16.00 Hz, 1H); 7.12-7.05 (m, 2H); 6.87 (d, J = 8.77 Hz, 1H); 6.30 (d, J = 16.00 Hz, 1H); 4.28 (q, J = 7.13 Hz, 2H); 4.04 (t, J = 6.58 Hz, 2H); 4.03 (t, J = 6.58 Hz, 2H); 1.84 (quin., J = 6.58 Hz, 4H); 1.58-1.22 (m, 39H); 0.91 (t, J = 6.58 Hz, 6H); ^{13}C NMR (300 MHz, $CDCl_3$) δ 167.2; 151.5; 149.4; 144.6; 127.5; 122.5; 115.8; 113.4; 112.7; 69.5; 69.2; 60.2; 31.9 (2C); 29.64 (2C); 29.61 (2C); 29.58 (2C); 29.57 (2C); 29.4; 29.34; 29.31 (2C); 29.2; 26.01; 25.98; 22.6 (2C); 14.3; 14.0 (2C).

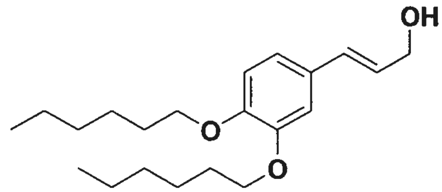

36e

3,4-bis-hexyloxy-cinnamyl alcohol (36e). To a solution of 3-(3,4-bis-hexyloxy-phenyl)-acrylic acid ethyl ester (**35e**, 0.67 g, 1.79 mmol) in anhydrous toluene (20 mL) at 0 °C was added DIBAL-H (4.48 mL, 1.0 M solution in hexanes) dropwise. The resulting solution was allowed to stir for 1 hour, warmed to room temperature and stirred for 24 hours. The reaction was quenched with H_2O (5 mL), poured into 2.0 M HCl (200 mL) and extracted with CH_2Cl_2 (3 × 75 mL). The combined organic layers were washed with H_2O (200 mL), brine (200 mL), dried over $MgSO_4$, filtered and the solvent removed *in vacuo* to afford **36e** (0.60 g, 100 %) as a clear, colourless oil; ^{1}H NMR (300 MHz, $CDCl_3$) δ 6.96 (d, J = 1.75 Hz, 1H); 6.90 (dd, J_1 = 8.22 Hz, J_2 = 1.75 Hz, 1H); 6.82 (d, J = 8.22 Hz, 1H); 6.52 (d, J = 15.78 Hz, 1H); 6.24 (dt, J_1 = 15.78 Hz, J_2 = 5.92 Hz, 1H); 4.31 (d, J = 5.92 Hz, 2H); 4.01 (t, J = 6.58 Hz, 2H); 4.00 (t, J = 6.58 Hz, 2H); 1.89-1.76 (m, 4H); 1.55-1.30 (m, 12H); 0.92 (t, J = 6.58 Hz, 6H); ^{13}C NMR (300 MHz, $CDCl_3$) δ 149.2; 149.1; 131.2; 129.9; 126.4; 119.8; 113.7; 69.34; 69.30; 63.8; 31.6 (2C); 29.30; 29.26; 25.7 (2C); 22.6 (2C); 14.0 (2C).

3,4-bis-octyloxy-cinnamyl alcohol (36f) was prepared in a method analogous to **36e** (0.70 g, 100 %); mp. 64-67 °C [lit.[52] 66 °C]; ^{1}H NMR (300 MHz, $CDCl_3$) δ 6.97 (d, J = 1.75 Hz, 1H); 6.92 (dd, J_1 = 8.22 Hz, J_2 = 1.75 Hz, 1H); 6.83 (d, J = 8.22 Hz, 1H); 6.55 (d, J = 15.89 Hz, 1H); 6.24 (dt, J_1 = 15.89 Hz, J_2 = 5.92 Hz, 1H); 4.31 (bs, 2H); 4.02 (t, J = 6.58 Hz, 2H); 4.01 (t, J = 6.58 Hz, 2H); 1.90-1.77 (m, 4H); 1.57-1.20 (m, 20H); 0.91 (t, J = 6.58 Hz, 6H); ^{13}C NMR (300 MHz, $CDCl_3$) δ 149.2; 131.4 (2C); 129.8; 126.3; 119.8; 113.7; 111.7; 69.4; 69.3; 63.9; 31.8 (2C); 29.4 (2C); 29.33; 29.29 (3C); 26.0 (2C); 22.7 (2C); 14.1 (2C).

3,4-bis-decyloxy-cinnamyl alcohol (**36g**) was prepared in a method analogous to **36e** (0.89 g, 100 %); ^{1}H NMR (300 MHz, $CDCl_3$) δ 6.97 (d, J = 1.75 Hz, 1H); 6.92 (dd, J_1 = 8.44 Hz, J_2 = 1.75 Hz, 1H); 6.83 (d, J = 8.44 Hz, 1H); 6.55 (d, J = 15.78 Hz, 1H); 6.24 (dt, J_1 = 15.78 Hz, J_2 = 5.92 Hz, 1H); 4.32 (bs, 2H); 4.02 (t, J = 6.58 Hz, 2H); 4.01 (t, J = 6.58 Hz, 2H); 1.89-1.77 (m, 4H); 1.55-1.21 (m, 28H); 0.91 (t, J = 6.58 Hz, 6H); ^{13}C NMR (300 MHz, $CDCl_3$) δ 149.2; 131.4 (2C); 129.8; 126.3; 119.8; 113.7; 111.7; 69.35; 69.29; 63.9; 31.9 (2C); 29.64 (2C); 29.59 (2C); 29.43 (2C); 29.35 (3C); 29.3; 26.05; 26.04; 22.7 (2C); 14.1 (2C).

3,4-bis-dodecyloxy-cinnamyl alcohol (**36h**) was prepared in a method analogous to **36e** (0.84 g, 93 %); mp. 62-65 °C [lit.[52] 65 °C]; ^{1}H NMR (300 MHz, $CDCl_3$) δ 6.97 (d, J = 1.75 Hz, 1H); 6.92 (dd, J_1 = 8.33 Hz, J_2 = 1.75 Hz, 1H); 6.83 (d, J = 8.33 Hz, 1H); 6.55 (d, J = 15.89 Hz, 1H); 6.24 (dt, J_1 = 15.89 Hz, J_2 = 5.92 Hz, 1H); 4.32 (bs, 2H); 4.02 (t, J = 6.58 Hz, 2H); 4.01 (t, J = 6.58 Hz, 2H); 1.89-1.77 (m, 4H); 1.55-1.21 (m, 37H); 0.90 (t, J = 6.58 Hz, 6H); ^{13}C NMR (300 MHz, $CDCl_3$) δ 149.2; 131.4 (2C); 12.98; 126.3; 119.8; 113.7; 111.7; 69.35; 69.30; 63.9; 31.9 (2C); 29.71 (2C); 29.65 (6C); 29.44 (2C); 29.37 (2C); 29.33; 29.29; 26.06; 26.04; 22.7 (2C); 14.1 (2C).

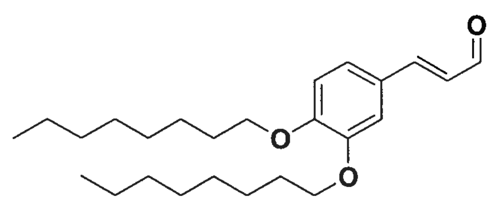

37f

3,4-bis-octyloxy-cinnamaldehyde (**37f**). To a solution of 2,3-dichloro-5,6-dicyano-benzoquinone (DDQ, 0.77 g, 3.41 mmol) in 1,4-dioxane (30 mL) was added 3,4-bis-octyloxy-cinnamyl alcohol (**36f**, 0.65 g, 1.66 mmol) as a solution in 1,4-dioxane (15 mL). The reaction mixture was allowed to stir for 1.0 hour, then filtered and the solvent removed *in vacuo*. Flash chromatography (EtOAc/hexanes 1:4) afforded **37f** (0.46 g, 71 %) as a white/brown powder; mp. 41-44 °C [lit.[52] 44 °C]; ^{1}H NMR (300 MHz, $CDCl_3$) δ 9.67 (d, J = 7.67 Hz, 1H); 7.41 (d, J = 15.78 Hz, 1H); 7.14 (dd, J_1 = 8.33 Hz, J_2 = 1.86

Hz, 1H); 7.10 (d, J = 1.86 Hz, 1H); 6.90 (d, J = 8.33 Hz, 1H); 6.61 (dd, J_1 = 15.78 Hz, J_2 = 7.67 Hz, 1H); 4.06 (t, J = 6.58 Hz, 2H); 4.04 (t, J = 6.58 Hz, 2H); 1.86 (quin., J = 6.58 Hz, 4H); 1.56-1.23 (m, 20H); 0.91 (t, J = 6.58 Hz, 6H); ^{13}C NMR (300 MHz, $CDCl_3$) δ 193.6; 153.1; 152.3; 149.3; 126.9; 126.5; 123.4; 112.9; 112.5; 69.4; 69.1; 31.8 (2C); 29.4; 29.33; 29.26; 29.25; 29.2; 29.1; 26.01; 25.98; 22.7 (2C); 14.1 (2C).

3,4-bis-decyloxy-cinnamaldehyde (**37g**) was prepared in a method analogous to **37f** (0.65 g, 77 %); ^{1}H NMR (300 MHz, $CDCl_3$) δ 9.67 (d, J = 7.67 Hz, 1H); 7.41 (d, J = 15.78 Hz, 1H); 7.14 (dd, J_1 = 8.22 Hz, J_2 = 1.86 Hz, 1H); 7.10 (d, J = 1.86 Hz, 1H); 6.90 (d, J = 8.22 Hz, 1H); 6.61 (dd, J_1 = 15.78 Hz, J_2 = 7.67 Hz, 1H); 4.06 (t, J = 6.58 Hz, 2H); 4.04 (t, J = 6.58 Hz, 2H); 1.86 (quin., J = 6.58 Hz, 4H); 1.56-1.19 (m, 28H); 0.90 (t, J = 6.58 Hz, 6H); ^{13}C NMR (300 MHz, $CDCl_3$) δ 193.6; 153.1; 152.3; 149.3; 126.9; 126.5; 123.4; 112.9; 112.5; 69.4; 69.1; 31.9 (2C); 29.63; 29.61; 29.58 (2C); 29.41; 29.37; 29.35 (2C); 29.2; 29.1; 26.01; 25.98; 22.7 (2C); 14.1 (2C).

3,4-bis-dodecyloxy-cinnamaldehyde (**37h**) was prepared in a method analogous to **37f** (0.70 g, 88 %); mp. 75-78 °C [lit.[52] 76 °C]; ^{1}H NMR (300 MHz, $CDCl_3$) δ 9.67 (d, J = 7.67 Hz, 1H); 7.41 (d, J = 15.78 Hz, 1H); 7.14 (dd, J_1 = 8.33 Hz, J_2 = 1.75 Hz, 1H); 7.10 (d, J = 1.75 Hz, 1H); 6.90 (d, J = 8.33 Hz, 1H); 6.61 (dd, J_1 = 15.78 Hz, J_2 = 7.67 Hz, 1H); 4.06 (t, J = 6.58 Hz, 2H); 4.04 (t, J = 6.58 Hz, 2H); 1.86 (quin., J = 6.58 Hz, 4H); 1.57-1.19 (m, 36H); 0.90 (t, J = 6.58 Hz, 6H); ^{13}C NMR (300 MHz, $CDCl_3$) δ 193.6; 153.1; 152.3; 149.3; 126.9; 126.5; 123.4; 112.9; 112.5; 69.4; 69.1; 31.9 (2C); 29.69 (2C); 29.66 (2C); 29.63 (2C); 29.61 (2C); 29.41; 29.37 (3C); 29.2; 29.1; 26.01; 25.98; 22.7 (2C); 14.1 (2C).

Chapter 3

Results and Discussion

3.1 General

A series of C_2 symmetric compounds with benzophenone, dibenzylidene acetone or 1,9-diphenyl-nona-1,3,6,8-tetraen-5-one cores were prepared. Derivatives were synthesized with either 1 or 2 linear alkoxy side chains which varied in length from C_6H_{13} to $C_{12}H_{25}$. The proposed synthesis of compounds with 3 alkoxy side chains, as well as the synthesis of 1,9-diphenyl-nona-1,3,6,8-tetraen-5-ones with 2 alkoxy side chains was not completed due to a number of difficulties encountered in the original synthetic plan which would result in longer, more complex syntheses for these compounds.

3.2 Synthesis

3.2.1 Mono-alkoxy Benzophenone Compounds 2a-d

The mono-alkoxy benzophenone compounds **2a-d** were prepared simply by a Williamson ether synthesis[26] to append the alkoxy side chains to 4,4'-dihydroxy-benzophenone **1** (**Scheme 3.1**).

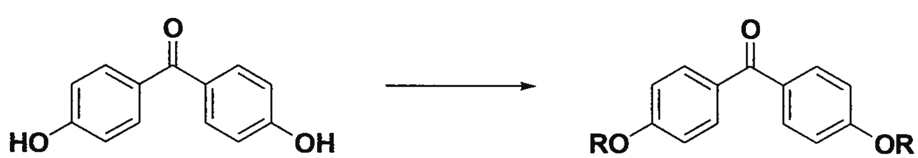

Scheme 3.1 Reagents and conditions: K_2CO_3, acetone, RBr, reflux 24 h. (R = C_6H_{13} (**a**), C_8H_{17} (**b**), $C_{10}H_{21}$ (**c**), $C_{12}H_{25}$ (**d**)).

The products were prepared in one step with yields ranging from 64 % (C_{12}) to 97 % (C_6). The compounds were characterized by FTIR, ^{1}H and ^{13}C NMR spectroscopy. **Figures 3.1-3.3** display the FTIR, ^{1}H NMR and ^{13}C NMR spectra for bis-(4-hexyloxy-phenyl)-methanone **2a**. Characteristic FTIR absorptions include the alkyl C-H stretches (2955, 2938, 2863 cm^{-1}), conjugated ketone C=O stretch (1636 cm^{-1}), aromatic C=C stretch (1604 cm^{-1}) and ether C-O stretch (1027 cm^{-1}). The ^{1}H NMR chemical shifts were assigned as: δ 7.79, 6.96 (aromatic C-**H**), 4.05 (O-C**H**$_2$-C), 1.84 (O-CH$_2$-C**H**$_2$-CH$_2$) 1.56-1.31 (C**H**$_2$-C**H**$_2$-C**H**$_2$-CH$_3$) and 0.94 (CH$_2$-C**H**$_3$). The ^{13}C NMR chemical shifts were assigned as: δ 194.5 (ketone **C**=O), 162.4, 132.2 (aromatic quaternary **C**), 130.6, 113.9 (aromatic **C**-H), 68.2 (O-**C**H$_2$), 31.6 (**C**H$_2$-CH$_2$-CH$_3$), 29.1 (O-CH$_2$-**C**H$_2$), 25.7 (O-CH$_2$-CH$_2$-**C**H$_2$), 22.6 (**C**H$_2$-CH$_3$) and 14.0 (CH$_2$-**C**H$_3$).

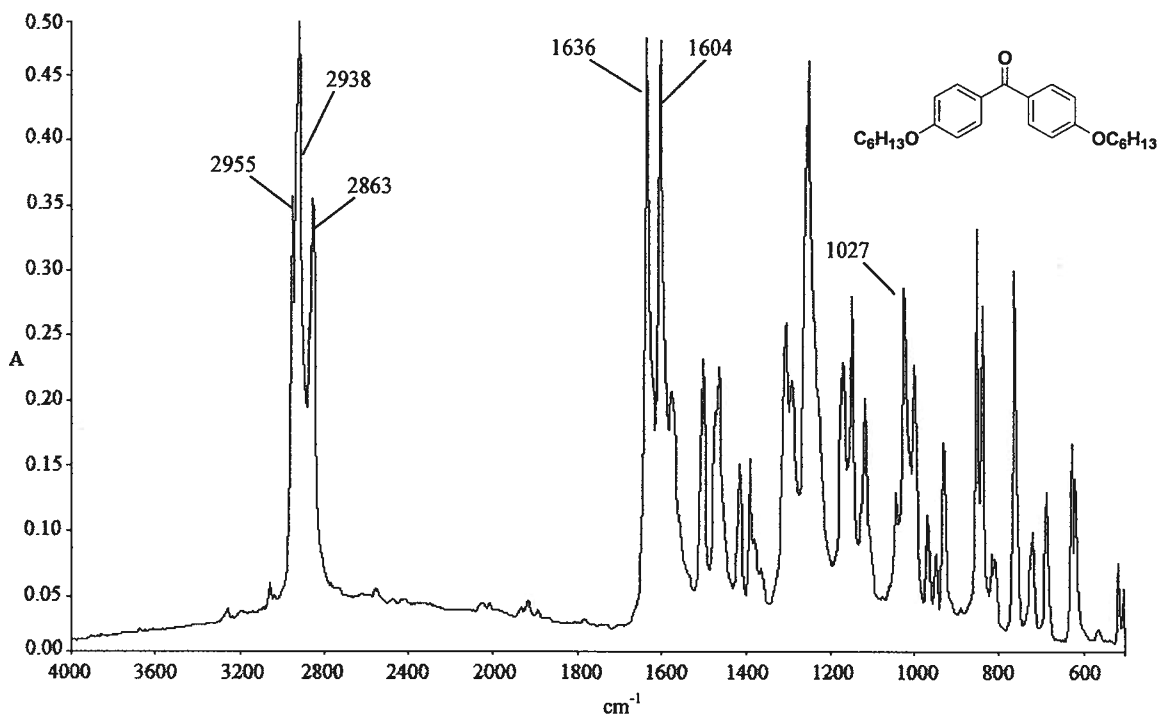

Figure 3.1: FTIR spectrum of **2a**.

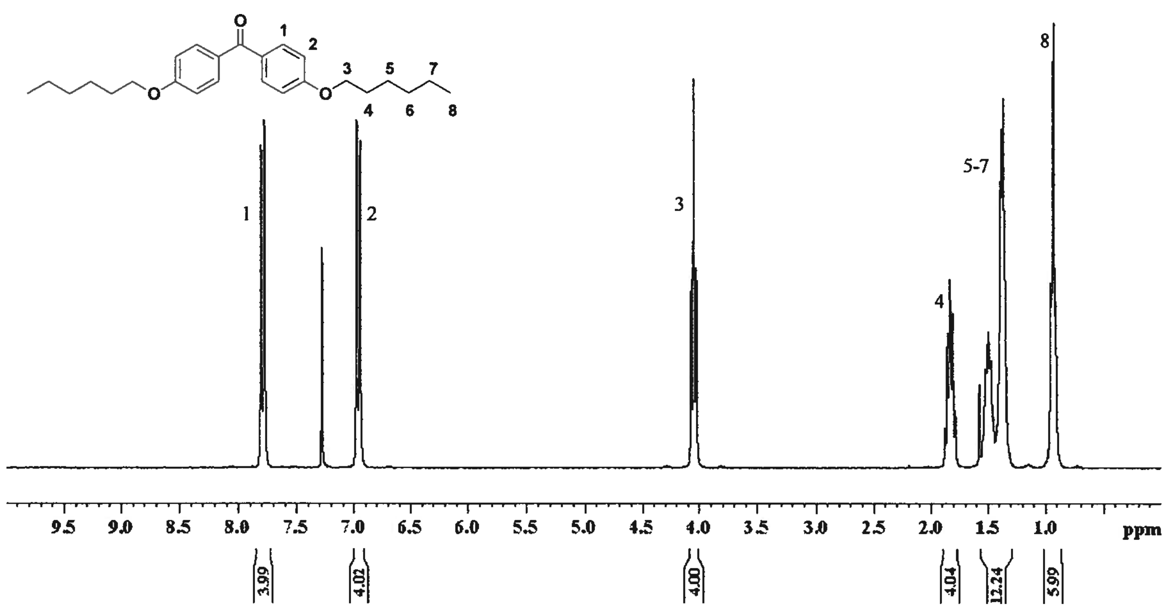

Figure 3.2: ^{1}H NMR spectrum of **2a**.

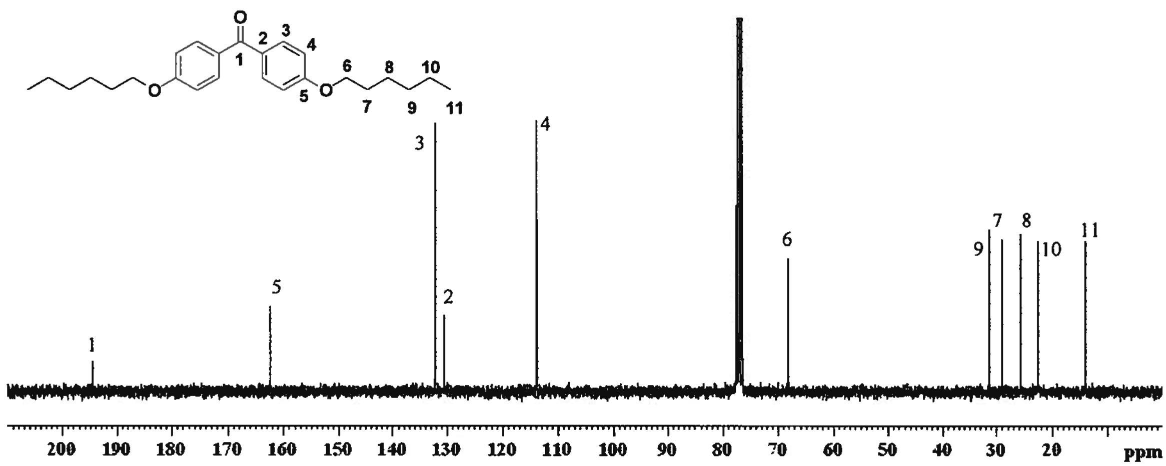

Figure 3.3: ^{13}C NMR spectrum of **2a**.

Appendix A contains FTIR, ^{1}H NMR and ^{13}C NMR spectra for the C_8, C_{10} and C_{12} derivatives **2b**, **2c** and **2d**.

3.2.2 Bis-alkoxy Benzophenone Compounds 9e-h

The synthesis of the first fragment of the bis-alkoxy substituted benzophenones began with the Fisher esterification[53] of commercially available 3,4-dihydroxy-benzoic acid (**3**) to give the methyl ester **4**. The alkoxy chains were appended again using the Williamson ether synthesis[26] to afford the methyl-3,4-bis-alkoxy benzoates **5e-h** in yields of 78 % (C_6) to 81 % (C_8) over two steps (**Scheme 3.2**).

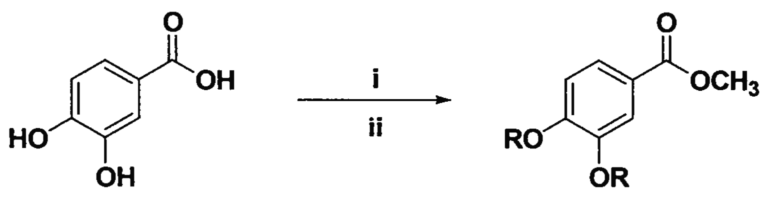

3 5e-h

Scheme 3.2 Reagents and conditions: i) H_2SO_4, MeOH, reflux 24 h; ii) K_2CO_3, acetone, RBr, reflux 48 h. (R = C_6H_{13}, C_8H_{17}, $C_{10}H_{21}$, $C_{12}H_{25}$)

Saponification of esters **5e-h**[40-42] achieved the desired 3,4-bis-alkoxy benzoic acid coupling precursors **6e-h** in yields ranging from 88 % (C_{10}) to 99 % (C_8) (**Scheme 3.3**).

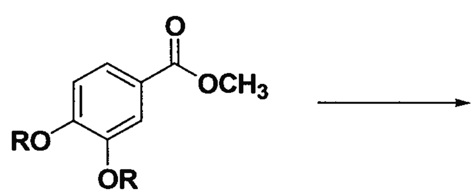

5e-h 6e-h

Scheme 3.3 Reagents and conditions: KOH, H_2O, MeOH, reflux 24 h.

The synthesis of the second coupling fragments was achieved simply by another Williamson ether synthesis[26] starting with catechol (**7**) and the using the appropriate n-alkyl bromide.[54] The substituted catechols **8e-h** were prepared in yields from 94 % (C_{10}) to 100 % (C_{12}). Coupling of the two fragments was accomplished by Friedel-Crafts acylation.[30] The benzoic acids **6e-h** were first converted to their respective acid chlorides, and then added to a solution containing aluminum chloride and catechol derivatives **8e-h** (**Scheme 3.4**). The Friedel-Crafts acylations to achieve benzophenones **9e-h** proceeded in yields ranging from 56 % (C_{12}) to 69 % (C_{10}).

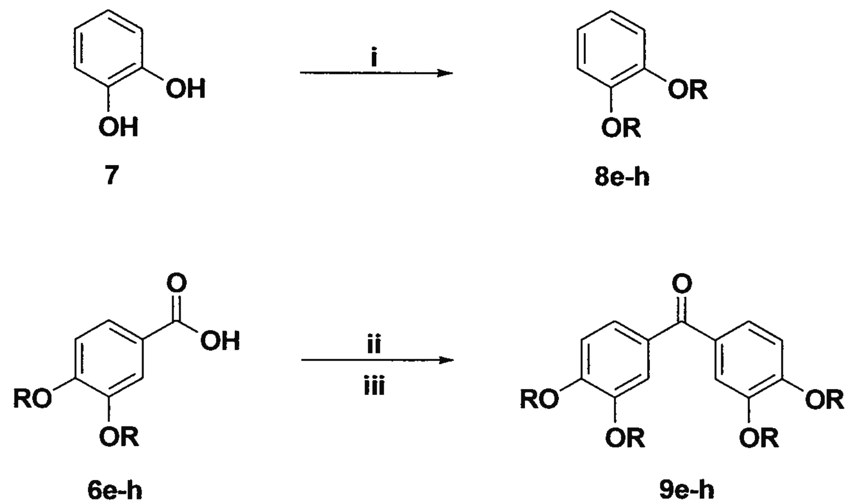

Scheme 3.4 Reagents and conditions: i) K_2CO_3, acetone, RBr, reflux 48 h. (R = C_6H_{13}, C_8H_{17}, $C_{10}H_{21}$, $C_{12}H_{25}$); ii) CH_2Cl_2, $HNEt_2$, $SOCl_2$, reflux 1.5 h; iii) $AlCl_3$, CH_2Cl_2, **8e-h** 0°C-rt. 24 h.

The bis-alkoxy benzophenones **9e-h** were prepared in four linear steps (five total steps) with overall yields ranging from 40 % (C_{12}) to 52 % (C_8). The compounds were characterized by FTIR, ^1H and ^{13}C NMR spectroscopy. **Figures 3.4-3.6** display FTIR, ^1H NMR and ^{13}C NMR spectra for bis-(3,4-bis-hexyloxy-phenyl)-methanone **9e**, respectively. Characteristic FTIR absorptions include the alkyl C-H stretches (2931, 2860 cm^{-1}), conjugated ketone C=O stretch (1649 cm^{-1}), aromatic C=C stretch (1595 cm^{-1}) and ether C-O stretch (1017 cm^{-1}). The ^1H NMR chemical shifts assigned were: δ 7.42, 7.37 and 6.90 (aromatic C-**H**), 4.09, 4.06 (O-C**H**$_2$-C), 1.93-1.79 (O-CH_2-C**H**$_2$-CH_2) 1.58-1.30 (C**H**$_2$-C**H**$_2$-C**H**$_2$-CH_3) and 0.93 (CH_2-C**H**$_3$). The ^{13}C NMR chemical shifts were assigned: δ 194.5 (ketone **C**=O), 152.8, 148.7 and 130.7 (aromatic quaternary **C**), 124.7, 114.7 and 111.5 (aromatic **C**-H), 69.3 and 69.1 (O-**C**H$_2$), 31.58 and 31.56 (**C**H$_2$-CH_2-CH_3), 29.2 and 29.1 (O-CH_2-**C**H$_2$), 25.69 and 25.66 (O-CH_2-CH_2-**C**H$_2$), 22.6 (**C**H$_2$-CH_3) and 14.0 (CH_2-**C**H$_3$).

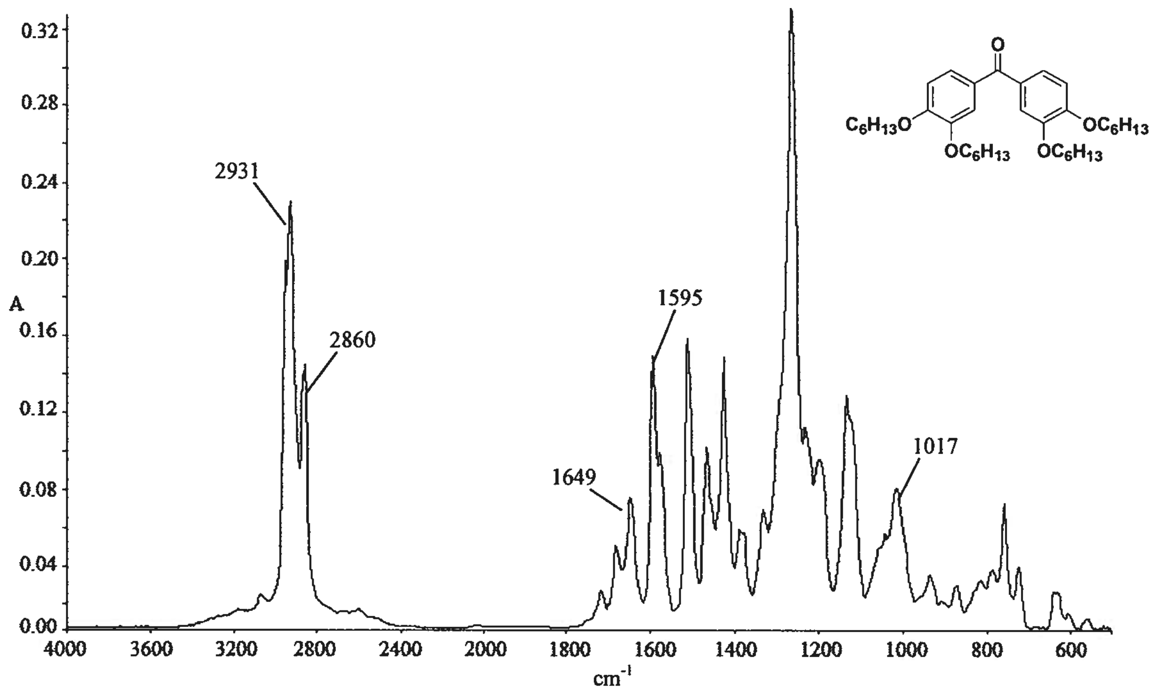

Figure 3.4: FTIR spectrum of **9e**.

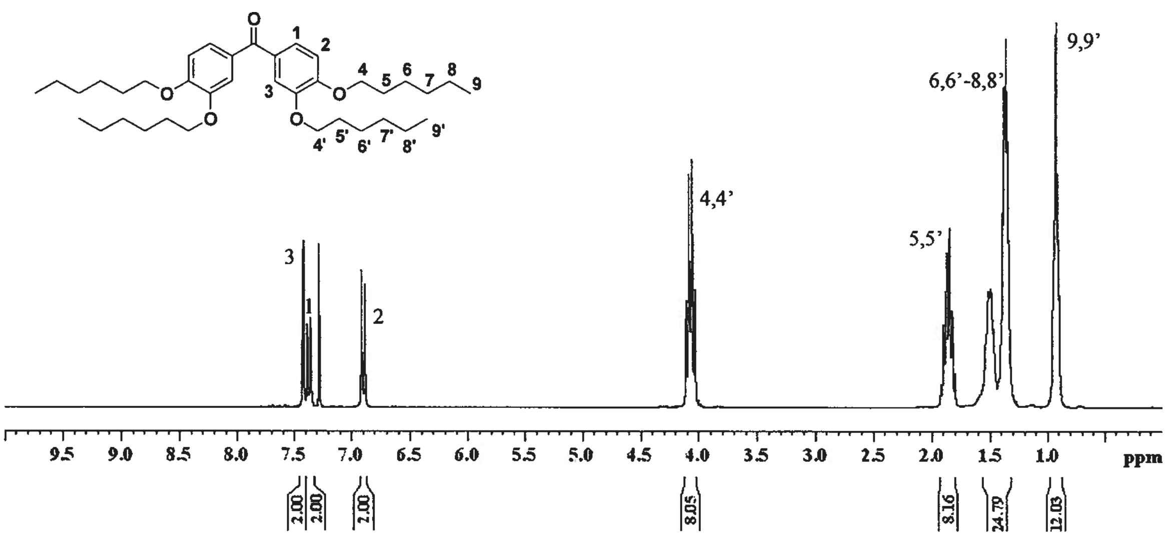

Figure 3.5: ^{1}H NMR spectrum of **9e**.

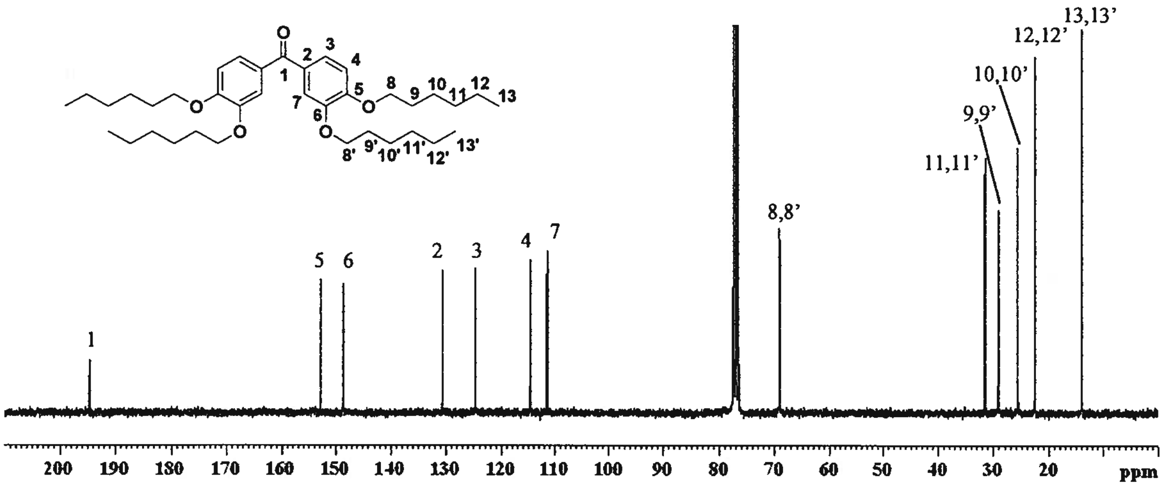

Figure 3.6: ^{13}C NMR spectrum of **9e**.

Appendix A contains FTIR, ^{1}H and ^{13}C NMR spectra for the C_8, C_{10} and C_{12} derivatives **9f, 9g** and **9h**, respectively.

3.2.3 Tris-alkoxy Benzophenone Compounds 16i-l

The synthesis of the tris-alkoxy substituted benzophenones began with the Fisher esterification[53] of commercially available gallic acid (**10**) to give the methyl ester **11**. The alkoxy chains were appended again using the Williamson ether synthesis[26] to afford the methyl-3,4,5-tris-alkoxy benzoates **12i-l** in yields of 62 % (C_6) to 69 % (C_1) over two steps (**Scheme 3.5**).

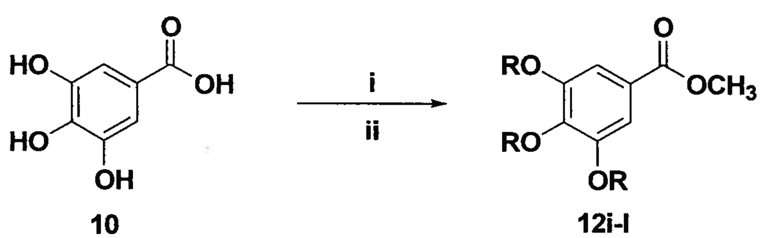

Scheme 3.5 Reagents and conditions: i) H_2SO_4, MeOH, reflux 24 h; ii) K_2CO_3, acetone, RBr, reflux 48 h. (R = C_6H_{13}, C_8H_{17}, $C_{10}H_{21}$, $C_{12}H_{25}$)

Saponification of the esters **12i-l** achieved the desired 3,4,5-tris-alkoxy benzoic acid coupling precursors **13i-l** in yields ranging from 85 % (C_{10}) to 94 % (C_{12}) (**Scheme 3.6**).

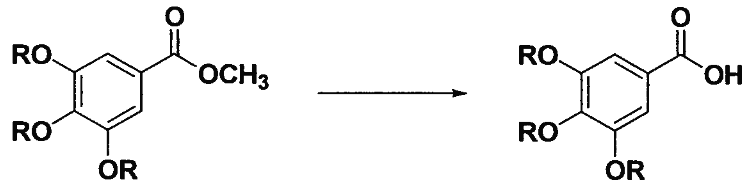

12i-l   13i-l

Scheme 3.6 Reagents and conditions: KOH, H_2O, MeOH, reflux 24 h.

The synthesis of the second coupling fragments was achieved simply by another Williamson ether synthesis[26] starting with pyrogallol (**14**) and the using the appropriate n-alkyl bromide. The substituted pyrogallols **15i-l** were prepared in yields from 74 % (C_{10}) to 87 % (C_6). Attempted coupling of the two C_8 fragments by Friedel-Crafts acylation[30] led to an asymmetric product **16j**, as identified by ^{1}H NMR. The benzoic acid **13j** was first converted to the corresponding acid chloride and added to a solution containing aluminum chloride and 1,2,3-tris-octyloxy benzene **15i** (**Scheme 3.7**).

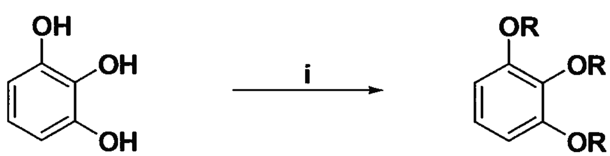

14   15i-l

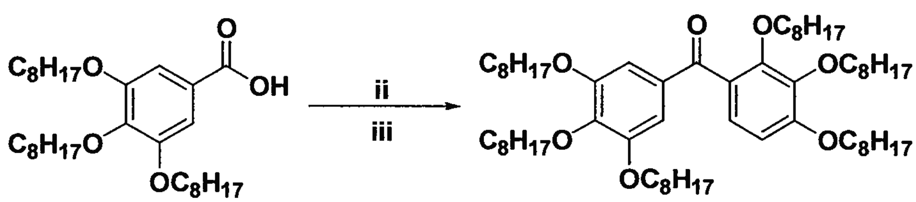

13j   16j

Scheme 3.7 Reagents and conditions: i) K_2CO_3, acetone, RBr, reflux 48 h. (R = C_6H_{13}, C_8H_{17}, $C_{10}H_{21}$, $C_{12}H_{25}$); ii) CH_2Cl_2, $HNEt_2$, $SOCl_2$, reflux 1.5 h; iii) $AlCl_3$, CH_2Cl_2, **24j** 0°C-rt. 24 h.

The reaction proceeded in 65 % yield. **Figure 3.7** displays the ^{1}H NMR spectrum for the (2,3,4-tri-octyloxy-phenyl)-(3,4,5-tri-octyloxy-phenyl)-methanone **16j**. The ^{1}H NMR chemical shifts were assigned as: δ 7.09, 7.04 and 6.70 (aromatic C-**H**), 4.08-3.91 (O-CH_2-C), 1.93-1.71 (O-CH_2-$\mathbf{CH_2}$-CH_2) 1.56-1.11 ($\mathbf{CH_2}$-$\mathbf{CH_2}$-$\mathbf{CH_2}$-$\mathbf{CH_2}$-$\mathbf{CH_2}$-CH_3) and 0.95-0.84 (CH_2-$\mathbf{CH_3}$).

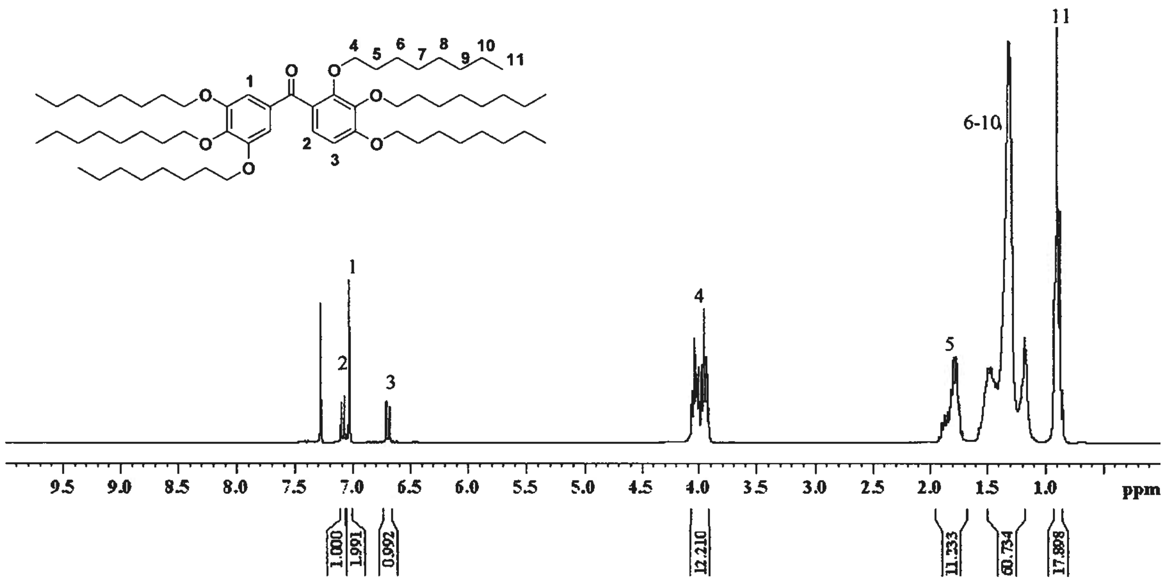

Figure 3.7: ^{1}H NMR spectrum of (2,3,4-tris-octyloxy-phenyl)-(3,4,5-tris-octyloxy-phenyl)-methanone **16j**.

The attempted synthesis of the tris-alkoxy benzophenones **16i-l** resulted in the synthesis of (2,3,4-tris-alkoxy-phenyl)-(3,4,5-tris-alkoxy-phenyl)-methanone (**Figure 3.8a**), instead of the desired bis-(3,4,5-tris-alkoxy-phenyl)-methanone (**Figure 3.8b**).

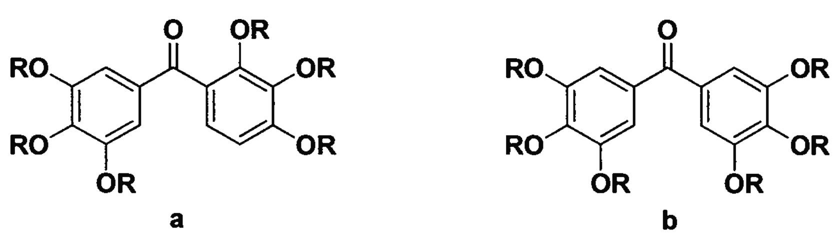

Figure 3.8: **a**) (2,3,4-tris-alkoxy-phenyl)-(3,4,5-tris-alkoxy-phenyl)-methanone; **b**) bis-(3,4,5-tris-alkoxy-phenyl)-methanone.

The resulting asymmetric product formed can be rationalized in terms of directing groups for electrophilic aromatic substitution. All three ether groups on the 1,2,3-tris-octyloxy benzene are activating *o*, *p* directors. The 1-octyloxy and 3-octyloxy groups will direct the acylation to the 4 or 6 position (which are equivalent), while the 2-octyloxy group will direct the acylation to the 1, 3 (blocked) or 5 position. Thus, the expected result is a majority of substitution at the 4 position, which is what was observed.

As the goal for this research was the synthesis and mesophase behaviour of C_2 symmetric liquid crystalline materials, the synthesis of these targets was abandoned. This decision was supported by the finding that increasing the number of alkoxy chains seems to attenuate liquid crystalline mesophase formation.

3.2.4 Mono-alkoxy Dibenzylidene Acetone Compounds 19a-d

The 4-alkoxy benzaldehydes **18a-d** were prepared by a Williamson ether synthesis[26] starting with 4-hydroxy-benzaldehyde (**17**) and the appropriate alkyl bromide in yields ranging from 86 % (C_{12}) to 100 % (C_6) (**Scheme 3.8**).[55]

17 **18a-d**

Scheme 3.8 Reagents and conditions: RBr, K_2CO_3, DMF, 20 h, 25 °C (R = C_6H_{13}, C_8H_{17}, $C_{10}H_{21}$, $C_{12}H_{25}$).

The mono-alkoxy dibenzylidene-acetone targets **19a-d** were prepared by a bidirectional aldol condensation between one equivalent of acetone and two equivalents of 4-alkoxy benzaldehydes **18a-d** (**Scheme 3.9**).[22] The mono-alkoxy dba compounds were achieved in two steps with overall yields ranging from 58 % (C_6; C_{12}) to 72 % (C_{10}).

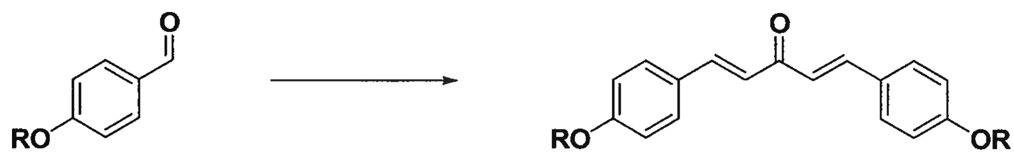

18a-d **19a-d**

Scheme 3.9: Reagents and conditions: Acetone, NaOH, H_2O, MeOH, 72 h, 25 °C (R = C_6H_{13}, C_8H_{17}, $C_{10}H_{21}$, $C_{12}H_{25}$).

The compounds were characterized by FTIR, ^{1}H and ^{13}C NMR spectroscopy. **Figures 3.9–3.11** display FTIR, ^{1}H NMR and ^{13}C NMR spectra for 1,5-bis-(4-hexyloxy-phenyl)-penta-1,4-dien-3-one **19a**, respectively. Characteristic FTIR absorptions include the alkyl C-H stretches (2934, 2869 cm^{-1}), ketone C=O stretch (1651 cm^{-1}), aromatic C=C stretch (1599 cm^{-1}) and ether C-O stretch (1030 cm^{-1}). The ^{1}H NMR chemical shifts were assigned as: δ 7.72, 6.97 (olefinic C-**H**, trans); 7.58, 6.94 (aromatic C-**H**); 4.02 (O-C**H**$_2$); 1.82 (O-CH$_2$-C**H**$_2$); 1.54-1.29 (C**H**$_2$-C**H**$_2$-C**H**$_2$-CH$_3$) and 0.93 (CH$_2$-C**H**$_3$). The stereochemistry of the olefins was assigned as E, based on the characteristic *J* coupling constants of 15.78 Hz.[56] The ^{13}C NMR chemical shifts were assigned as: δ 188.9 (ketone **C**=O); 161.2, 127.4 (aromatic quaternary **C**); 142.7, 123.4 (olefinic **C**-H); 130.1, 114.9 (aromatic **C**-H); 68.2 (O-**C**H$_2$); 31.6 (**C**H$_2$-CH$_2$-CH$_3$); 29.1 (O-CH$_2$-**C**H$_2$); 25.7 (O-CH$_2$-CH$_2$-**C**H$_2$); 22.6 (**C**H$_2$-CH$_3$) and 14.0 (CH$_2$-**C**H$_3$).

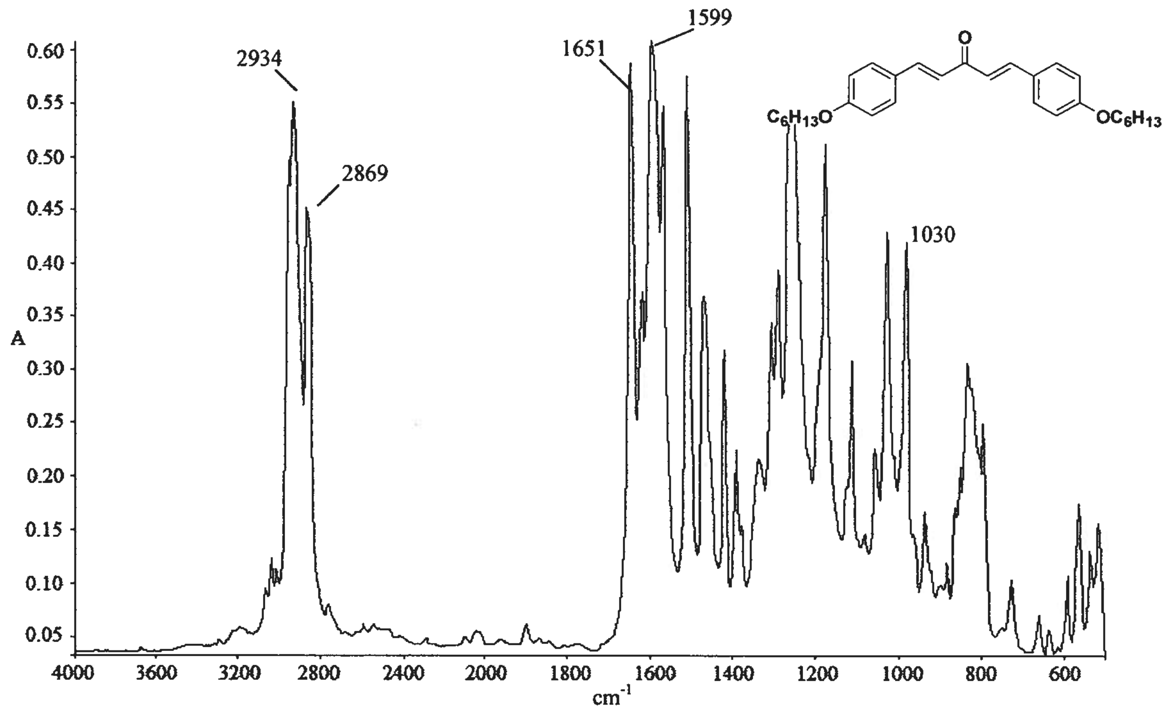

Figure 3.9: FTIR spectrum of **19a**

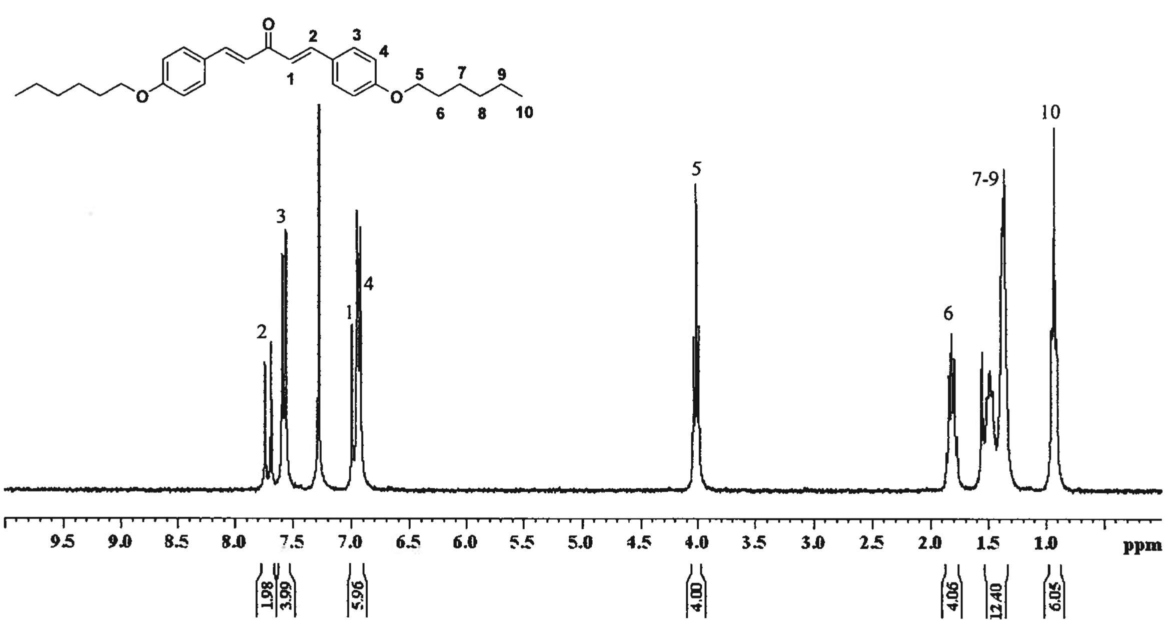

Figure 3.10: ^{1}H NMR spectrum of **19a**.

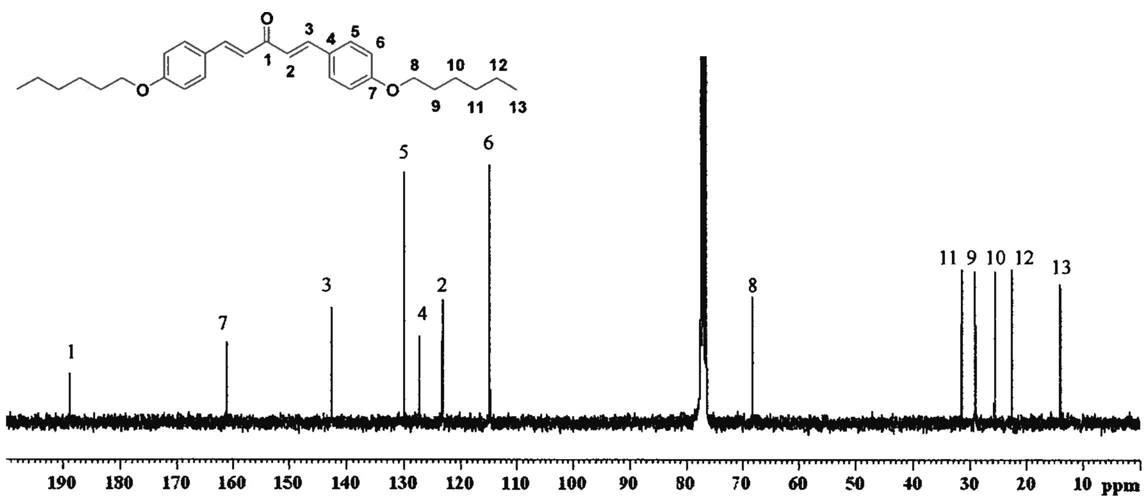

Figure 3.11: ^{13}C NMR spectrum of **19a**.

Appendix A contains FTIR, ^{1}H NMR and ^{13}C NMR spectra for the C_8, C_{10} and C_{12} derivatives **19b**, **19c**, and **19d**.

3.2.5 Bis-alkoxy Dibenzylidene Acetone Compounds 23e-h

The 3,4-bis-alkoxy dba compounds **23e-h** were prepared in a method analogous to that of the mono-alkoxy dba compounds **19a-d**, with the exception that instead of a bidirectional aldol condensation, two stepwise aldol condensations were employed.

The 3,4-bis-alkoxy benzaldehydes **21e-h** were prepared by a Williamson ether synthesis[26] starting from 3,4-bis-hydroxy-benzaldehyde (**20**) and the appropriate n-alkyl bromide (**Scheme 3.10**).[48,57] **21e-h** were prepared in yields ranging from 89 % (C_8) to 100 % (C_{10}).

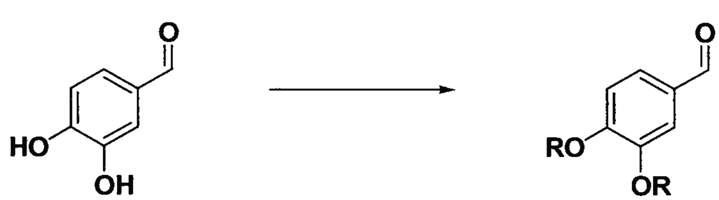

20

21e-h

Scheme 3.10: Reagents and conditions: RBr, K_2CO_3, DMF, 20 h, 25 ° C (R = C_6H_{13}, C_8H_{17}, $C_{10}H_{21}$, $C_{12}H_{25}$).

The intended synthetic route of a bidirectional aldol condensation proved difficult, resulting in an inseparable mix of both the mono-aldol condensation and bis-aldol condensation products. This was avoided through the use of stepwise aldol condensations (**Scheme 3.11**). The first condensation to afford **22e-h** proceeded in yields ranging from 70 % (C_8; C_{10}) to 100 % (C_{12}) and the second condensation to afford products **23e-h** proceeded in yields ranging from 50 % (C_{10}) to 61 % (C_8).

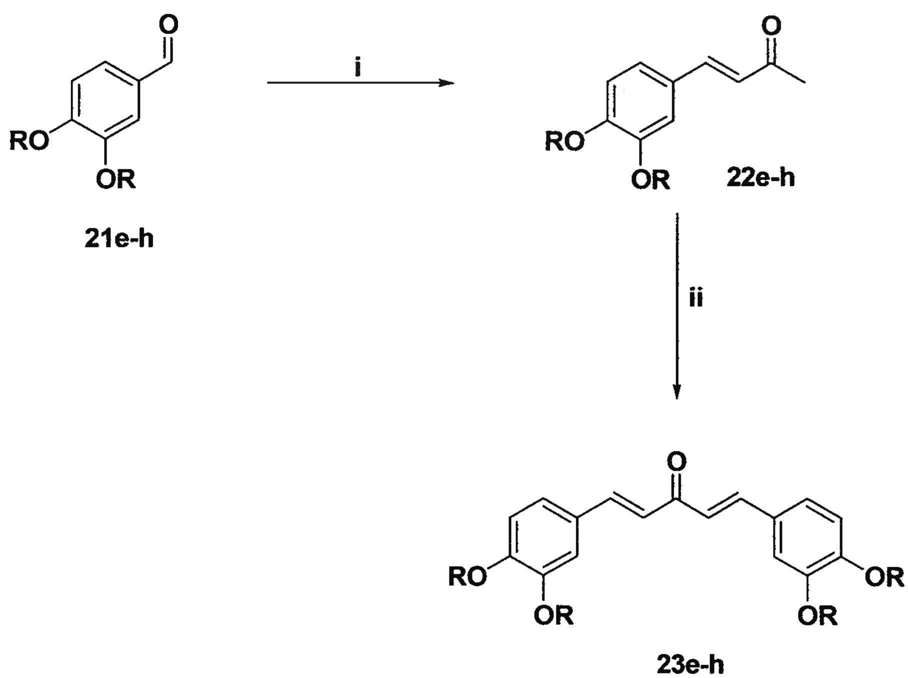

Scheme 3.11: Reagents and conditions: i) NaOMe, acetone, MeOH, reflux 24 h. ii) **21e-h**, NaOMe, MeOH, reflux 48 h.

The 3,4-bis-alkoxy dba compounds **23e-h** were prepared in three steps with overall yields between 35 % (C_{10}) and 55 % (C_{12}). The compounds were characterized by FTIR, ^1H and ^{13}C NMR spectroscopy. **Figures 3.12–3.14** display FTIR, ^1H NMR and ^{13}C NMR Spectra for 1,5-bis-(3,4-bis-hexyloxy-phenyl)-penta-1,4-dien-3-one **23e**. Characteristic FTIR absorptions include the alkyl C-H stretches (2955, 2931, 2860 cm^{-1}), ketone C=O stretch (1648 cm^{-1}), aromatic C=C stretch (1595 cm^{-1}) and ether C-O stretch (1017 cm^{-1}). The ^1H NMR chemical shifts were assigned as: δ 7.69, 6.95 (olefinic C-**H**, trans); 7.21-7.15, 6.90 (aromatic C-**H**); 4.07, 4.06 (O-C**H**$_2$); 1.87, 1.86 (O-CH$_2$-C**H**$_2$); 1.56-1.26 (C**H**$_2$-C**H**$_2$-

$\mathbf{CH_2}$-CH_3); and 0.93 (CH_2-$\mathbf{CH_3}$). Again the stereochemistry of the olefins was assigned as E, based on the characteristic *J* coupling constant of 15.78 Hz.[56] The ^{13}C NMR chemical shifts were assigned as: δ 188.8 (ketone **C**=O); 151.6, 149.2, 127.8 (aromatic quaternary **C**); 143.1, 123.5 (olefinic **C**-H); 123.1, 113.0, 112.6 (aromatic **C**-H); 69.4, 69.1 (O-$\mathbf{CH_2}$); 31.59, 31.56 ($\mathbf{CH_2}$-CH_2-CH_3); 29.2, 29.1 (O-CH_2-$\mathbf{CH_2}$); 25.71, 25.67 (O-CH_2-CH_2-$\mathbf{CH_2}$); 22.62, 22.59 ($\mathbf{CH_2}$-CH_3) and 14.03, 14.01 (CH_2-$\mathbf{CH_3}$).

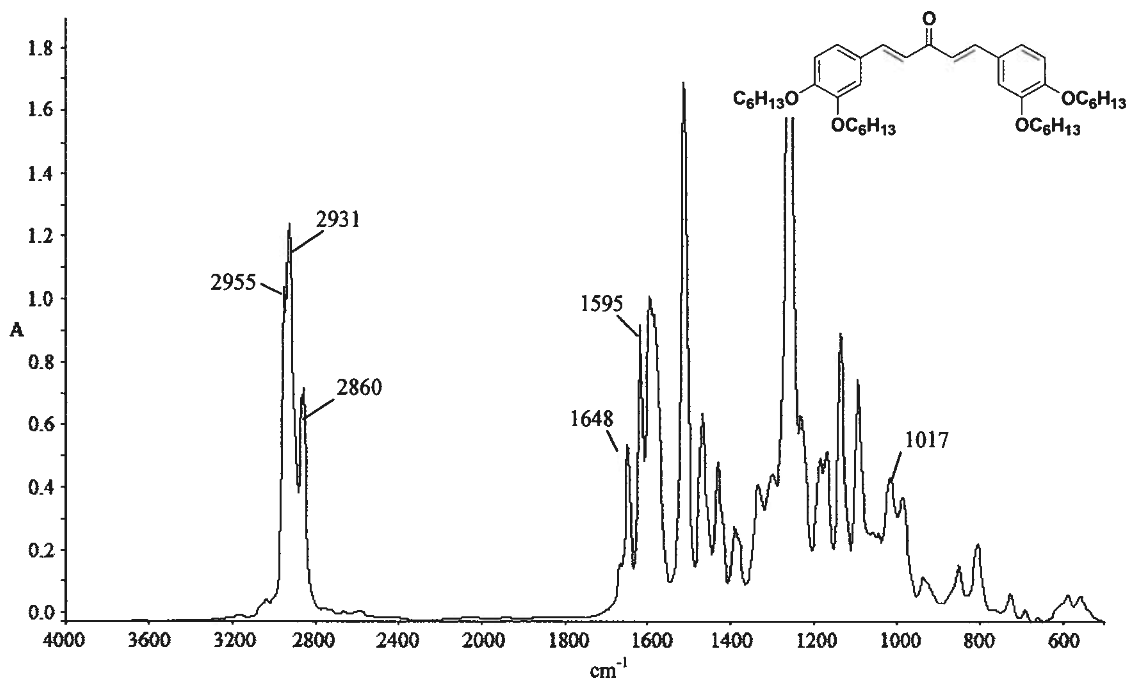

Figure 3.12: FTIR spectrum of **23e**.

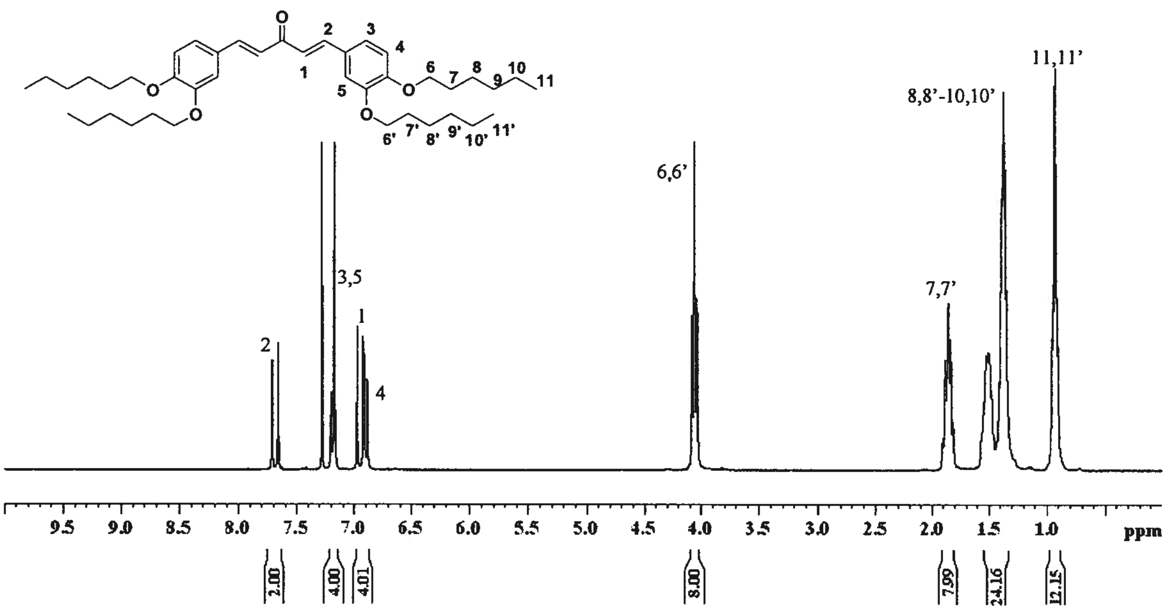

Figure 3.13: ^{1}H NMR spectrum of **23e**.

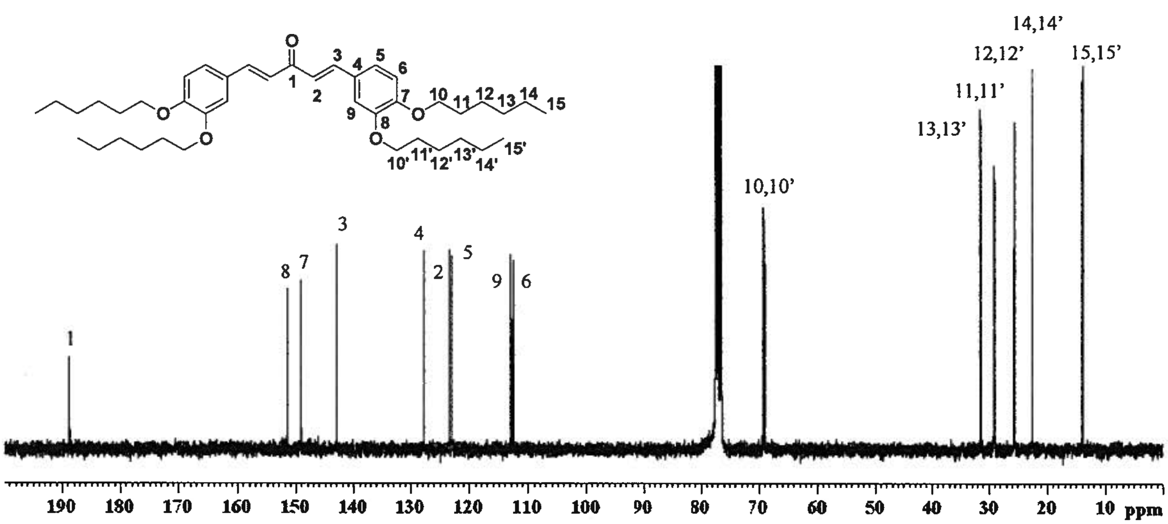

Figure 3.14: ^{13}C NMR spectrum of **23e**.

Appendix A contains FTIR, ^{1}H NMR and ^{13}C NMR spectra for the C_8, C_{10} and C_{12} derivatives **23f, 23g,** and **23h.**

3.2.6 Tris-alkoxy Dibenzylidene Acetone Compounds 27i-l

The synthesis of the tris-alkoxy dba compounds began with the synthesis of 3,4,5-tris-alkoxy benzaldehydes **25i-l** from methyl-3,4,5-tris-alkoxy benzoates **12i-l** (**Scheme 3.5,** *vide supra*). Attempted partial reduction to the aldehyde **25i-l** using 1.0 equivalent of di-isobutyl aluminum hydride (DIBAL-H)[58] led to a 1:1 mixture of the totally reduced alcohol **24i-l** and the unreacted starting ester **12i-l** (**Scheme 3.12**).

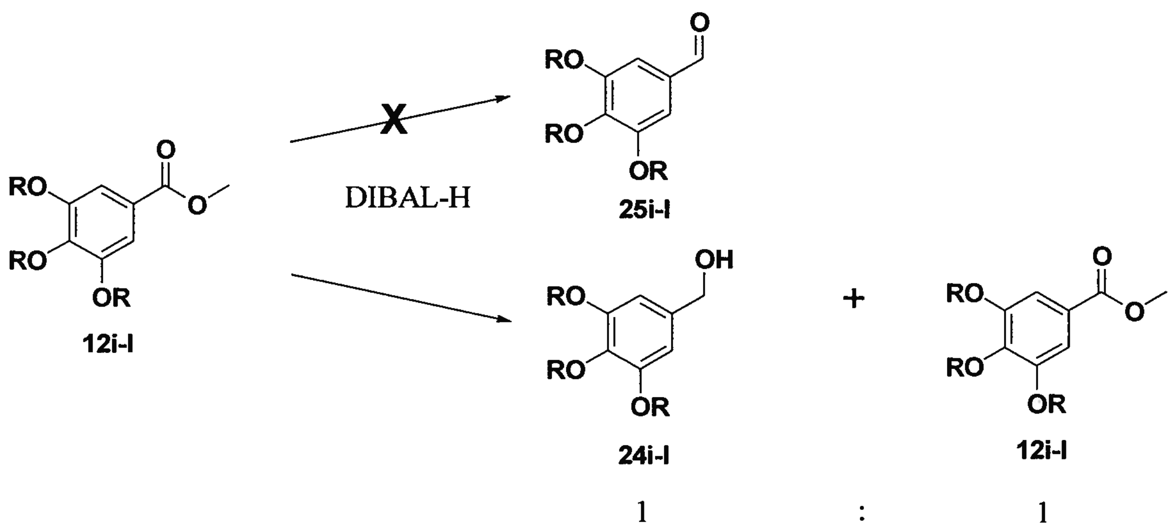

Scheme 3.12 Reagents and conditions: 1.0 eq. DIBAL-H in toluene, -78°C.

Instead, total reduction to the alcohol using $LiAlH_4$[59] and reoxidation to the aldehyde using PCC[60,61] was carried out. The two step reduction/oxidation sequence afforded aldehydes **25i-l** in yields ranging from 79 % (C_{12}) to 100 % (C_8) (**Scheme 3.13**).

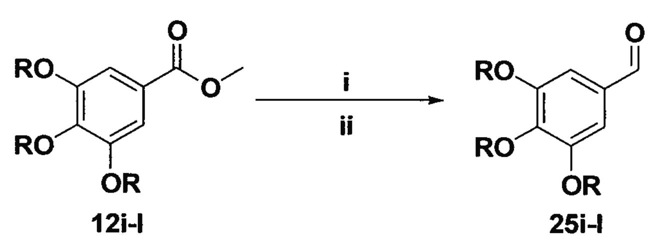

Scheme 3.13 Reagents and conditions: i) $LiAlH_4$, THF 0 °C to rt. 24 h.; ii) PCC, DCM, rt. 2h.

Following the procedure for the bis-alkoxy dba compounds, stepwise aldol condensations were attempted instead of the proposed bidirectional aldol condensation. The first condensation proceeded in moderate yields (38 % (C_8) to 67 % (C_{12}), **Scheme 3.14**), but the second condensation proved exceedingly difficult. A variety of conditions were attempted, including various solvents (MeOH, EtOH, THF, DMF, DMSO, DCM), different bases (NaOH, KOH, NaOMe, pyridine, piperidine, NaH) and temperatures (0 °C to 100 °C). All reactions were characterized by the disappearance of starting materials by TLC, but no products were observed by ^{1}H NMR. With the ultimate goal being a simple, easily reproducible system, the synthesis of the tris-alkoxy dba compounds **27i-l** was abandoned.

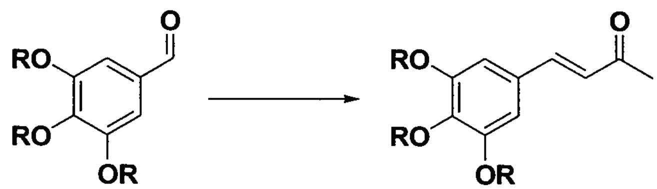

25i-l **26i-l**

Scheme 3.14 Reagents and conditions: Acetone, NaOMe, rt. 1.0 h.

3.2.7 Mono-Alkoxy 1,9-Diphenyl-nona-1,3,6,8-tetraen-5-one Compounds 34a-d

The synthesis of the mono-alkoxy 1,9-diphenyl-nona-1,3,6,8-tetraen-5-one compounds began with the Fischer esterification[51] of commercially available *p*-coumaric acid (**28**)[62] and installation of the alkoxy chains by the Williamson ether synthesis[26] (**Scheme 3.15**). Compounds **30a-d** were obtained in 87 % (R = C_{10}) to 95 % (R = C_8) yield over two steps.

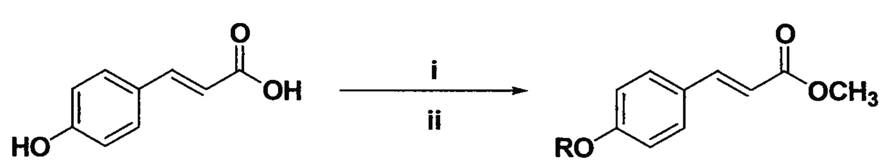

28 **30a-d**

Scheme 3.15 Reagents and conditions: i)H_2SO_4, MeOH, reflux 24h; ii)K_2CO_3, RBr, acetone, reflux 24h (R = C_6H_{13}, C_8H_{17}, $C_{10}H_{21}$, $C_{12}H_{25}$).

Again, attempted partial reduction to the aldehydes **32a-d** using 1.0 equivalent of DIBAL-H[58] afforded a 1:1 mixture of the totally reduced alcohol **31a-d** and the unreacted starting ester **30a-d** (**Scheme 3.16**).

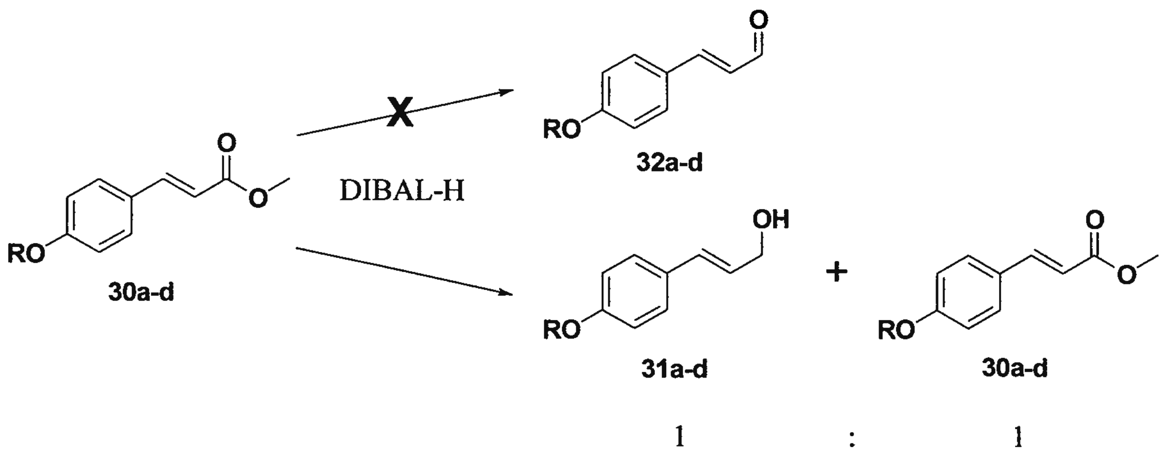

Scheme 3.16 Reagents and conditions: 1.0 eq. DIBAL-H in toluene, -78°C.

To circumvent this problem, a strategy of total reduction to the alcohols **31a-d** and subsequent reoxidation to the aldehydes **32a-d** was again employed. The reduction using $LiAlH_4$[59] did not proceed as desired, but instead led to both reduction of the ester as well as hydrogenation of the olefin (**Scheme 3.17**).

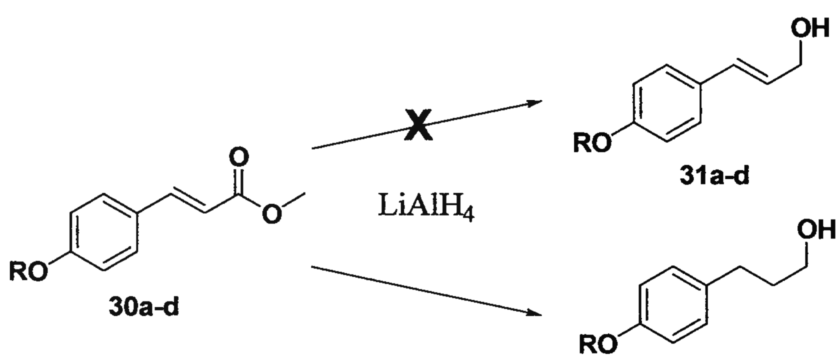

Scheme 3.17 Reagents and conditions: 1.1 eq. LAH, THF, 0°C.

This unexpected result is known,[63] but seems to be limited to structural analogues of *p*-coumaric acid. The reduction was achieved using an excess of DIBAL-H, producing the corresponding alcohols **31a-d** in good yield (**Scheme 3.19,** *vide infra*).

Attempted oxidation using the Corey-Suggs reagent PCC[60] yielded a mixture of the desired aldehyde as a minor product and olefin oxidative cleavage as the major product (**Scheme 3.18**). The unexpected oxidative cleavage of aryl substituted olefins using PCC was reported in 1985,[64] but has since been rarely cited.[65]

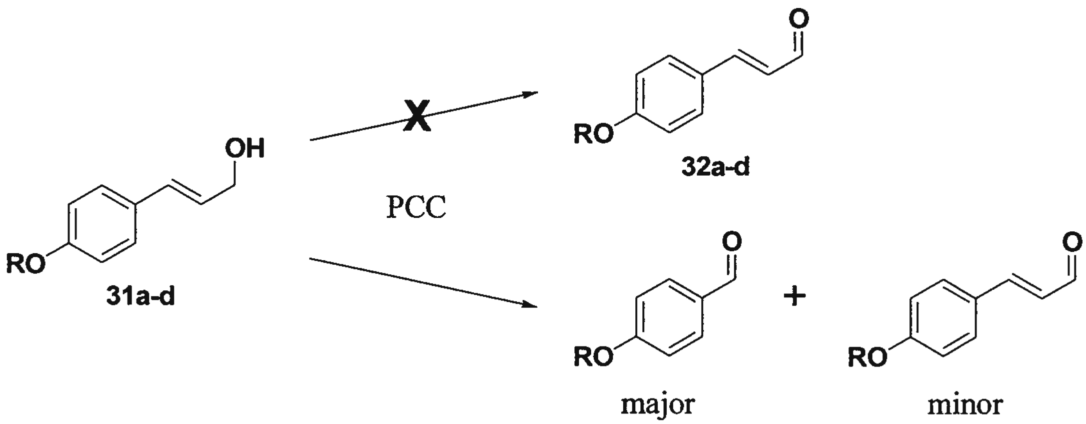

Scheme 3.18 Reagents and conditions: 1.5 eq. PCC, DCM, 25°C, 3 h.

Alternatively, oxidation using DDQ in dioxane[66] was employed and yielded the desired aldehydes **32a-d** (**Scheme 3.19**). Overall yields for the combined reduction/oxidation sequence ranged from 92 % (R = C_{10}) to 96 % (R = C_8).

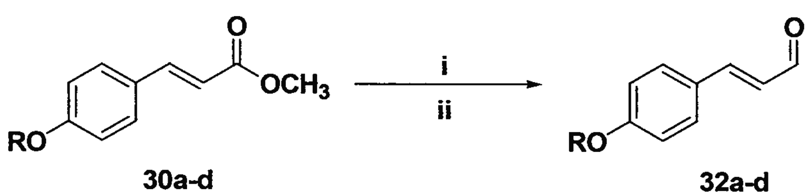

Scheme 3.19 Reagents and conditions: i) 2.1 eq. DIBAL-H, toluene, 0 °C to 25 °C, 24 h; ii) 1.05 eq. DDQ, dioxane, 25 °C, 30 min.

The attempted one-pot bidirectional aldol condensation again proved difficult, yielding an inseparable mixture of both the desired product **34a-d** and the mono-aldol condensation product 6-(4-alkoxy-phenyl)-hexa-3,5-dien-2-ones **33a-d**. Instead, a strategy of two sequential aldol condensations was employed, first between one equivalent of the 4-alkoxy-cinnamaldehydes **32a-d** and an excess of acetone to afford **33a-d**, and then another aldol condensation between **33a-d** and a second equivalent of the 4-alkoxy-cinnamaldehydes **32a-d** (**Scheme 3.20**). This strategy produced the final target compounds **34a-d** in six linear steps with overall yields ranging between 42 % (C_{10}) and 56 % (C_{12}).

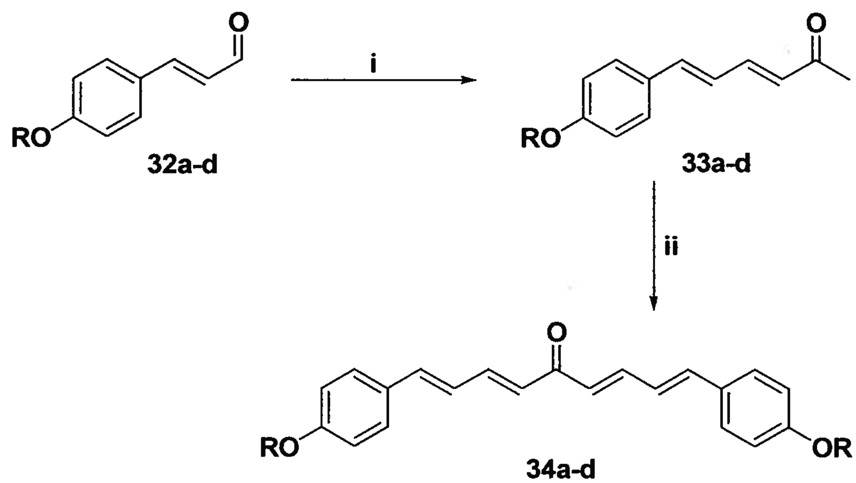

Scheme 3.20 Reagents and conditions: i) 5.0 eq. acetone, NaOH, H_2O, MeOH, reflux 24 h; ii) **32a-d,** NaOMe (25% wt in MeOH), THF, 25 °C, 30 min.

Figures 3.15-3.17 display FTIR, ^{1}H and ^{13}C NMR spectra for the 1,9-Bis-(4-hexyloxy-phenyl)-nona-1,3,6,8-tetraen-5-one **34a**. Characteristic FTIR absorptions include the alkyl C-H stretches (2926, 2851 cm^{-1}), ketone C=O stretch (1655 cm^{-1}), aromatic C=C stretch (1592 cm^{-1}) and ether C-O stretch (1071 cm^{-1}). The ^{1}H NMR chemical shifts were assigned as: δ 7.48, 6.95, 6.84, 6.53 (olefinic C-**H**), 7.44, 6.90 (aromatic C-**H**), 4.00 (O-**CH$_2$**), 1.81 (O-CH_2-**CH$_2$**) 1.55-1.30 (**CH$_2$**-**CH$_2$**-**CH$_2$**-CH_3) and 0.91 (CH_2-**CH$_3$**). The stereochemistry of all of the olefins was assigned as E, based on the characteristic *J* coupling constants of 15.13 Hz and 15.46 Hz.[56] The ^{13}C NMR chemical shifts were assigned as: δ 189.0 (ketone **C**=O), 160.2, 128.8 (aromatic quaternary **C**), 128.7, 114.9 (aromatic **C**-H), 143.3, 141.2, 128.1, 124.8 (olefinic **C**-H), 68.2 (O-**C**H$_2$), 31.6 (**C**H$_2$-CH_2-CH_3), 25.7 (O-CH_2-CH_2-**C**H$_2$), 29.2 (O-CH_2-**C**H$_2$), 22.6 (**C**H$_2$-CH_3) and 14.0 (CH_2-**C**H$_3$).

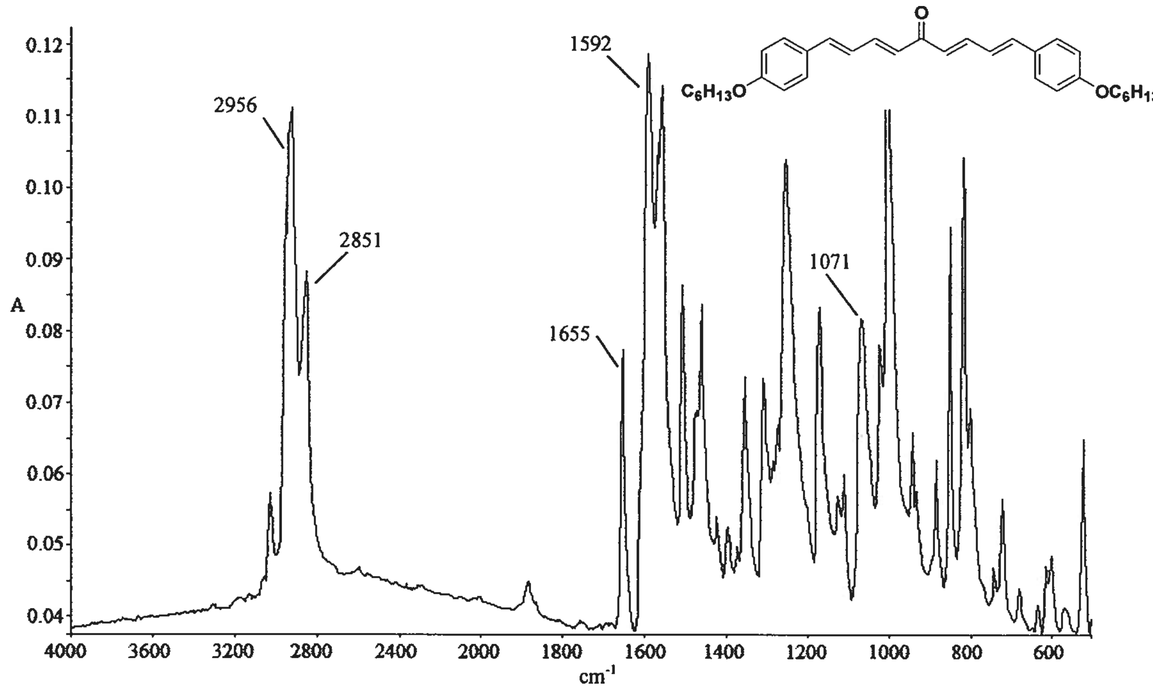

Figure 3.15: FTIR spectrum of **34a**.

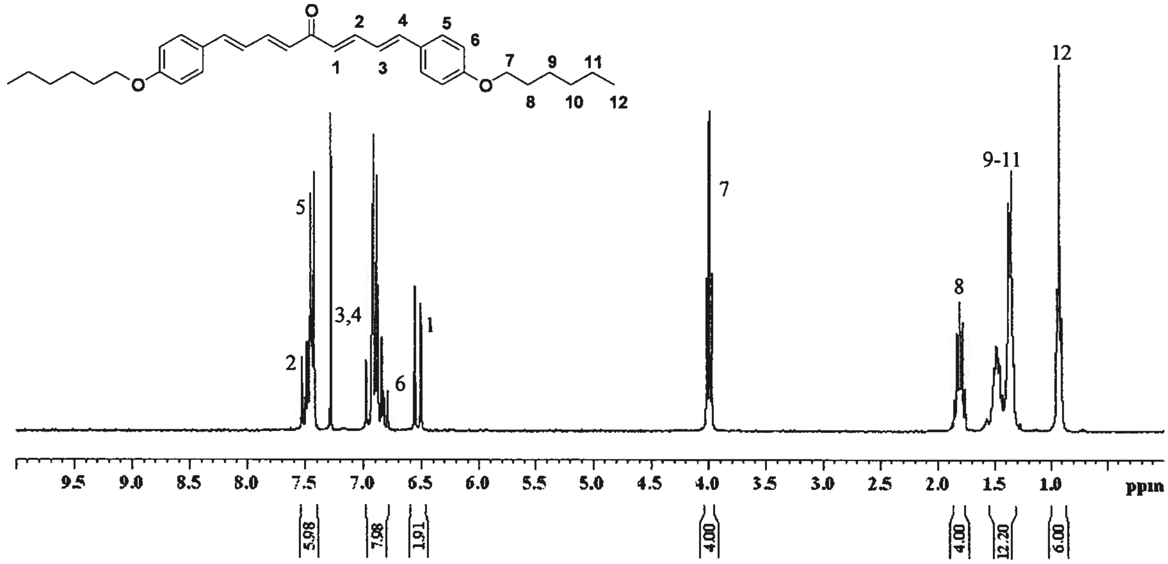

Figure 3.16: ^{1}H NMR spectrum of **34a**.

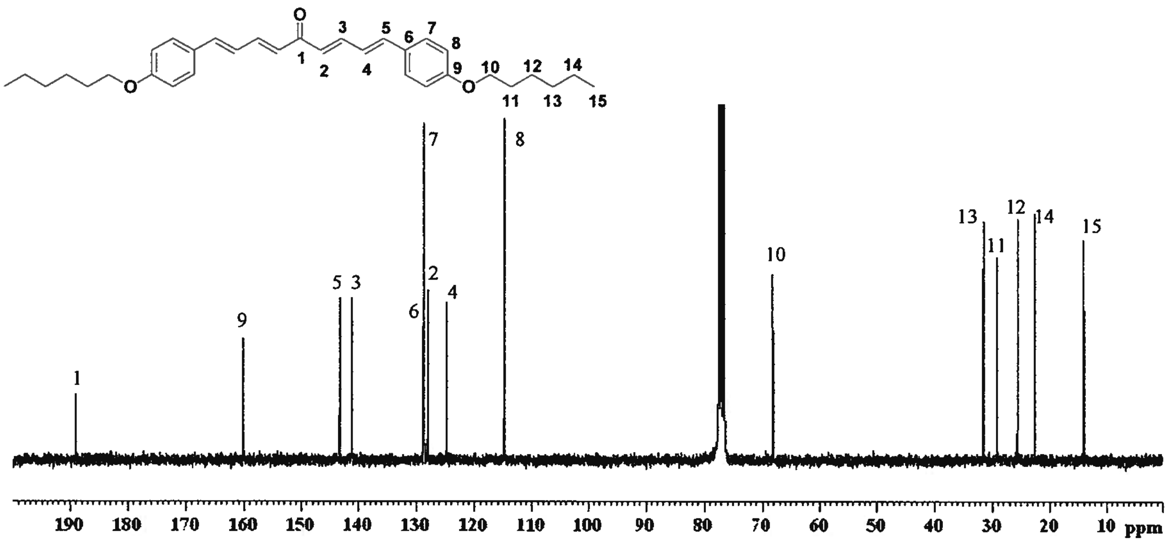

Figure 3.17: ^{13}C NMR spectrum of **34a**.

Appendix A contains FTIR, ^{1}H and ^{13}C NMR spectra for the C_8, C_{10} and C_{12} derivatives **34b, 34c** and **34d**.

3.2.8 Bis-Alkoxy 1,9-Diphenyl-nona-1,3,6,8-tetraen-5-one Compounds 38e-h

The synthesis of the bis-alkoxy 1,9-diphenyl-nona-1,3,6,8-tetraen-5-one compounds began with the Knoevenagel condensation[33,67] of 3,4-bis-alkoxy benzaldehydes **21e-h** with mono-ethyl malonic acid (**Scheme 3.21**). Compounds **35e-h** were obtained in 85% (R = C_6 to 96% (R = C_{12}) yield.

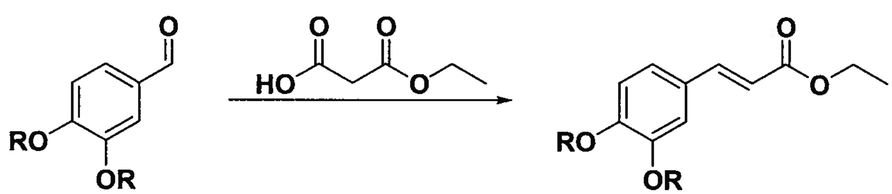

21e-h **35e-h**

Scheme 3.21 Reagents and conditions: i) Pyridine, piperidine, 100 °C 24h (R = C_6H_{13}, C_8H_{17}, $C_{10}H_{21}$, $C_{12}H_{25}$).

The same reduction/oxidation sequence performed above yielded the aldehydes **37e-h** in yields ranging from 71 % (C_8) to 82 % (C_{12}) over two steps (**Scheme 3.22**).

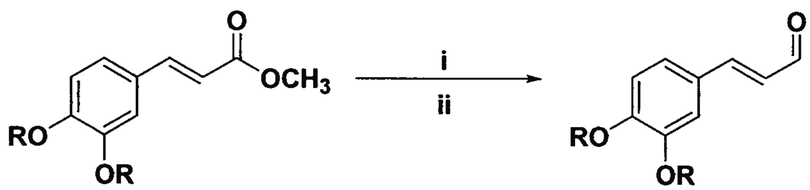

35e-h

37e-h

Scheme 3.22 Reagents and conditions: i) 2.1 eq. DIBAL-H, toluene, 0 °C to 25 °C, 24 h; ii) 1.05 eq. DDQ, dioxane, 25 °C, 30 min.

The attempted aldol condensation strategy employed above proved difficult. The reactions were monitored by TLC and ^{1}H NMR. The disappearance of starting material was observed, but no formation of products was visible by ^{1}H NMR. Based on the successes of the mesophase properties of the mono-alkoxy derivatives (*vide infra*) and the difficulties encountered in the synthesis, the bis-alkoxy and tris-alkoxy 1,9-diphenyl-nona-1,3,6,8-tetraen-5-one targets were abandoned.

3.2.9 Tris-alkoxy 1,9-Diphenyl-nona-1,3,6,8-tetraen-5-one Compounds 38i-l

The synthesis of the tris-alkoxy 1,9-diphenyl-nona-1,3,6,8-tetraen-5-ones **38i-l** was not completed due to experimental difficulties and the desire for a simple, easily reproducible synthesis.

3.3 Differential Scanning Calorimetry

3.3.1 Mono-alkoxy Benzophenone Compounds 2a-d

DSC analysis showed that the mono-C_6 benzophenone derivative **2a** displayed two endothermic transitions on heating; 66.3 °C with an enthalpy change (ΔH) of 2.96 kJ/mol and 103.6 °C (ΔH = 37.85 kJ/mol) and two exothermic transitions on cooling; at 93.4 °C (ΔH = 38.10 kJ/mol) and 62.8 °C (ΔH = 2.08 kJ/mol). Based on the relatively small ΔH value of the first endothermic transition, it was characterized as a crystal to crystal transition. The second endothermic transition was characterized as a crystal to isotropic liquid transition.

The mono-C_8 derivative **2b** also displayed two endothermic transitions on heating, the first at 88.9 °C (ΔH = 3.87 kJ/mol) and the second at 98.2 °C (ΔH = 45.13 kJ/mol), and two exothermic transitions on cooling; 90.8 °C (ΔH = 45.14 kJ/mol) and 87.5 °C (ΔH = 2.32 kJ/mol). Similar to **2a**, the first endothermic transition was characterized as a crystal to crystal transition based on the ΔH value, while the second endothermic transition was characterized as a crystal to isotropic liquid transition.

The mono-C_{10} derivative **2c** showed only one endothermic transition on heating at 100.2 °C (ΔH = 73.65 kJ/mol), and one exothermic transition on cooling at 93.7 °C (ΔH = 72.55 kJ/mol). These transitions correspond to the crystal to isotropic liquid transition (melting) and the isotropic liquid to crystal transition (crystallization), respectively.

The mono-C_{12} derivative **2d** also showed only one endothermic transition on heating at 103.2 °C (ΔH = 79.08 kJ/mol), and one exothermic transition on cooling at 98.9 °C (ΔH = 86.71 kJ/mol). Again, these transitions correspond to the melting and crystallization phase transitions, respectively.

It should be noted that all four DSC thermograms for the mono-alkoxy benzophenones **2a-d** displayed a loop on the exothermic transition from isotropic liquid to crystalline solid (*vide infra*). This phenomenon is known as 'self-heating' and is indicative of high energy, sharp transitions.[68] During crystallization, enough heat is released that the sample temperature increases by a small amount, causing a loop in the DSC thermogram. This phenomenon was not seen in any other samples, and is under further investigation.

Based on these findings, it was determined that the mono-alkoxy benzophenones were likely non-mesogenic and this was confirmed by POM. **Figures 3.18** through **3.21** display the DSC thermograms for **2a, 2b, 2c** and **2d,** respectively.

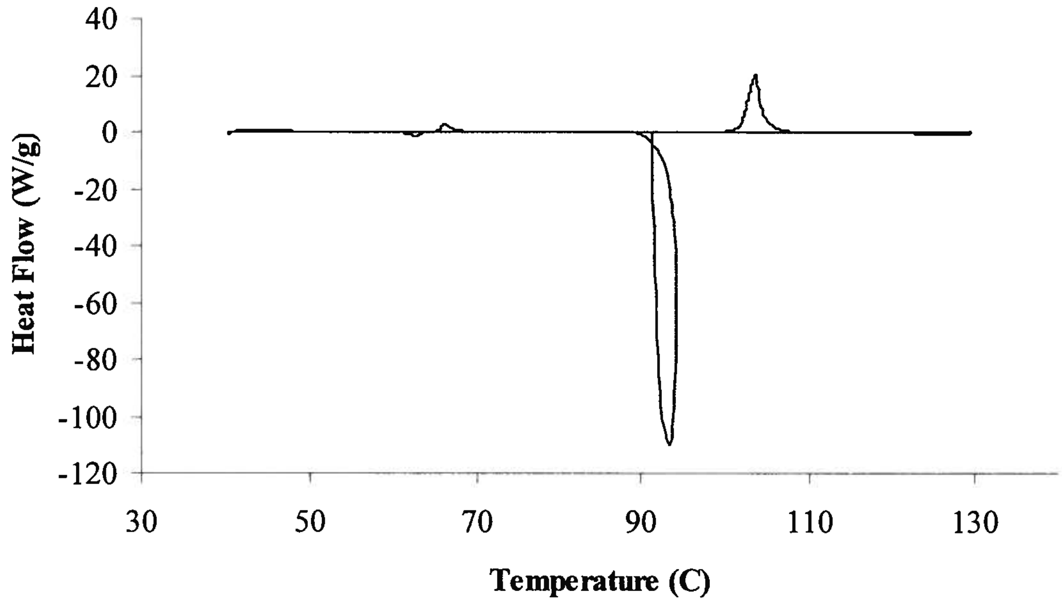

Figure 3.18: DSC thermogram of **2a**. Heating rate: 10 °C/min. Cooling rate: 5 °C/min.

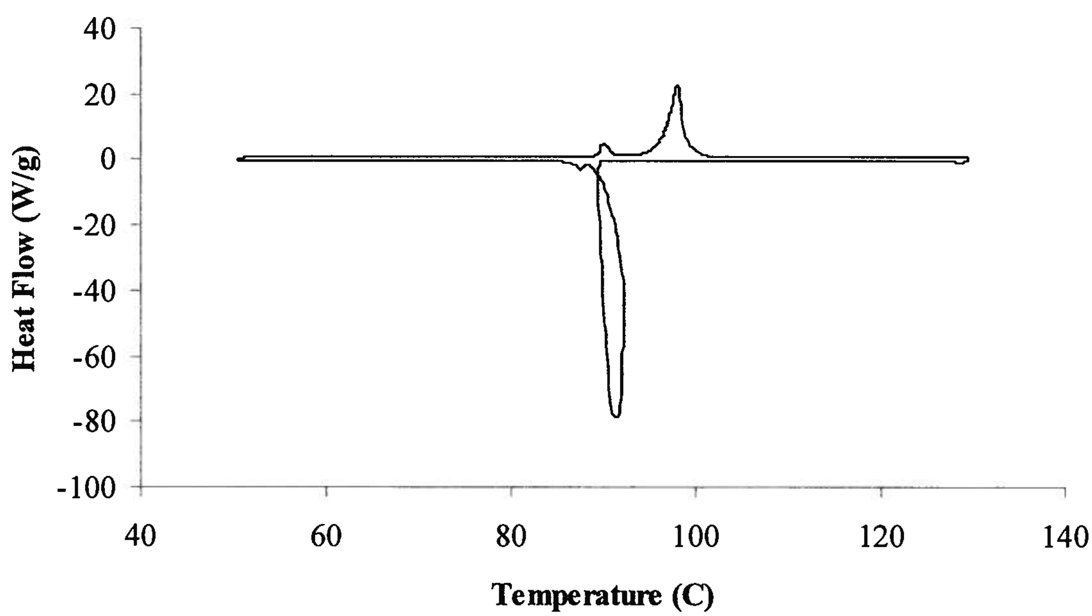

Figure 3.19: DSC thermogram of **2b**. Heating rate: 10 °C/min. Cooling rate: 5 °C/min.

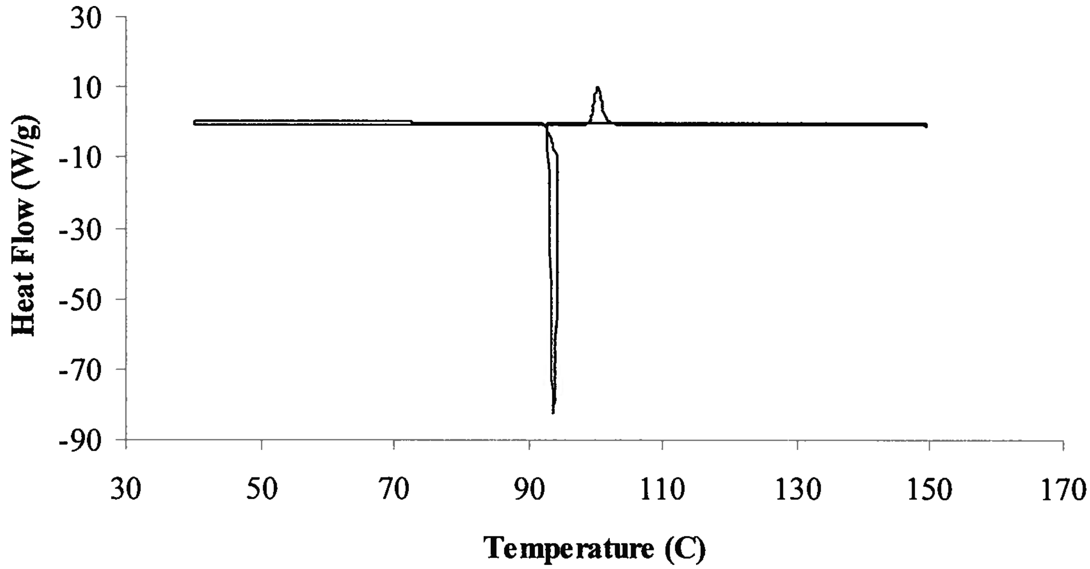

Figure 3.20: DSC thermogram of **2c**. Heating rate: 5 °C/min. Cooling rate: 2 °C/min.

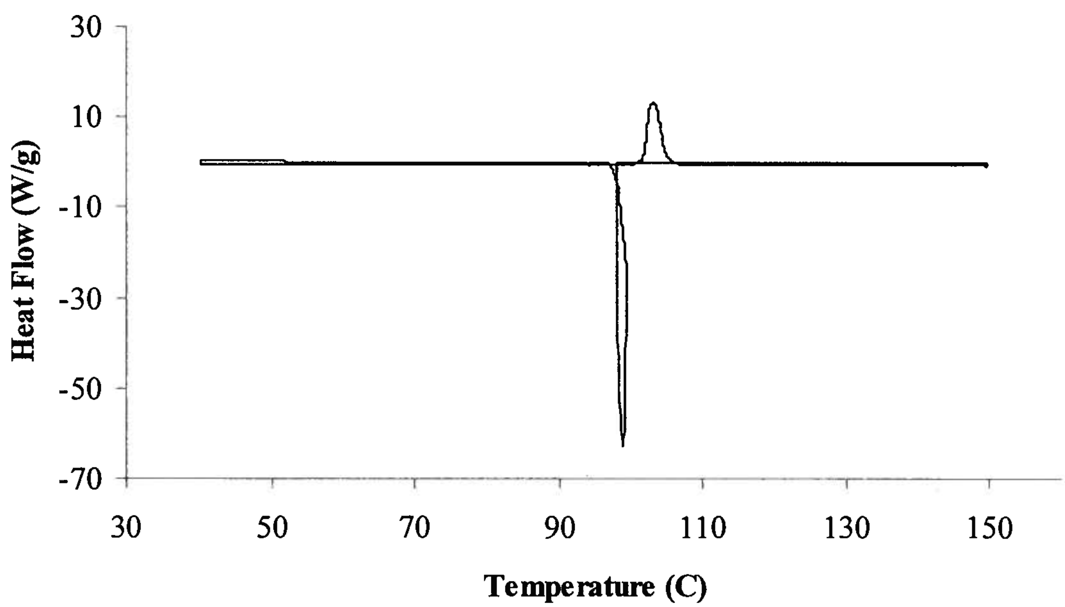

Figure 3.21: DSC thermogram of **2d**. Heating rate: 5 °C/min. Cooling rate: 2 °C/min.

3.3.2 Bis-alkoxy Benzophenone Compounds 9e-h

DSC analysis showed that the bis-C_6 benzophenone derivative **9e** displayed endothermic transitions at -16.5 °C (ΔH = 5.94 kJ/mol), 26.4 °C (ΔH = 24.12 kJ/mol), and 45.8 °C (ΔH = 53.36 kJ/mol). The first two endothermic transitions were followed immediately by exothermic transitions at -11.9 °C (ΔH = 7.90 kJ/mol) and 29.8 °C (ΔH = 32.08 kJ/mol), respectively. There was only one exothermic transition on cooling, at -14.9 °C (ΔH = 3.46 kJ/mol). The exothermic transitions on heating are likely crystallization transitions due to supercooling of the isotropic liquid, which is characterized by a crystallization temperature much below that of the clearing temperature.[5] The first endothermic transition is probably a crystal to crystal transition while the second and third transitions likely correspond to a mesophase.

The bis-C_8 derivative **9f** showed only one endothermic transition on heating, at 56.9 °C (ΔH = 66.26 kJ/mol) that was immediately preceded by a small exothermic transition (46.2 °C, ΔH = 3.93 kJ/mol) and one exothermic transition on cooling, at 11.3 °C (ΔH = 45.92 kJ/mol). Similar to **9e**, the exothermic transition on heating is most likely a crystallization due to supercooling of the isotropic liquid.

The bis-C_{10} derivative **9g** also showed only one endothermic transition on heating, at 64.2 °C (ΔH = 79.75 kJ/mol) and one exothermic transition on cooling, at 39.7 °C (ΔH = 76.06 kJ/mol). These transitions correspond to the melting and crystallization phase transitions, respectively.

The bis-C_{12} derivative **9h** again showed only one endothermic transition on heating, at 71.8 °C (ΔH = 88.36 kJ/mol) and one exothermic transition on cooling, at 47.0 °C (ΔH = 81.69 kJ/mol). These transitions correspond to the melting and crystallization phase transitions, respectively.

Based on these findings, it was determined that the bis-C_6 benzophenone **9e** was probably mesogenic, whereas the bis-C_8, bis-C_{10} and bis-C_{12} benzophenones **9f**, **9g** and **9h** were not. The liquid crystallinity was confirmed by POM (*vide infra*).

Figures 3.22 through **3.25** display the DSC thermograms for **9e**, **9f**, **9g**, and **9h**, respectively.

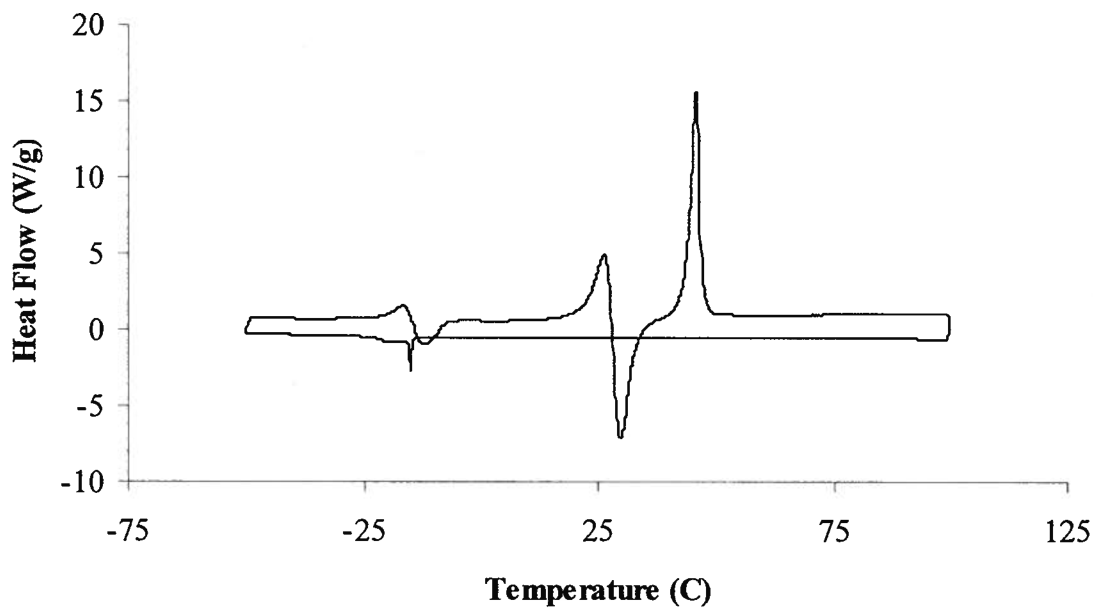

Figure 3.22: DSC thermogram of **9e**. Heating rate: 10 °C/min. Cooling rate: 5 °C/min.

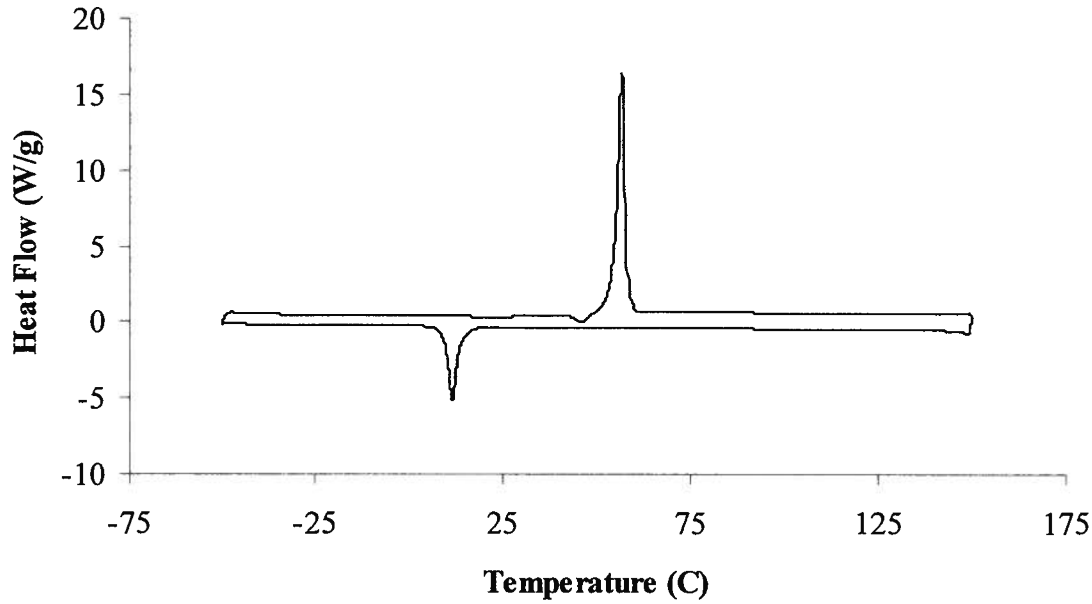

Figure 3.23: DSC thermogram of **9f**. Heating rate: 10 °C/min. Cooling rate: 5 °C/min.

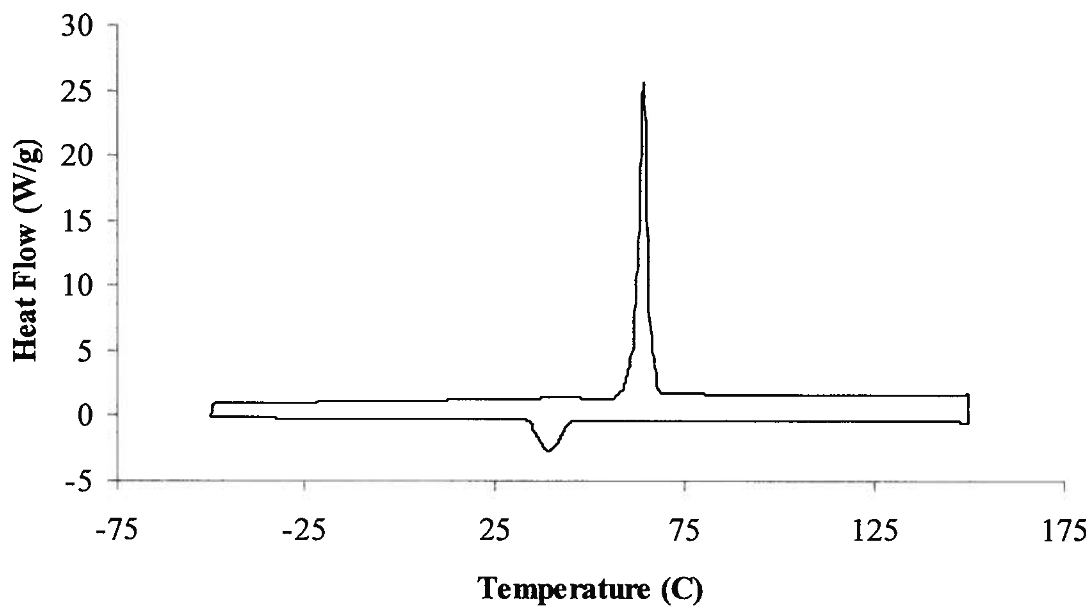

Figure 3.24: DSC thermogram of **9g**. Heating rate: 10 °C/min. Cooling rate: 2 °C/min.

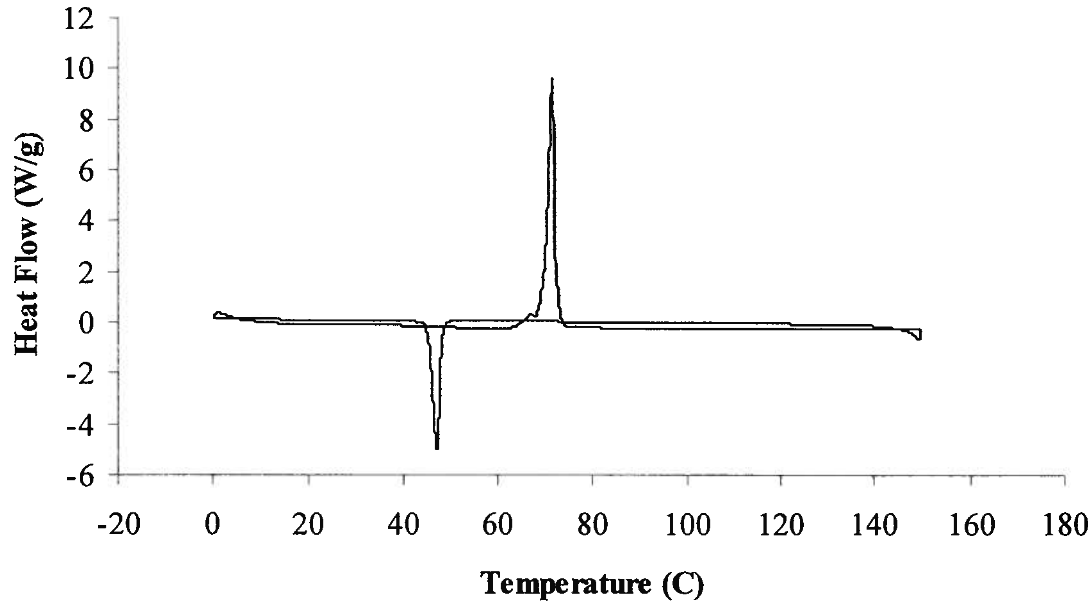

Figure 3.25: DSC thermogram of **9h**. Heating rate: 10 °C/min. Cooling rate: 5 °C/min.

3.3.3 Mono-alkoxy Dibenzylidene Acetone Compounds 19a-d

DSC analysis revealed that the mono-C_6 dba derivative **19a** showed only one endothermic transition on heating, at 109.8 °C (ΔH = 27.64 kJ/mol) and one exothermic transition on cooling, at 101.6 °C (ΔH = 27.29 kJ/mol). These transitions correspond to the melting and crystallization transitions, respectively.

The mono-C_8 derivative **19b** displayed two endothermic transitions at 81.5 °C (ΔH = 18.06 kJ/mol) and 101.6 °C (ΔH = 44.46 kJ/mol). There was only one exothermic transition on cooling (rate = 1 °C/min), at 92.4 °C (ΔH = 51.01 kJ/mol). Based on the small ΔH value of the first endothermic transition relative to the second, it was characterized as a crystal to crystal transition. The second endothermic transition was characterized as a crystal to isotropic liquid transition.

The mono-C_{10} derivative **19c** also displayed two endothermic transitions on heating, at 90.9 °C (ΔH = 14.05 kJ/mol) and 101.4 °C (ΔH = 23.50 kJ/mol). Again, there was only one exothermic transition on cooling (rate = 1 °C/min), at 94.8 °C (ΔH = 29.10 kJ/mol). Similarly to **19b**, the first endothermic transition was characterized as a crystal to crystal transition.

The mono-C_{12} derivatives **19d** showed only one endothermic transition on heating, at 95.4 °C (ΔH = 66.00 kJ/mol) and one exothermic transition on cooling, at 90.7 °C (ΔH = 53.43 kJ/mol). These transitions correspond to the melting and crystallization transitions, respectively.

Based on these results, it was determined that the mono-alkoxy dba compounds **19a-d** were non-mesogenic. These findings were confirmed by POM to verify the nature of the first endothermic transitions for **19b** and **19c**.

Figures 3.26 through **3.29** display the DSC thermograms for **19a, 19b, 19c,** and **19d,** respectively.

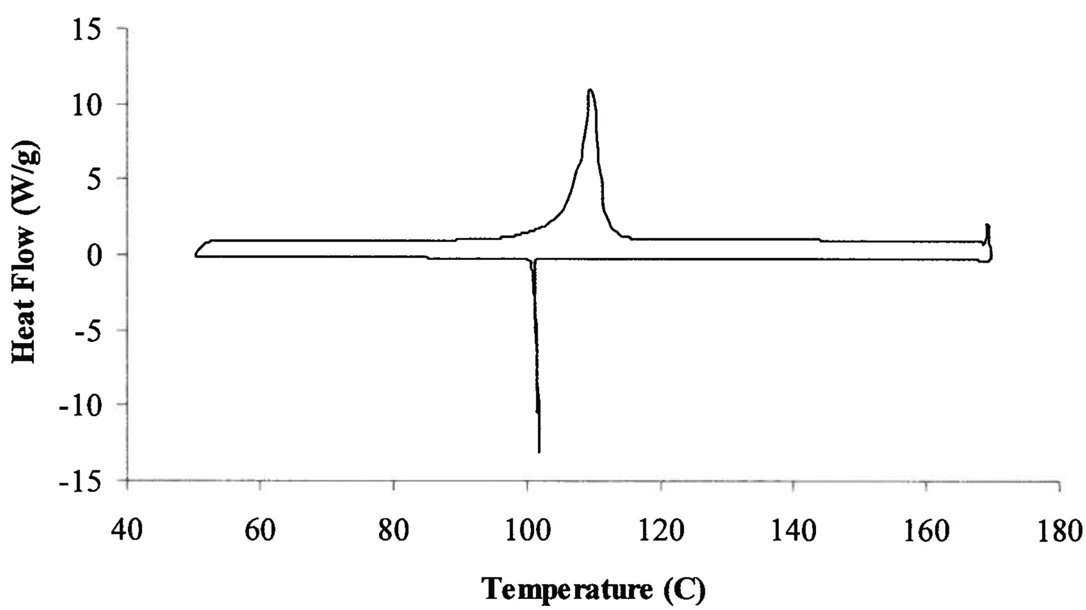

Figure 3.26: DSC thermogram of **19a**. Heating Rate: 10 °C/min. Cooling rate: 1 °C/min.

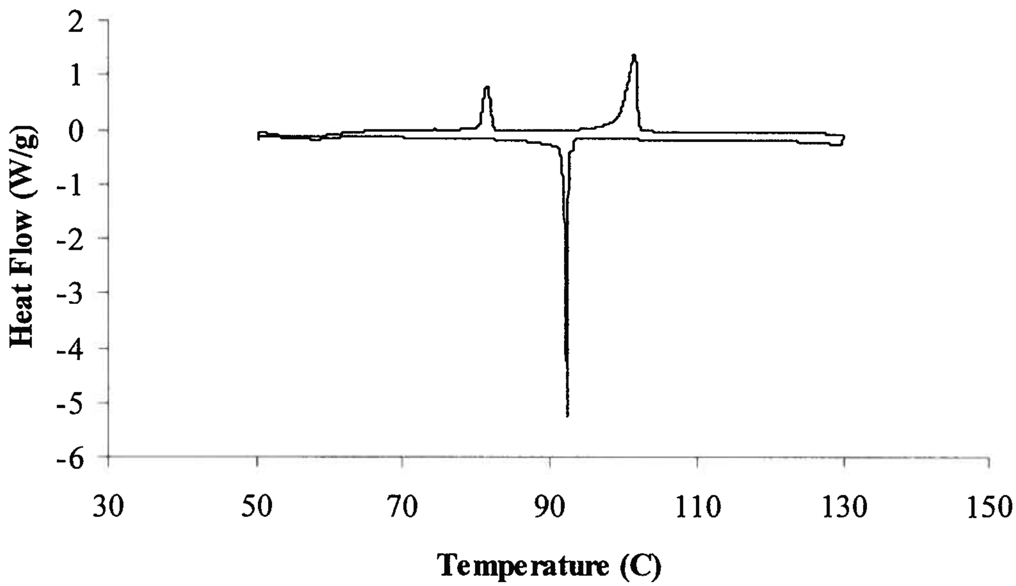

Figure 3.27: DSC thermogram of **19b**. Heating Rate: 10 °C/min. Cooling Rate: 1° C/min.

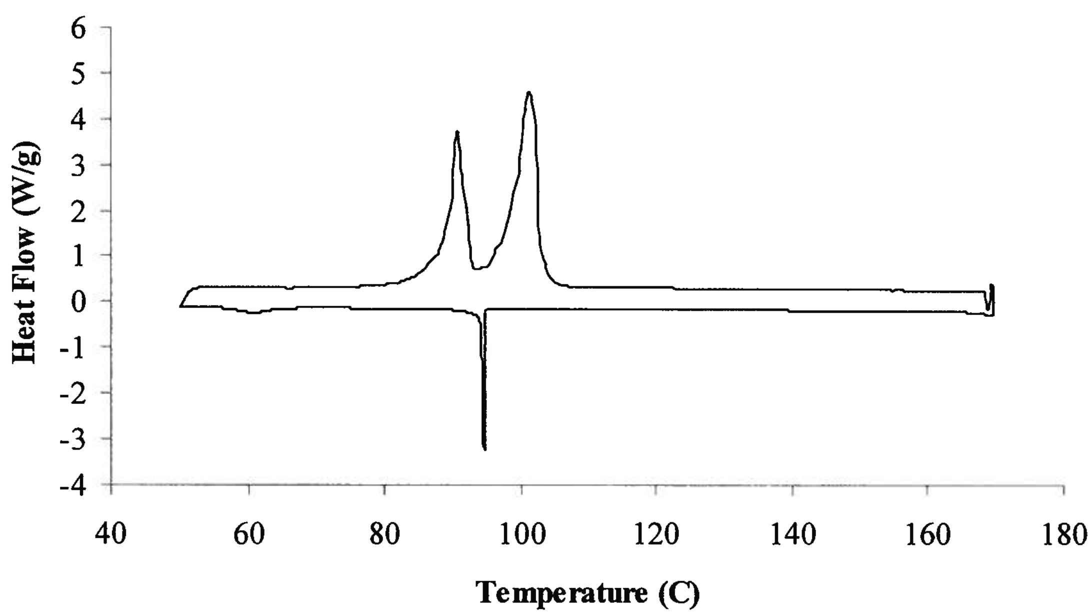

Figure 3.28: DSC thermogram of **19c**. Heating Rate: 10 °C/min. Cooling Rate: 1° C/min.

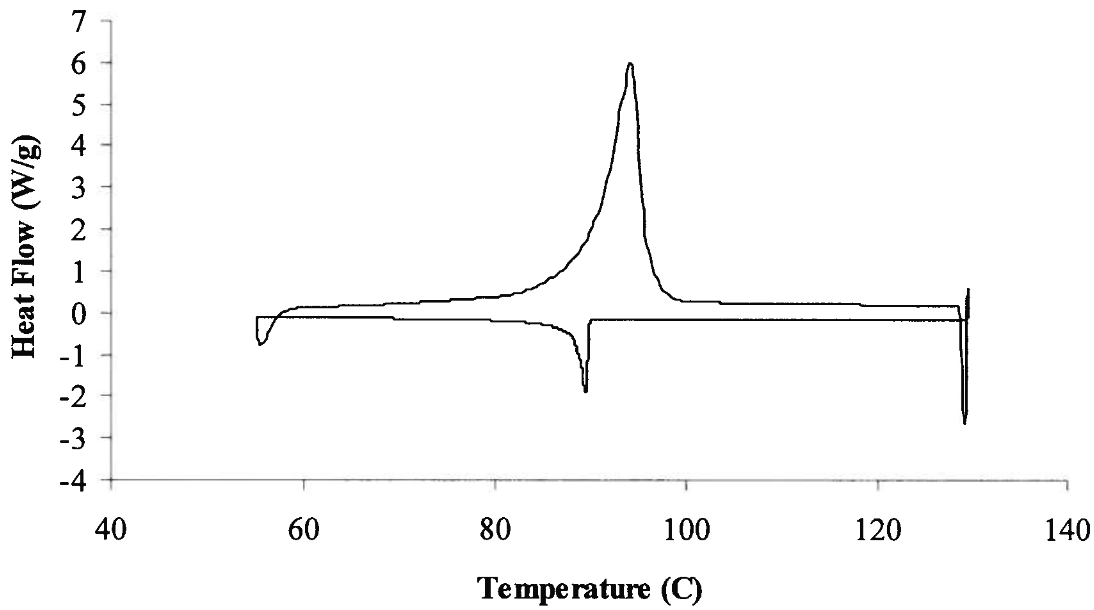

Figure 3.29: DSC thermogram of **19d**. Heating Rate: 10 °C/min. Cooling rate: 1 °C/min.

3.3.4 Bis-alkoxy Dibenzylidene Acetone Compounds 23e-h

DSC analysis revealed that the bis-C_6 dba derivative **23e** displayed two endothermic transitions, at 54.8 °C (ΔH = 42.89 kJ/mol) and 62.9 °C (ΔH = 10.87 kJ/mol) on the first heating cycle. There were no exothermic transitions observed on cooling. The endothermic transitions most likely correspond to a liquid crystalline phase. On the second and subsequent heating cycles, only one endothermic transition (at 54.8 °C) was observed. Changing the heating and cooling rates (1, 2, 5 and 10 °C) had no impact on this behaviour.

The bis-C_8 derivative **23f** showed two exothermic transitions on heating; at 3.2 °C (ΔH = 8.10 kJ/mol) and 30.9 °C (ΔH = 12.33 kJ/mol) before the endothermic melting transition at 65.4 °C (ΔH = 57.59 kJ/mol). There was only one exothermic transition on cooling, at 23.0 °C (ΔH = 2.20 kJ/mol).

The bis-C_{10} derivative **23g** displayed an exothermic transition on heating at 39.1 °C (ΔH = 5.39 kJ/mol) and an endothermic transition at 73.1 °C with a shoulder peak at 70.1 °C (total ΔH = 62.54 kJ/mol). On cooling, two overlapping exothermic transitions were observed: at 26.6 °C (ΔH = 23.08 kJ/mol) and 21.1 °C (ΔH = 8.57 kJ/mol). The shoulder peak observed near the clearing point and overlapping peaks near the crystallization point likely corresponds to a narrow liquid crystalline phase.

The bis-C_{12} derivative **23h** showed an exothermic transition at 51.2 °C (ΔH = 13.00 kJ/mol), and an endothermic transition at 72.1 °C (ΔH = 45.89 kJ/mol) on heating. On cooling, only one sharp exothermic transition was observed, at 31.4 °C (ΔH = 35.33 kJ/mol).

The exothermic transitions observed on heating for **23f, 23g** and **23h** are most likely crystallizations due to supercooling of the isotropic liquid. Based on the above results, the bis-C_6 and bis-C_{10} dba compounds **23e** and **23g** are likely mesogenic, while the bis-C_{12} dba compound **23h** is not. The bis-C_8 derivative **23f** does not appear to be mesogenic, and was confirmed by POM (*vide infra*).

Figures 3.30 through **3.33** display the DSC thermograms for **23e, 23f, 23g,** and **23h,** respectively.

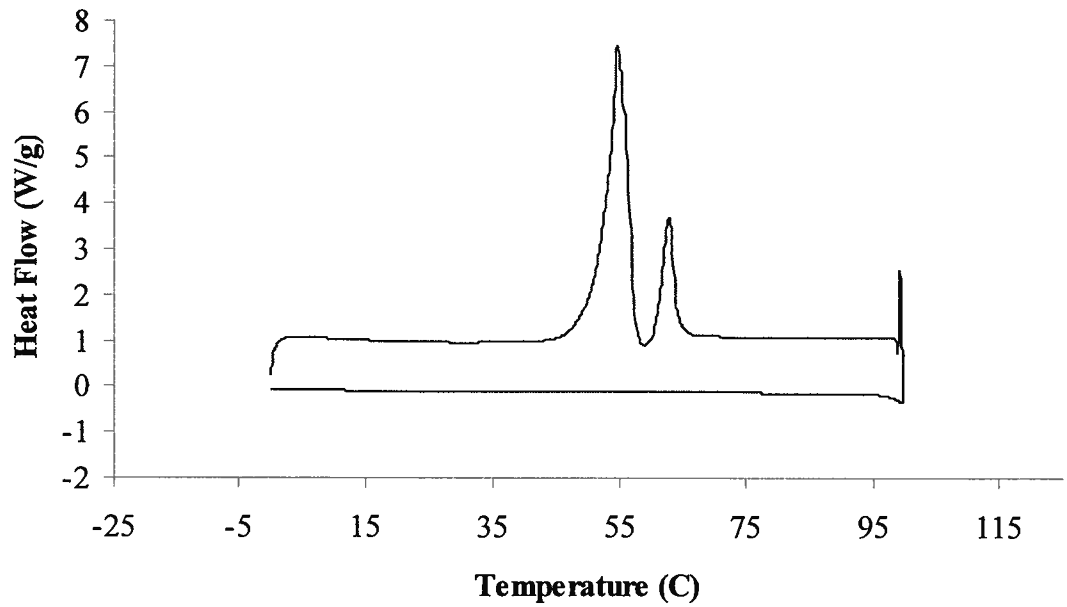

Figure 3.30: DSC thermogram of **23e**. Heating Rate: 10 °C/min. Cooling Rate: 1 °C/min.

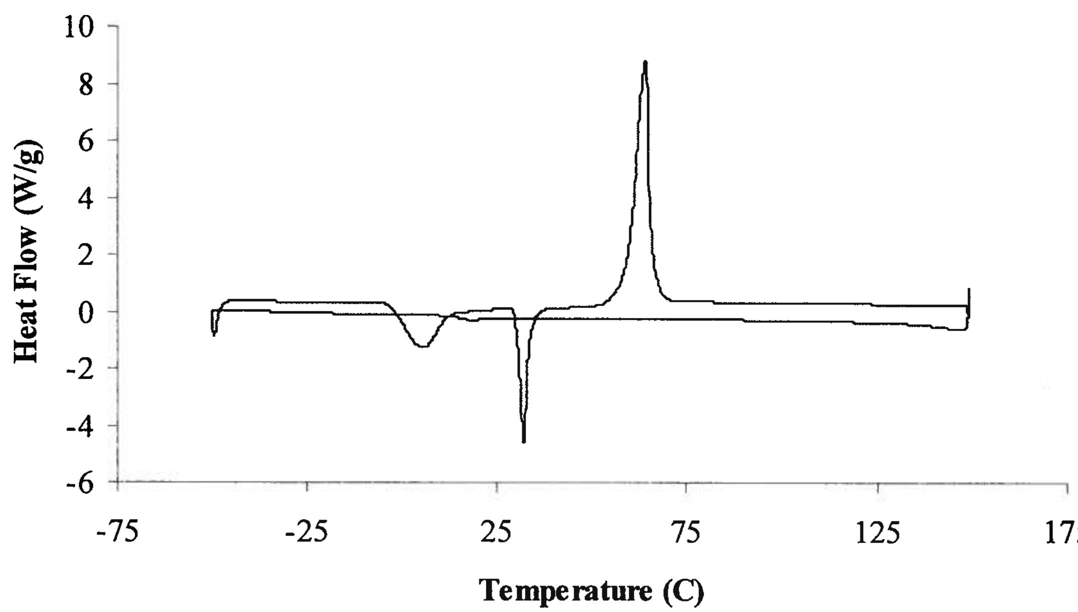

Figure 3.31: DSC thermogram of **23f**. Heating Rate: 10 °C/min. Cooling Rate: 5 °C/min.

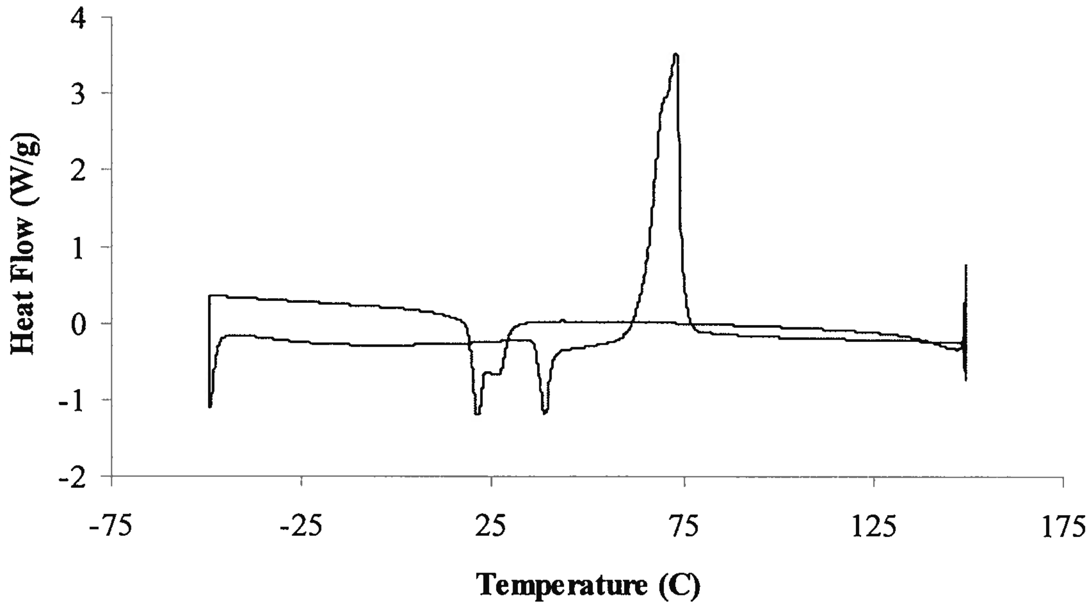

Figure 3.32: DSC thermogram of **23g**. Heating Rate: 10 °C/min. Cooling Rate: 5 ° C/min.

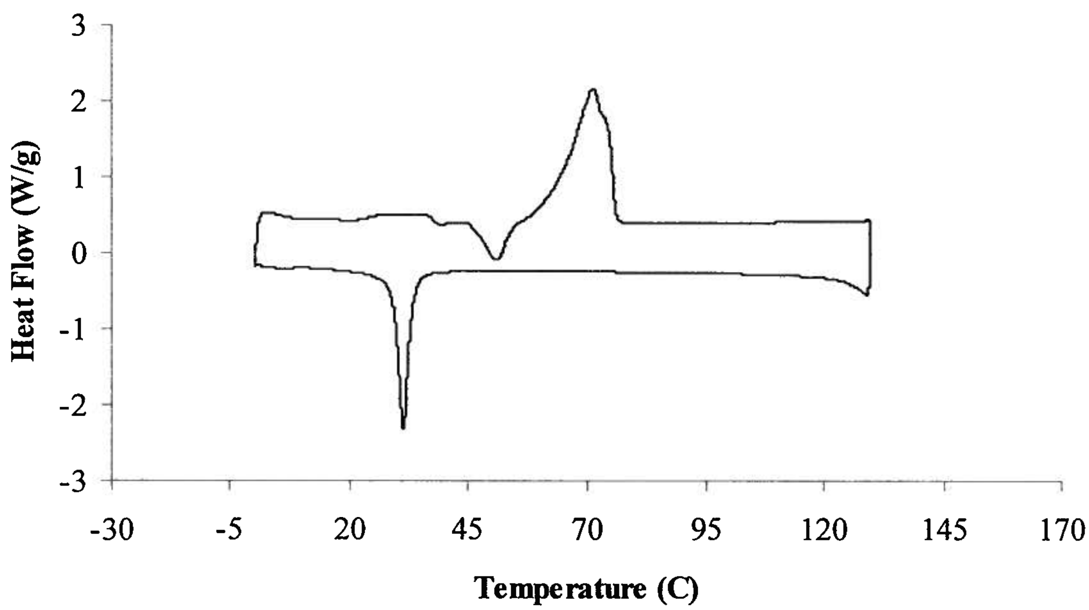

Figure 3.33: DSC thermogram of **23h**. Heating Rate: 10 °C/min. Cooling Rate: 5 °C/min.

3.3.5 Mono-alkoxy 1,9-Diphenyl-nona-1,3,6,8-tetraen-5-one Compounds 34a-d

DSC analysis of the mono-C_6 1,9-diphenyl-nona-1,3,6,8-tetraen-5-one derivative **34a** showed only one endothermic transition on heating at 149.7 °C (ΔH = 81.41 kJ/mol), but displayed two exothermic transitions at a cooling rate of 10 °C/min at 131.8 °C (ΔH = 70.60 kJ/mol) and 128.5 °C (ΔH = 8.34 kJ/mol). This likely corresponds to a liquid crystalline phase on cooling.

The mono-C_8 derivative **34b** displayed endothermic transitions at 11.6 °C (ΔH = 3.37 kJ/mol) and 136.8 °C (ΔH = 27.84 kJ/mol) on heating, and at 135.1 °C (ΔH = 0.43 kJ/mol), 128.5 °C (ΔH = 24.82 kJ/mol) and 8.0 °C (ΔH = 1.76 kJ/mol) on cooling. Based on the relatively small ΔH values, the first endothermic transition on heating and the third exothermic transition on cooling are most likely crystal to crystal transitions. The first exothermic transition on cooling probably represents the isotropic liquid to liquid crystal transition, while the second exothermic transition is likely the liquid crystal to crystal transition.

The mono-C_{10} derivative **34c** displayed endothermic transitions at 34.9 °C (ΔH = 1.66 kJ/mol), 40.3 °C (ΔH = 3.39 kJ/mol), 117.5 °C (ΔH = 14.27 kJ/mol) and at 130.9 °C (ΔH = 14.42 kJ/mol) on heating, and exothermic transitions at 121.4 °C (ΔH = 10.76 kJ/mol) and 33.2 °C (ΔH = 3.46 kJ/mol) on cooling. Based on the ΔH values the first and second endothermic transitions, as well as the second exothermic transition, were characterized as crystal to crystal transitions. The third endothermic transition probably represents a melting transition to the liquid crystalline phase, while the fourth endothermic transition probably represents the clearing point.

The C_{12} derivative **34d** displayed endothermic transitions at 121.1 °C (ΔH = 17.52 kJ/mol) and 125.3 °C (ΔH = 6.71 kJ/mol) on heating, and exothermic transitions at 117.9 °C (ΔH = 3.32 kJ/mol) and 62.9 °C (ΔH = 10.30 kJ/mol) on cooling. These transitions are indicative of a liquid crystalline phase both on heating and cooling.

Based on these findings, it is likely that all four mono-alkoxy 1,9-diphenyl-nona-1,3,6,8-tetraen-5-ones **34a-d** are liquid crystalline. The C_6, C_8 and C_{10} derivatives **34a, 34b** and **34c** are likely monotropic (displaying liquid crystallinity only when the temperature changes in one direction), while the C_{12} derivative **34d** is likely enantiotropic (displaying liquid crystallinity both on heating and cooling).

Figures 3.34 through **3.37** display DSC thermograms for the 1,9-diphenyl-nona-1,3,6,8-tetraen-5-ones **34a-d**.

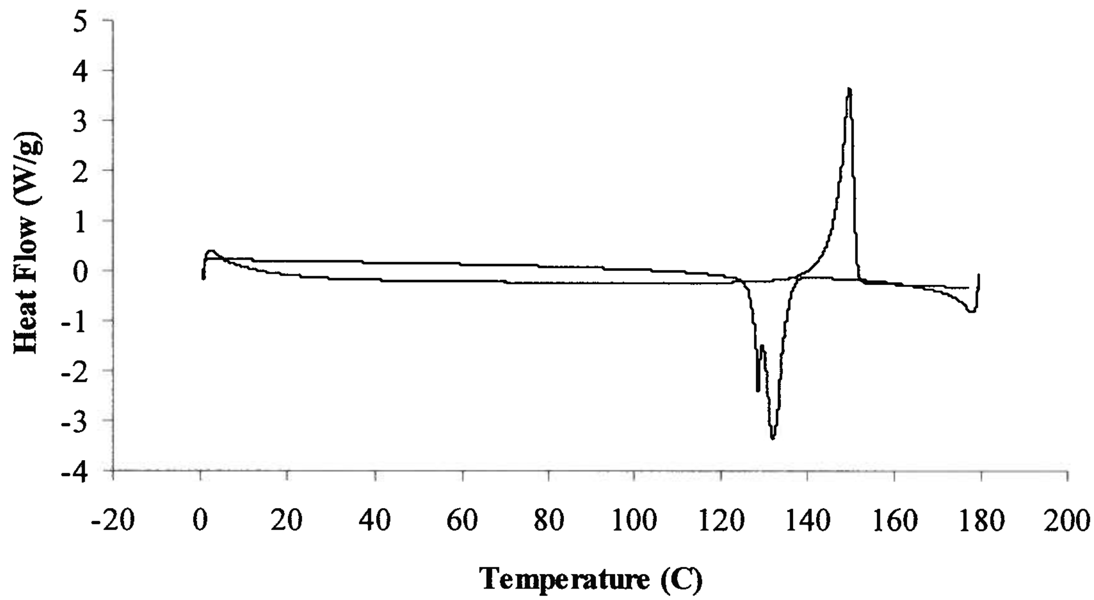

Figure 3.34: DSC thermogram of **34a**. Heating Rate: 10 °C/min. Cooling Rate: 5 °C/min.

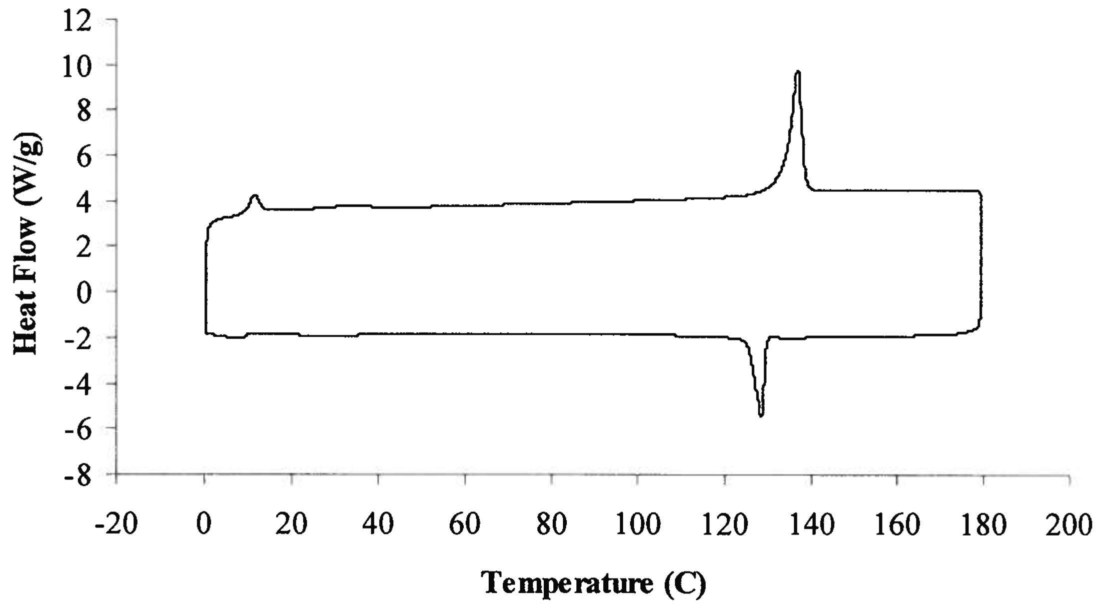

Figure 3.35: DSC thermogram of **34b**. Heating Rate: 10 °C/min. Cooling Rate: 5 °C/min.

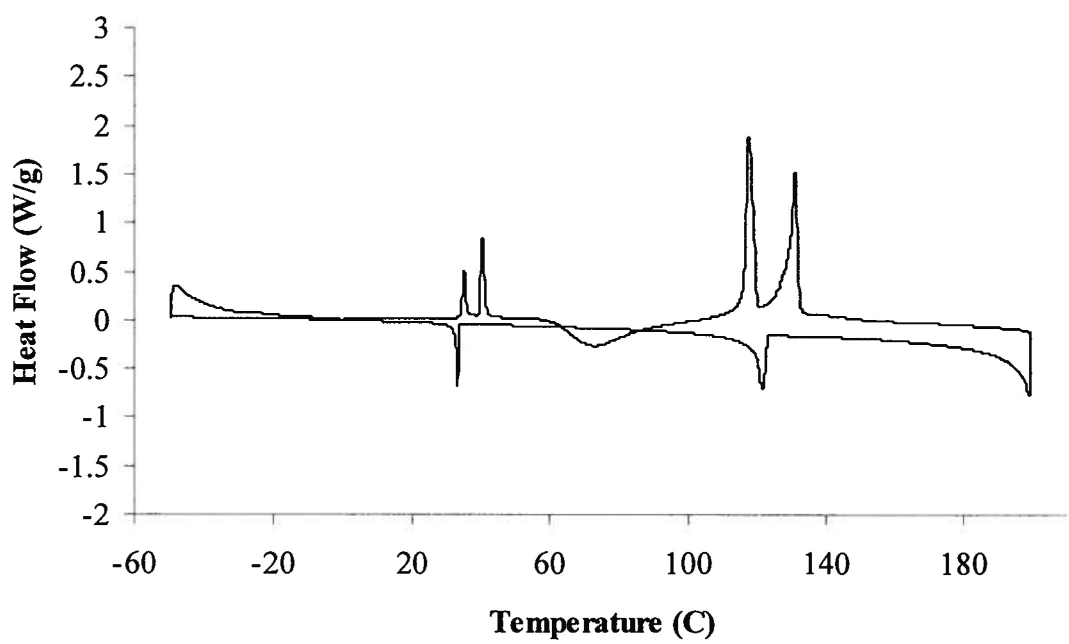

Figure 3.36: DSC thermogram of **34c**. Heating Rate: 10 °C/min. Cooling Rate: 5 °C/min.

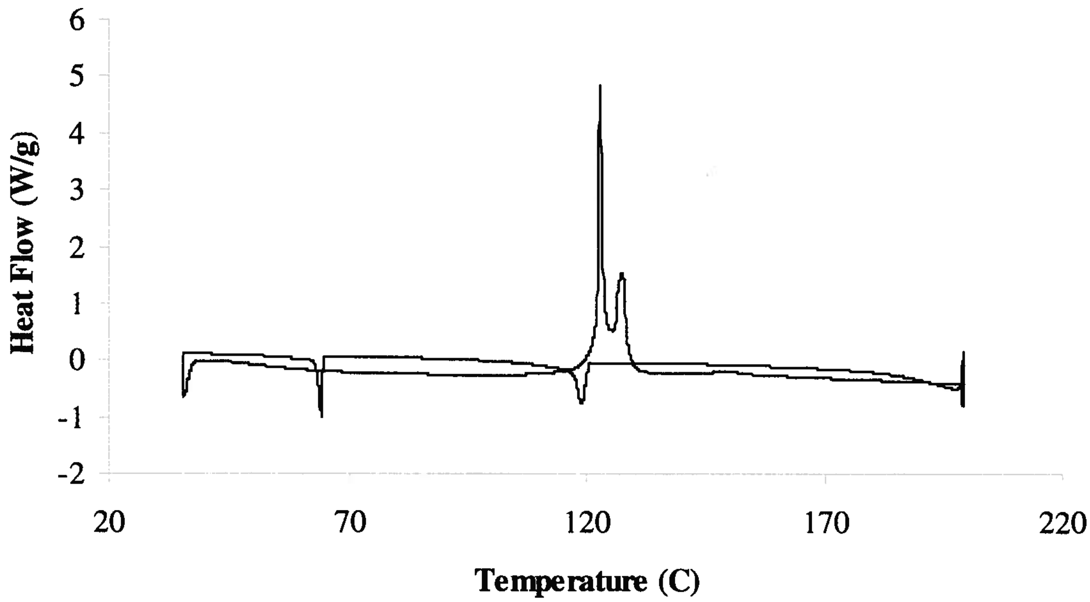

Figure 3.37: DSC thermogram of **34d**. Heating Rate: 10 °C/min. Cooling Rate: 5 °C/min.

It was determined that the mono-alkoxy benzophenones **2a-d** and mono-alkoxy dibenzylidene acetones **19a-d** were non-mesogenic, while the mono-alkoxy 1,9-diphenyl-nona-1,3,6,8-tetraen-5-ones **34a-d** likely were mesogenic. For the bis-alkoxy compounds, it was determined that the bis-C_6 benzophenone **9e**, as well as the bis-C_6 and bis-C_{10} dibenzylidene acetones **23e** and **23g**, were likely mesogenic, while the bis-C_8, bis-C_{10} and bis-C_{12} benzophenones **9f**, **9g** and **9h** and bis-C_{12} dibenzylidene acetone **23h** were not. The bis-C_8 dibenzylidene acetone **23f** did not appear liquid crystalline by DSC, but as the C_6 and C_{10} analogues did, it is also likely liquid crystalline. These findings were further investigated by POM.

3.4 Polarizing Optical Microscopy

All compounds displaying suitable phase transition enthalpies by DSC were observed using a Polarizing Optical Microscope (POM) equipped with a hot stage and temperature controller. Typical phase transition enthalpies are on the order of 30-50 kJ/mol for crystal to liquid crystal or crystal to isotropic transitions and 1-8 kJ/mol for liquid crystal to liquid crystal or liquid crystal to isotropic transitions.[5] The materials were heated to the clearing point and cooled to observe the liquid crystalline mesophase textures. The liquid crystallinity of the phases was verified by shearing the microscope coverslip to ensure fluidity.

3.4.1 Mono-Alkoxy Benzophenone Compounds 2a-d

Using POM, the first endothermic transitions of both the C_6 and C_8 derivatives **2a** and **2b** were both confirmed as crystal to crystal transitions. The absence of a liquid crystalline phase is consistent with the small transition enthalpies observed by DSC (*vide supra*).

3.4.2 Bis-Alkoxy Benzophenone Compounds 9e-h

The liquid crystalline mesophase of the C_6 derivative **9e** was identified as smectic A based on the characteristic focal conics texture.[69] **Figure 3.38** displays representative POM images of **9e** taken at a magnification of 10× in the: i) crystalline phase (Cr), ii) smectic A liquid crystalline phase (Sm A), and iii) isotropic liquid phase (I).

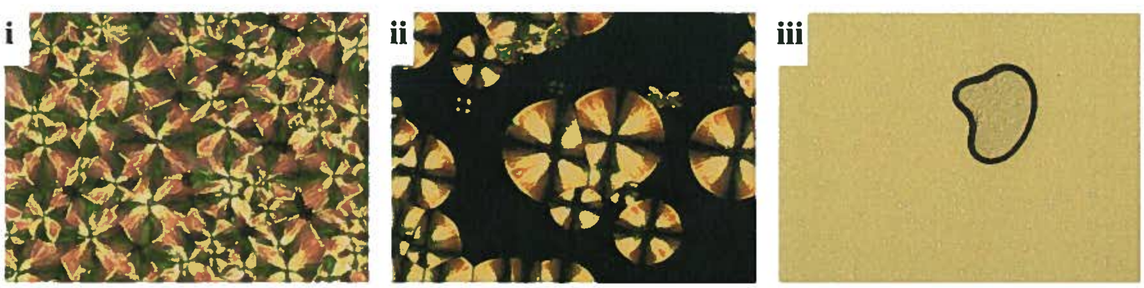

Figure 3.38: POM images of **9e** taken at a magnification of 10× i) -25 °C Cr ii) 30 °C Sm A (CP)[a] iii) 50 °C I. [a]CP = Crossed Polars.

The mesophase behaviour of benzophenone compounds **2a-h** is summarized in **Table 3.1**.

Table 3.1: Phase behaviour of **2a-d** and **9e-h**. [a]Transition temperatures were determined by DSC. [b]Cr = Crystalline, Sm = Smectic, I = Isotropic.

	Phase	T_t (°C)[a] →	Phase[b]
2a	Cr_1	⇌ (66.3 / 62.8) Cr_2 ⇌ (103.6 / 93.4)	I
2b	Cr_1	⇌ (89.9 / 87.5) Cr_2 ⇌ (98.2 / 90.8)	I
2c	Cr	⇌ (100.2 / 93.7)	I
2d	Cr	⇌ (103.2 / 98.9)	I
9e	Cr_1	→ -16.5 Cr_2 → 26.4 Sm A → 45.8; ← -14.9	I
9f	Cr	⇌ (56.9 / 11.3)	I
9g	Cr	⇌ (64.2 / 39.7)	I
9h	Cr	⇌ (71.8 / 47.0)	I

3.4.3 Mono-Alkoxy Dibenzylidene Acetone Compounds 19a-d

Based on the transition enthalpies of the first transition for the C_8 and C_{10} mono-alkoxy dba derivatives **19b** and **19c** (18.06 kJ/mol and 14.05 kJ/mol, respectively), these two transitions were labelled as crystal to crystal transitions. This was confirmed using POM, by observing the absence of a liquid crystalline phase.

3.4.4 Bis-Alkoxy Dibenzylidene Acetone Compounds 23e-h

The liquid crystalline mesophases of the C_6, C_8, and C_{10} mono-alkoxy dba derivatives **23e**, **23f** and **23g** were all characterized by POM. The C_6 derivative **23e** displayed a nematic mesophase between 54.8 °C and 62.9 °C on heating, but underwent a very slow crystallization at lower temperatures (0 °C) on cooling. **Figure 3.39** displays representative POM images of **23e** taken at a magnification of 20× in the i) crystalline phase (Cr), ii) nematic liquid crystalline phase (N), and iii) isotropic liquid phase (I).

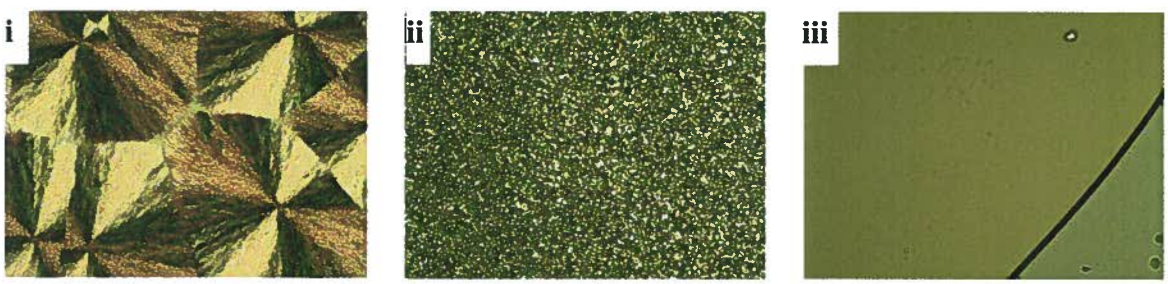

Figure 3.39: POM images of **23e** taken at a magnification of 20× i) 25 °C Cr ii) 55 °C N iii) 70 °C I

The C_8 derivative **23f** displayed a very short-lived, unstable nematic mesophase during the melting process at 62 °C, which was not visible on the DSC thermogram. The exothermic transitions observed by DSC on heating were both characterized as crystal to crystal transitions, and were not observed by POM. **Figure 3.40** displays representative POM images of **23f** taken at a magnification of 20× in the i) crystalline phase (Cr), ii) nematic liquid crystalline phase (N), and iii) isotropic liquid phase (I).

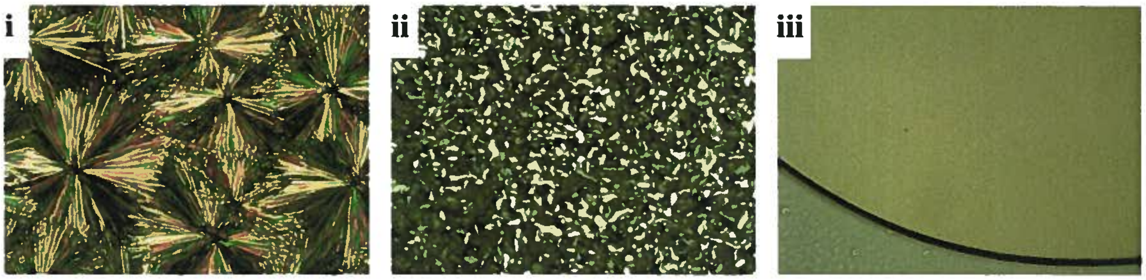

Figure 3.40: POM images of **23f** taken at a magnification of 20× i) 25 °C Cr ii) 62 °C N iii) 70 °C I

The C_{10} derivative **23g** again displayed a short-lived nematic mesophase on heating during the melting process at 71 °C, and a longer-lived nematic phase on cooling between 26.6 °C and 21.1 °C. The exothermic transition observed by DSC on heating was characterized as a crystal to crystal transition, and wasn't observed by POM. **Figure 3.41** displays representative POM images of **23g** taken at a magnification of 20× in the i) crystalline phase (Cr), ii) nematic liquid crystalline phase (N), and iii) isotropic liquid phase (I).

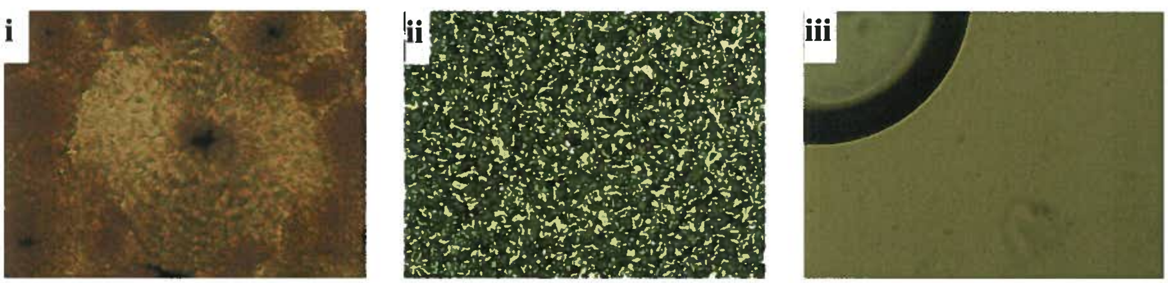

Figure 3.41: POM images of **23g** taken at a magnification of 20× i) 20 °C Cr ii) 25 °C N iii) 100 °C I

The mesophase behaviour of dba compounds **19a-d** and **23e-h** is summarized in **Table 3.2**.

Table 3.2: Phase behaviour of **19a-d** and **23e-h**. [a]Transition temperatures were determined by DSC. [b]Cr = Crystalline, N = Nematic, I = Isotropic.

	Phase → T_t (°C)[a] → Phase[b] (heating)	Cooling
19a	Cr → 109.8 → I	I → 101.6 → Cr
19b	Cr_1 → 81.5 → Cr_2 → 101.6 → I	I → 92.4 → Cr_1
19c	Cr_1 → 90.9 → Cr_2 → 101.4 → I	I → 94.8 → Cr_1
19d	Cr → 95.4 → I	I → 90.7 → Cr
23e	Cr → 54.8 → N → 62.9 → I	n/a
23f	Cr_1 → 3.2 → Cr_2 → 30.9 → Cr_3 → 62.0 → N → 65.4 → I	I → 23.0 → Cr_1
23g	Cr_1 → 39.1 → Cr_2 → 71.5 → I	I → 26.6 → N → 21.1 → Cr_1
23h	Cr_1 → 51.2 → Cr_2 → 72.1 → I	I → 31.4 → Cr_1

3.4.5 Mono-Alkoxy 1,9-Diphenyl-nona-1,3,6,8-tetraen-5-ones 34a-d

The liquid crystalline mesophases of the mono-alkoxy 1,9-diphenyl-nona-1,3,6,8-tetraen-5-ones **34a-d** were all characterized using POM. The C_6 derivative **34a** was found to exhibit a nematic mesophase on cooling to 130 °C from the isotropic liquid. **Figure 3.26** displays representative POM images of C_6 derivative **34a** taken at a magnification of 10× in the i) crystalline phase (Cr), ii) nematic liquid crystalline phase (N), and iii) isotropic liquid phase (I).

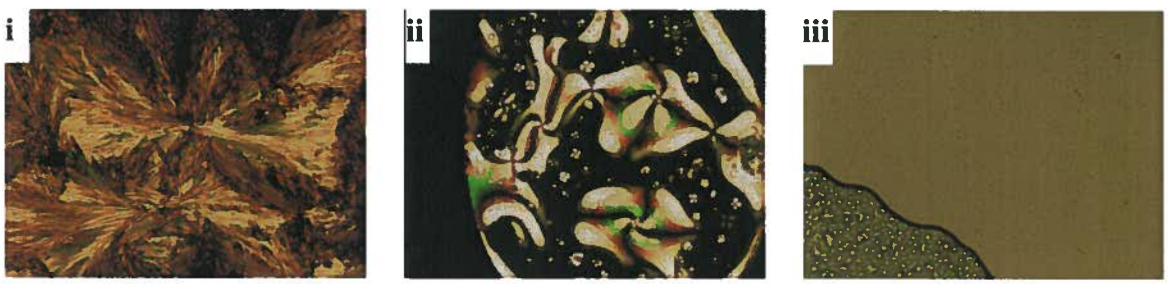

Figure 3.42: POM images of **34a** taken at a magnification of 10× i) 25 °C Cr ii) 130 °C N (CP)[a] iii) 155 °C I. [a]CP = Crossed Polars

The C_8 derivative **34b** underwent a phase transition from isotropic liquid to nematic mesophase on cooling at 135 °C which was unstable and melted back to the isotropic liquid as cooling continued until 128 °C when the isotropic liquid crystallized. The exothermic transition at 8 °C by DSC was characterized as a crystal to crystal transition based on the transition enthalpy value. **Figure 3.43** displays representative POM images of C_8 derivative **34b** taken at a magnification of 10× in the: i) crystalline phase (Cr), ii) nematic liquid crystalline phase (N) and iii) isotropic liquid phase (I).

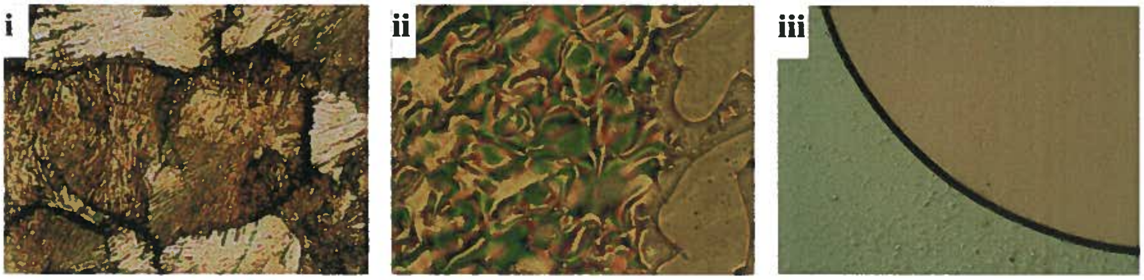

Figure 3.43: POM images of **34b** taken at a magnification of 10× i) 25 °C Cr ii) 136 °C N iii) 140 °C I

The C_{10} derivative **34c** was found to exhibit a nematic liquid crystalline phase between 130.9 °C and 117.5 °C on cooling. The endothermic phase transitions at 34.9 °C and 40.3 °C and exothermic transition at 33.2 °C were characterized as crystal to crystal transitions based on the DSC transition enthalpy values and lack of liquid crystallinity by POM. **Figure 3.44** displays representative POM images of C_{10} derivative **34c** taken at a magnification of 10× in the: i) crystalline phase (Cr), ii) nematic liquid crystalline phase (N) and iii) isotropic liquid phase (I).

Figure 3.44: POM images of **34c** taken at a magnification of 10× i) 25 °C Cr ii) 125 °C N iii)140 °C I

The C_{12} derivative **34d** exhibited a nematic liquid crystalline phase on cooling from the isotropic liquid between 118 °C and 63 °C. **Figure 3.46** displays POM images of **34d** taken at a magnification of 10× in the: i) crystalline phase (Cr), ii) nematic mesophase (N), and iii) isotropic liquid phase (I).

Figure 3.45: POM images of **34d** taken at a magnification of 10× i) 25 °C Cr ii) 122 °C N iii) 140 °C I

The mesophase behaviour of the 1,9-diphenyl-nona-1,3,6,8-tetraen-5-one compounds **34a-d** is summarized in **Table 3.3**.

Table 3.3: Phase behaviour of **34a-d**. [a]Transition temperatures were determined by DSC. [b]Cr = Crystalline, N = Nematic, I = Isotropic.

	Phase ——— T_t (°C)[a] ———→ Phase[b]
34a	Cr —149.7→ I; I —131.8→ N —128.5→ Cr
34b	Cr_1 ⇌ Cr_2 (11.6 / 8.0); Cr_2 —136.8→ I; I —135.0→ N —128.5→ Cr_2
34c	Cr_1 —34.9→ Cr_2 —40.3→ Cr_3; Cr_3 —33.2→ Cr_1; Cr_3 —117.5→ N —130.9→ I; I —121.4→ Cr_3
34d	Cr ⇌ N (121.1 / 62.9); N ⇌ I (125.3 / 117.9)

Based on the above results, benzophenone and dibenzylidene acetone are not suitable cores for liquid crystalline materials with only one alkoxy side chain. 1,9-Diphenyl-nona-1,3,6,8-tetraen-5-one cores, on the other hand, are. When the number of alkoxy chains is increased for benzophenone and dibenzylidene acetone, the compounds are more likely to be mesogenic. Furthermore, it can be stated that the alkoxy side chain length, the number of alkoxy side chains, as well as the size and extent of conjugation of the rigid core all affect molecular self-assembly into liquid crystalline mesophases.

The alkoxy side chain length affects liquid crystalline formation, but the length required to induce liquid crystalline formation seems to be dependent upon the size of the core. For the largest core size, the mono-alkoxy 1,9-diphenyl-nona-1,3,6,8-tetraen-5-ones **34a-d**, all four chain lengths: C_6H_{13}, C_8H_{17}, $C_{10}H_{21}$ and $C_{12}H_{25}$ led to liquid crystalline behaviour. The clearing temperature decreased with increasing alkoxy side chain length, and a similar trend in the size of the mesophase range was observed. The C_6 and C_8 derivatives **34a** and **34b** displayed monotropic mesophases on cooling with temperature ranges on the order of 3-4 °C, while the C_{10} derivative **34c** displayed the widest monotropic mesophase on heating (13.4 °C). The C_{12} derivative **34d**, meanwhile, exhibited a liquid crystalline mesophase between 121.1 °C and 125.3 °C on heating, and between 117.9 °C and 62.9 °C (a range of 55 °C) on cooling.

The bis-alkoxy benzophenones **9e-h,** on the other hand, showed a distinct increase in the clearing temperature with increasing alkoxy side chain length. Similarly, the bis-alkoxy dibenzylidene acetones **23e-h** showed a mild increase in clearing temperature with increasing alkoxy side chain length. The size of the mesophase range for **23e-h** did not show a correlation with alkoxy side chain length.

Interestingly, the non-mesogenic mono-alkoxy benzophenones **2a-d** showed no correlation between the melting temperature and alkoxy side chain length, while the non-mesogenic mono-alkoxy dibenzylidene acetone compounds **19a-d** showed a decrease in the melting temperature with increasing alkoxy side chain length.

For the largest core, the 1,9-diphenyl-nona-1,3,6,8-tetraen-5-one compounds, these results agree with the hypothesis that longer alkoxy chains should lead to mesophases with broader temperature ranges as well as decreased melting points. However, for the bis-alkoxy dibenzylidene acetone compounds, the above trend was not observed. In addition, it seems that for mesophase formation for this class of molecules, the alkoxy side chain length required is dependent on the size of the core.

The number of alkoxy side chains also impacts the formation of liquid crystalline mesophases. It appears that for this class of C_2 symmetric molecules, increasing the number of alkoxy side chains helps induce mesophase formation. The mono-alkoxy benzophenones **2a-d** and mono-alkoxy dibenzylidene acetones **19a-d** were all non-mesogenic. However, when the number of side chains was increased from 1 to 2 for the benzophenone cores, the C_6 derivative **9e** was mesogenic, and when the number of side chains was increased from 1 to 2 for the dibenzylidene acetone cores, the C_6, C_8 and C_{10} derivatives **23a**, **23b** and **23c** all appeared mesogenic. This result supports the hypothesis that increasing the number of alkoxy chains will help the self-assembly into liquid crystalline mesophases.

Finally, the core size and extent of conjugation plays a strong role in the self-assembly into liquid crystalline mesophases. While none of the mono-alkoxy benzophenones **2a-d** or dibenzylidene acetones **19a-d** exhibited liquid crystalline phases, all of the 1,9-diphenyl-nona-1,3,6,8-tetraen-5-ones **34a-d** exhibited a nematic liquid crystalline phase. Clearly, larger core size and increased conjugation is required to induce liquid crystallinity when compared to the smaller, less conjugated analogues. In addition, for the bis-alkoxy benzophenones **9e-h**, only the C_6 derivative **9e** was liquid crystalline, while for the bis-alkoxy dibenzylidene acetones **23e-h**, the C_6, C_8 and C_{10} derivatives **23e**, **23f** and **23g** were liquid crystalline. It is apparent that increasing the core size from benzophenone to dibenzylidene acetone helps induce liquid crystallinity for the bis-alkoxy derivatives. Thus, these findings are in agreement with the hypothesis that increased core size and conjugation should increase the π stacking ability, resulting in mesophase formation.

Chapter 4

Conclusions

4.1 Conclusions

The hypothesis for this research was that alkoxy side chain length, the number of alkoxy side chains, and the core size and conjugation would all strongly impact liquid crystalline phase formation. Longer alkoxy chains should lead to mesophases with broader temperature ranges as well as decreased melting temperatures T_m.[16] In addition, the number of alkoxy side chains would increase differentiation between the aromatic core and aliphatic side chain. This should lead to greater organization in the liquid phase which, in turn, should lead to broader temperature range mesophases. Furthermore, the addition of multiple side chains should decrease the alkoxy chain length required to induce liquid crystalline phase formation. Finally, increasing the core size and conjugation from benzophenone (**a**) to dibenzylidene acetone (**b**) to 1,9-diphenyl-nona-1,3,6,8-tetra-en-5-one (**b**) should increase the ability of the molecules to π stack, which should result in more stable, broader temperature range mesophases.

In this thesis a series of compounds consisting of benzophenone (**a**), dibenzylidene-acetone (**b**) or 1,9-diphenyl-nona-1,3,6,8-tetraen-5-one (**c**) cores with either one or two linear alkoxy side chains varying in length from C_6H_{13} to $C_{12}H_{25}$ were prepared. The compounds were characterized by FTIR, ^{1}H NMR and ^{13}C NMR spectroscopy. The liquid crystalline phase behaviour was investigated by differential scanning calorimetry and polarizing optical microscopy, and factors influencing liquid crystallinity, e.g. alkoxy side-chain length and number of side chains, as well as mesogen core size and conjugation were studied.

4.1.1 Synthesis

It was determined that alkoxy chain length, the number of alkoxy side chains and core size and the extent of conjugation all affected reaction yields.

For the various Williamson ether synthesis[25] reactions, yields tended to increase with increasing alkoxy chain length. By contrast, the increased alkoxy chain lengths seemed to attenuate further reaction: the yields for the aldol condensation reactions tended to decrease with increasing chain length, owing probably to lower solubility and slower diffusion in solution.

Similarly, both the increased core size and extent of conjugation, as well as the increased number of alkoxy chains seems to inhibit reactivity. For the mono-alkoxy dba compounds, a bidirectional aldol condensation was achieved at room temperature. For the bis-alkoxy dba compounds and mono-alkoxy 1,9-diphenyl-nona-1,3,6,8-tetraen-5-one compounds, stepwise aldol condensations and elevated temperatures were required to achieve the desired molecules. Again, this is most likely due to solubility and diffusion issues.

The mono-alkoxy benzophenones **2a-d** were prepared in one step with yields ranging from 64 % to 97 %. The key synthetic step was a Williamson ether synthesis[25] to append the alkoxy chains.

The bis-alkoxy benzophenone compounds **9e-h** were prepared in four linear steps (five total steps) with overall yields ranging from 40 % to 52 %. The key synthetic step was a Friedel-Crafts acylation[29] to couple the 1,2-bis-alkoxy benzenes with the 3,4-bis-alkoxy benzoic acids.

The mono-alkoxy dba compounds **19a-d** were prepared in two steps with overall yields ranging from 58 % to 72 %. The key synthetic step was a bidirectional aldol condensation between 4-alkoxy benzaldehydes and acetone.

The bis-alkoxy dba compounds **23e-h** were prepared in three synthetic steps with overall yields ranging from 35% to 55%. The key synthetic steps were two stepwise aldol condensations to construct the dba core.

The mono-alkoxy 1,9-diphenyl-nona-1,3,6,8-tetraen-5-one compounds **34a-d** were prepared in six linear steps with overall yields ranging from 42 % to 56 %. The key synthetic steps were stepwise aldol condensations between acetone and 4-alkoxy cinnamaldehydes.

4.1.2 Mesophase Formation

It was found that the alkoxy side chain length, the number of alkoxy side chains, and the size of the rigid core all affected the self-assembly into liquid crystalline phases. The alkoxy side chain length affected mesophase formation, but the length required to induce liquid crystallinity seemed dependent on the size of the core. The mono-alkoxy benzophenones were non-mesogenic and showed no relationship between melting points and side chain lengths. By contrast, the mono-alkoxy dibenzylidene acetones were also non-mesogenic, but showed decreased melting points with increased side chain length. For the largest 1,9-diphenyl-nona-1,3,6,8-tetra-en-5-one core, all four alkoxy chain lengths induced liquid crystalline mesophase formation, with the clearing temperature decreasing and mesophase temperature range increasing with increasing alkoxy side chain length.

For the bis-alkoxy benzophenones, only the C_6 derivative was mesogenic, while the C_8, C_{10} and C_{12} derivatives were not, and the clearing point increased with increasing side chain length. The C_6, C_8 and C_{10} bis-alkoxy dibenzylidene acetone derivatives were mesogenic, while the C_{12} derivative was not, and the clearing temperature increased with increasing side chain length. Interestingly, there was no observable trend in the temperature range of the resulting mesophases. These findings are inconsistent, as one result (compounds **34a-d**) agrees with the stated hypothesis that increased alkoxy side-chain length will widen or increase the temperature range of the mesophases, while the other (compounds **9e-h**) disagrees with this hypothesis.

Similarly, mesophase formation was affected by the number of alkoxy side-chains. For this class of C_2 symmetric molecules, increasing the number of alkoxy side chains helps induce mesophase formation. Neither the mono-alkoxy benzophenones nor mono-alkoxy dibenzylidene acetones were mesogenic, while half of their bis-alkoxy analogues were liquid crystalline. For the bis-alkoxy benzophenones, only the C_6 derivative was mesogenic while the C_8, C_{10} and C_{12} derivatives were not. For the bis-alkoxy dibenzylidene acetones, the C_6, C_8 and C_{10} derivatives were mesogenic while the C_{12} derivative was not. These findings agree strongly with the hypothesis that increasing the number of alkoxy chains should lead to greater molecular assembly in the liquid phase, leading in turn to mesophase formation.

Finally, core size and the extent of conjugation in the core played an important part in self-assembly and mesophase formation. Increasing the core size led to a greater tendency for the materials to form liquid crystalline phases: for the 1,9-diphenyl-nona-1,3,6,8-tetraen-5-one core, all four side chain lengths resulted in liquid crystalline mesophases, compared to the benzophenone and the dibenzylidene acetone cores, neither of which were mesogenic for the mono-alkoxy variants. In addition, increasing the core size led to a decreased melting point and increased clearing temperature. Likewise, for the bis-alkoxy analogues of the benzophenones and dibenzylidene acetones, it seems that increasing core size helps induce liquid crystallinity. While only the bis-C_6 benzophenone was mesogenic, when the core size was increased to dibenzylidene acetone, the C_6, C_8 and C_{10} compounds were mesogenic. These findings are in agreement with the hypothesis that increased core size and conjugation should increase the π stacking ability, resulting in more stable mesophase.

In this study, it was found benzophenone, dibenzylidene acetone and 1,9-diphenyl-nona-1,3,6,8-tetraen-5-one compounds are suitable cores for liquid crystalline materials. In addition, is was determined that for this class of C_2 symmetric molecules, alkoxy side chain length, the number of alkoxy side chains and the core size and extent of conjugation all have an impact on the ability of C_2 symmetric molecules to self-assemble into liquid crystalline phases. The variables affecting mesophase formation is an important area of research which will aid in our understanding of the ordering of liquid crystalline systems. These findings will help when designing new liquid crystalline materials in order to exploit the potential applications of liquid crystals.

Chapter 5

Future Work

5.1 Recommendations for Future Work

There are many aspects of this research that can be further investigated to better understand the factors influencing the self-assembly of C_2 symmetric bent-core mesogens. Among the aspects which could affect mesophase formation that could be further investigated are: 1) the upper and lower limits of alkoxy chain length required, 2) the effect of alkoxy chain regiochemistry, 3) the effect of multiple ($n > 2$) alkoxy chains and 4) the effect of symmetry.

5.1.1 The Upper and Lower Limits of Alkoxy Chain Length Required to Induce Mesophase Formation

One aspect of this research that could be examined further is the limits on alkoxy chain length to induce liquid crystalline mesophase formation.

All four of the mono-alkoxy 1,9-diphenyl-nona-1,3,6,8-tetra-en-5-one compounds prepared were mesogenic, with the C_6 and C_8 derivatives displaying only a very narrow monotropic mesophase. The C_{10} analogue had a wider monotropic mesophase and the C_{12} displayed the widest mesophase. It would be of interest to know at what point the alkoxy chain is too short or is too long to induce mesophase formation for this class of molecule.

Similarly, the bis-alkoxy dibenzylidene acetones were liquid crystalline for the C_6, C_8, C_{10} derivatives, but not for the C_{12} derivative. It would be of value to know the lower limit for mesophase formation. More specifically, would the 3,4-bis-butyloxy derivative be liquid crystalline?

5.1.2 The Effect of Alkoxy Chain Regiochemistry on Mesophase Formation

A second aspect of this research that could be investigated more thoroughly is the effect of alkoxy chain regiochemistry on liquid crystalline mesophase formation. The regiochemistry of the alkoxy side chain could impact both the sterics and the electronics of the system.

All of the mono-alkoxy compounds prepared contained the side chain at the 4 position of the aromatic ring. To investigate the effect of regiochemistry, mono-alkoxy compounds containing the side chain at the 2 and 3 positions could be prepared. **Figure 5.1** displays 2-alkoxy and 3-alkoxy 1,9-diphenyl-nona-1,3,6,8-tetraen-5-one derivatives.

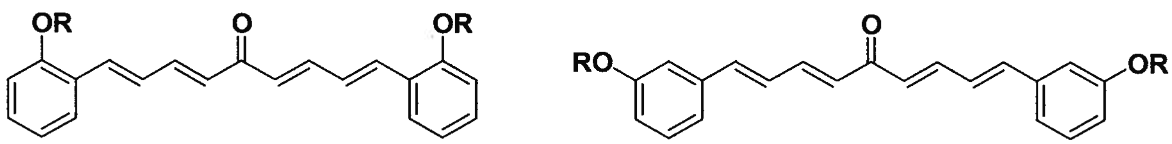

Figure 5.1: 2-alkoxy and 3-alkoxy 1,9-diphenyl-nona-1,3,6,8-tetraen-5-ones.

In addition to the steric effects of changing the regiochemistry of the alkoxy side chain, there are also electronic effects that could impact liquid crystalline mesophase formation. With the alkoxy chain at the 2 or 4 position, it is conjugated into the aromatic core, whereas with the alkoxy chain at the 3 position, it is not. This could lead to interesting stereoelectronic effects.

Similarly, all of the bis-alkoxy compounds prepared contained the side chains at the 3 and 4 positions of the aromatic ring. Bis-alkoxy compounds with side chains at the 2, 3; 2, 4; 2, 5 or 3, 5 positions could be prepared, which would again allow investigation of both the steric and electronic effects of side chain regiochemistry on liquid crystalline mesophase formation.

In the case where the side chains are at the 2 and 4 positions, both would be conjugated into the aromatic system. In the case where the side chains are at the 3 and 5 positions, neither would be conjugated into the aromatic system. It would be interesting to see whether these slight changes had an impact on the ability of the system to self-assemble when compared to the studied case of the 3,4-bis-alkoxy derivative, with one alkoxy group conjugated into the core, and the other not. **Figure 5.2** displays some possible variants of bis-alkoxy dba compounds.

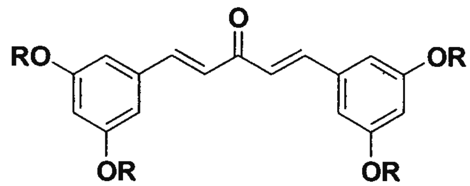

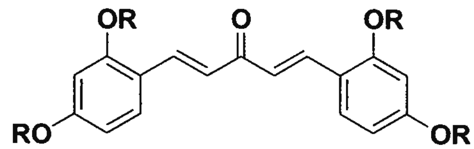

Figure 5.2: 3,5-bis alkoxy and 2,4-bis-alkoxy dibenzylidene acetones.

It would also be interesting to study the steric effects of placing the alkoxy chains closer to the aromatic core. A 2,5-bis-alkoxy compound might have the alkoxy chains too close to the core, interrupting the π-stacking that is so critical for self-assembly. **Figure 5.3** displays a 2,5-bis-alkoxy dba derivative.

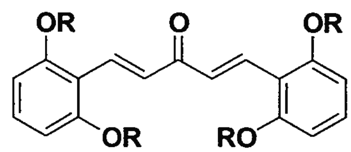

Figure 5.3: 2,5-bis-alkoxy dibenzylidene acetone.

5.1.3 The Effect of Multiple (n > 2) Alkoxy Chains on Mesophase Formation

A third aspect of this research that could be studied in more detail is the effect of multiple (n > 2) alkoxy chains on liquid crystalline mesophase formation. When the number of alkoxy side chains is increased from 1 to 2, liquid crystalline mesophase formation seems to be enhanced. It would be beneficial to investigate the effect of 3, 4 or even 5 alkoxy chains. With an increased number of alkoxy chains, the differentiation of hydrophobic and hydrophilic regions might be enhanced, possibly leading to wider, more stable mesophases. **Figure 5.4** displays some possible examples of compounds with multiple alkoxy chains.

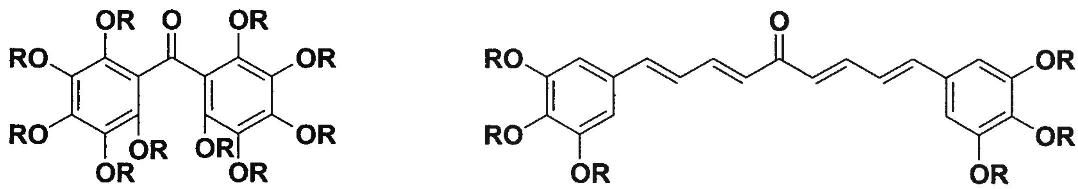

Figure 5.4: Examples of possible mesogens containing multiple alkoxy chains.

5.1.4 The Effect of Symmetry on Mesophase Formation

A final aspect of this research that could be elaborated on is the effect of symmetry on liquid crystalline mesophase formation. All of the compounds prepared exhibited C_2 symmetry.

One possible extension would be to prepare compounds which are not C_2 symmetric, but instead whose sides display differing numbers of side chains or side chains in differing positions. **Figure 5.5** displays some possible examples of non-C_2 symmetric dibenzylidene acetone derivatives.

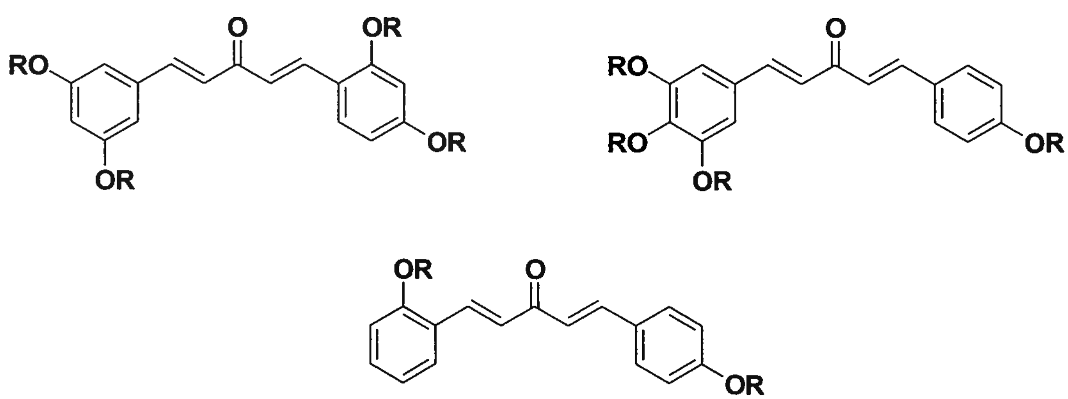

Figure 5.5: Examples of non-C_2 symmetric dibenzylidene acetone derivatives.

Chapter 6

References

(1) Collings, P. J. *Liquid Crystals: Nature's Delicate Phase of Matter*; Princeton University Press: New Jersey, 1990.

(2) Reinitzer, F. Beitrage zur Kenntniss des Cholesterins *Monatschefte fur Chemie* **1888**, *9*, 421-441.

(3) Lehmann, O. Uber Fliessende Krystalle *Zeitschrift fur Physikalische Chemie* **1889**, *4*, 462-472.

(4) Stegemeyer, H. *Liquid Crystals;* Springer, New York: 1994.

(5) Gray, G.W. *Thermotropic Liquid Crystals;* John Wiley and Sons, Chichester, England: 1987.

(6) Skoog, D. A., Holler, F. J., Nieman, T. A. *Principles of Instrumental Analysis, 5th Ed.* Thomson Learning, Toronto, 1998.

(7) Freudenmann, R., Behnisch, B., Hanack, M. Synthesis of Conjugated-Bridged Triphenylenes and Applications in OLEDs. *Journal of Materials Chemistry* **2001**, *11*, 1618-1624.

(8) Schmidt-Mende, L., Fechtenkotter, A., Mullen, K., Moons, E., Friend, R. H., Mackenzie, J. D. Self-organized Discotic Liquid Crystals for High-Efficiency Organic Photovoltaics. *Science*, **2001**, *293*, 1119-1122.

(9) (a) Vlachos, P., Mansoor, B., Aldred, M. P., O'Nell, M., Kelly, S. M. Charge-Transport in Crystalline Organic Semiconductors with Liquid Crystalline Order. *Chemical Communications.* **2005**, 2921-2923. (b) Aldred, M. P., Eastwood, A. J., Kelly, S. M.; Vlachos, P.; Contret, A. E. A.; Farrar, S. R.; Mansoor, B.; O'Nell, M.; Chung Tsoi, W. Light-emitting Fluorene Photoreactive Liquid Crystals for Organic Electroluminescence. *Chemistry of Materials* **2004**, *16*, 4928-4936. (c)

Barche, J.; Janietz, S.; Ahles, M.; Schmechel, R.; von Seggern, H. Cross-Linked Liquid Crystalline Materials-A Possible Strategy to Ordered Organic Semiconductors. *Chemistry of Materials* **2004**, *16*, 4286-4291. (d) van de Craats, A. M.; Stutzmann, N.; Bunk, O.; Nielsen, M. M.; Watson, M.; Mullen, K.; Chanzy, H. D.; Sirrnghaus, H.; Friend, R. H. Meso-Epitaxial Solution Growth of Self-Organizing Discotic Liquid Crystalline Semiconductors. *Advanced Materials.* **2003**, *15*, 495-499. (e) Mochizuki, H.; Hasui, T.; Kawamoto, M.; Shiono, T.; Ikeda, T.; Adachi, C.; Taniguchib, Y.; Shirotac, Y. Novel Liquid Crystalline and Amorphous Materials Containing Oxadiazole and Amine Moieties for Electroluminescent Devices. *Chemical Communications* **2000**, 1923-1924.

(10) (a) Tanaka, S., Adachi, C., Koyama T., Taniguchi, Y. Organic Light Emitting Diodes Using Triphenylene Derivatives as a Hole Transport Material. *Chemistry Letters* **1998,** 975-976. (b) Bacher, A., Bleyl, I., Erdelen, C. H., Haarer, D., Paulus, W., Schmidt, H.-W. Low Molecular Weight and Polymeric Triphenylenes as Hole Transport Materials in Organic Two-Layer LEDs. *Advanced Materials* **1997**, *9*, 1031-1035. (c) Christ, T., Glusen, B., Greiner, A., Kettner, A., Sander, R., Stumpflen, V., Tsukruk, V., Wenndorf, J. H. Columnar Discotics for Light Emitting Diodes. *Advanced Materials* **1997**, *9*, 48-52.

(11) Chandrasekhar, S. *Liquid Crystals, 2nd Edition.* Cambridge University Press, Cambridge, UK: 1992.

(12) Jeong, M., J., Park, J. H., Lee, C., Chang, J. Y. Discotic Liquid Hydrazone Compounds: Synthesis and Mesomorphic Properties. *Organic Letters* **2006,** *8*, 2221-2224.

(13) Foster, E. J., Jones, R. B., Lavigueur, C., Williams, V. E. Structural Factors Controlling the Self-Assembly of Columnar Liquid Crystals. *Journal of the American Chemical Society* **2006**, *128*, 8569-8574.

(14) van de Craats, A. M., Warman, J. M. The Core-Size Effect on the Mobility of Charge in Discotic Liquid Crystalline Materials. *Advanced Materials* **2001**, *13*, 130-133.

(15) Wang, C.-S., Wang, I.-W., Cheng, K.-L., Lai, C. K. The Effect of Polar Substituents on the Heterocyclic Benzoxazoles. *Tetrahedron* **2006**, *62*, 9383-9392.

(16) Lai, C. K., Liu, H.-C., Li, F.-J., Cheng, K.-L., Sheu, H.-S. Heterocyclic Benzoxazole-Based Liquid Crystals. *Liquid Crystals* **2005**, *32*, 85-94.

(17) Engel, M. K., Bassoul, P., Bosio, L., Lehmanns, H., Hanacks, M., Simon, J. Mesomorphic Molecular Materials: Influence of Chain Length on the Structural Properties of Octa-Alkyl Substituted Phthalocyanines. *Liquid Crystals* **1993**, *15*, 709-722.

(18) Destrade, C., Nguyen, H. T., Gasparoux, H. Mesogenic and Nonmesogenic Central Rigid Cores. *Molecular Crystals and Liquid Crystals* **1980,** *59*, 273-288.

(19) Koden, M., Yagyu, T., Takenaka, S., Terauchi, H., Kusabayashi, S. The Effect of the Alkyl Chain Length on the Liquid Crystalline Properties of *p*-Substituted Cholesterol 4-Benzoylbenzoates. *Chemistry Letters* **1981**, 269-272.

(20) (a) Bhowmik, P. K., Han, H. Fully Aromatic Thermotropic Liquid Crystalline Polyesters of 3-Phenyl-4-4'-Biphenol with 4,4'-Benzophenone Dicarboxylic Acid. *Journal of Polymer Science, Part A: Polymer Chemistry* **1995**, *33*, 415-426. (b) Han, H., Bhowmik, P. K. Wholly Aromatic Thermotropic Liquid Crystalline Polyesters of 4,4'-Bisphenol, Substituted Biphenols and 1,1'-Binaphthyl-4,4'-diol with 3,4'-Benzophenone Dicarboxylic Acid. *Journal of Polymer Science, Part A: Polymer Chemistry* **1995**, *33*, 211-225. (c) Stagnaro, P., Tavella, F., Costa, G.,

Valenti, B. New Thermotropic Copoly(Keto Esters) Based on 3,4'-Disubstituted Benzophenones. *Macromolecular Chemistry and Physics* **1997**, 198, 2599-2611.

(21) (a) Baeyer, A. Dibenzalacetone and Triphenylmethane *Berichte der Deutschen Chemischen Gesellschaft* **1907**, *40*, 3083-3090.

(22) (a) Takahashi, Y., Ito, Ts., Sakai, S., Ishii, Y. Novel Palladium(0) Complex; Bis(dibenzylideneacetone)palladium(0). *Journal of the Chemical Society D: Chemical Communications* **1970**, *17*, 1065-1066. (b) Ishii, Y., Hasegawa, S., Kimura, S., Itoh, K. Novel Trinuclear Palladium(0) Complexes. Tris(tribenzylideneacetone)tripalladium(solvent) Complexes and Their Reactions. *Journal of Organometallic Chemistry* **1974**, *73*, 411-418.

(23) (a) Bennett, G. M., Jones, B. Mesomorphism and Polymorphism of Some *p*-Alkoxybenzoic and *p*-Alkoxycinnamic Acids. *Journal of the Chemical Society* **1939**, 420-425. (b) Gray, G. W., Jones, B. Mesomorphism and Chemical Constitution. II. The Trans-*p*-n-alkoxycinnamic Acids. *Journal of the Chemical Society* **1954**, 1467-1470.

(24) Praefcke, K., Kohne, B., Gundogan, B., Demus, D., Diele. S., Pelzl, G. Liquid Crystal Compounds. 53. 2,3,4-Trihexyloxycinnamic Acid – the First Example of a Novel Series of Biaxial Nematic Liquid Crystals. *Molecular Crystals and Liquid Crystals* **1990**, *7*, 27-32.

(25) Ragauskas, A. J., Williams, C. K., Davison, B. H., Britovsek, G., Cairney, J., Eckert, C. A., Frederick Jr., W. J., Hallett, J. P., Leak, D. L., Liotta, C. L., Mielenz, J. R., Murphy, R., Templer, R., Tschaplinski, T. The Path Forward for Biofuels and Biomaterials **Science**, *311*, 484-489.

(26) Williamson, A. W. On Etherification. *Quarterly Journal of the Chemical Society of London* **1852,** *4*, 229-239.

(27) Sugawara, T., Murata, S., Kimura, K., Iwamura, H., Sugawara, Y., Iwasaki, H. Design of Molecular Assembly of Diphenylcarbenes having Ferromagnetic Intermolecular Interactions. *Journal of the American Chemical Society* **1985**, *107*, 5293-5294.

(28) Schultz, A., Diele, S., Lschat, S., Nimuz, M. Novel Columnar Tetraphenylethenes via Mcmurry Coupling. *Advanced Functional Materials* **2001**, *11*, 441-446.

(29) (a) Nuckolls, C., Guo, X., Kim, P., Xiao, S., Myers, M. *PCT Int. Appl.* **2007**, 48pp. (b) Nuckolls, C., Guo, X., Kim, P. *PCT Int. Appl.* **2007**, 49pp. (c) Martinotto, L., Peruzzotti, F., Del Brenna, M. *PCT Int. Appl.* **2001**, 34pp.

(30) Friedel, C., Crafts, J. M. Sur Une Nouvelle Methode Generale de Synthese d'Hydrocarbures, d'Acetones, etc. *Comptes Rendus des Seances de L'Academie des Sciences* **1877**, *84*, 1392.

(31) Xiao, S., Tang, J., Beetz, T., Guo, X., Tremblay, N., Siegrist, T., Zhu, Y., Steigerwald, M., Nuckolls, C. Transferring Self-Assembled, Nanoscale Cables into Electrical Devices. *Journal of the American Chemical Society* **2006**, *128*, 10700-10701.

(32) Fairlamb, I. J. S.; Kapdi, A. R.; Lee, A. F. η^2-dba Complexes of Pd(0): The Substituent Effect in Suzuki-Miyaura Coupling. *Organic Letters* **2004,** *6,* 4435-4438.

(33) Knoevenagel, E., Baebenroth, F., Wollweber, O. Condensation of Malonic Acid with Aromatic Aldehydes by Means of Ammonia and Amines. *Berichte der Deutschen Chemischen Gesselschaft* **1898**, *31*, 2596-2619.

(34) Although ^{1}H decoupled ^{13}C NMR is not a quantitative technique, integration of overlapping signals allowed the number of individual carbon signals present in the overlapped signal to be estimated. The acquisition and processing parameters for both ^{1}H and ^{13}C NMR spectra are outlined in **Appendix B**.

(35) Pettit, G. R., Numata, A., Cragg, G. M., Herald, D. L., Takada, T., Iwamoto, C., Riesen, R., Schmidt, J. M., Doubek, D. L., Goswami, A. Isolation and Structures of Schleicherastatins 1-7 and Schleicheols 1 and 2 from the Teak Forest Medicinal Tree Schleichera Oleosa. *Journal of Natural Products* **2000**, *63*, 72-78.

(36) Percec, V., Rudick, J. G., Peterca, M., Wagner, M., Obata, M., Mitchell, C. M., Cho, W.-D., Balagurusamy, V. S. K., Heiney, P. A. Thermoreversible Cis-cisoidal to Cis-transoidal Isomerization of Helical Dendronized Polyphenylacetylenes. *Journal of the American Chemical Society* **2005**, *127*, 15257-15264.

(37) Percec, V., Holerca, M. N., Magonov, S. N., Yeardley, D. J. P., Ungar, G., Duan, H., Hudson, S. D. Poly(oxazolines)s with Tapered Minidendritic Side Groups. The Simplest Cylindrical Models To Investigate the Formation of Two-Dimensional and Three-Dimensional Order by Direct Visualization. *Biomacromolecules* **2001**, *2*, 706-728.

(38) Percec, V.; Ahn, C.-H.; Cho, W.-D.; Jamieson, A. M.; Kim, J.; Leman, T.; Schmidt, M.; Gerle, M.; Moeller, M.; Prokhorova, S. A.; Sheiko, S. S.; Cheng, S. Z. D.; Zhang, A.; Ungar, G.; Yeardley, D. J. P. Visualizable Cylindrical Macromolecules with Controlled Stiffness from Backbones Containing Libraries of Self-Assembling Dendritic Side Groups. *Journal of the American Chemical Society* **1998**, *120*, 8619-8631.

(39) Nguyen, H. T., Destrade, C., Malthete, J. New Biforked Mesogen Series. *Liquid Crystals* **1990**, *8*, 797-811.

(40) Rowe, K. E., Bruce, D. W. The Synthesis and Mesomorphism of Di-, Tetra- and Hexa-Catenar Liquid Crystal Based on 2,2'-Bipyridine. *Journal of Materials Chemistry* **1998**, *8,* 331-341.

(41) Suarez, S., Mamula, O., Scopelliti, R., Donnio, B., Guillon, D., Terazzi, E., Piguet, C., Buenzli, J.-C. G. Lanthanide Luminescent Mesomorphic Complexes with Macrocylces Derived from Diaza-18-crown-6. *New Journal of Chemistry* **2005**, *29*, 1323-1334.

(42) Ropponen, J., Nummelin, S., Rissanen, K. Bisfunctionalized Janus Molecules *Organic Letters* **2004**, *6*, 2495-2497.

(43) Binnemans, K., Sleven, J., De Feyter, S., De Schryver, F. C., Donnio, B., Guillon, D. Structure and Mesomorphic Behavior of Alkoxy-Substituted Bis(phthalocyaninato)lanthanide(III) Complexes. *Chemistry of Materials* **2003**, *15*, 3930-3938.

(44) Ohta, K., Jacquemin, L., Sirlin, C., Bosio, L., Simon, J. Influence of the Nature of the Side Chains on the Mesomorphic Properties of Octasubstituted Phthalocyanine Derivatives. Annelides. XXIX. *New Journal of Chemistry* **1988**, *12*, 751-754.

(45) Briggs, L. H., Cambie, R. C. Constituents of Eugenia Maire. II. Identification of Mairin and Constituents of the Leaves. *Journal of the Chemical Society* **1961**, 4684-4685.

(46) Terazzi, E., Torelli, S., Bernardinelli, G., Rivera, J.-P., Benech, J.-M., Bourgogne, C., Donnio, B., Guillon, D., Imbert, D., Buenzli, J.-C. G., Pinto, A., Jeannerat, D., Piguet, C. Molecular Control of Macroscopic Cubic, Columnar, and Lamellar Organizations in Luminescent Lanthanide-Containing Thermotropic Liquid Crystals. *Journal of the American Chemical Society* **2005**, *127*, 888-903.

(47) Cardinaels, T., Ramaekers, J., Nockemann, P., Driesen, K., Van Hecke, K., Van Meervelt, L., Lei, S., De Feyter, S., Guillon, D., Donnio, B., Binnemans, K. Imidazo[4,5-f]-1,10-phenanthrolines: Versatile Ligands for the Design of Metallomesogens. *Chemistry of Materials* **2008**, *20*, 1278-1291.

(48) Mukkamala, R., Burns Jr., C. L., Catchings III, R. M., Weiss, R. G. Photopolymerization of Carbohydrate-Based Discotic Mesogens. Syntheses and Phase Properties of 1,2,3,4,6-Penta-O-(trans-3,4-dialkoxycinnamoyl)-(D)-glucopyranoses and Their Oligomers. *Journal of the American Chemical Society* **1996**, *118*, 9498-9508.

(49) Meier, H., Prass, E., Zerban, G., Kosteyn, F. Investigation on the Formation of Liquid Crystals by Distyrylbenzenes with Alkoxy Chains. *Zeitschrift fuer Naturforschung, B: Chemical Sciences* **1998**, *43*, 889-896.

(50) Speranza, G., Martignoni, A., Manitto, P. Studies on Aloe. Part 5. Iso-aloeresin A, a Minor Constituent of Cape Aloe. *Journal of Natural Products* **1988**, *51*, 588-590.

(51) Brettle, R., Dunmur, D. A., Hindley, N. J., Marson, C. M. Synthesis of New Liquid Crystalline Compounds Based on 1,4-diarylbuta-1,3-dienes. *Journal of the Chemical Society, Perkin Transactions 1: Organic and Bio-Organic Chemistry* **1993**, 775-781.

(52) Davis, R., Kumar, N. S. S., Abraham, S., Suresh, C. H., Rath, N. P., Tamaoki, N., Das, S. Molecular Packing and Solid-State Fluorescence of Alkoxy-Cyano Substituted Diphenylbutadienes: Structure of the Luminescent Aggregates. *Journal of Physical Chemistry C* **2008**, *112*, 2137-2146.

(53) Fischer, E., Speier, A. Preparation of Ethereal Salts *Berichte der Deutschen Chemischen Gesellschaft* **1895**, *28*, 3252-3258.

(54) (a) Schloeg, M., Rieger, B. Dialkoxy-Substituted, C1-Symmetric Metallocenes: Synthesis and Catalytic Behavior in the Propylene Polymerization Reaction. *Zeitschrift fuer Naturforschung, B: Chemical Sciences* **2004**, *59*, 233. (b) McKenna, M. D., Barbera, J., Marcos, M., Serrano, J. L. Discotic Liquid Crystalline Poly(Propylene Imine) Dendrimers Based on Triphenylene. *Journal of the American Chemical Society* **2005**, *127*, 619-625. (c) Tahara, K., Furukawa, S., Uji-i, H., Uchino, T., Ichikawa, T., Zhang, J., Mamdouh, W., Sonoda, M., De Schryver, F. C., De Feyter, S., Tobe, Y. Two-Dimersonal Porous Molecular Networks of Dehydrobenzo[12]annulene Derivatives via Alkyl Chain Interdigitation. *Journal of the American Chemical Society* **2006**, *128*, 16613-16625.

(55) (a) Tang, Y.; Mei, C.; Li, S.; Wang, Y.; Wang, X.; Wang, L.; Yan, D. Ye, C. Synthesis and Characterization of a Three-Ring Bent-Core Compound. *Chinese Science Bulletin* **2005**, *50,* 1849-1853. (b) Brun, A., Etemad-Maghadam, G. New Double-Chain and Aromatic (α-hydroxyalkyl)phosphorous amphiphiles. *Synthesis*, **2002**, *10*, 1385-1390. (c) Lensen, M. C., Elemans, J. A. A. W., van Dingenen, S. J. T., Gerritsen, J. W., Speller, S., Rowan, A. E., Nolte, R. J. M. Giant Porphyrin Disks: Control of Their Self-Assembly at Liquid-Solid Interfaces Through Metal-Ligand Interactions. *Chemistry a European Journal* **2007**, *13*, 7948-7956.

(56) Field, L. D., Sternhell, S., Kalman, J. R. *Organic Structures from Spectra, 3rd Ed.;* John Wiley and Sons, Chichester, England: 2002.

(57) Kosteyn, F., Zerban, G., Meier, H. 4,4'-Distyrylazobenzene as a Mesogen. *Chemische Berichte* **1992,** *125*, 893-897.

(58) Winterfeldt, E. Applications of Diisobutylaluminum Hydride (DIBAH) and Triisobutylaluminum (TIBA) as Reducing Agents in Organic Synthesis. *Synthesis* **1975**, *7* 617-630.

(59) (a) Finholt, A. E., Bond Jr., A. C., Schlesinger, H. I. Lithium Aluminum Hydride, Aluminum Hydirde and Lithium Gallium Hydride, and Some of Their Applications in Organic and Inorganic Chemistry. *Journal of the American Chemical Society* **1947**, *69*, 1199-1203. (b) Nystrom, R. F., Brown, W. G. Reductions of Organic Compounds by Lithium Aluminum Hydride. I. Aldehydes, Ketones, Esters, Acid Chlorides, and Acid Anhydrides. *Journal of the American Chemical Society* **1947,** *69*, 1197-1199.

(60) Corey, E. J., Suggs, J. W. Pyridinium Chlorochromate. Efficient Reagent for Oxidation of Primary and Secondary Alcohols to Carbonyl Compounds. *Tetrahedron Letters* **1975,** *16,* 2647-2650.

(61) Chien, C.-W., Liu, K.-T., and Lai, C. K. Heterocyclic Columnar Pyrimidines: Synthesis, Characterization and Mesomorphic Properties. *Liquid Crystals* **2004**, *31*, 1007-1017.

(62) Patel, C. K., Owen, C. P., Aidoo-Gyamfi, K., Ahmed, S. Strucutre-Activity Relationship Determination Study of a Series of Novel Compounds as Potential Inhibitors of the Enzyme Estron Sulfatase (ES). *Letters in Drug Design and Discovery* **2004**, *1*, 35-44.

(63) Nystrom, R. F., Brown, W. G. Reduction of Organic Compound by Lithium Aluminum Hydride. II. Carboxylic Acids. *Journal of the American Chemical Society* **1947,** *69*, 2548-2549.

(64) Narasimhan, V., Rathore, R., Chandrasekaran, S. Highly Selective Oxidative Cleavage of Aryl Substituted Olefins with Pyridinium Chlorochromate. *Synthetic Communications* **1985**, *15*, 769-774.

(65) (a) Fernandes, R. A., Kumar, P. PCC-Mediated Novel Oxidation Reactions of Homobenzylic and Homoallylic Alcohols. *Tetrahedron Letters* **2003**, *44*, 1275.

(b) Thomas, A. F., Bessiere, Y. Limonone. *Natural Products Reports* **1989**, *6*, 291-309. (c) Muzart, J. Synthesis of Unsaturated Carbonyl Compounds via a Chromium-Mediated Allylic Oxidation by 70 % Tert-Butyl Hydroperoxide. *Tetrahedron Letters* **1987**, *28*, 4665-4668. (d) Parish, E. J. Chitrakorn, S., Wei, T. Y. Pyridinium Chlorochromate-Mediated Allylic and Benzylic Oxidation. *Synthetic Communications* **1986**, *16*, 1371-1375.

(66) Kumar, N. S. S., Varghese, S. Narayan, G., Das, S. Hierarchical Self-Assembly of Donor-Acceptor-Substituted Butadiene Amphiphiles into Photoresponsive Vesicles and Gels. *Angewandte Chemie International Edition* **2006**, *45,* 6317-6321.

(67) Mazur, M., Hope-Ross, K., Kadla, J. F., Sederoff, R., Chang, H.-M. Synthesis of Hydoxyphenylpropanoid β-D-glucosides. *Journal of Wood Chemistry and Technology* **2007**, *27*, 1-8.

(68) Wang, T., Liu, R. Y., Zhu, M. L., Zhang, J. S. Activation Energy of Self-Heating Process Studied by DSC. *Journal of Thermal Analysis and Calorimetry* **2002**, *70*, 507-519.

(69) (a) Gray, G. W., Goodby, J. W. G. *Smectic Liquid Crystals;* Heydon & Son: Philadelphia, 1984. (b) Demus, D., Richter, L. *Textures of Liquid Crystals*; Verlag Chemie Weinheim: New York, 1978.

Appendix A

Selected Spectra

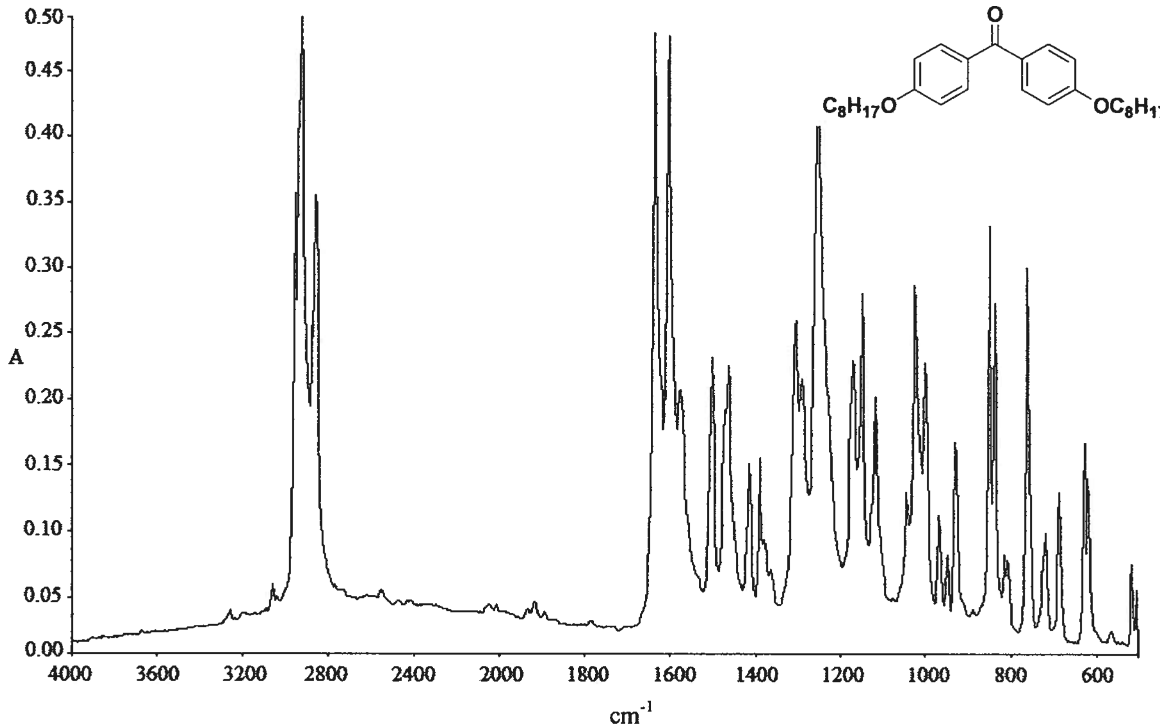

Figure A1: FTIR spectrum of **2b**.

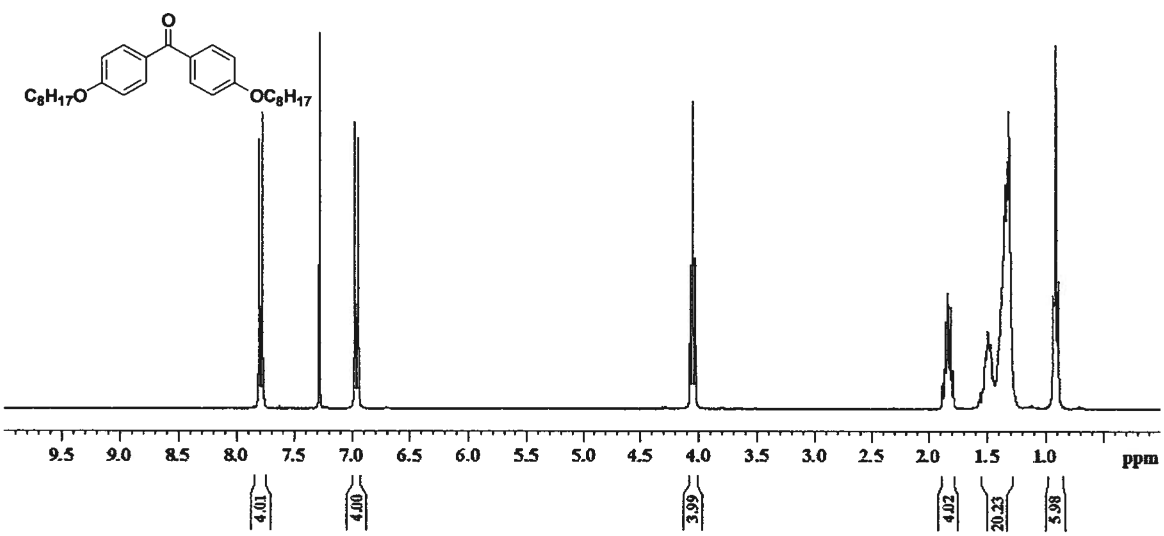

Figure A2: ^{1}H NMR spectrum of **2b**.

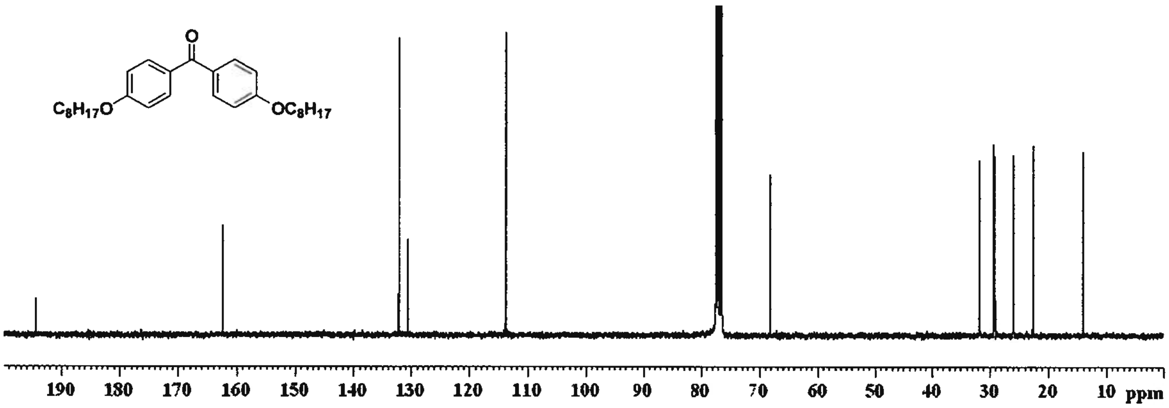

Figure A3: ^{13}C NMR spectrum of **2b**.

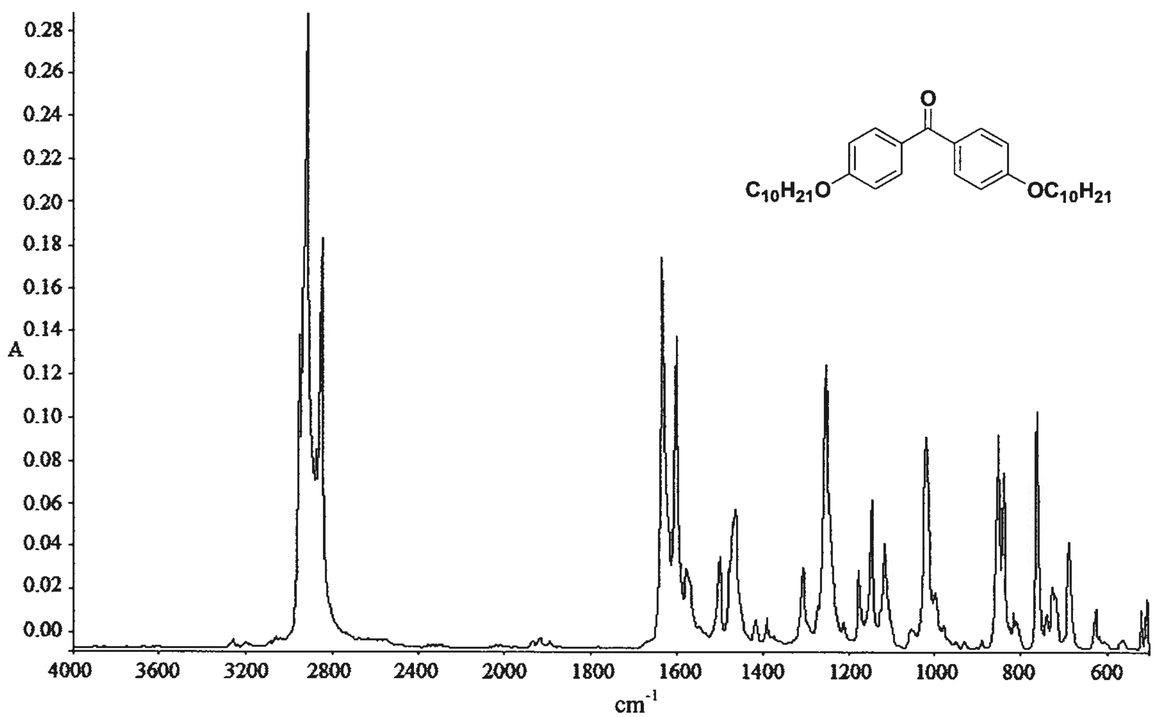

Figure A4: FTIR spectrum of **2c**.

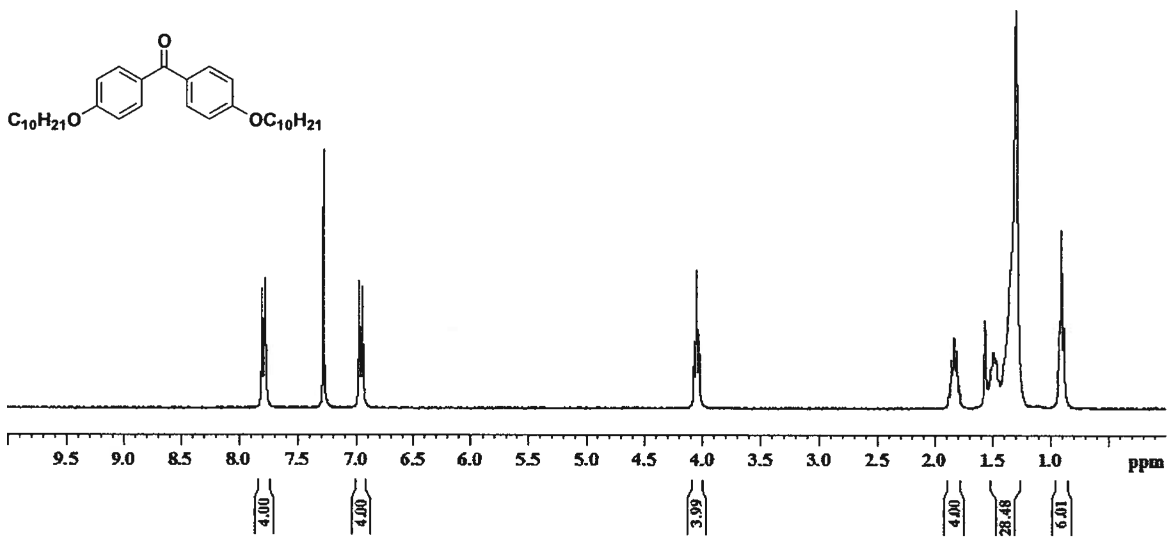

Figure A5: ^{1}H NMR spectrum of **2c**.

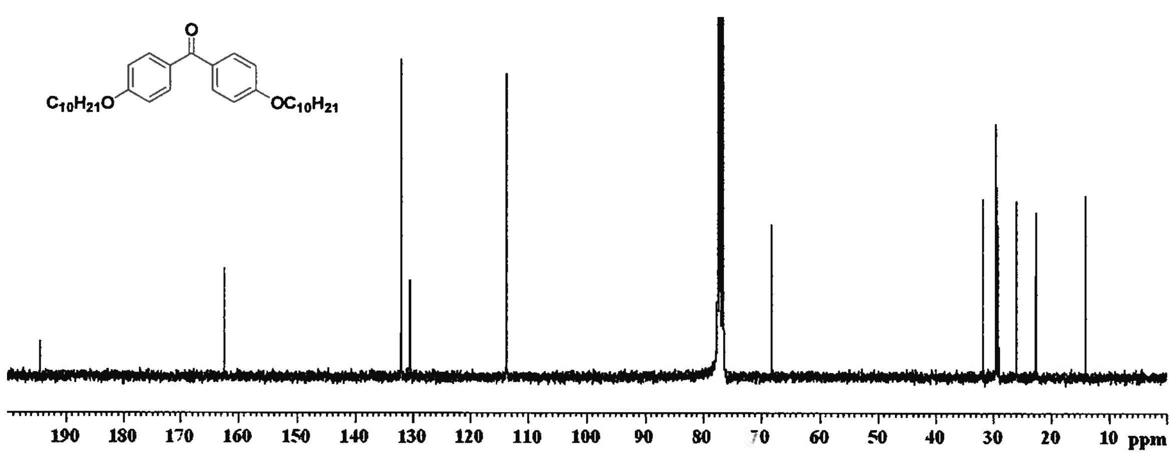

Figure A6: ^{13}C NMR spectrum of **2c**.

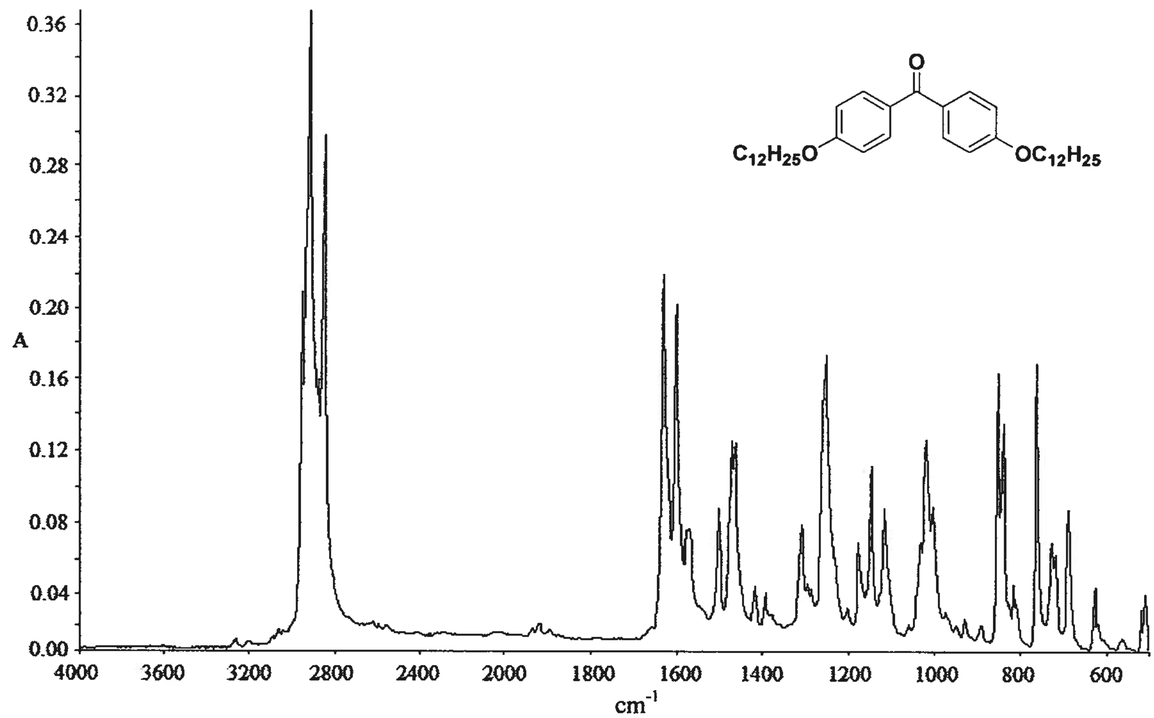

Figure A7: FTIR spectrum of **2d**.

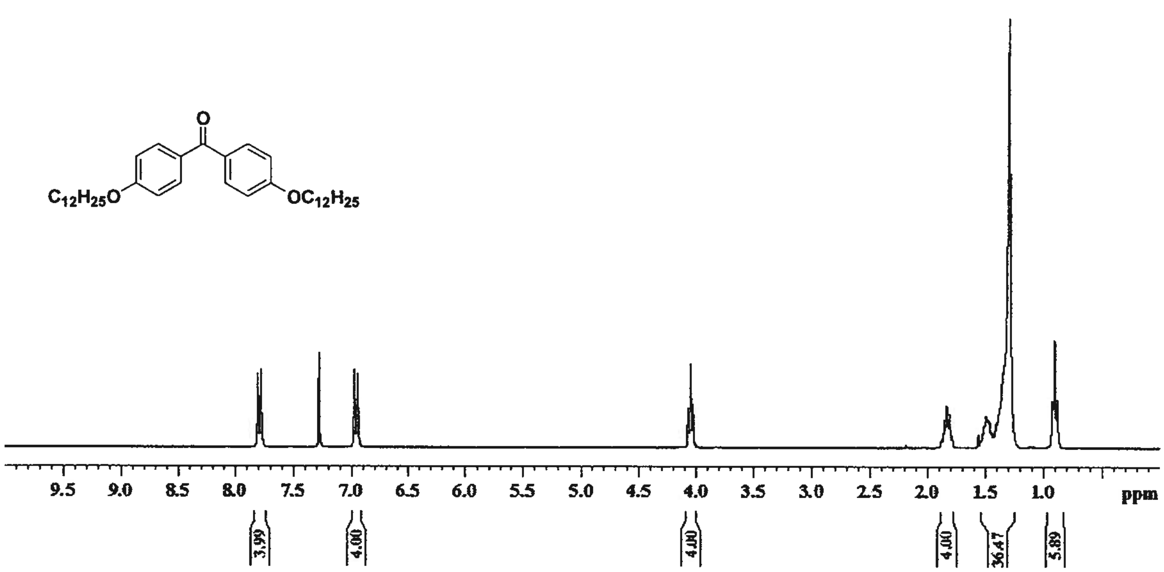

Figure A8: ^{1}H NMR spectrum of **2d**.

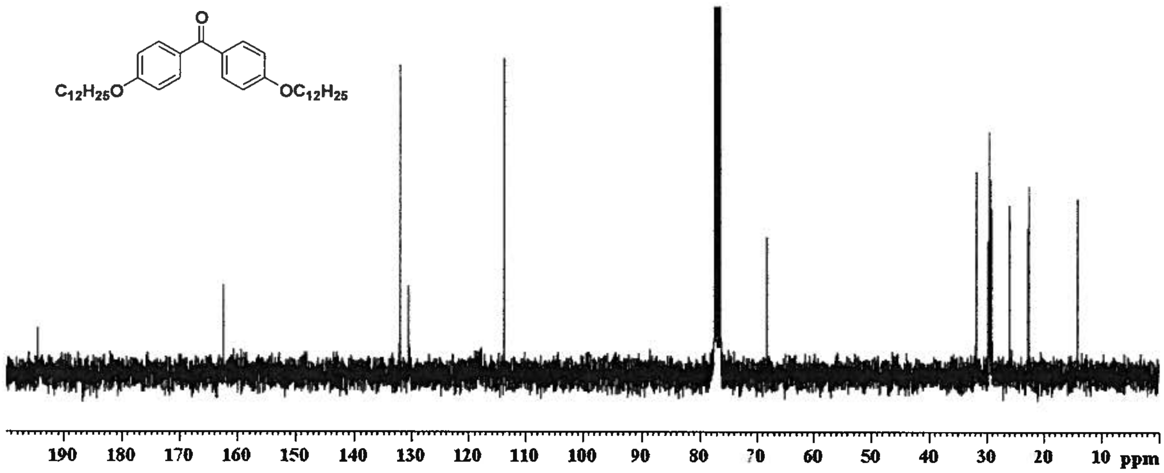

Figure A9: ^{13}C NMR spectrum of **2d**.

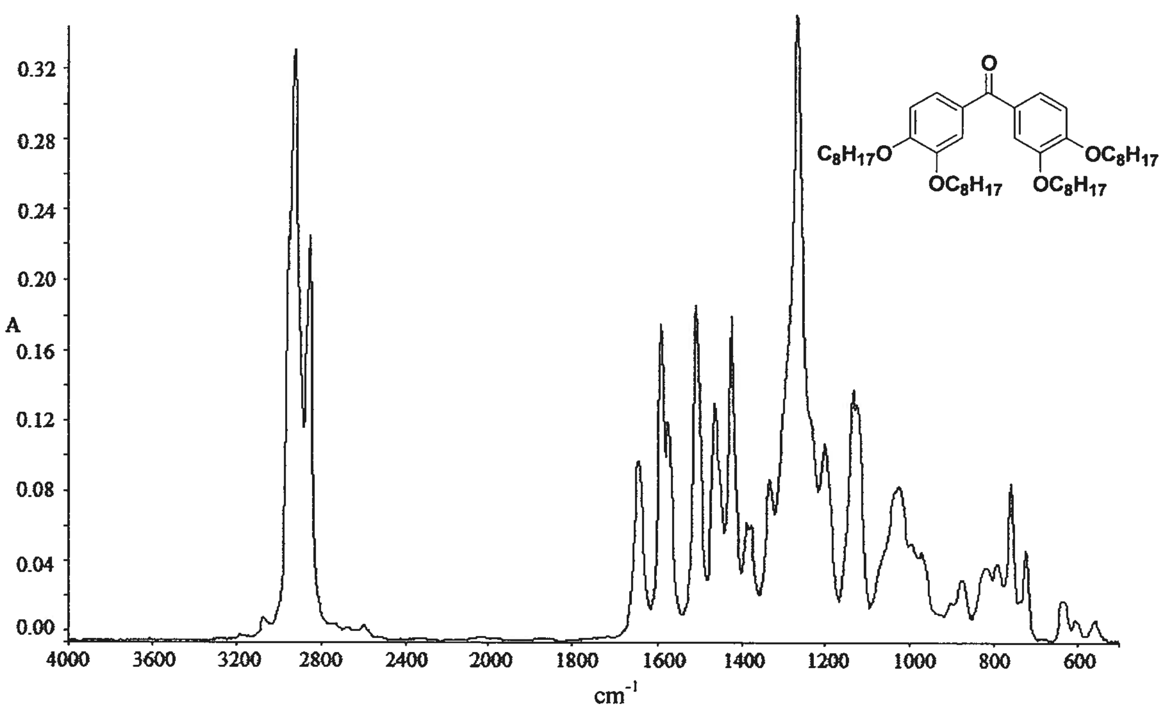

Figure A10: FTIR spectrum of **9f**.

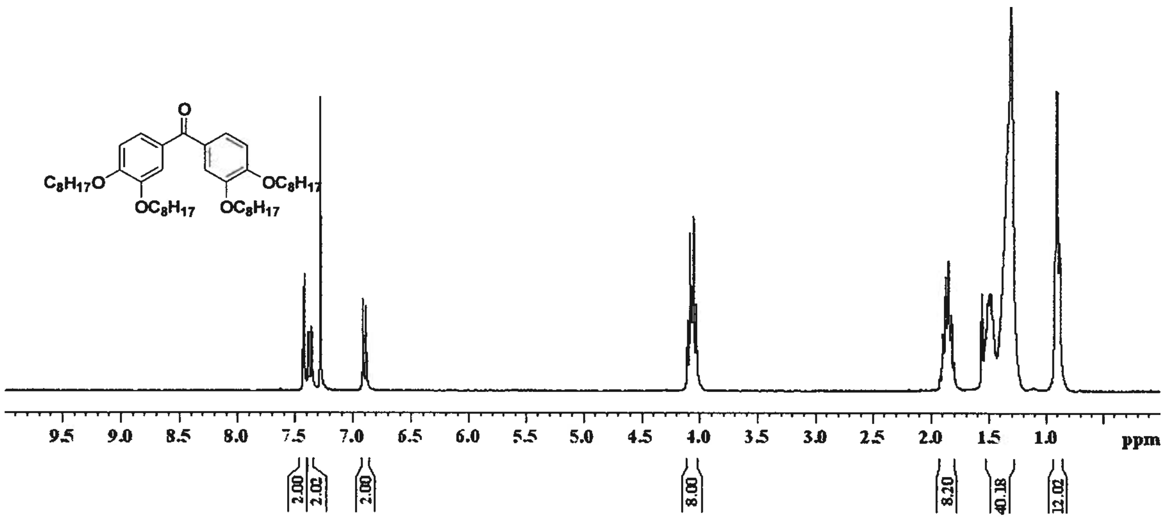

Figure A11: ^{1}H NMR spectrum of **9f**.

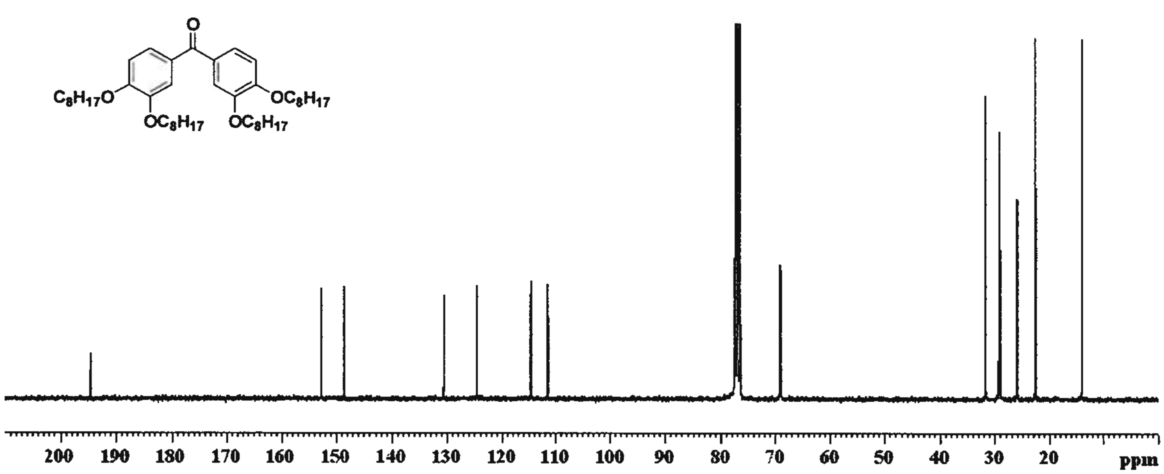

Figure A12: ^{13}C NMR spectrum of **9f**.

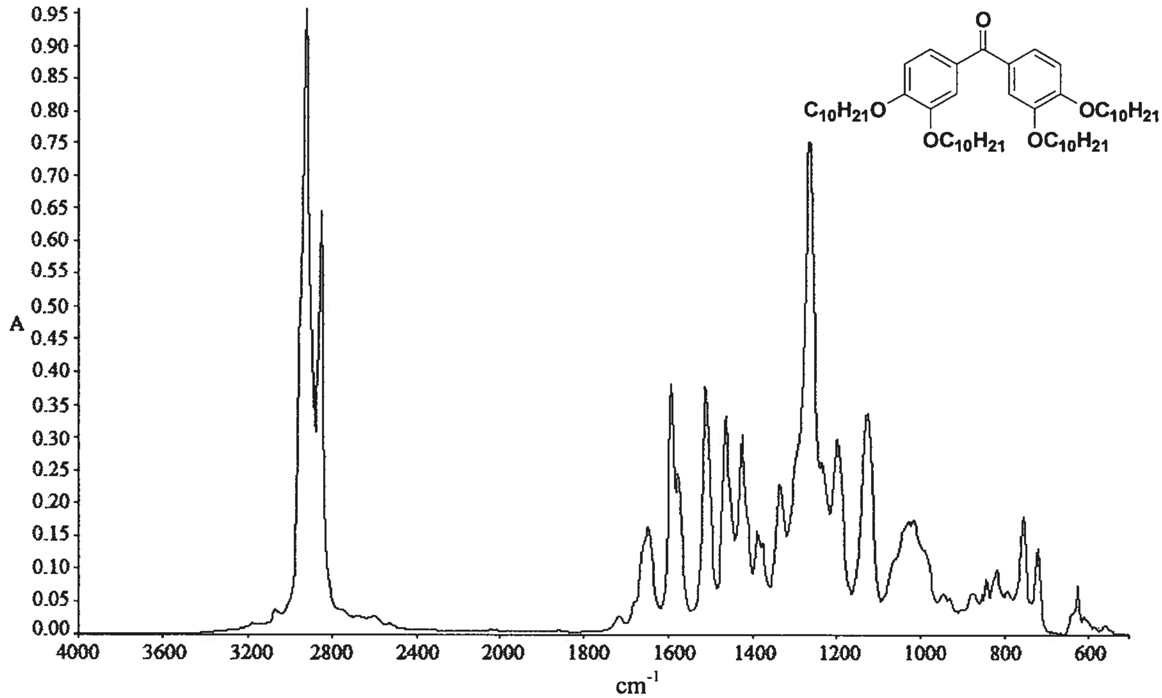

Figure A13: FTIR spectrum of **9g**.

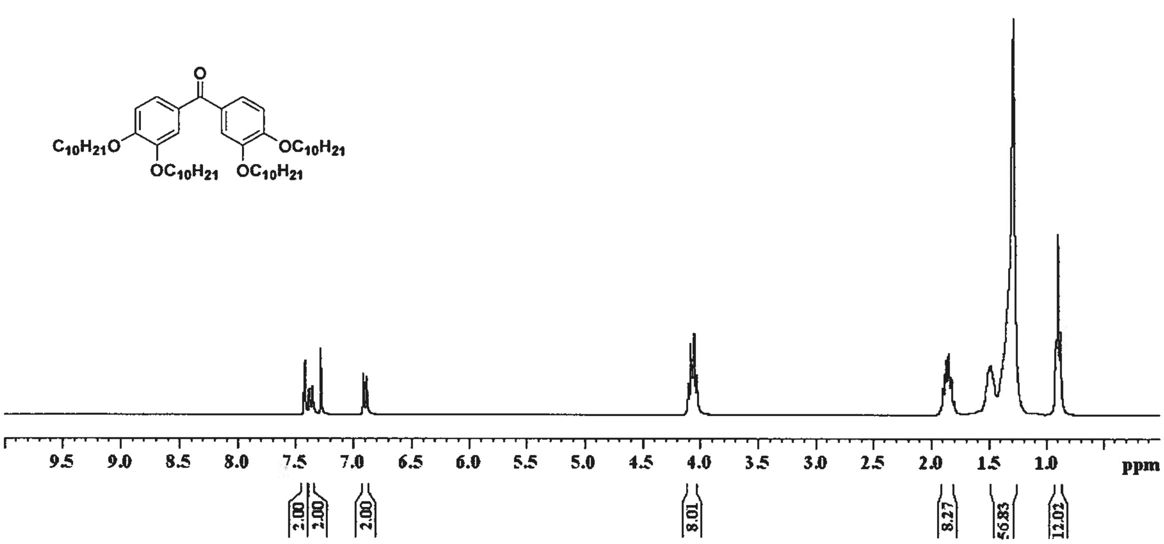

Figure A14: ^{1}H NMR spectrum of **9g**.

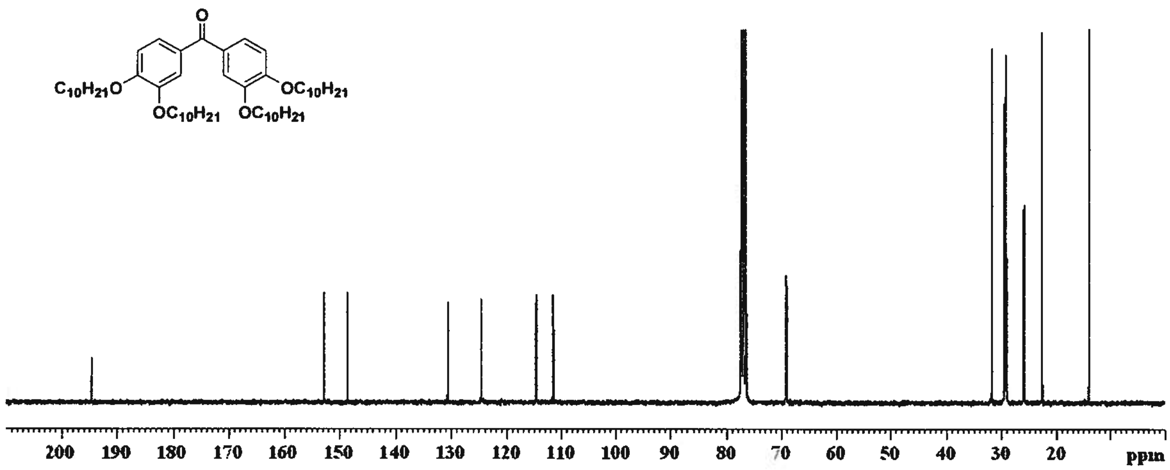

Figure A15: ^{13}C NMR spectrum of **9g**.

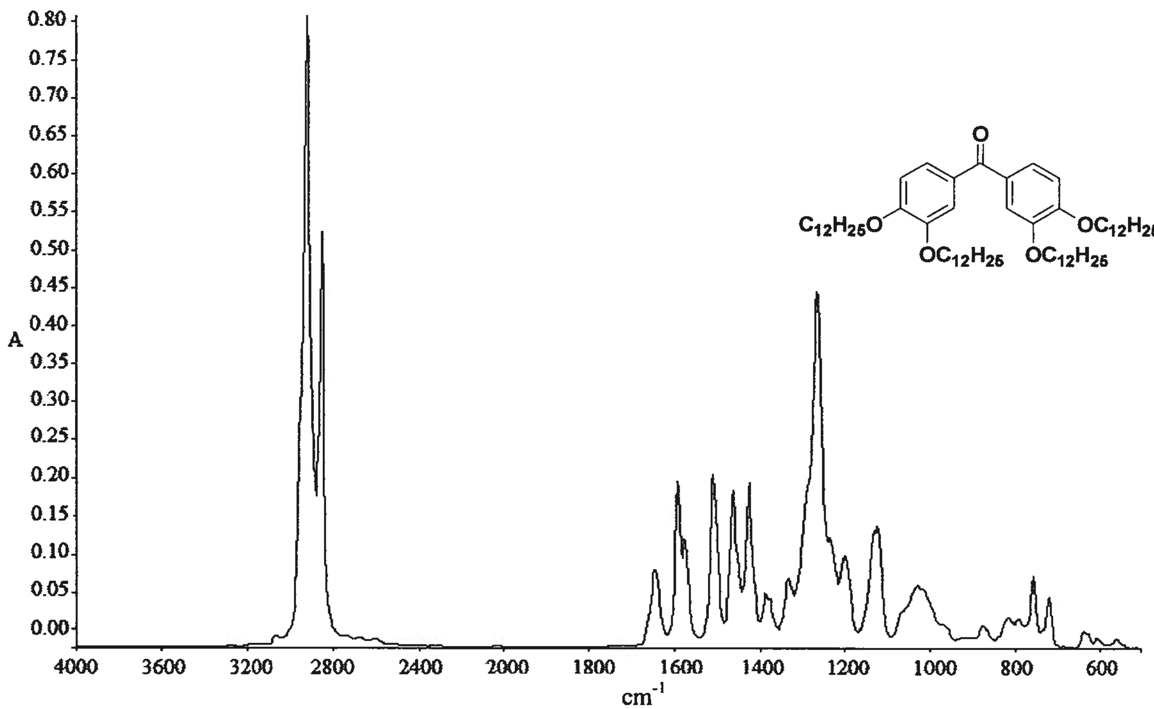

Figure A16: FTIR spectrum of **9h**.

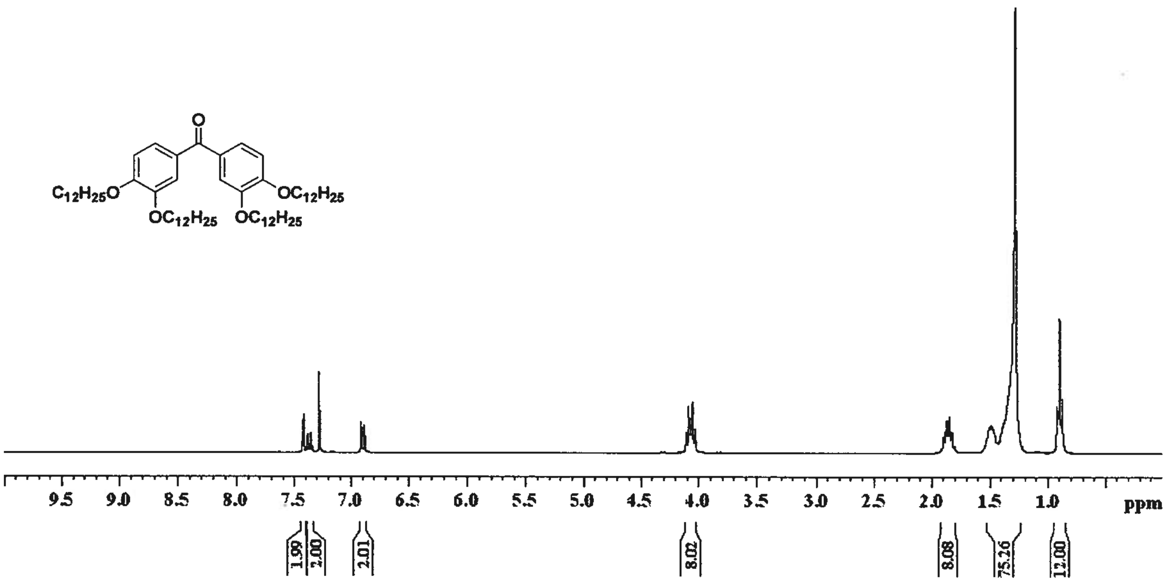

Figure A17: ^{1}H NMR spectrum of **9h**.

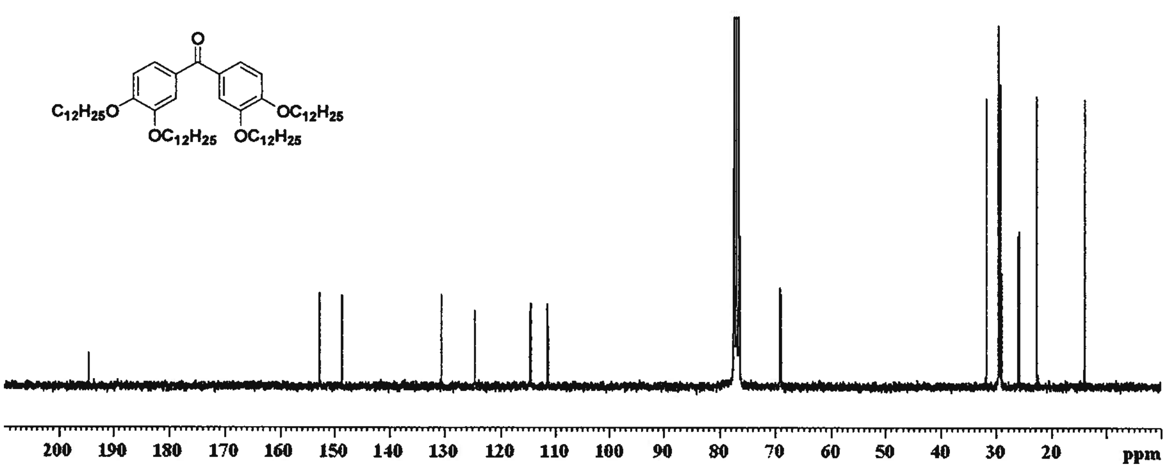

Figure A18: ^{13}C NMR spectrum of **9h**.

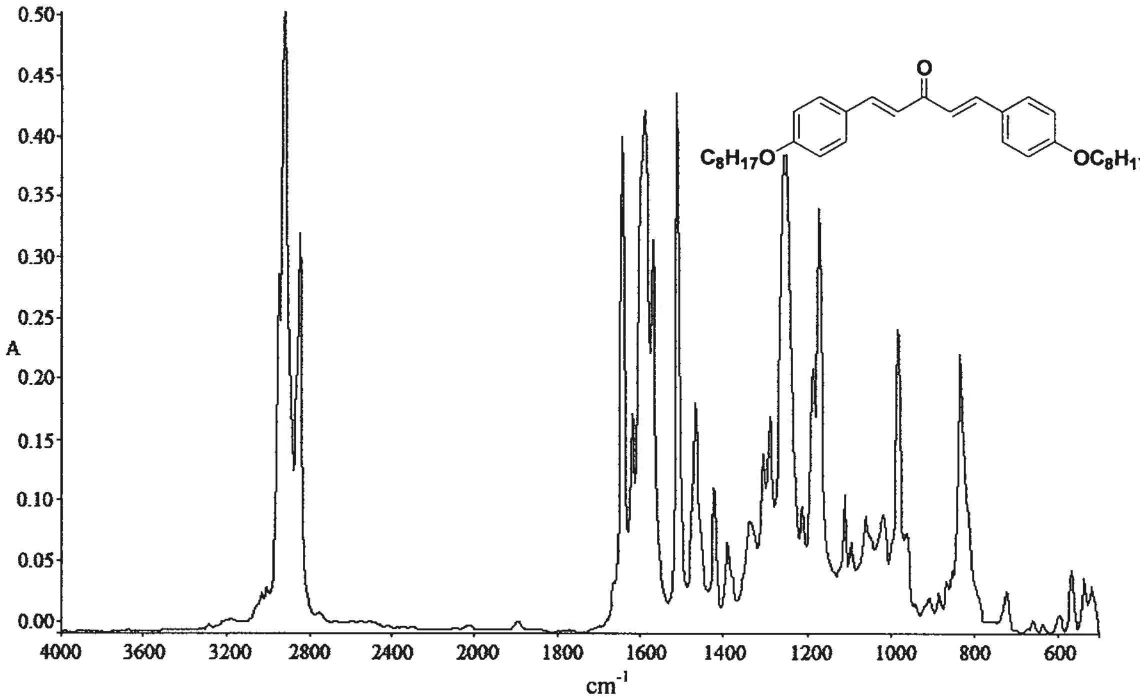

Figure A19: FTIR spectrum of **19b**.

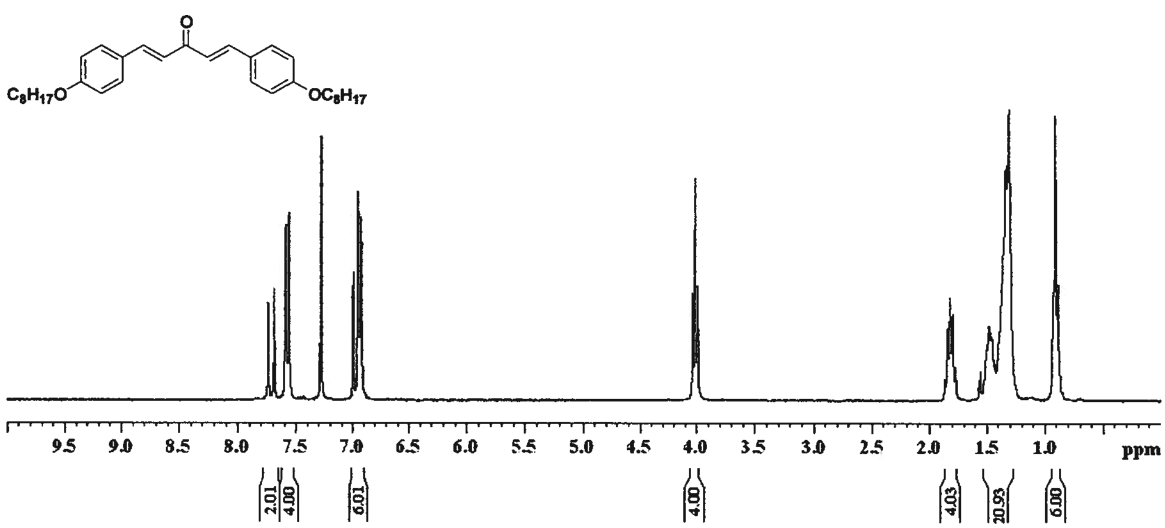

Figure A20: ^{1}H NMR spectrum of **19b**.

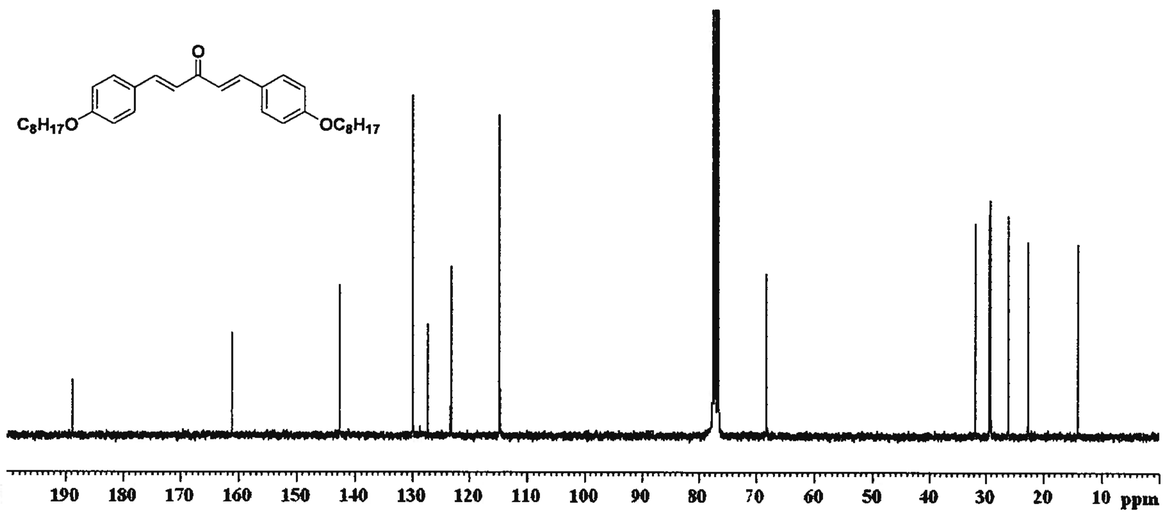

Figure A21: ^{13}C NMR spectrum of **19b**.

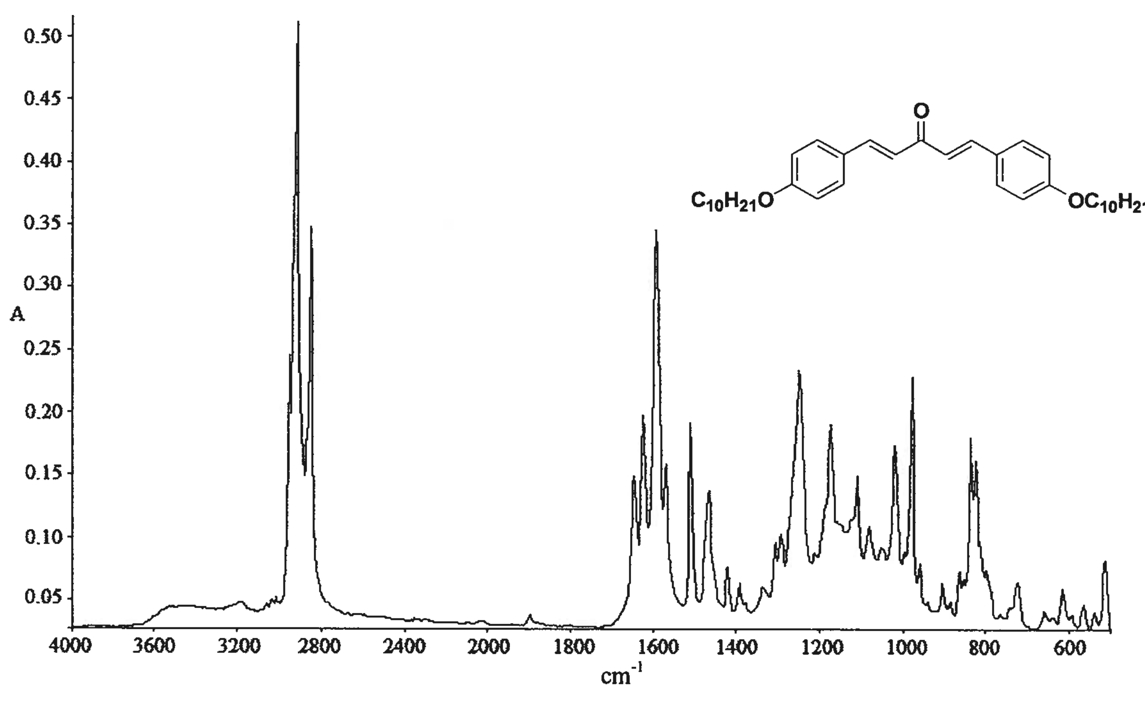

Figure A22: FTIR spectrum of **19c**.

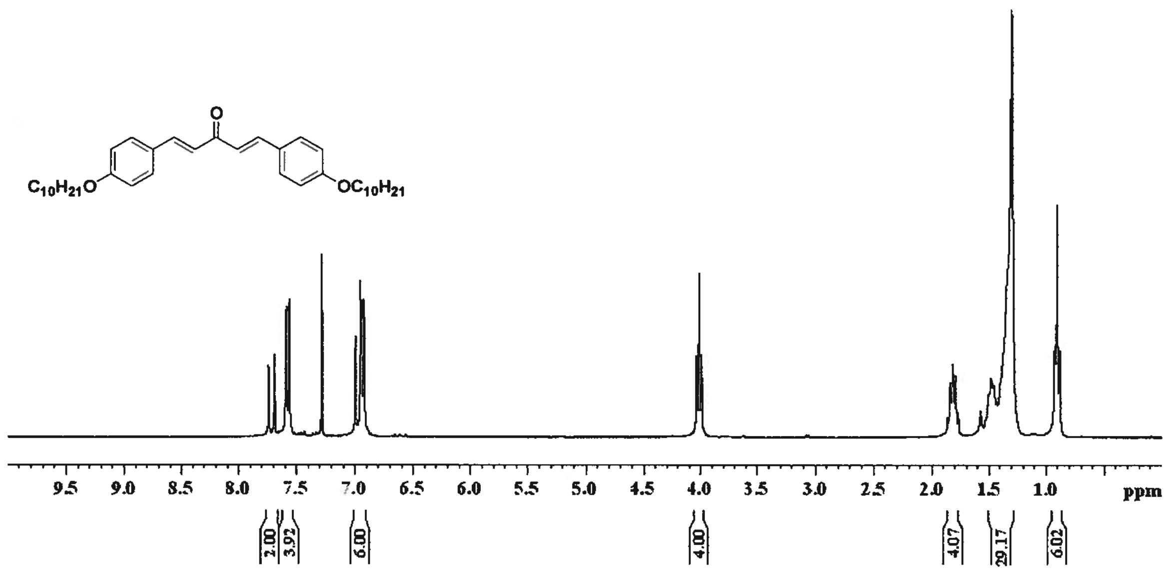

Figure A23: ^{1}H NMR spectrum of **19c**.

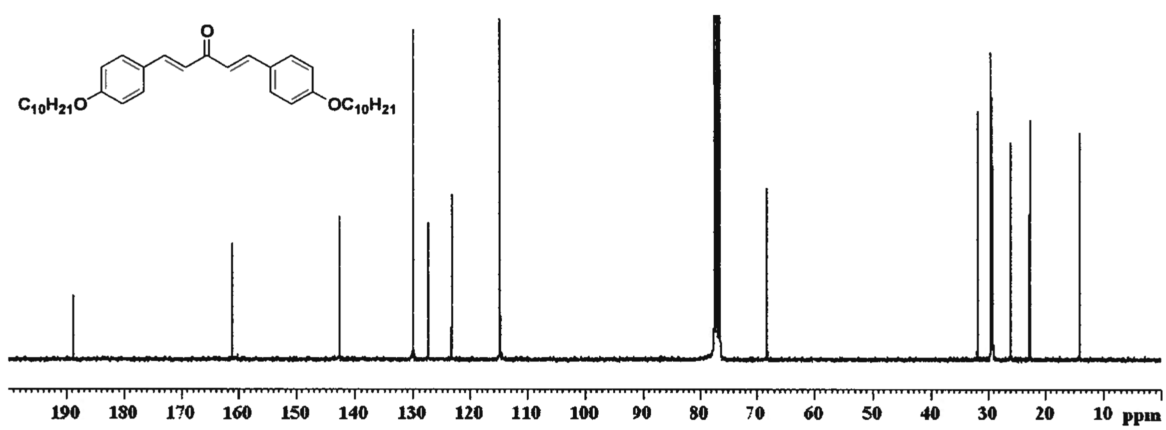

Figure A24: ^{13}C NMR spectrum of **19c**.

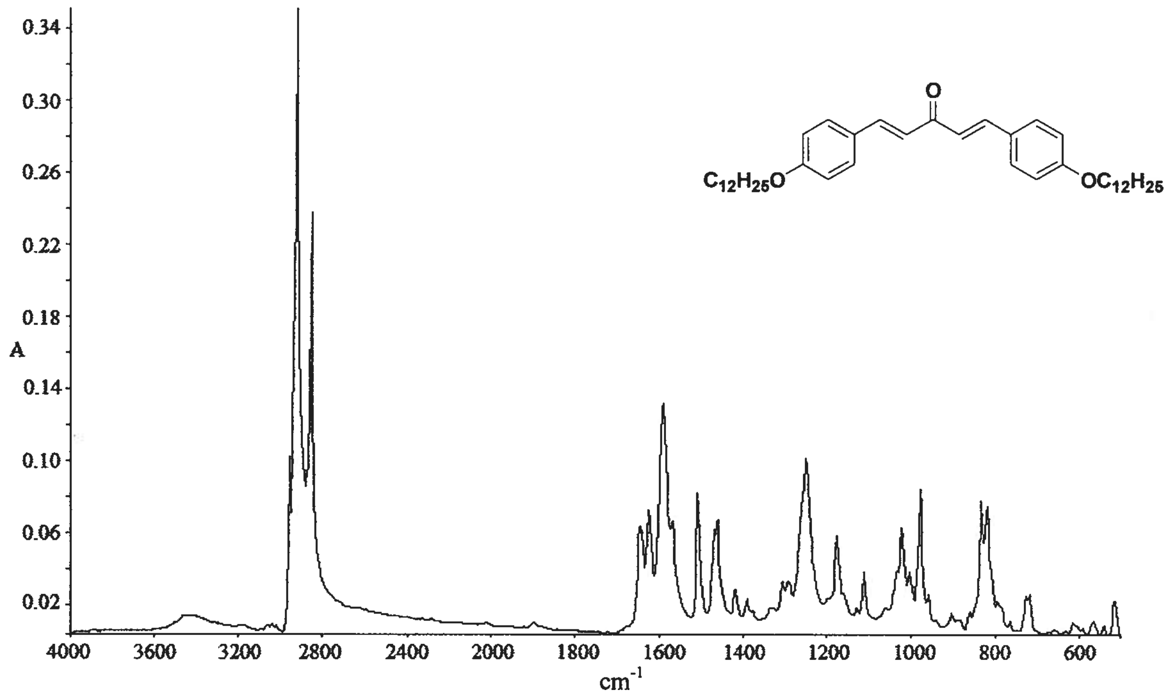

Figure A25: FTIR spectrum of **19d**.

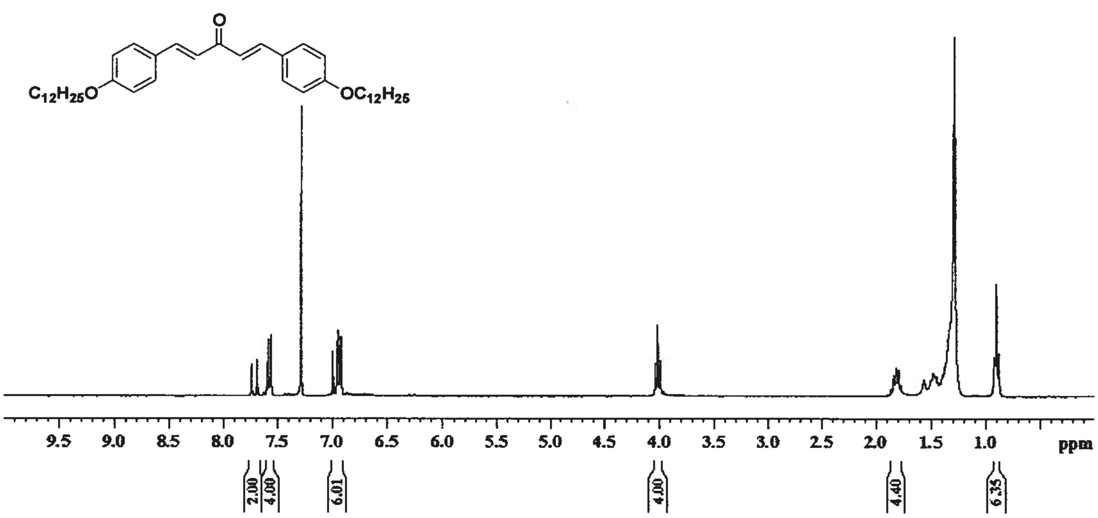

Figure A26: ^{1}H NMR spectrum of **19d**.

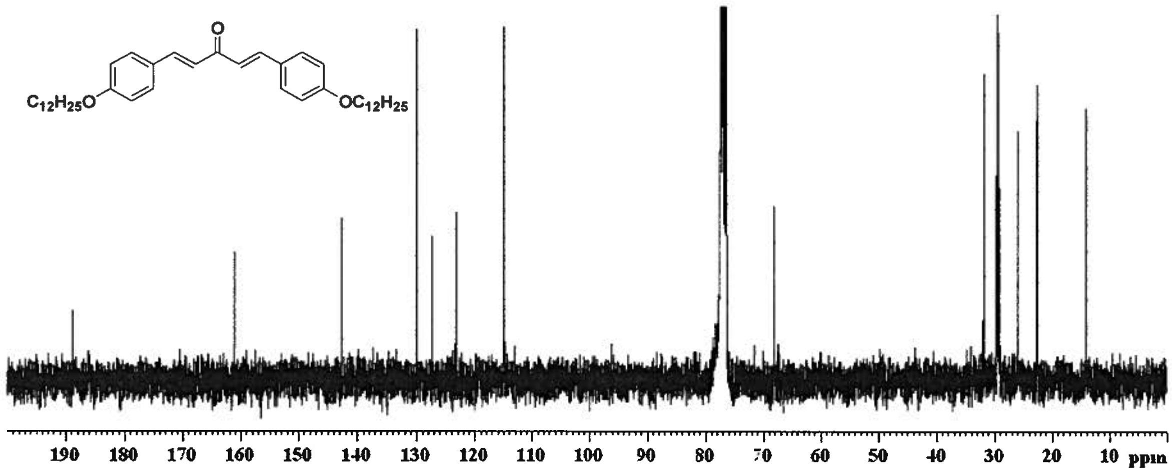

Figure A27: ^{13}C NMR spectrum of **19d**.

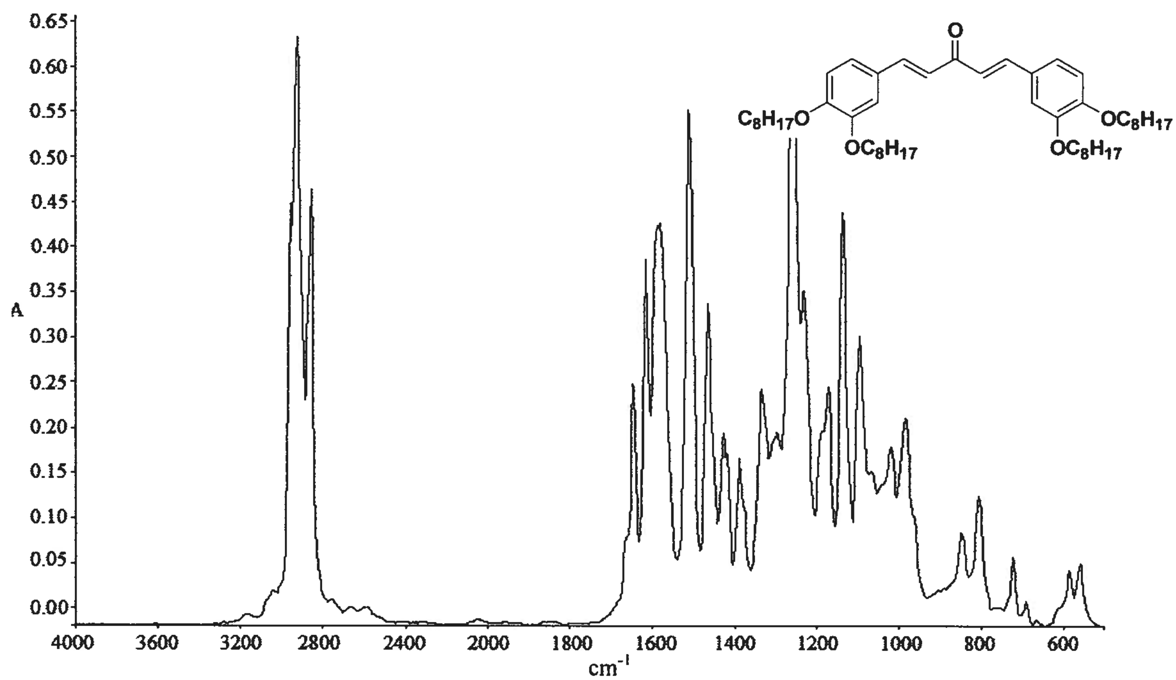

Figure A28: FTIR spectrum of **23f**.

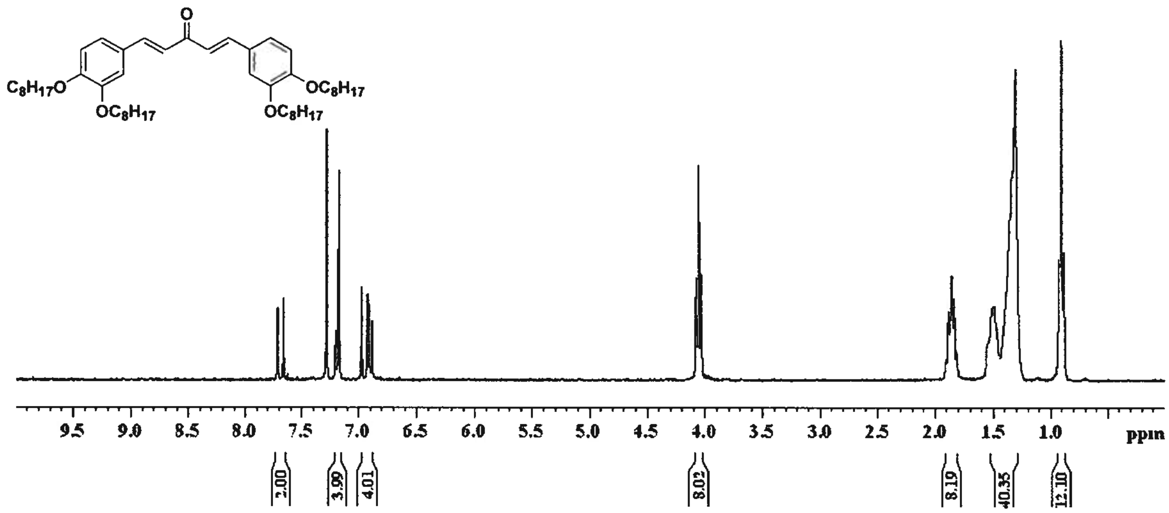

Figure A29: ^{1}H NMR spectrum of **23f**.

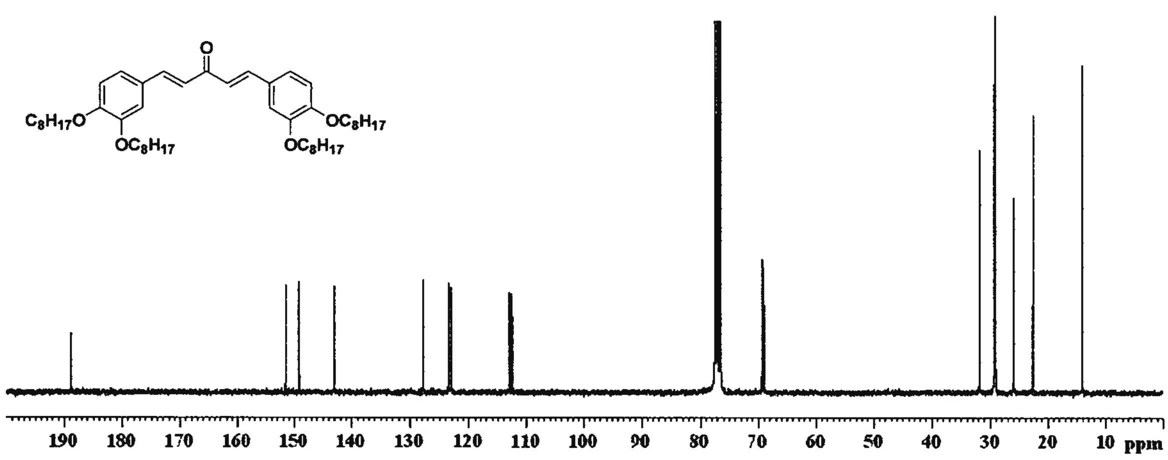

Figure A30: ^{13}C NMR spectrum of **23f**.

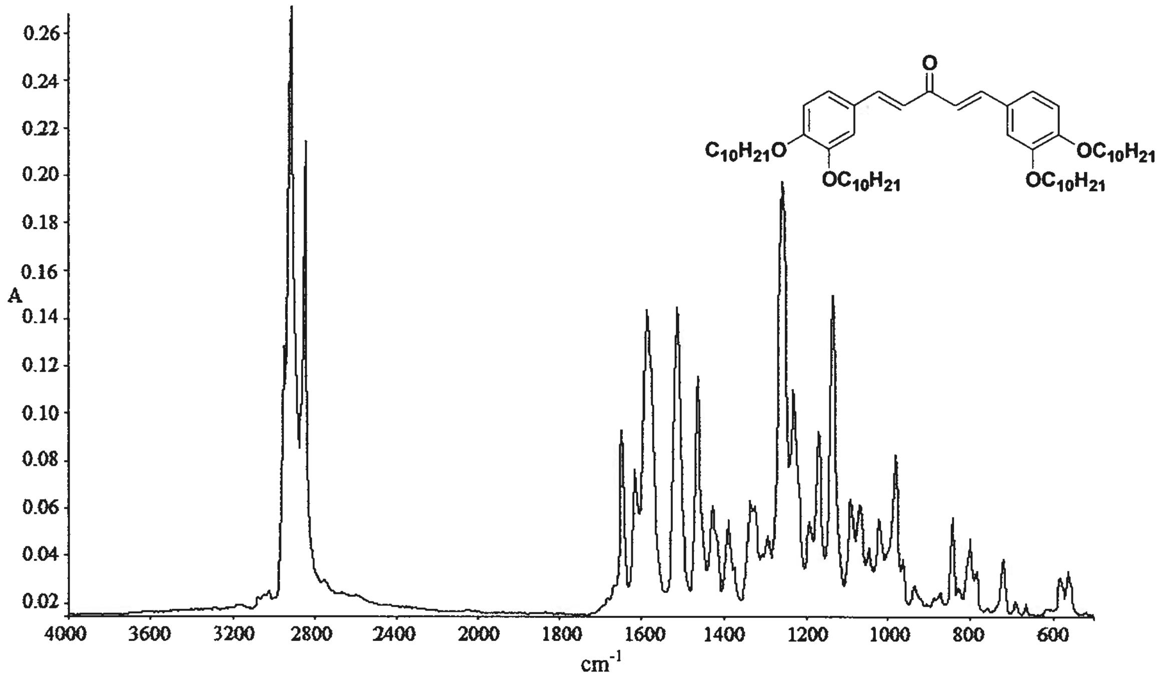

Figure A31: FTIR spectrum of **23g**.

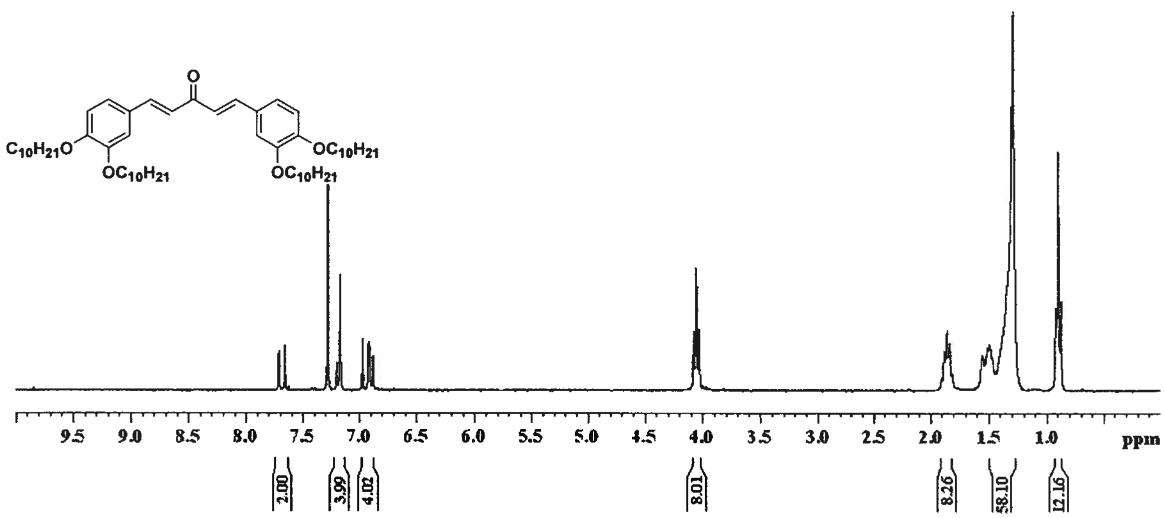

Figure A32: ^{1}H NMR spectrum of **23g**.

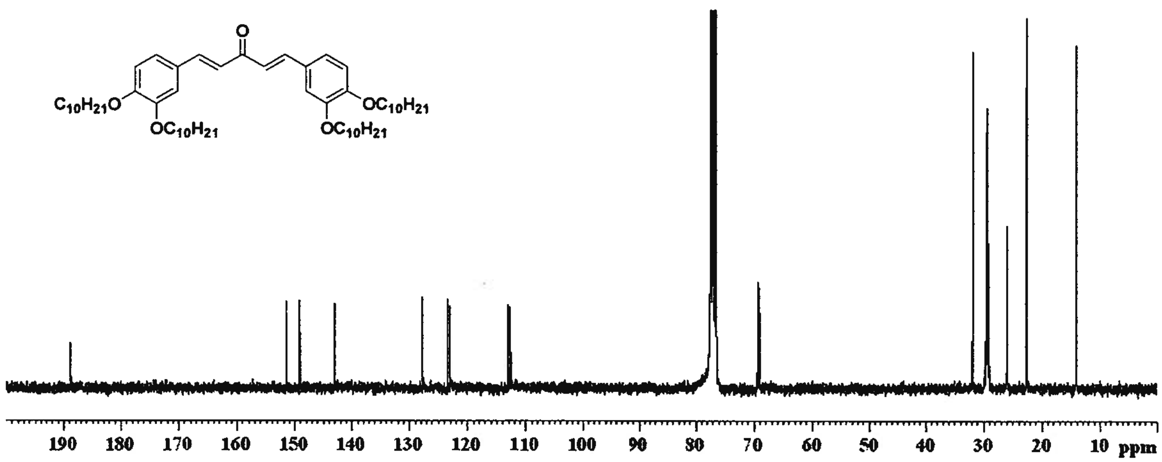

Figure A33: ^{13}C NMR spectrum of **23g**.

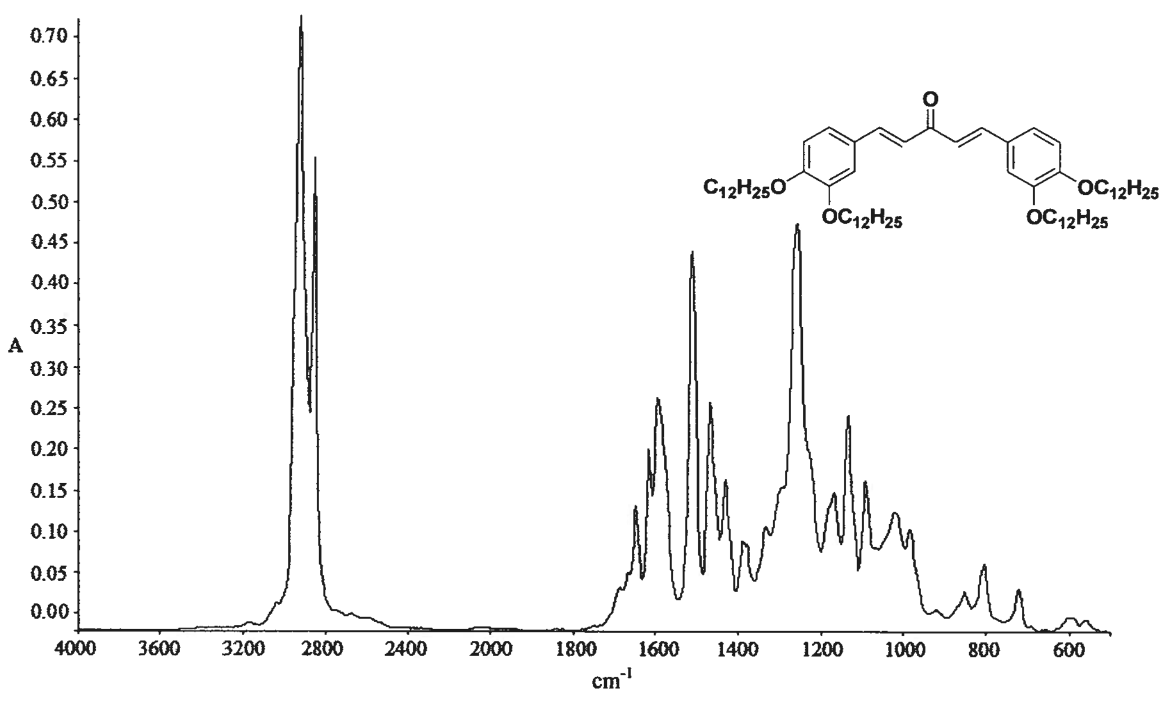

Figure A34: FTIR spectrum of **23h**.

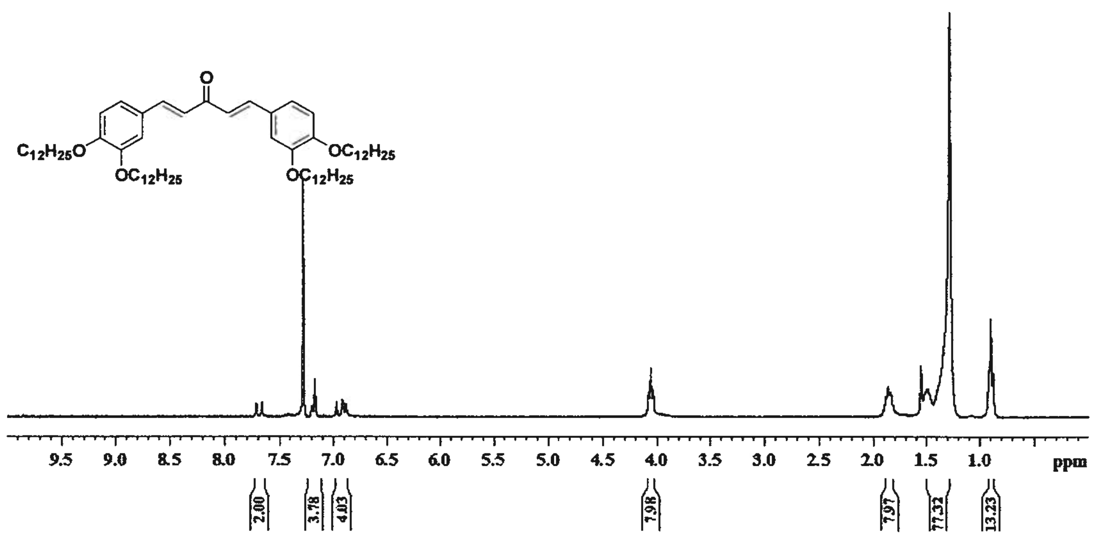

Figure A35: ^{1}H NMR spectrum of **23h**.

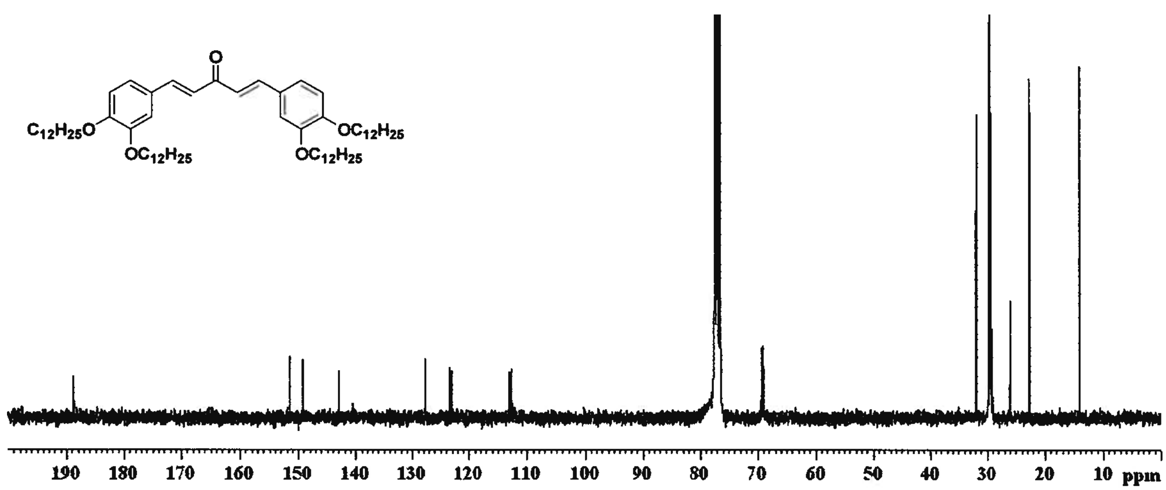

Figure A36: ^{13}C NMR spectrum of **23h**.

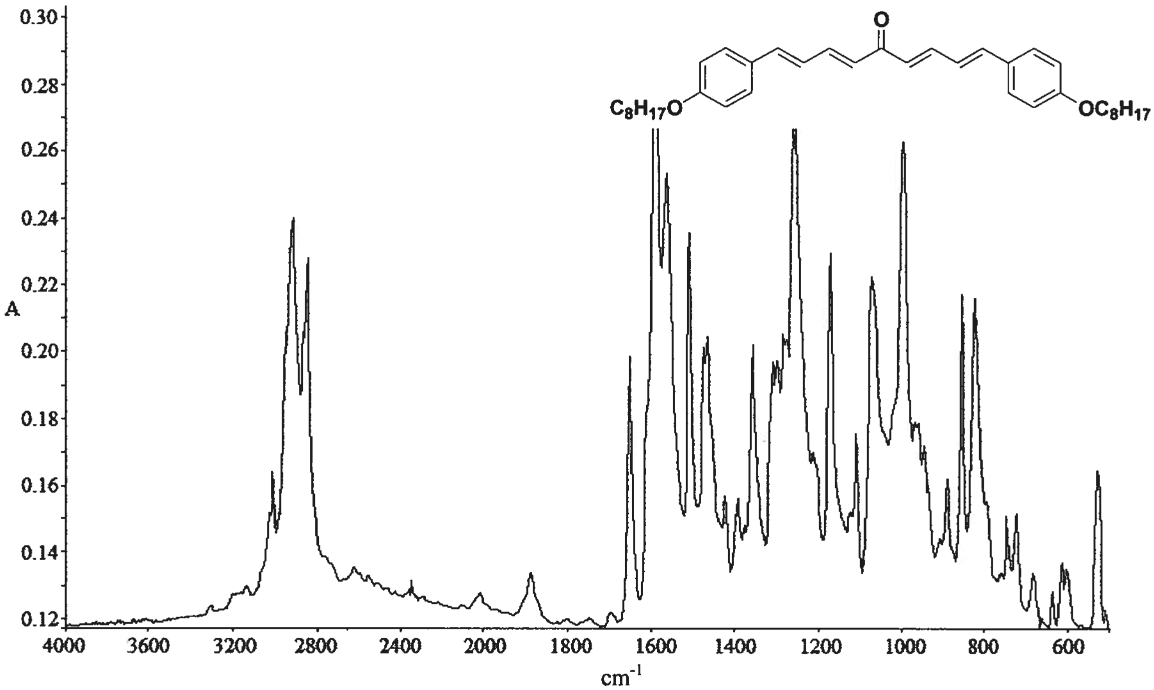

Figure A37: FTIR spectrum of **34b**.

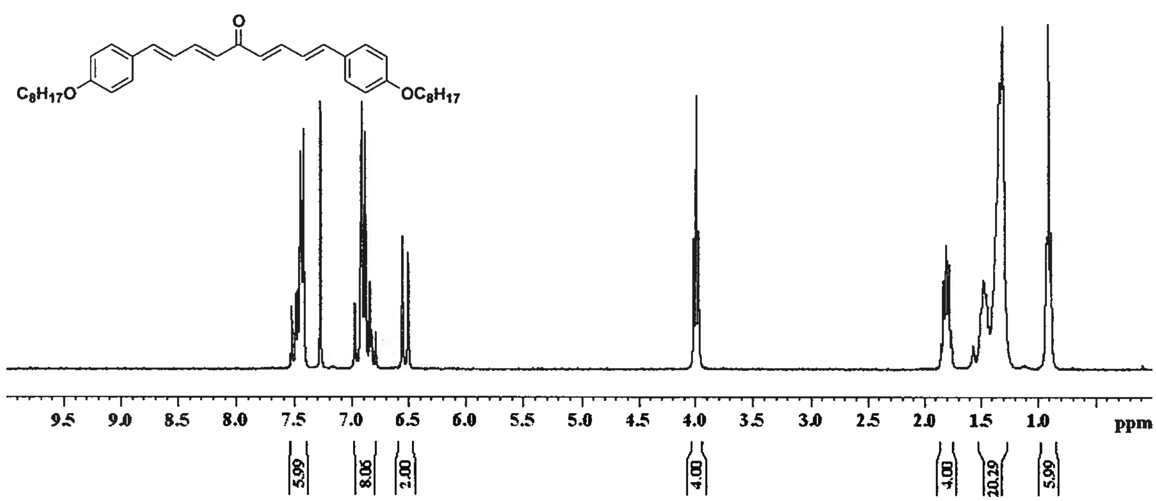

Figure A38: ^{1}H NMR spectrum of **34b**.

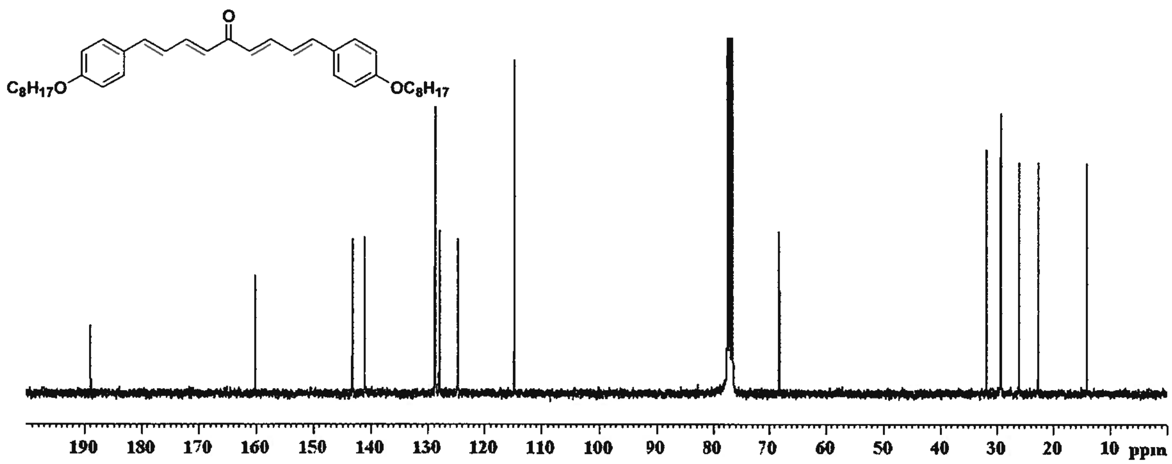

Figure A38: ^{13}C NMR spectrum of **34b**.

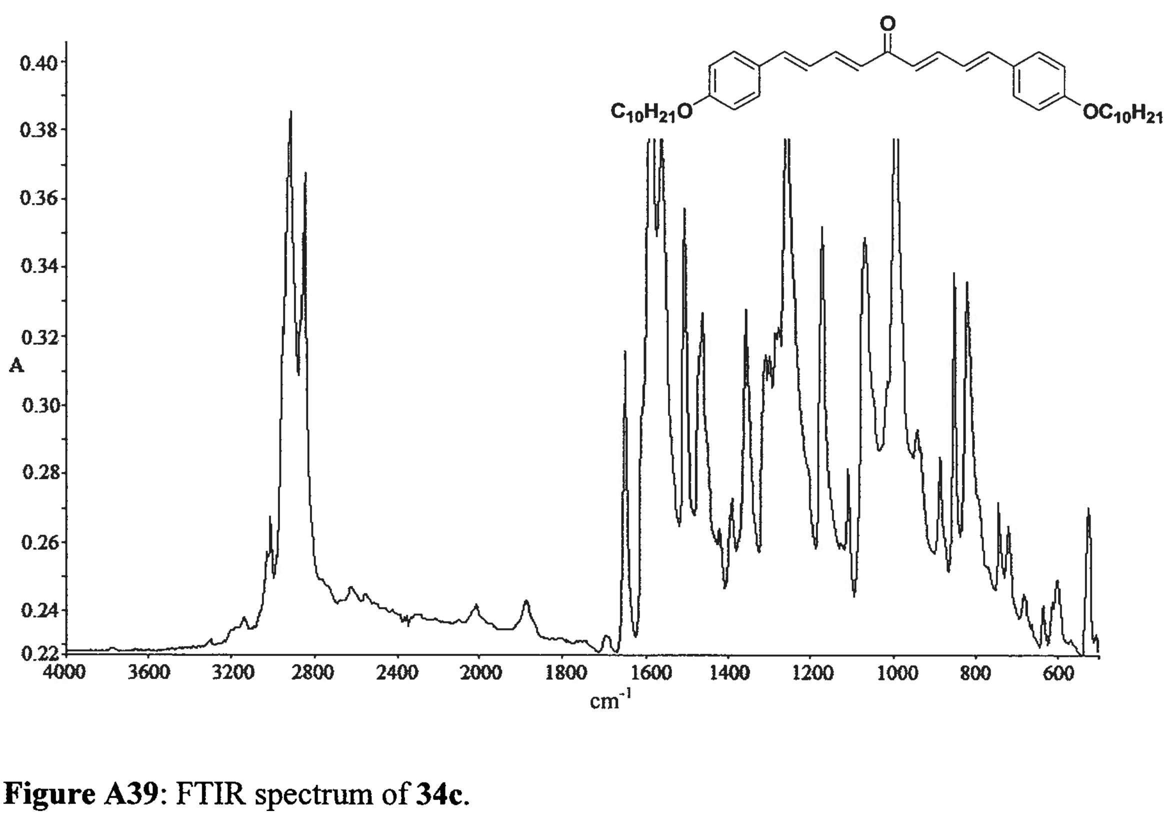

Figure A39: FTIR spectrum of **34c**.

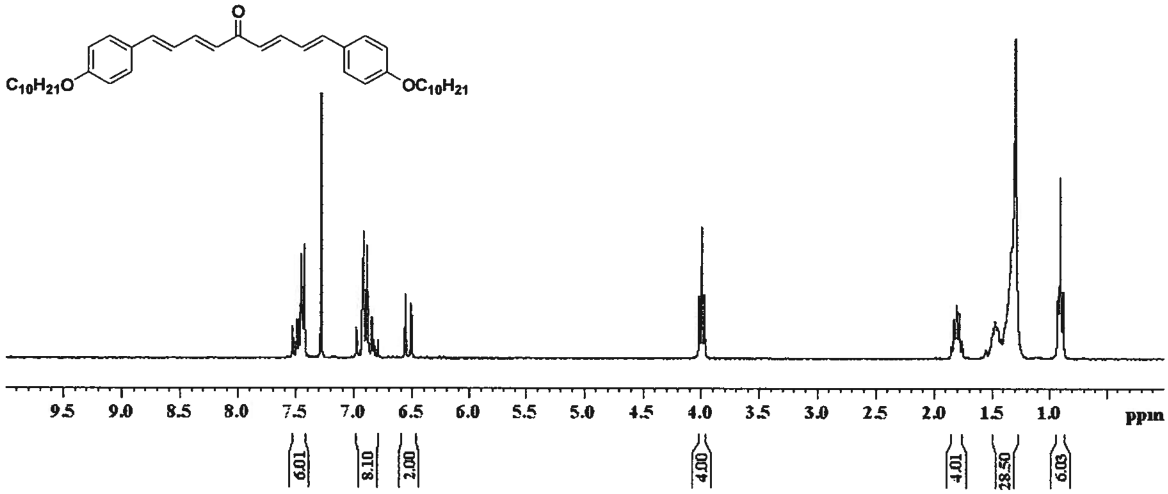

Figure A40: ^{1}H NMR spectrum of **34c**.

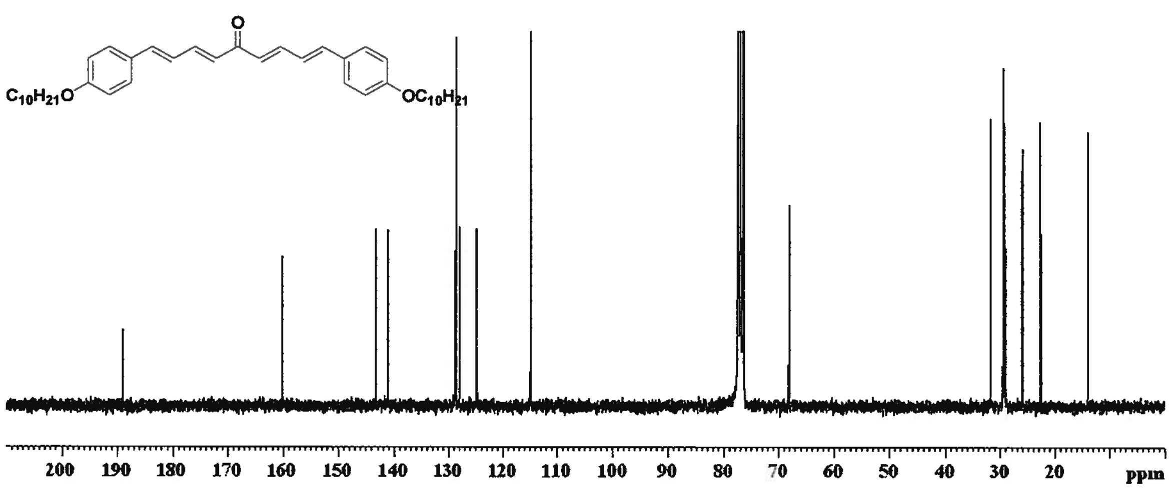

Figure A41: ^{13}C NMR spectrum of **34c**.

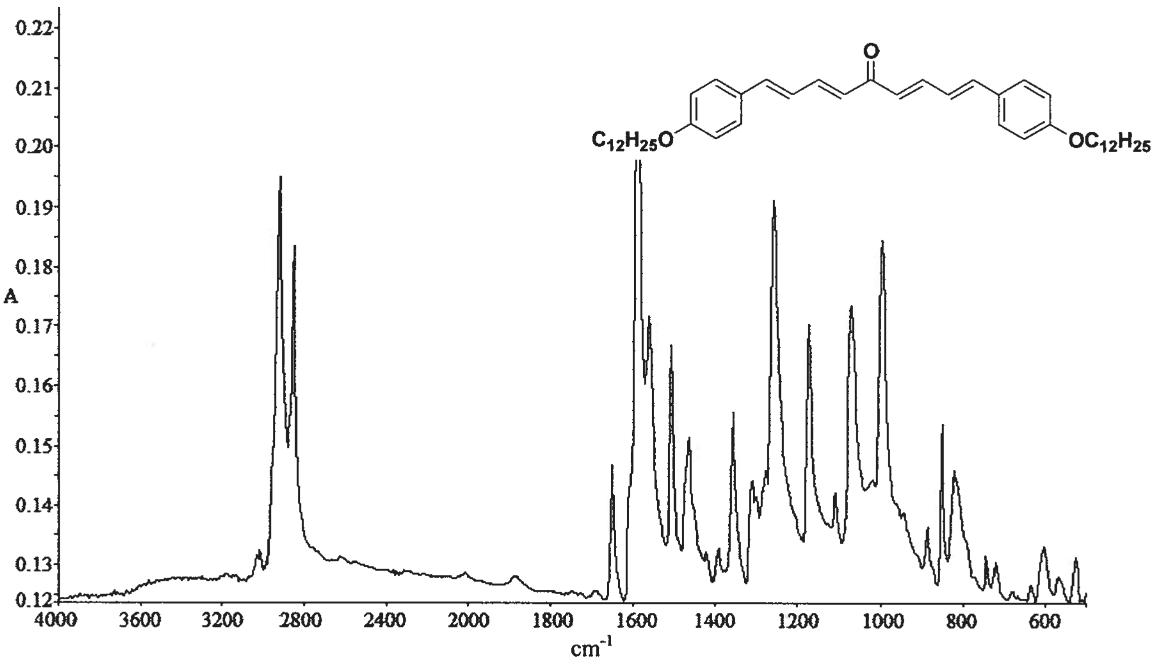

Figure A42: FTIR spectrum of **34d**.

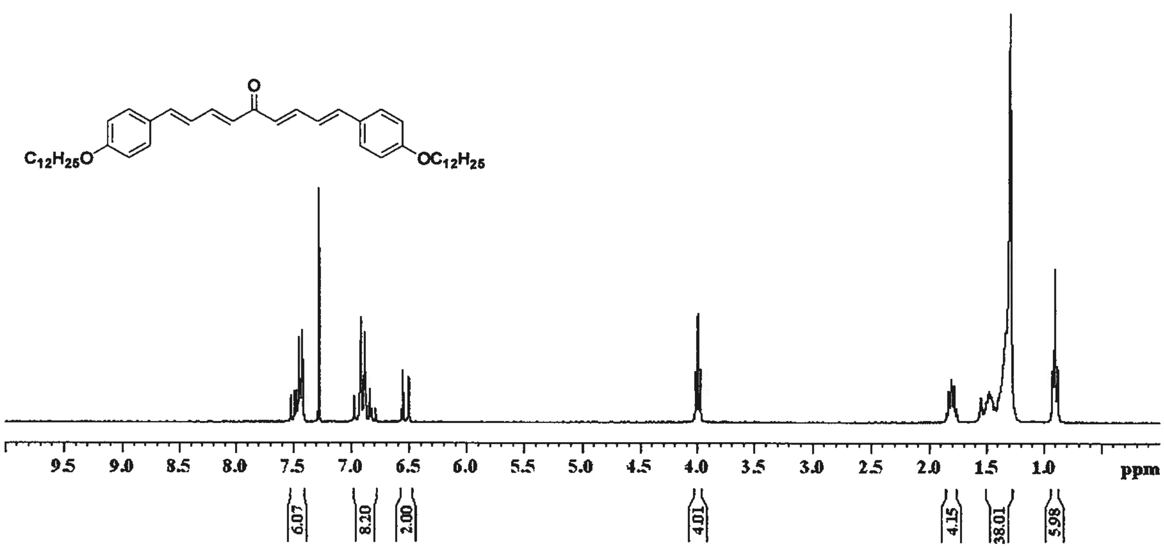

Figure A43: [1]H NMR spectrum of **34d**.

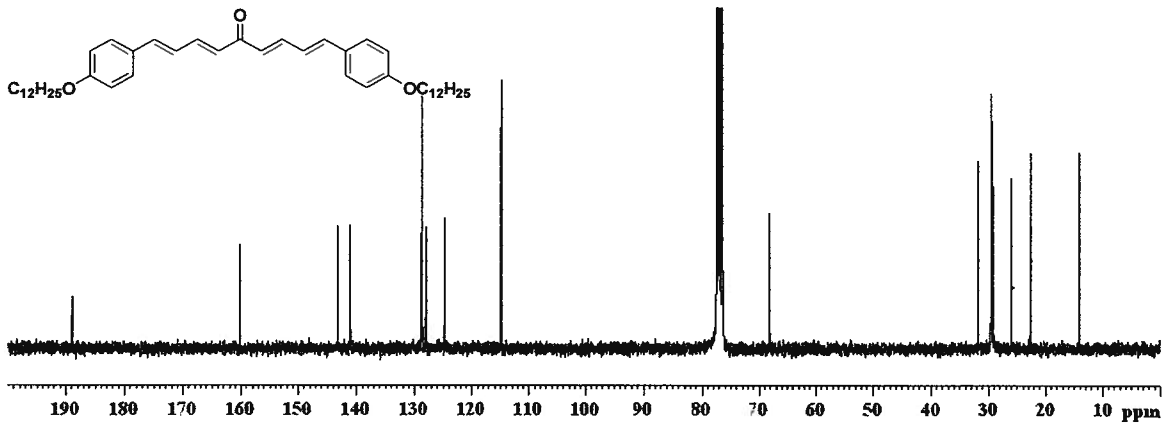

Figure A44: ^{13}C NMR spectrum of **34d**.

Appendix B

NMR Acquisition Parameters

Table B1: ^{1}H and ^{13}C NMR Acquisition and Processing Parameters

^{1}**H NMR Parameters**	^{13}**C NMR Parameters**
F2 - Acquisition Parameters INSTRUM: av300 PROBHD: 5 mm PABBO BB- PULPROG: zg30 TD: 16384 SOLVENT: CDCl3 NS: 16 DS: 2 SWH: 3591.954 Hz FIDRES: 0.219235 Hz AQ: 2.2807028 sec RG: 456.1 DW: 139.200 μsec DE: 6.00 μsec TE: 298.2 K D1: 1.00000000 sec MCREST: 0.00000000 sec MCWRK: 0.01500000 sec ---CHANNEL f1--- NUC1: 1H P1: 10.30 μsec PL1: -3.00 dB SFO1: 300.1315007 MHz	**F2 - Acquisition Parameters** INSTRUM: av300 PROBHD: 5 mm PABBO BB- PULPROG: zgpg30 TD: 32768 SOLVENT: CDCl3 NS: 3072 DS: 4 SWH: 17985.611 Hz FIDRES: 0.548877 Hz AQ: 0.9110004 sec RG: 7298.2 DW: 27.800 μsec DE: 6.00 μsec TE: 298.2 K D1: 1.50000000 sec d11: 0.03000000 sec MCREST: 0.00000000 sec MCWRK: 0.01500000 sec ---CHANNEL f1--- NUC1: 13C P1: 5.70 μsec PL1: -6.00 dB SFO1: 75.4752953 MHz

	---CHANNEL f2--- CPDPRG2: waltz16 NUC2: 1H PCPD2: 80.00 μsec PL2: -3.00 dB PL12: 14.81 dB PL13: 15.00 dB SFO2: 300.1312005
F2 – Processing Parameters SI: 32768 SF: 300.1300000 MHz WDW: EM SSB: 0 LB: 0.30 Hz GB: 0 PC: 1.40	**F2 – Processing Parameters** SI: 32768 SF: 75.4677490 MHz WDW: EM SSB: 0 LB: 1.00 Hz GB: 0 PC: 1.00

Appendix C

Table of Enthalpy Changes in DSC Thermograms

Table C1: Transition enthalpy changes in DSC thermograms of **2a-d** and **9e-f**.

Compound	Transition Temperature (°C)	Transition Enthalpy Change (kJ/mol)
2a	66.3 103.6 93.4 62.8	2.96 37.85 -38.10 -2.08
2b	89.9 98.2 87.5 90.8	3.87 45.13 -45.14 -2.32
2c	100.2 93.7	73.65 -72.55
2d	103.2 98.9	79.08 -86.71
9e	-16.5 26.4 45.8 -14.9	5.94 24.14 53.36 -3.46
9f	56.9 11.3	66.26 -45.92
9g	64.2 39.7	79.75 -76.06
9h	71.8 47.0	88.36 -81.69

Table C2: Transition enthalpy changes in DSC thermograms of **19a-d** and **23e-f**.

Compound	Transition Temperature (°C)	Transition Enthalpy Change (kJ/mol)
19a	109.8 101.6	27.64 -27.29
19b	81.5 101.6 92.4	18.06 44.46 -51.01
19c	90.9 101.4 94.8	14.05 23.50 -29.10
19d	95.4 90.7	66.00 53.43
23e	54.8 62.9	42.89 10.87
23f	3.2 30.9 62.0 65.4 23.0	-8.10 -12.33 - 57.59 -2.20
23g	39.1 71.5 26.6 21.1	5.39 62.54 -23.08 -8.57
23h	51.2 72.1 31.4	-13.00 45.89 -35.33

Table C3: Transition enthalpy changes in DSC thermograms of **34a-d**.

Compound	Transition Temperature (°C)	Transition Enthalpy Change (kJ/mol)
34a	149.7	81.41
	131.8	-70.60
	128.5	-8.34
34b	11.6	3.37
	136.8	27.84
	135.0	-0.43
	128.5	-24.82
	8.0	-1.76
34c	34.9	1.66
	40.3	3.39
	117.5	14.27
	130.9	14.42
	121.4	-10.76
	33.2	-3.46
34d	121.1	17.52
	125.3	6.71
	117.9	-3.32
	62.9	-10.30